# Belowground plasticity of European beech – Studies on the variability of beech fine root system size, structure, morphology, and anatomy, and on their impact on soil organic matter in the top- and subsoil of six beech forests with different bedrock types in Northern Germany

Dissertation
for the award of the degree
„Doctor rerum naturalium“,
Georg-August University of Göttingen

within the doctoral program Biological Diversity and Ecology
of the Georg-August University School of Science (GAUSS)

submitted by
**Kristina Kirfel**
from
Kreuzberg (DE)

Göttingen, July 2018

Thesis Committee

Prof. Dr. Christoph Leuschner

Plant Ecology and Ecosystems Research, Georg-August University of Göttingen

Prof. Dr. Dirk Hölscher

Tropical Silviculture and Forest Ecology, Georg-August University of Göttingen

Dr. Dietrich Hertel

Plant Ecology and Ecosystems Research, Georg-August University of Göttingen

Members of the Examination Board

Reviewer: Prof. Dr. Christoph Leuschner

Plant Ecology and Ecosystems Research, Georg-August University of Göttingen

Second Reviewer: Prof. Dr. Dirk Hölscher

Tropical Silviculture and Forest Ecology, Georg-August University of Göttingen

Date of the oral examination: 29th of August, 2018

The difficulty lies not in the new ideas, but in escaping from the old ones, which ramify, for those brought up as most of us have been, into every corner of our minds.

- JOHN MAYNARD KEYNES -

# TABLE OF CONTENTS

**CHAPTER 1**

**General Introduction ..... 1**

1.1 Background ..... 3

1.2 General study aims ..... 9

1.3 Paper outline ..... 9

1.4 Project Framework ..... 12

1.5 References ..... 15

**CHAPTER 2**

**Material and Methods ..... 21**

2.1 Study Sites ..... 23

2.2 Methods ..... 26

2.3 References ..... 29

**CHAPTER 3**

**Effects of bedrock type and soil chemistry on the fine root system and fine root morphology of European beech – A study on the belowground plasticity of trees ..... 31**

3.1 Abstract ..... 33

3.2 Introduction ..... 34

3.3 Material and Methods ..... 39

3.4 Results ..... 43

3.5 Discussion ..... 55

3.6 Conclusions ..... 60

3.7 References ..... 66

**CHAPTER 4**

**Influence of Root Diameter and Soil Depth on the Xylem Anatomy of Fine- to Medium-Sized Roots of Mature Beech Trees in the Top- and Subsoil ..... 73**

4.1 Abstract ..... 75

4.2 Introduction ..... 76

4.3 Material and Methods ..... 79

4.4 Results ..... 82

4.5 Discussion ..... 89

4.6 Conclusion ..... 95

4.7 References ..... 99

**CHAPTER 5**

**Factors controlling the variability of organic matter in the top- and subsoil of a sandy Dystric Cambisol under beech forest ..... 109**

5.1 Abstract ..... 111

5.2 Introduction ..... 112

5.3 Materials and Methods ..... 114

5.4 Results ..... 120

5.5 Discussion ..... 127

5.6 Conclusions ..... 130

5.7 References ..... 132

**CHAPTER 6**

**Spatial distribution and chemical composition of soil organic matter fractions in rhizosphere and non-rhizosphere soil under European beech (*Fagus sylvatica* L.) ..... 139**

6.1 Abstract ..... 141

6.2 Introduction ..... 143

6.3 Materials and Methods ..... 144

6.4 Results ..... 152

5.5 Discussion ..... 158

5.6 Conclusions ..... 161

6.7 References ..... 164

**CHAPTER 7**

**Soil organic carbon stocks in topsoil and subsoil controlled by parent material, carbon input in the rhizosphere, and microbial-derived compounds ..... 171**

7.1 Abstract ..... 173

7.2 Introduction ..... 175

7.3 Materials and Methods ..... 177

7.4 Results ..... 184

7.5 Discussion ..... 193

7.6 Conclusions ..... 200

7.7 References ..... 203

**CHAPTER 8**

**Synthesis ..... 217**

8.1 Synthesis ..... 219

8.2 References ..... 230

**CHAPTER 9**

**Summary ..... 239**

9.1 Summary ..... 241

**CHAPTER 10**

**Appendix ..... 243**

10.1 Index of Tables ..... 245

10.2 Index of Figures ..... 249

10.3 Curriculum Vitae ..... **Fehler! Textmarke nicht definiert.**

10.4 Acknowledgements ..... 253

10.5 Declaration of originality and certificate of ownership ..... 257

# LIST OF ABBREVIATIONS

| | |
|---|---|
| AIC | Akaike information criterion |
| $Al_d$ | Dithionite-citrate-extractable Al (mg $g^{-1}$) |
| $Al_o$ | Oxalate-extractable and Al (mg $g^{-1}$) |
| $A_{lumen}$:$A_{xylem}$ | Relative vessel lumen area (%) |
| ANOVA | Analysis of variance |
| $A_{xylem}$ | Xylem cross-sectional area ($mm^2$) |
| BS | Base saturation (%) |
| CEC | Cation exchange capacity (µmolc $g^{-1}$) |
| CFE | Chloroform fumigation extraction |
| $C_{mic}$ | Microbial biomass C (µg $g^{-1}$) |
| CPMAS $^{13}C$ NMR | Cross-polarization magic angle spinning $^{13}C$ nuclear magnetic resonance |
| CV | Coefficient of variation |
| *D* | Mean vessel diameter (mm) |
| DFG | Deutsche Forschungsgemeinschaft |
| $D_h$ | Hydraulically weighted vessel diameter (mm) |
| DI | Deionized water |
| DOC | Dissolved organic carbon |
| DW | Dry weight |
| $E_c$ | Carbon enrichment factor |
| $Fe_d$ | Dithionite-citrate-extractable Fe (mg $g^{-1}$) |
| $Fe_o$ | Oxalate-extractable Fe (mg $g^{-1}$) |
| FRB | Fine root biomass (g $m^{-2}$) |
| FRN | Fine root necromass (g $m^{-2}$) |

| | |
|---|---|
| $K_p$ | Potential hydraulic conductivity kg $m^{-1}$ $MPa^{-1}$ $s^{-1}$ |
| LME | Linear mixed effect |
| MD | Mean root diameter (mm) |
| $N_t$ | Total nitrogen (mg $kg^{-1}$) |
| OC | Organic carbon |
| OL | Organic layer |
| OM | Organic matter |
| oPOM | POM occluded within aggregates |
| PCA | Principal components analysis |
| POM | Particulate organic matter |
| RAI | Root area index ($m^2$ root area $m^{-2}$ ground area) |
| RLI | Root length index (m root length $m^{-2}$ ground area) |
| RTA | Root tip abundance (n $m^{-2}$ ground area) |
| RTD | Root tip density (n $L^{-1}$) |
| RTF | Root tip frequency (n $mg^{-1}$ root dry mass) |
| SD | Standard deviation |
| SOC | Soil organic carbon (%) |
| SPT | Sodium polytungstate |
| SRA | Specific root area ($cm^2$ $g^{-1}$) |
| SRL | Specific root length (cm $g^{-1}$) |
| SSA | Specific surface area ($m^2$ $g^{-1}$) |
| VD | Vessel density (n $mm^{-2}$) |
| VIF | Variance inflation factors |
| XRD | X-ray Powder Diffraction |

# CHAPTER 1

# General Introduction

## 1.1 Background

Tree roots are of fundamental functional importance on the individual tree as well as on the ecosystem level. In simplified terms, woody coarse roots (≥ 2 mm in diameter) serve anchorage, transport, and storage functions, while non-woody fine roots (< 2 mm in diameter)[1] primarily serve nutrient and water uptake (Helmisaari et al. 2000; Pregitzer 2002). Moreover, roots play a key role in ecosystem functioning with regards to biogeochemical cycling in terrestrial ecosystems (Pregitzer et al. 2002; Yuan and Chen 2010; McCormack et al. 2015): besides their acquisition and transport function for water and nutrients upwards, they are pathways for carbon and nutrients in the downward direction, they facilitate deep water infiltration, affect the weathering of minerals, and they have an impact on the activity of soil fauna (Schenk and Jackson 2002).

Despite their importance, our knowledge on fine root system size, structure, morphology, and anatomy of trees under different environmental conditions is still scarce, thereby limiting our understanding of the role of belowground systems in ecological processes (Reich 2002; Comas and Eissenstat 2009). Since root studies are in the majority confined to the upper soil horizons (Gill and Burke 2002; Schenk and Jackson 2002, 2005), this is particularly true for the subsoil, which is the lower part of the soil above the non-weathered parent material, between topsoil and substratum. The lack of studies on trees' root systems can be attributed to the methodological difficulties and the enormous work load imposed by the study of fine roots in mature forests (Vogt et al. 1996):

"The fine roots of perennial plants are a royal pain to study." (Pregitzer 2002, p. 267)

### *Deep roots*

Sampling of deep roots is even more time-consuming, technically demanding, and costly (Maeght et al. 2013) – this is one reason for the scarcity of studies investigating the abundance, distribution, and function of subsoil roots. The usually small share of roots in subsoil layers compared to the bulk of root mass in the topsoil may be another reason for the negligence of deep

[1] Although an established definition of fine roots in terms of diameter-size range does not exist, conventionally roots with a diameter smaller than 2 mm are termed fine roots (Fogel 1983; Vogt et al. 1983).

roots in most studies; however, there is an increasing interest in investigating deep roots since some studies indicate that their activity and functional importance is much more substantive than their abundance may suggest (Stone and Kalisz 1991; Canadell et al. 1996; Lehmann 2003). The large volume of subsoil often constitutes an important reservoir for water and nutrients, which plants can tap with deep roots (Stone and Comerford 1994): soil moisture may be equal or higher in the subsoil than in the uppermost horizons, and the absorption of water by deep-reaching roots can secure trees' water supply during dry periods (Nepstad et al. 1994). Furthermore, considerable amounts of plant-available Ca, Mg, N, and S may be present below 20 cm soil depth (Jobbággy and Jackson 2001). And subsoils also play an important role in C cycling: > 50 % of the total profile SOC is stored in soils below 20 cm depth (Gill et al. 1999).

Although it is uncontroversial that deep roots may fulfill important roles in plant nutrient and water supply as well as in ecosystem functioning, their function and their development, whether genetically or environmentally driven, is not well understood (Schenk and Jackson 2002; Maeght et al. 2013). The deployment of deep roots appears to be dependent on tree species and their specific strategies to ensure sufficient water and nutrient supply also in stressful environments and in dry periods, modulated by the prevailing environmental conditions, most importantly physical and chemical soil properties (Lehmann 2003): for instance, deep roots are much more likely to occur in coarse- compared to medium-textured soils, most probably because the limited storage-capacities of these soils for plant-available water require to tap greater soil volumes to meet plants' water demand (Jackson et al. 2000; Schenk and Jackson 2002, 2005; Mainiero and Kazda 2006).

***Root system development***

Information on the plasticity of mature trees' fine root systems in terms of biomass, distribution, and morphology is in general still limited, not only with regards to the subsoil (Leuschner et al. 2004). More than 50 years ago Bradshaw (1965) specified that "plasticity is shown by a genotype when its expression is able to be altered by environmental influences". It is well-recognized that root system development is governed by a combination of endogenous (genetics and hormonal influences (Santner et al. 2009)) and exogenous factors (external physical and biochemical

factors, soil temperature, moisture and inorganic nutrients, soil organisms (Leuschner and Hertel 2003; Maeght et al. 2013)) (Hodge 2006; Pierret et al. 2007; Hartmann and Von Wilpert 2014).

Most decisively, the plasticity in root system architecture is considered to be a strategy directed at optimizing resource uptake from the soil under different environmental conditions (Yanai et al. 1995), a continuous response to the variability in soil resource availability in space and time (Harper et al. 1991). Soils are in the majority markedly heterogeneous on a spatial as well as on a temporal scale with regards to resource distribution, which has led the scientific community to describe soils as "patchy" environments (Hodge 2006). It is well established that root form is determined by root function (within the limits of a species' genetic make-up), and that particularly fine roots can be considered to be the modular unit of plants' belowground systems (Pregitzer et al. 2002; Pierret et al. 2007; Maeght et al. 2013): plants may increase their absorptive area via increasing their root system size or via alteration in morphological traits in order to optimize the acquisition of essential nutrients (Hodge 2004; Ostonen et al. 2007; Comas and Eissenstat 2009). Morphological parameters like specific root length (SRL, cm $g^{-1}$)and (SRA, $cm^2$ $g^{-1}$) can be thought of as factors indicating the ratio of root benefit (resource acquisition) to root cost (root construction and maintenance) (Eissenstat and Yanai 1997; Eissenstat et al. 2000; Pregitzer et al. 2002; Ostonen et al. 2007). Developing this conceptual model further, fine roots' morphological traits are thought to be shaped by the soil conditions they meet and are therefore indicative for the mineral nutrition of trees at certain sites, since nutrient uptake from the soil solution is a function of both soil and root properties (Yanai et al. 1995): roots might react to low nutrient availability with the production of thinner roots, which have a larger specific surface area per unit of carbon expenditure compared to thicker roots and can take up more nutrients at a given resource investment. How the variation in specific root traits and variation in soil chemical and/or physical characteristics are exactly linked is not well understood (Pregitzer et al. 2002; Comas and Eissenstat 2004; Pierret et al. 2007; Pregitzer 2008; Chen et al. 2016), for the main part because intra-species comparative studies particularly on fine root system morphology under different environmental regimes are rare (Leuschner et al. 2004). Furthermore, plants may, but were not always shown to (Caldwell et al. 1996) respond to soil heterogeneity with root proliferation into patches, where resources are available (Hodge 2004), or with physiological,

morphological, and / or anatomical adjustments in the root system in order to optimize resource capture (Fitter 1994; Forde and Lorenzo 2001; Pregitzer et al. 2002).

Overall, our knowledge about the linkages between structural, physiological, morphological, and anatomical root system adjustment and root function is still extremely limited (Pregitzer et al. 2002) and a generalization of strategies in terms of plastic responses in root traits could not be established yet (Ryser 2006).

### *The role of roots in the C cycle of forests*

In terms of terrestrial C cycling, fine roots play a major role in forest ecosystems (Rasse et al. 2005; Comas and Eissenstat 2009): although their share in tree biomass may be less than 2%, they consume up to 75% of forests' annual net primary production (Keyes and Grier 1981; Fogel and Hunt 1983; Fogel 1985; Vogt et al. 1996; Gill and Jackson 2000). Dead fine roots and rhizodeposits are a major source of soil organic carbon (SOC) in soils, particularly in subsoils (Rasse et al. 2005; Comas and Eissenstat 2009; Tefs and Gleixner 2012); however, how tree roots exactly impact the spatial distribution, turnover and storage of soil organic matter (SOM) as well as its chemical composition is not fully understood, yet (Angst et al. 2016). The SOC concentration in subsoils is most often comparably low, but because the volume of subsoils generally exceeds that of topsoils by several magnitudes, 30-60% of the global SOC is stored in the horizons below the topsoil (Chabbi et al. 2009; Harrison et al. 2011; Koarashi et al. 2012; Harper and Tibett 2013). Soils contain the largest terrestrial organic carbon (OC) pool (Jobbágy and Jackson 2000; Janzen 2005), and forest soils contain up to 70% of all SOC (Jobbágy and Jackson, 2000), which emphasizes the need to quantify belowground C-fluxes, including subsoil properties and deep root systems, of forests to fully understand global C cycling (Jackson et al. 1997; Pollierer et al. 2007). Despite a comparably high number of studies investigating SOC contents and stocks, most studies are confined to the topsoil and therefore quantitative information on subsoil SOC stocks, cycling, and storage mechanisms are scarce (Rumpel and Kögel-Knabner 2011). In this regard, only little information is available on the effects of contrasting parent material on the SOC cycle (Barré et al. 2017; Heckmann et al. 2009).

### *Fagus sylvatica*

European beech (*Fagus sylvatica* L.) is the most prevalent broadleaf tree species in Germany: it covers about 1.680.072 ha or 15.4 % of the forest area in Germany (Bundeswaldinventur 2012) - only pine and spruce cover a higher percentage of the forested area. Prior to deforestation and management of forests, more than 300 000 $km^2$ of Central Europe were covered by European beech (Leuschner et al. 2006). Today, beech and mixed beech forests are still the most important and characteristic alliance in terms of spatial extension in Central Europe (Fig. 1.1) (Leuschner and Ellenberg 2017). The success of the tree species is due to its tolerance of a very broad range of site conditions and its ability to outcompete other native tree species owing to its shade-tolerance at juvenile stage and by the production of shade at adult stage (Hertel 1999; Leuschner and Ellenberg 2017). It thrives on almost all geological substrates and Central European forest soil types, whether highly acidic or alkaline, if sufficient drainage is given. Due to its sensitivity to hypoxia, European beech is absent on gleysols or other hydromorphic soils and does not grow in waterlogged depressions either. European beech also tolerates a broad range of climatic conditions: naturally, it would cover around 2/3 of the land area of Central Europe, apart from azonal habitats with too cold or dry conditions (Leuschner et al. 2006; Bohn and Gollub 2007).

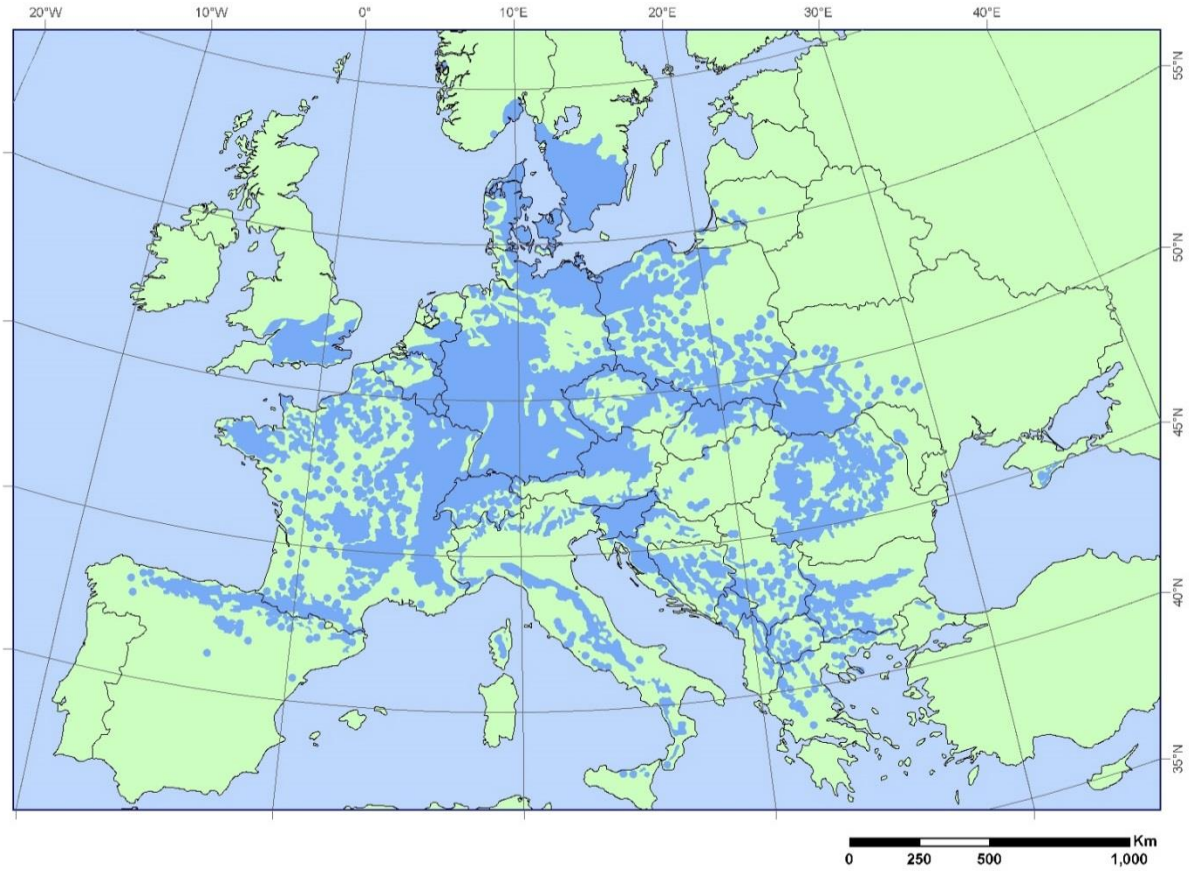


**FIGURE 1.1**: **Distribution map of *Fagus sylvatica*** (adapted from EUFORGEN 2018)

## 1.2 General study aims

The present thesis investigates the belowground plasticity of *Fagus sylvatica L.* in a comparative approach in six mature European beech forests on different bedrock in Northern Germany. The studies aimed to reveal species-specific adaptations in beech fine root system size, structure, morphology and anatomy as well as their impact on SOC content, distribution, and quality in the top- and subsoil of the study sites along an edaphic gradient.

Major study aims were to

i. quantify total stand fine root biomass and necromass and to analyze variation in fine root distribution patterns in dependence on soil acidity and depth,
ii. investigate beech fine root morphological adaptations to different regimes of nutrient availability in soils,
iii. analyze the intraspecific variability in xylem anatomical and derived hydraulic traits of small- and medium-sized beech roots with particular focus to soil depth-dependent variation,
iv. assess the impact of beech roots on the amount, spatial distribution and chemical composition of SOM with regards to the effect of different parent materials.

## 1.3 Paper outline

This dissertation is subdivided into five studies which deal with different aspects of fine root biomass and necromass, root distribution and morphology, anatomical and derived hydraulic properties and the role of fine roots in the carbon cycle of top- and subsoils under European beech forests along an edaphic gradient.

**CHAPTER 3:**

**Effects of bedrock type and soil chemistry on the fine root system and fine root morphology of European beech – A study on the belowground plasticity of trees**

In this comparative study, the variation in beech fine root system size, distribution, and morphology was investigated in six mature stands on different bedrock down to the rock surface. The following hypotheses were tested:

(i) The stand total of fine root biomass increases with increasing soil acidity and decreasing base saturation,

(ii) fine root biomass density shows a steeper decrease from topsoil to subsoil in more acidic soil profiles,

(iii) the stand total of fine root biomass is smaller in shallow soil profiles with low bedrock depth, irrespective of soil acidity,

(iv) the live:dead ratio of fine root mass decreases with increasing soil acidity, while fine root necromass increases,

(v) fine roots in acidic soils have a higher specific root length and area and smaller mean root diameter in order to increase uptake efficiency under nutrient-deficient conditions, and

(vi) the frequency of fine root tips and root tip abundance per soil volume increase with increasing soil acidity.

**CHAPTER 4:**

**Influence of Root Diameter and Soil Depth on the Xylem Anatomy of Fine- to Medium-Sized Roots of Mature Beech Trees in the Top- and Subsoil**

In this study, the intraspecific variability in xylem anatomical and derived hydraulic traits of small- to medium-sized roots (1-10 mm in diameter) was analyzed in the top- and subsoil down to a depth of 200 cm in one mature *Fagus sylvatica* L. forest stand in Northern Germany.

The following hypotheses were tested:

(i) Vessel diameter and hydraulic conductivity are a function of root diameter and, thus, of root age,

(ii) the variability in xylem anatomical and hydraulic traits in similar-sized roots is high at a given soil depth with some roots exhibiting characteristics of “high-conductivity roots”, and

(iii) vessel diameter and consequently hydraulic conductivity increase with increasing soil depth.

**CHAPTER 5:**

**Factors controlling the variability of organic matter in the top- and subsoil of a sandy Dystric Cambisol under beech forest**

This study aimed to analyze the amounts and distribution of SOC and to elucidate the turnover and storage mechanisms throughout deep soil profiles of a sandy Dystric Cambisol on Pleistocene glacial deposits under beech forest in Northern Germany.

In particular the goals of this study were to

(i) identify the factors controlling the SOC distribution in subsoils to better understand the mechanisms that engender the greater variability of subsoil OC, in order to

(ii) allow a better estimation of OC contents in subsoils, and

(iii) help to guide future management strategies for increasing subsoil OC stocks.

**CHAPTER 6:**

**Spatial distribution and chemical composition of soil organic matter fractions in rhizosphere and non-rhizosphere soil under European beech (*Fagus sylvatica L.*)**

This study focuses on the impact of individual trees and their root system on the spatial distribution and chemical composition of SOM fractions and the storage of SOC in subsoils.

Research was guided by the hypothesis that

(i) individual trees measurably influence the measured chemical composition of SOM fractions, and this influence decreases with increasing distance to the trees' stem base.

**CHAPTER 7:**

**Soil organic carbon stocks in topsoil and subsoil controlled by parent material, carbon input in the rhizosphere, and microbial-derived compounds**

The aim of this study was to

(i) emphasize how differences in parent material influence the amount and distribution of SOC in the top- and subsoil, in particular by investigating

   a. the way in which substrate properties affect the input of OM
   b. how differences in substrate properties impact SOC stabilization mechanisms.

## 1.4 Project Framework

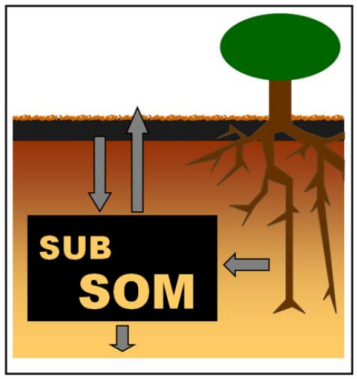


The current studies were conducted in the frame of research unit FOR1806 "The Forgotten Part of Carbon Cycling: Organic Matter Storage and Turnover in Subsoils (SUBSOM)", funded by Deutsche Forschungsgemeinschaft (DFG). The overall aim of the research unit was to improve the understanding of carbon cycling in subsoils by identifying processes and controlling factors of subsoil carbon turnover by means of a transdisciplinary approach. The results are a prerequisite for numerical modelling of C-dynamics in subsoils and moreover serve to improve the management and prediction of climate change effects on soil C-pools.

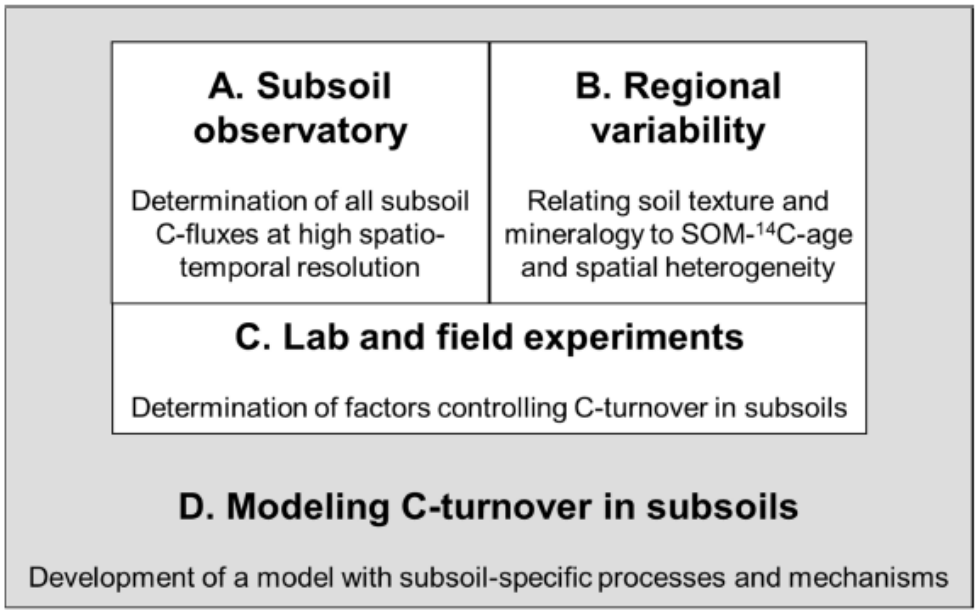


**FIGURE 1.2**: **Project concept with four methodological approaches** (Marschner et al. 2012)

The research unit consisted of nine closely interlinked subprojects implemented by several working groups at different research institutes within Germany (Table 1.1). Four distinct methodological approaches were combined in order to model the C-dynamics in the subsoil (Fig. 1.2). At six research sites, which are described in chapter 2, field C-flux measurements, detailed analyses of subsoil properties, in-situ and laboratory experiments were conducted:

A. A subsoil observatory for determining C-fluxes in the subsoil was set up in the Grinderwald forest. At a high spatial and temporal resolution, all relevant fluxes were collected in-situ and quantified.
B. At all six study sites, soil samples were taken at a high spatial resolution and characterized comprehensively. The selection of study sites in the same climatic region but developed on different bedrock types allowed to study the role of different parent materials for the stabilization and spatial distribution of subsoil organic matter.
C. In order to identify the determinants of SOC stability in the subsoil, field (e.g. $^{13}C$ tracers, reciprocal transfer of soil samples within the profile) and laboratory incubation experiments with disturbed and intact soil samples were conducted.
D. A numerical model for SOC turnover which integrated the subsoil-specific controlling factors for SOC sequestration has been developed.

**TABLE 1.1: Subprojects of the SUBSOM research unit**

| **Number of subproject** | **Title of subproject** |
|---|---|
| PC | Project coordination: field site management, data synthesis and modelling of subsoil C turnover. |
| P1 | Effects of water content, input of roots and DOC, spatial inaccessibility on C-turnover and spatial variability of subsoil properties. |
| P2 | Organic matter composition in the subsoil: contribution of root litter and microbial-derived compounds. |
| P3 | $^{14}C$ content of specific compounds in subsoils. |
| P4 | Micro-scaled hydraulic heterogeneity in subsoils. |
| P5 | Origin and fate of dissolved organic matter in the subsoil. |
| P6 | Vertical partitioning of $CO_2$ production and effects of temperature, oxygen and root location within the soil profile on C-turnover. |
| P7 | Root distribution and dynamics and their contribution to subsoil C-fluxes. |
| P8 | Spatial heterogeneity and substrate availability as limiting factors for subsoil C-turnover. |
| P9 | Biological regulation of subsoil C-cycling under field conditions. |

The present doctoral thesis was conducted within the frame of the subproject “Root distribution and dynamics and their contribution to subsoil C-fluxes” (P7) in a working group at the Department of Plant Ecology and Ecosystems Research at the Georg-August University of Göttingen. The main goals of this subproject were to investigate the vertical distribution and activity of fine roots in soils under beech forest to analyze the role of roots in the C-cycle of subsoils as well as in the water and nutrient cycles of soils.

## 1.5 References


Angst, G., Kögel-Knabner, I., Kirfel, K., Hertel, D., and Mueller, C. W. (2016) Spatial distribution and chemical composition of soil organic matter fractions in rhizosphere and non-rhizosphere soil under European beech (*Fagus sylvatica* L.). Geoderma 264: 179-187.

Barre, P., Durand, H., Chenu, C., Meunier, P., Montagne, D., Castel, G., Billiou, D., Soucémarianadin, L., and Cecillon, L. (2017) Geological control of soil organic carbon and nitrogen stocks at the landscape scale. Geoderma 285: 50-56.

Bohn, U., and Gollub, G. (2007) Buchenwälder als natürliche Vegetation in Europa. Natur und Landschaft 82: 391-397.

Bradshaw, A.D. (1965) Evolutionary significance of phenotypic plasticity in plants. Advances in Genetics 13:115–155.

Bundeswaldinventur (2012) https://bwi.info/. Accessed in July 2018.

Canadell, J., Jackson, R.B., Ehleringer, J.R., Mooney, H.A., Sala, O.E., and Schulze, E.-D. (1996) Maximum rooting depth of vegetation types at the global scale. Oecologia 108:583-595.

Chabbi, A., Kögel-Knabner, I., and Rumpel, C. (2009) Stabilised carbon in subsoil horizons is located in spatially distinct parts of the soil profile. Soil Biology and Biochemistry 41(2):256-261.

Chen, W., Koide, R.T., Adams, T.S., DeForest, J.L., Cheng, L., and Eissenstat, D.M. (2016) Root morphology and mycorrhizal symbioses together shape nutrient foraging strategies of temperate trees. PNAS 113(31): 8741-8746.

Comas, L.H., and Eissenstat, D.M. (2009) Patterns in root trait variation among 25 co-existing North American forest species. New Phytologist 182: 919–928.

Comas, L. H., and Eissenstat, D. M. (2004) Linking fine root traits to maximum potential growth rate among 11 mature temperate tree species. Functional Ecology 18(3): 388-397.

Eissenstat, D. M., and Yanai, R. D. (1997) The ecology of root lifespan. Advances in Ecological Research 27: 1–60.

Eissenstat, D.M., Wells, C.E., Yanai, R.D., and Whitbeck, J. L. (2000) Building roots in a changing environment: implications for root longevity. New Phytol. 147: 33-42.

EUFORGEN 2018. http://www.euforgen.org/. Accessed in July 2018.

Fitter, A.H. (1994) Architecture and biomass allocation as components of the plastic response of root systems to soil heterogeneity. In: Caldwell, M.M., Pearcy, R.W. (eds.) Exploitation of environmental heterogeneity by plants. Academic Press, 305–323, San Diego, USA.

Fogel, R. (1985) Roots as primary producers in below-ground ecosystems. In: Fitter, A.H., Atkinson, D., Read, D.J., and Usher, M.B. (eds.) Ecological Interactions in Soil: Plants, Microbes, and Animals (Special Publication No. 4 of the British Ecological Society). Blackwell Scientific Publications, 23–36, Oxford, UK.

Fogel, R. (1983) Root turnover and productivity of coniferous forest. Plant & Soil 71: 75–85.

Forde, B., and Lorenzo, H. (2001) The nutritional control of root development. Plant and soil 232(1-2):51-68.

Gill, R.A., and Burke, I.C. (2002) Influence of soil depth on the decomposition of Bouteloua gracilis roots in the shortgrass step. Plant Soil 241: 233-242.

Gill, R.A., and Jackson, R.B. (2000) Global patterns of root turnover for terrestrial ecosystems. New Phytologist 147: 13–31.

Gill, R.A., Burke, I.C., Milchunas, D.G., and Lauenroth, W.K. (1999) Relationship between root biomass and soil organic matter pools in the shortgrass steppe of eastern Colorado: Implications for decomposition through a soil profile. Ecosystems 2: 226–236.

Harper, R. J., and Tibbett, M. (2013). The hidden organic carbon in deep mineral soils. Plant Soil 368: 641–648. doi: 10.1007/s11104-013-1600-9.

Harper, J.L., Jones, M., and Sackville Hamilton, N.R. (1991) The evolution of roots and the problems of analyzing their behavior. In: Atkinson, D. (ed.) Plant Root Growth: An Ecological Perspective. Blackwell Scientific Publications, 3–22, Oxford, UK.

Harrison, R., Footen, P., and Strahm, B. (2011) Deep soil horizons: contribution and importance to soil carbon pools and in assessing whole-ecosystem response to management and global change. For. Sci. 57: 67–76.

Hartmann, P., and von Wilpert, K. (2014) Fine-root distributions of Central European forest soils and their interaction with site and soil properties. Can.J.For.Res. 44: 71-81.

Heckman, K., Welty-Bernard, A., Rasmussen, C., and Schwartz, E. (2009) Geologic controls of soil carbon cycling and microbial dynamics in temperate conifer forests. Chemical Geology 267(1-2): 12-23.

Helmisaari HS., Lehto T., and Makkonen K. (2000) Fine Roots and Soil Properties. In: Mälkönen E. (ed.) Forest Condition in a Changing Environment. Forestry Sciences, vol 65., 203-217, Springer, Dordrecht.

Hertel, D. (1999) Das Feinwurzelsystem von Rein-und Mischbeständen der-Rotbuche: Struktur, Dynamik und interspezifische Konkurrenz. Dissertationes Botanicae, 317. J. Cramer, Berlin, Stuttgart.

Hodge, A. (2004) The plastic plant: root responses to heterogeneous supplies of nutrients. New Phytologist 162: 9–24.

Hodge, A. (2006) Plastic plants and patchy soils. Journal of Experimental Botany 57(2): 401–411.

Jackson, R.B., Mooney, H.A., and Schulze, E.D. (1997) A global budget for fine root biomass, surface area, and nutrient contents. Proceedings of the National Academy of Sciences United States of America 94: 7362–7366.

Jackson, R.B., Sperry, J.S., and Dawson, T.E. (2000) Root water uptake and transport: using physiological processes in global predictions. Trends Plant Sci. 5 (11): 482–488.

Janzen, H. H. (2005) Soil carbon: A measure of ecosystem response in a changing world?. Canadian Journal of Soil Science 85(Special Issue): 467-480.

Jobbágy, E. G., and Jackson, R. B. (2000) The vertical distribution of soil organic carbon and its relation to climate and vegetation. Ecological applications 10(2): 423-436.

Jobbágy, E. G., and Jackson, R. B. (2001) The distribution of soil nutrients with depth: global patterns and the imprint of plants. Biogeochemistry 53(1): 51-77.

Keyes, M.R., and Grier, C.C. (1981) Above- and below-ground net production in 40-year-old Douglas-fir stands on low and high productivity sites. Canadian Journal of Forest Research 11: 599-605.

Koarashi, J., Hockaday, W. C., Masiello, C. A., and Trumbore, S. E. (2012) Dynamics of decadally cycling carbon in subsurface soils. J. Geophys. 117: G03033. doi: 10.1029/2012JG002034

Lehmann, J. (2003) Subsoil root activity in tree-based cropping systems. Plant and Soil 255: 319–331.

Leuschner, C., and Ellenberg, H. (2017) Ecology of Central European Forests. Vegetation Ecology of Central Europe, Vol I, Springer Nature, Cham, Switzerland.

Leuschner, C. and Hertel, D. (2003) Fine Root Biomass of Temperate Forests in Relation to Soil Acidity and Fertility, Climate, Age and Species. Progress in Botany 64: 405-438.

Leuschner, C., Hertel, D., Schmid, I., Koch, O., Muhs, A., and Hölscher, D. (2004) Stand fine root biomass and fine root morphology in old-growth beech forests as a function of precipitation and soil fertility. Plant and Soil 258: 43–56.

Leuschner, C., Meier, I.C., and Hertel, D. (2006) On the niche breadth of *Fagus sylvatica*: soil nutrient status in 50 Central European beech stands on a broad range of bedrock types. Annals of Forest Science 63:355–68.

Maeght J.-L-, Rewald, B., and Pierret, A. (2013) How to study deep roots — and why it matters. Frontiers in plant science 4: 1-14.

Mainiero, R., and Kazda, M. (2006) Depth-related fine root dynamics of *Fagus sylvatica* during exceptional drought. Forest Ecology and Management 237: 135–142.

Marschner, B., Bachmann, J., Flessa, H., Göbel, M.-O., Guggenberger, G., Helfrich, M., Hertel, D., Kandeler, E., Kögel-Knabner, I., Leuschner, C., Ludwig, B., Mikutta, R., Müller, C.W., Priesack, E., and Rethemeyer, J. (2012) The Forgotten Part of Carbon Cycling: Organic Matter Storage and Turnover in Subsoils [SUBSOM]. Proposal for a DFG research unit (FOR 1806). Bochum, Germany.

McCormack, M.L., Dickie, I.A., Eissenstat, D.M., Fahey, T.J., Fernandez, C.W., Guo, D., Helmisaari, H.-S., Hobbie, E.A., Iversen, C.M., Jackson, R.B., Leppälammi-Kujansuu, J., Norby, R.J., Phillips, R.P., Pregitzer, K.S., Pritchard, S.G., Rewald, B., and Zadworny, M. (2015) Redefining fine roots improves understanding of below-ground contributions to terrestrial biosphere processes. New Phytologist 207: 505–518.

Nepstad, D.C., de Carvalho, C.R., Davidson, E.A., Jipp, P.H., Lefebvre, P.A., Negreiros, G.H., da Silva, E.D., Stone, T.A., Trumbore, S.E., and Vieira, S. (1994) The role of deep roots in the hydrological and carbon cycles of Amazonian forests and pastures. Nature 372: 666–669.

Ostonen, I., Püttsepp, Ü., Biel, C., Alberton, O., Bakker, M. R., Lõhmus, K., Majdi, H., Metcalfe, D., Olsthoorn, A. F. M., Pronk, A., Vanguelova, E., Weih, M., and Brunner, I. (2007) Specific root length as an indicator of environmental change. Plant Biosystems - An International Journal Dealing with all Aspects of Plant Biology 141(3): 426-442. DOI: 10.1080/11263500701626069

Pierret, A., Doussan, C., Capowiez, Y., Bastardie, F., and Pagès, L. (2007) Root Functional Architecture: A Framework for Modeling the Interplay between Roots and Soil. Vadose Zone Journal 6(2): 269-281.

Pollierer, M.M., Langel, R. Körner, C., Maraun, M., and Scheu, S. (2007) The underestimated importance of belowground carbon input for forest soil animal food webs. Ecology Letters 10: 729–736.

Pregitzer, K. S. (2002) Fine roots of trees – a new perspective. New Phytologist 154: 267-270. doi:10.1046/j.1469-8137.2002.00413_1.x

Pregitzer, K.S. (2008) Tree root architecture – form and function. New Phytologist 180: 562–564.

Pregitzer, K.S., DeForest, J.L., Burton, A.J., Allen, M.F., Ruess, R.W., and Hendrick, R.L. (2002) Fine root architecture of nine North American trees. Ecological Monographs 72: 293–309.

Rasse, D.P., Rumpel, C., and Dignac, M.-F. (2005) Is soil carbon mostly root carbon? Mechanisms for a specific stabilization. Plant and Soil 269: 341-356.

Reich, P.B. (2002) Root-Shoot Relations: Optimality in Acclimation and Adaptation or the "Emperor's New Clothes"? In: Waisel, Y., Eshel, A., and Kafkafi, U. (eds.) Plant Roots: The Hidden Half, 205–220, Dekker, New York.

Rumpel, C., and Kögel-Knabner, I. (2011) Deep soil organic matter—a key but poorly understood component of terrestrial C cycle. Plant and soil 338(1-2): 143-158.

Ryser, P. (2006) The mysterious root length. Plant Soil 286: 1–6.

Schenk, H. J., and Jackson, R. B. (2002) The global biogeography of roots. Ecological Monographs 72: 311–328.

Schenk, H. J., and Jackson, R. B. (2005) Mapping the global distribution of deep roots in relation to climate and soil characteristics. Geoderma 126: 129-140.

Stone, E. L., and Comerford, N. B. (1994) Plant and animal activity below the solum. Proceedings on a Symposium on Whole Regolith Pedology: 57-74.

Stone, E.L., and Kalisz, P.J. (1991) On the maximum extent of tree roots. Forest Ecology and Management 46: 59-102.

Tefs, C., and Gleixner, G. (2012) Importance of root derived carbon for soil organic matter storage in a temperate old-growth beech forest–Evidence from C, N and $^{14}C$ content. Forest Ecology and Management 263: 131-137.

Vogt, K.A., Vogt, D.J., Palmiotto, P.A., Boon, B., O´Hara, J., and Asbjornsen, H. (1996) Review of root dynamics in forest ecosystems grouped by climate, climatic forest type and species. Plant Soil 187: 159-219.

Vogt, K.A., Grier, C.C., Meier, C.E.. and Keyes, M.R. (1983) Organic matter and nutrient dynamics in forest floors of young and mature Abies amabilis stands in western Washington, as suggested by fine root input. Ecol. Monogr. 53: 139–157.

Yanai, R.D., Fahey, T.J., and Miller, S.L. (1995) Efficiency of nutrient acquisition by fine roots and mycorrhizae. In: Smith, W.K., and Hinkley, T.M. (eds.) Resource Physiology of Conifers, 75-103, Academic Press, New York.

Yuan, Z.Y., and Chen, Y.H. (2010) Fine root biomass, production, turnover rates, and nutrient contents in boreal forest ecosystems in relation to species, climate, fertility, and stand age: literature review and meta-analyses. Critical Rev. Plant Sci. 29: 204-221.

# CHAPTER 2

# Material and Methods

## 2.1 Study Sites

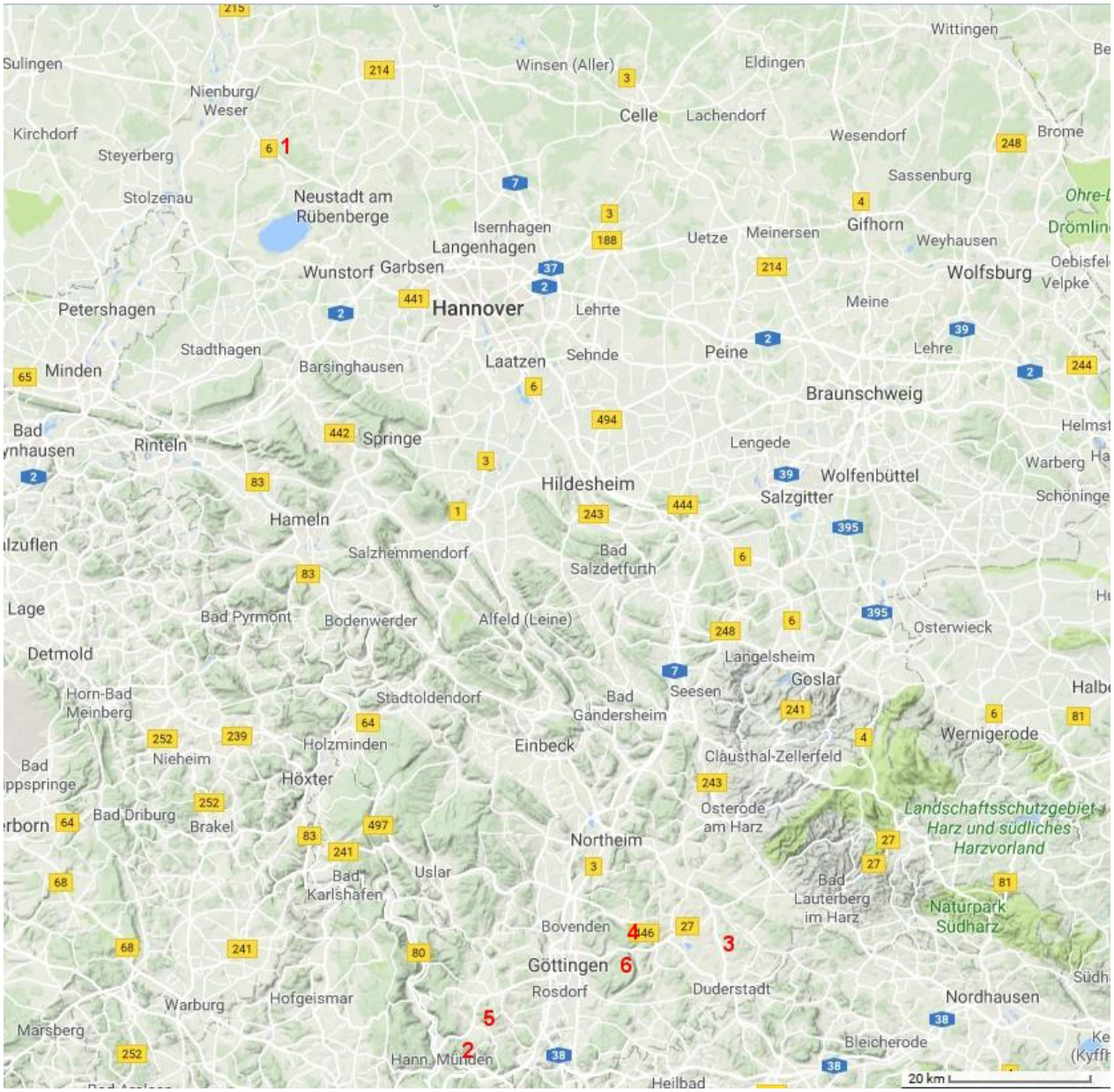


**FIGURE 2.1**: **Map with the locations of the study sites (red numbers) in Lower Saxony** (1: GR; 2: HM; 3: RU; 4: EG; 5: DR; 6: GW) (adapted from Google Maps 2018)

In order to investigate the impact of differential parent materials, nutrient availability, and soil depth on different characteristics of the fine root system of beech as well as on SOM stocks in the top- and subsoil, we selected six study sites (Table 2.1) for the criteria

i) similarity in climatic conditions,

ii) sufficient comparability with regards to forest structural characteristics, and

iii) variability in terms of soil characteristics.

The six study sites are mature European beech forests (*Fagus sylvatica* L.) on different bedrock in Lower Saxony, Germany, covering the whole spectrum of soil types colonized by beech in this region. The Grinderwald site (GR) is located 33 km northwest of Hannover in the Pleistocene lowlands on glacial moraine deposits (Saalian), the other five study sites are located in the vicinity of Goettingen in Hannoversch Muenden (HM), Ruedershausen (RU), Ebergoetzen (EG), Dransfeld (DR) and Goettinger Wald (GW) in the central German uplands on Mesozoic or Tertiary bedrock (Fig. 2.1).

For minimizing additional influences by variation in climatic conditions, all sites are within the cool-temperate climatic zone and feature similar conditions with mean annual precipitation between 709 and 902 mm and mean annual temperature ranging between 7.1 and 8.7 °C (World Clim data base). The stands are either pure beech stands or dominated by *F. sylvatica* L. with admixture of single trees of other species. The cumulative basal area of the stands ranged from 22.8 to 43.2 $m^2$ $ha^{-1}$ with mean dbh varying between 33.1 and 50.2 cm and stem density varying between 111 and 300 $ha^{-1}$. With tree ages between 95 and 166 years, all stands could be qualified as mature. Three sites (GR, HM, RU) are characterized by deep soil profiles (> 200 cm), the soils of the other three sites are comparably shallow (< 80 cm) (EG, DR, GW).

**TABLE 2.1: Locational and soil characteristics of the six study sites grouped into deep and shallow profiles**

| | Deep profiles | | | Shallow profiles | | |
|---|---|---|---|---|---|---|
| Plot no. | 1 | 2 | 3 | 4 | 5 | 6 |
| Site | Grinderwald (GR) | Hann.Muenden (HM) | Ruedershausen (RU) | Ebergoetzen (EG) | Dransfeld (DR) | Goettinger Wald (GW) |
| Substrate type | Pleistocene sand | Tertiary sand | Loess | Sandstone | Basalt | Limestone |
| Location | N Lower Saxony | S Lower Saxony | S Lower Saxony | S Lower Saxony | S Lower Saxony | S Lower Saxony |
| Coordinates | 52° 34' 22.115'' N | 51° 26' 25.64'' N | 51° 34' 51.52'' N | 51° 34' 45.89'' N | 51° 28' 35.60'' N | 51° 32' 43.69'' N |
| | 9° 18' 49.762'' E | 09° 41' 24.25'' E | 10° 14' 43.03'' E | 10° 03' 59.52'' E | 09° 45' 32.46'' E | 10° 02' 34.95'' E |
| Elevation (m a.s.l.) | 106 | 280 | 211 | 295 | 492 | 414 |
| Inclination / Exposition | slight inclined SW | slight inclined O | slight inclined NO | level | slight inclined W | slight inclined NW |
| Mean annual temperature | 8.7 | 8.1 | 8.1 | 7.7 | 7.1 | 7.1 |
| Annual precipitation (mm) | 718 | 761 | 709 | 772 | 902 | 881 |
| Forest community | Luzulo-Fagetum | Luzulo-Fagetum | Galio odorati-Fagetum | Luzulo-Fagetum | Galio odorati-Fagetum | Hordelymo-Fagetum |
| Mean tree height (m) | 26.8 | 35.3 | 32.9 | 36.1 | 29.1 | 26.3 |
| Tree age (years) | 100 | 118 | 95 | 133 | 153 | 166 |
| Mean dbh (cm) | 33.1 | 45.2 | 40.2 | 46.7 | 50.2 | 32.9 |
| Stem density ($ha^{-1}$) | 287 | 144 | 256 | 111 | 133 | 300 |
| Plot basal area ($m^2\ ha^{-1}$) | 27.1 | 24.6 | 37.3 | 22.8 | 43.2 | 29.4 |
| Bedrock | Pleistocene glacio- | Tertiary sand | Quaternary loess | Triassic sandstone | Tertiary basalt | Triassic limestone |
| Soil type [1] | Dystric Cambisol | Dystric Cambisol | Semi-eutric Cambisol | Dystric Cambisol | Eutric Cambisol | Chromic Cambisol |
| Organic layer | Leptomoder | Hemimor | Leptomoder | Leptomoder | Mullmoder | Vermimull |
| Thickness of organic layer | 35 | 44 | 20 | 19 | 37 | 18 |
| Maximum profile depth (cm) | ≥ 200 | ≥ 200 | ≥ 200 | 60-80 | 60-80 | 60-80 |
| Upper subsoil (cm) | 20 - 110 | 20 - 110 | 20 - 110 | 20 - 50 | 20 - 50 | 20 - 50 |
| Lower subsoil (cm) | 110 - 200 | 110 - 200 | 110 - 200 | 50 - 80 | 50 - 80 | 50 - 80 |
| SOC (%) | | | | | | |
| Topsoil (0-20 cm) | 1.15 | 1.60 | 0.99 | 1.40 | 3.60 | 2.50 |
| Upper subsoil | 0.20 | 0.25 | 0.46 | 0.33 | 2.10 | 1.60 |
| Lower subsoil | 0.06 | 0.05 | 0.33 | 0.13 | 1.30 | 1.40 |
| Texture | | | | | | |
| Topsoil (0-20 cm) | Sandy loam | Sandy loam | Silt | Loam | Silt loam | Silt loam |
| Upper subsoil | Loamy sand | Sandy loam | Silt | Silt loam | Silt loam | Silt |
| Lower subsoil | Loamy sand | Sandy loam | Silt | Silt loam | Silt | Silt |
| CEC ($\mu molc\ g^{-1}$) | | | | | | |
| Topsoil (0-20 cm) | 25.1 | 32.6 | 52.8 | 50.9 | 100.1 | 117.8 |
| Upper subsoil | 16.4 | 10.4 | 78.6 | 52.2 | 83.9 | 303.5 |
| Lower subsoil | 14.9 | 12.2 | 98.7 | 84.7 | 175.9 | 204.3 |

## 2.2 Methods

Table 2.2 gives an overview of the sampling designs, the investigated traits and the methods used in this study. More detailed information is given in the 'Materials and Methods' sections in chapters 3, 4, 5, 6, and 7.

**TABLE 2.2: Overview of sampling designs, studies traits, and methods used**

| Chapter No. | Sampling design | Studied traits | Methods |
|---|---|---|---|
| 3 | All six study sites<br>Soil coring method<br>3 soil pits per site, 200 cm depth (or to bedrock depth at EG, DR, GW)<br>Organic layer, 0-10 cm, 10-20 cm, 20-40 cm layers of mineral soil: 6 soil cores (ø 3.5 cm) per pit<br>Soil profile below 40 cm depth: depth intervals of 20 cm, 3 soil cores (ø 12.3 cm, sample volume of ~2.4 L) per soil depth and pit | ***Fine root biomass and necromass*** | Extraction of rootlets > 10 mm length<br>Separation of into live and dead roots, subsequently into fine (≤ 2 mm) and coarse (> 2 mm) roots under the stereo-microscope<br>Criteria for distinction of live and dead roots: periderm colour, tissue elasticity, cohesion of cortex, periderm and stele (Hertel et al. 2013)<br>Root fragments < 10 mm length: estimation of mass of small rootlets using soil depth-specific regression equations relating the mass of dead fine roots < 10 mm length to dead rootlets ≥ 10 mm length; established for every third sample using a method introduced by van Praag et al. (1988) and modified by Hertel (1999)<br>All live and dead root samples were dried at 70° C and weighed. |
| | | ***Fine root morphology*** | |
| | | Specific root length (SRL), specific root area (SRA), mean root diameter (MD) of live fine roots | Scan of the fine root biomass of each sample (EPSON expression 1680, EPSON America Inc.), analysis with use of WinRHIZO 2005c (Régent Instruments Inc., Quebec, Canada) |
| | | Fine root length index (RLI), fine root area index (RAI) | Calculated by multiplying SRL or SRA with the fine root biomass of the respective depth layers and integrating fine root length or surface area over the whole soil profile |
| | | Root tip frequency (RTF) | Determined by counting all turgescent tips of two live fine root strands per sample and relating the number to the respective root dm |

**TABLE 2.2 (continued): Overview of sampling designs, studies traits, and methods used**

| Chapter No. | Sampling design | Studied traits | Methods |
|---|---|---|---|
| 4 | GR site, 3 soil pits, 7 soil depths from 0-20 cm to 160-200 cm<br>Collection of fine-, small- and medium-sized beech root segments of ~ 10 cm length<br>Per soil pit and depth, selection of 6-10 root segments covering all root diameters between 1 and 10 mm, yielding 197 analyzed root segments in total<br>Excavation of 4 complete root strands belonging to 3 different tree individuals located in the organic and topsoil layer; from each strand, 6-10 segments were processed, yielding 42 analyzed segments in total | ***Xylem anatomical traits*** ($A_{xylem,}$ VD, $A_{lumen,}$ $D$, $D_h$)<br>***Derived hydraulic traits*** ($K_p$) | All root samples were stained with safranin; using a sliding microtome, 10-20 mm semi-thin transverse sections were cut. Images of every cross-sectional transverse section were taken with a stereo-microscope equipped with an automatic stage and a digital camera (SteREOV20, Carl Zeiss MicroImaging GmbH, Göttingen, Germany) at 100x magnification.<br>Image analysis with use of Adobe Photoshop CS6 (version 13.0 x 64, Adobe Systems Incorporated, United States) and the particle analysis function from ImageJ (version 1.49 v). |
| | | ***Root age*** | Counting of growth rings |
| 5 | GR site, soil coring method;<br>Grid sampling: transects of 330 cm length, 200 cm depth, regular grid with vertical and horizontal dimensions of 185 cm and 315 cm, respectively;<br>sampling in steps of 45 cm horizontally, in steps of 25 cm vertically at each grid intersection with round steel corer (8.5 cm in diameter, 6 cm height), yielding 64 soil samples per transect<br>resulting in a total of 192 samples for the whole site; | ***Soil properties***<br>SOC, $N_t$<br>$^{13}C/^{12}C$ isotope ratios<br>pH<br>Soil texture | <br>Vario EL analyzer (Elementar, Hanau, Germany)<br>Isotope ratio mass spectrometer (Thermo Fisher Scientific Delta plus, Bremen, Germany)<br>Measured in 0.01 M $CaCl_2$ with a ration of soil to solution of 1:2.5;<br>Laser particle sizer (Analysette 22, Fritsch, Idar-Oberstein, Germany) |
| | | ***Fine root biomass and necromass*** | see above |
| | | ***Microbial biomass C*** | Chloroform fumigation extraction (CFE) method |
| 6 | GR site<br>Grid sampling (see above) | ***Fine root biomass and necromass*** | see above |
| | | ***Soil texture, POM, oPOM*** | Combined density and particle size fractionation |
| | | ***Soil and POM C and N contents*** | EA elemental analyzer (EuroVector, Milan, Italy) |
| | | ***Specific surface area of clay fraction*** | Multi-point BET method (Brunauer et al. 1938) using Autosorb-1 analyzer (Quantachrome, Syosset, NY, USA) |
| | | ***OC chemistry*** (leaf litter, fine roots, OL material, POM, clay fraction) | $^{13}C$ CPMAS NMR spectroscopy (Bruker AvanceIII Spectrometer) |

**TABLE 2.2 (continued): Overview of sampling designs, studies traits, and methods used**

| Chapter No. | Sampling design | Studied traits | Methods |
|---|---|---|---|
| 7 | All six study sites, soil coring method, 3 soil pits per site; soil samples were taken in 10 cm and 85 cm depth at 2 spots per depth increment directly at the stem base and at 135 cm distance to the tree using a round steel corer (8.5 cm in diameter, 6 cm height) | ***Fine root biomass and necromass*** | see above |
| | | ***Microbial biomarkers*** from bulk soil samples (glucosamine, mannosamine, galactosamine, muramic acid) | Measurement using a Trace GC Ultra coupled to and ISQ mass spectrometer (ThermoFisher Scientific, Waltham, USA) after extraction following Zhang and Amelung (1996) and Liang et al. (2012) |
| | | ***Soil texture, POM, oPOM*** | Combined density and particle size fractionation |
| | | ***C and N contents*** of bulk soil and SOM fractions | EA elemental analyzer (EuroVector, Milan, Italy) |
| | | $^{14}$***C contents*** of the clay fraction | Radiocarbon analysis measured on a 6 MV Tandetron AMS (HVE, The Netherlands) |

## 2.3 References

Brunauer, S., Emmett, P.H., and Teller, E. (1938) Adsorption of gases in multimolecular layers. J. Am. Chem. Soc. 60 (2): 309–319.

Google Maps (2018) https://www.google.de/maps. Access date: 13th July, 2018.

Hertel, D. (1999) Das Feinwurzelsystem von Rein-und Mischbeständen der-Rotbuche: Struktur, Dynamik und interspezifische Konkurrenz. Dissertationes Botanicae 317, J. Cramer, Berlin, Stuttgart.

Hertel, D., Strecker, T., Müller-Haubold, H., and Leuschner, C. (2013) Fine root biomass and dynamics in beech forests across a precipitation gradient – is optimal resource partitioning theory applicable to water-limited mature trees? Journal of Ecology 101:1183–1200.

Liang, C., Read, H.W., Balser, T.C. (2012) GC-based detection of aldononitrile acetate derivatized glucosamine and muramic acid for microbial residue determination in soil. Journal of Visualized Experiments e3767. http://dx.doi.org/10.3791/3767.

Van Praag, H.J., Sougnez-Remy, S., Weissen, F., and Carletti, G. (1988) Root turnover in a beech and a spruce stand of the Belgian Ardennes. Plant and soil 105(1):87-103.

Zhang, X., and Amelung, W. (1996) Gas chromatographic determination of muramic acid, glucosamine, mannosamine, and galactosamine in soils. Soil Biology and Biochemistry 28: 1201–1206. http://dx.doi.org/10.1016/0038-0717(96)00117-4.

# CHAPTER 3

# Effects of bedrock type and soil chemistry on the fine root system and fine root morphology of European beech – A study on the belowground plasticity of trees

Kristina KIRFEL, Stefanie HEINZE, Dietrich HERTEL, and Christoph LEUSCHNER

## 3.1 Abstract

We studied the fine root system of *Fagus sylvatica* in six mature stands on different bedrock down to the rock surface (or to 2 m) to investigate whether (1) the stand total of fine root biomass (FRB) increases, while the fine root live:dead ratio decreases, with decreasing soil base richness, (2) specific root area (SRA) and root tip frequency increase with a decrease in base richness, and (3) FRB is related to profile depth. The three beech stands on deep soil (> 2 m profile depth) had on average by 38 % larger FRB totals than the stands on shallow soil (60-80 cm), suggesting that limited root space is an important determinant of fine root system size in *F. sylvatica*. Despite large variation among sites, soil chemistry influenced root morphology only little: fine root diameter depended on soil C/N ratio and root tip frequency on base saturation in a few soil horizons. Much larger morphological differences were found between topsoil and subsoil roots within a profile. We conclude that the fine root system of *F. sylvatica* varies under similar climatic conditions remarkably little between base-poor and base-rich sites, in contrast to the pronounced topsoil-subsoil differences in root morphology and fine root density.

**Keywords:** base saturation, depth distribution, *Fagus sylvatica*, live:dead ratio, profile depth, root system plasticity, root tips, specific root area, subsoil

## 3.2 Introduction

Fine roots (conventionally defined as roots <2 mm in diameter) represent only a few percent of the biomass of a tree, but play a key role in tree ecophysiology and in the biogeochemical cycling of forests (Pregitzer et al. 2002; Yuan and Chen 2010; McCormack et al. 2015). Fine roots are pathways for water and nutrients in upward direction, and for carbon and nutrients in downward direction in the soil. Due to the rapid turnover of the finest rootlets, fine roots have been estimated to consume up to 33% of global net primary production (Jackson, Mooney and Schulze 1997; Gill and Jackson 2000) or a third to more than half of annual canopy carbon gain in mature forests (Keyes and Grier 1981; Fogel and Hunt 1983; Fogel 1985; Vogt et al. 1996; Gill and Jackson 2000; Leuschner and Ellenberg 2017). Dying fine roots and rhizodeposits released by fine roots are an important source of soil organic carbon (Rasse et al. 2005, Comas and Eissenstat 2009). Fine roots feed the net of mycorrhizal fungi with carbohydrates, affect the weathering of minerals, and may have an impact on the activity of microbiota in the rhizosphere and the soil fauna (Schenk and Jackson 2002). Despite its importance, fine root functioning and its response to environmental change are only partly understood. Our knowledge is particularly limited with respect to roots in the subsoil, which is defined by most authors as the profile below 20 or 30 cm depth. Deep roots have been studied much less intensively than topsoil roots, because access is more time-consuming, technically demanding and costly (Gill and Burke 2002; Schenk and Jackson 2002, 2005, Maeght et al. 2013). While fine root abundance in deeper soil layers may be low, their importance for water and nutrient acquisition and for soil development is often greater than their share in root biomass (Stone and Kalisz 1991; Canadell et al. 1996; Lehmann 2003). The same is valid for the C content in subsoils, which is often comparably low, but more than half of the total soil C stocks of terrestrial ecosystems is found in the horizons below the topsoil, emphasizing the need to investigate subsoil properties and deep root systems in greater detail for fully understanding C cycling in forests (Harrison et al. 2011; Koarashi et al. 2012; Harper and Tibett 2013).

One of the least studied aspects of tree root ecology is the plasticity of root systems to variation in soil properties. More than 50 years ago, Bradshaw (1965) specified that “plasticity is shown by a genotype, when its expression is able to be altered by environmental influences”. More recently, Yanai et al. (1995) defined plasticity in root system development as a strategy directed at

optimizing resource uptake from the soil under different environmental conditions. Most soils show considerable small-scale heterogeneity in both vertical and horizontal direction, reflected in gradients in bulk density, soil moisture, soil organic carbon and nutrient concentration, which influence root growth and vitality, but are in part also the result of root activity itself. This has led the scientific community to describe soils as "patchy" environments (Hodge 2006). In vertical direction, not only the mass of fine, coarse and large roots per soil volume changes dramatically in response to vertical gradients in soil chemistry and physics, but the morphology and functioning of fine roots may change as well in order to optimize the acquisition of essential nutrients (Forde and Lorenzo 2001; Ostonen et al. 2007). Temporal variation in resource availability is also large in most soils. Great variation in soil properties is further encountered when different soil types along a gradient from acidic, base-poor to neutral or alkaline, base-rich soils are colonized by the same tree species. For example, European beech (*Fagus sylvatica* L.) forms in Central Europe productive stands on a great variety of bedrock and soil types, which range from sandy infertile Pleistocene soils such as dystric Cambisols with very low cation exchange capacity and base saturation to fertile eutric Cambisols or Luvisols with high base saturation, and Leptosols on limestone rich in calcium carbonate. Wood biomass and yield data from managed forests suggest that the large variation in soil chemical properties tolerated by beech imprints remarkably little on the aboveground productivity and the canopy structure of this species, as long as water availability is not limiting (Leuschner and Ellenberg 2017). It is not clear whether the belowground response of *F. sylvatica* to this variation in soil chemistry is governed by greater morphological and functional plasticity than is the aboveground response. A few studies in mature forests along soil pH, temperature and precipitation gradients indicate that temperate tree species may modify their root system structure and size considerably (e.g. Leuschner and Hertel 2003; Finér et al. 2007; Hertel et al. 2013), suggesting particularly high plasticity in the root system.

Plants may respond to resource heterogeneity with root proliferation into soil patches, where water and/or nutrients are available (Hodge 2004). The response can include physiological and root morphological adjustments in order to optimize resource capture (Fitter 1994; Forde and Lorenzo 2001; Pregitzer et al. 2002, Ostonen et al. 2007; Comas and Eissenstat 2009). Many reactions in the root system appear to be highly species-specific (Campbell et al. 1991; Farley and

Fitter 1999; Finér et al. 2007; Hartmann and von Wilpert 2014), seem to be specific to certain nutrients (Hendrick and Pregitzer 1997; Forde and Lorenzo 2001; Neatrour et al. 2005) and to depend on overall site fertility, relating to the plant's demand for specific nutrients (Forde and Lorenzo 2001; Hodge 2004). Root development is governed by a combination of endogenous (genetic constitution, hormonal regulation, carbohydrate supply, Santner et al. 2009) and exogenous factors (climate, soil moisture, nutrient availability, rhizosphere chemistry, interacting soil fungi and procaryotes (Leuschner and Hertel 2003; Hodge 2006; Pierret et al. 2007; Maeght et al. 2013, Hartmann and Von Wilpert 2014)), which are difficult to disentangle and poorly understood (Pregitzer et al. 2002).

As our knowledge about changes in the fine root biomass and root system structure of mature trees in dependence on environmental conditions is still rudimentary, particularly with respect to subsoil roots, we conducted a comparative study on the fine root system of mature F. sylvatica stands to 2 m soil depth along an extended soil chemical gradient. By selecting beech stands of similar age and stand structure growing under similar climate, we were able to examine relationships between soil chemical properties and soil depth, and stand fine root biomass, fine root depth distribution and fine root morphology of a single tree species, while largely controlling for tree species, stand structure and climate effects. Caused by large variation in bedrock type and also profile depth, the availability of plant nutrient macro-elements (N, P, Ca, K, Mg) varies greatly across this gradient. Assuming that the fine root system of beech responds to this variation in edaphic conditions with modifications in total fine root biomass, root distribution and root morphology in order to maximize resource uptake, we formulated six guiding hypotheses: (i) The stand total of fine root biomass increases with increasing soil acidity and decreasing base saturation, (ii) fine root biomass density shows a steeper decrease from topsoil to subsoil in more acidic soil profiles, (iii) the stand total of fine root biomass is smaller in shallow soil profiles with low bedrock depth, irrespective of soil acidity, (iv) the live:dead ratio of fine root mass decreases with increasing soil acidity, while fine root necromass increases, (v) fine roots in acidic soils have a higher specific root length and area and smaller mean root diameter in order to increase uptake efficiency under nutrient-deficient conditions, and (vi) the frequency of fine root tips and root tip abundance per soil volume increase with increasing soil acidity.

**TABLE 3.1: Topographic, climatologic and stand structural characteristics of the six studied mature beech forests on different bedrock type in northern Germany. The sites are arranged from left to right in a sequence of increasing base richness of the soil, with the plots # 1-3 representing deep profiles (>2 m profile depth), while the profiles # 4-6 are shallow profiles (<0.8 m depth).**

| | Deep profiles | | | Shallow profiles | | |
|---|---|---|---|---|---|---|
| Plot no. | 1 | 2 | 3 | 4 | 5 | 6 |
| Site | Grinderwald (GR) | Hann.Muenden (HM) | Ruedershausen (RU) | Ebergoetzen (EG) | Dransfeld (DR) | Goettinger Wald (GW) |
| Substrate type | Pleistocene sand | Tertiary sand | Loess | Sandstone | Basalt | Limestone |
| Location | N Lower Saxony | S Lower Saxony | S Lower Saxony | S Lower Saxony | S Lower Saxony | S Lower Saxony |
| Coordinates | 52° 34' 22.115'' N | 51° 26' 25.64'' N | 51° 34' 51.52'' N | 51° 34' 45.89'' N | 51° 28' 35.60'' N | 51° 32' 43.69'' N |
| | 9° 18' 49.762'' E | 09° 41' 24.25'' E | 10° 14' 43.03'' E | 10° 03' 59.52'' E | 09° 45' 32.46'' E | 10° 02' 34.95'' E |
| Elevation (m a.s.l.) | 106 | 280 | 211 | 295 | 492 | 414 |
| Inclination / Exposition | slight inclined SW | slight inclined O | slight inclined NO | level | slight inclined W | slight inclined NW |
| Mean annual temperature | 8.7 | 8.1 | 8.1 | 7.7 | 7.1 | 7.1 |
| Annual precipitation (mm) | 718 | 761 | 709 | 772 | 902 | 881 |
| Forest community | Luzulo-Fagetum | Luzulo-Fagetum | Galio odorati-Fagetum | Luzulo-Fagetum | Galio odorati-Fagetum | Hordelymo-Fagetum |
| Mean tree height (m) | 26.8 | 35.3 | 32.9 | 36.1 | 29.1 | 26.3 |
| Tree age (years) | 100 | 118 | 95 | 133 | 153 | 166 |
| Mean dbh (cm) | 33.1 | 45.2 | 40.2 | 46.7 | 50.2 | 32.9 |
| Stem density ($ha^{-1}$) | 287 | 144 | 256 | 111 | 133 | 300 |
| Plot basal area ($m^2$ $ha^{-1}$) | 27.1 | 24.6 | 37.3 | 22.8 | 43.2 | 29.4 |

**TABLE 3.2: Soil characteristics of the six beech forests on different bedrock type. 'Upper subsoil' stands for 20-110 cm soil depth at the GR, RU and HM sites with deep profiles, and 20-50 cm depth in the shallow profiles of the EG, DR and GW sites. 'Lower subsoil' stands for 110-200 cm soil depth at the GR, RU and HM sites, and 50-80 cm depth at the EG, DR and GW sites.**

| | Deep profiles | | | Shallow profiles | | |
|---|---|---|---|---|---|---|
| Plot no. | 1 | 2 | 3 | 4 | 5 | 6 |
| Site | Grinderwald (GR) | Hann. Muenden (HM) | Ruedershausen (RU) | Ebergoetzen (EG) | Dransfeld (DR) | Goettinger Wald (GW) |
| Bedrock | Pleistocene glacio-fluviatile deposits (Saale) | Tertiary sand | Quaternary loess | Triassic sandstone | Tertiary basalt | Triassic limestone |
| Soil type [1] | Dystric Cambisol | Dystric Cambisol | Semi-eutric Cambisol | Dystric Cambisol | Eutric Cambisol | Chromic Cambisol |
| Organic layer | Leptomoder | Hemimor | Leptomoder | Leptomoder | Mullmoder | Vermimull |
| Thickness of organic layer (mm) | 35 | 44 | 20 | 19 | 37 | 18 |
| Maximum profile depth (cm) | ≥ 200 | ≥ 200 | ≥ 200 | 60-80 | 60-80 | 60-80 |
| Upper subsoil (cm) | 20 - 110 | 20 - 110 | 20 - 110 | 20 - 50 | 20 - 50 | 20 - 50 |
| Lower subsoil (cm) | 110 - 200 | 110 - 200 | 110 - 200 | 50 - 80 | 50 - 80 | 50 - 80 |
| SOC (%) | | | | | | |
| Topsoil (0-20 cm) | 1.15 | 1.60 | 0.99 | 1.40 | 3.60 | 2.50 |
| Upper subsoil | 0.20 | 0.25 | 0.46 | 0.33 | 2.10 | 1.60 |
| Lower subsoil | 0.06 | 0.05 | 0.33 | 0.13 | 1.30 | 1.40 |
| C/N | | | | | | |
| Topsoil (0-20 cm) | 26.3 | 20.8 | 12.8 | 17.4 | 14.1 | 13.6 |
| Upper subsoil | 14.3 | 12.3 | 8.2 | 10.7 | 13.2 | 11.4 |
| Lower subsoil | 13.1 | 8.9 | 5.7 | 5.4 | 15.0 | 11.6 |
| pH ($CaCl_2$) | | | | | | |
| Topsoil (0-20 cm) | 3.5 | 3.7 | 3.6 | 4.0 | 3.7 | 4.3 |
| Upper subsoil | 4.1 | 4.1 | 3.7 | 3.9 | 4.1 | 5.5 |
| Lower subsoil | 4.0 | 3.9 | 4.0 | 3.8 | 4.8 | 6.6 |
| Texture [1] | | | | | | |
| Topsoil (0-20 cm) | Sandy loam | Sandy loam | Silt | Loam | Silt loam | Silt loam |
| Upper subsoil | Loamy sand | Sandy loam | Silt | Silt loam | Silt loam | Silt |
| Lower subsoil | Loamy sand | Sandy loam | Silt | Silt loam | Silt | Silt |
| Bulk density (g $cm^{-3}$) | | | | | | |
| Topsoil (0-20 cm) | 1.2 | 1.2 | 1.1 | 1.1 | n.a | 1.2 |
| Upper subsoil | 1.5 | 1.4 | 1.4 | 1.5 | n.a | 1.4 |
| Lower subsoil | 1.5 | 1.4 | 1.5 | 1.2 | n.a | 1.3 |
| Cation exchange capacity | | | | | | |
| (µmolc $g^{-1}$) | (mmolc $g^{-1}$) | | | | | |
| Topsoil (0-20 cm) | 25.1 | 32.6 | 52.8 | 50.9 | 100.1 | 117.8 |
| Upper subsoil | 16.4 | 10.4 | 78.6 | 52.2 | 83.9 | 303.5 |
| Lower subsoil | 14.9 | 12.2 | 98.7 | 84.7 | 175.9 | 204.3 |
| Base saturation (%) | | | | | | |
| Topsoil (0-20 cm) | 9.0 | 4.8 | 16.3 | 26.8 | 14.2 | 57.4 |
| Upper subsoil | 6.3 | 9.3 | 39.4 | 24.5 | 51.0 | 99.8 |
| Lower subsoil | 6.2 | 10.7 | 99.5 | 22.7 | 97.5 | 96.5 |

## 3.3 Material and Methods

### *Study sites*

The study was conducted in six mature European beech forests on different bedrock in Lower Saxony, Germany, covering the whole spectrum of soil types colonized by beech in this region. Five study sites (HM, RU, EG, DR, GW) are located in the central German uplands on Mesozoic or Tertiary bedrock in the surroundings of Goettingen, one site (GR) is situated 33 km northwest of Hannover in the Pleistocene lowlands on glacial moraine deposits (Saalian). The climate of the study region is cool-temperate with mean annual temperature ranging between 7.1 and 8.7 °C, and mean annual precipitation between 709 and 902 mm (World Clim data base). The stands are either pure beech stands or dominated by F. sylvatica with admixture of single trees of other species and sufficiently comparable in terms of forest structure (26–36 m in height, 111–300 stems $ha^{-1}$) and age (95-166 years) (Table 3.1). Three sites are characterized by deep soil profiles (> 2 m), which developed from Pleistocene fluvial and aeolian sandy deposits (GR), Tertiary sand (HM), or Quaternary loess (RU). The soils of the other three sites developed from Triassic sandstone (EG), Tertiary basalt (DR) or Triassic limestone (GW), and are comparatively shallow with a maximum profile depth of 60-80 cm. Due to the largely different bedrock types, the soils differ widely in their chemical and physical properties, in particularly in terms of soil texture, cation exchange capacity and base saturation (Table 3.2).

### *Soil sampling and analyses*

Soil sampling was conducted in June 2013 (GR) and May 2014 (HM, RU, EG, DR, GW) along three randomly distributed transects per site with a minimal distance of 10 m from each other, each aligned towards a main tree. The transects of 330 cm length were excavated to a maximum depth of 200 cm (or to a maximum depth of 80 cm at the shallow sites EG, DR and GW). Samples were taken in a regular grid with vertical and horizontal dimensions of 185 and 315 cm, respectively (Angst et al., 2016). The regular grid started close (10–50 cm) to a main tree (*Fagus sylvatica* L.) and extended horizontally in steps of 45 cm and downwards in 25 cm-steps. Soil samples were taken at each grid intersection with a circular steel core sampler (diameter: 8.5 cm, height: 6 cm) at 0, 45, 90, 135, 180, 225, 270, 315 cm horizontal distance and 10, 35, and 60 cm

depth at all sites, and additionally at 85, 110, 135, 160, and 185 cm depth at the sites GR, HM and RU. Thus, a total of 24 (EG, DR, GW) or 64 (GR, HM, RU) soil samples were taken in each transect, resulting in a total of 72 or 192 samples per site. Immediately after sampling, the fresh soil samples were sieved (< 2 mm) to remove stones and roots. The soil samples were stored after sieving in polyethylene bags at 4 °C.

For the analysis of soil organic carbon and total nitrogen, the soil samples were prepared through drying for 3 d at 50 °C and grinding by a planet micromill (Fritsch Pulverisette 7). Total C and N contents were determined by gas chromatography (Vario EL elemental analyzer, Elementar, Hanau, Germany).

The pH of the fresh soil samples was measured in a 0.01 M $CaCl_2$ solution (ratio soil to liquid: 1:2.5). Since all samples were free of carbonate, all C referred to organic C. For the analysis of soil texture, soil samples with a SOC content >1.2 % were pretreated with $H_2O_2$ to oxidize the organic matter. Soil texture was analyzed with a particle sizer (Analysette 22, Fritsch, Idar-Oberstein, Germany); the samples were separated into two size fractions (>0.2 and < 0.2 mm) with a 0.2 mm sieve, and each fraction was measured separately to increase the accuracy of the measurement. The base saturation and cation exchange capacity (CEC) of the samples were determined through ICP analysis after $BaCl_2$ percolation.

***Root sampling and fine root system analysis***

We used the soil coring method to study beech fine root density (in g d.m. $m^{-3}$ soil volume) and abundance (in g $m^{-2}$ ground area per soil layer) in the top- and subsoil of profiles dug to 2 m depth, or to the surface of the bedrock. In each forest, a plot of ca. 30 x 30 m was demarcated, and each three subplots of ca. 25 m² size were placed by random in the direct neighborhood of the stems of a mature beech tree. Each six samples from the forest floor and the upper mineral soil layer were extracted at random locations using a soil corer of 3.5 cm in diameter; the extracted soil cores were sliced into the organic layer, and the 0-10 cm, 10-20 cm and 20-40 cm layers of the mineral soil. For every sample, the thickness of the organic layer (consisting of the L, Of, Oh layers) was measured at the undisturbed wall left after the extraction of the soil core. Samples of the lower profile (≥ 40 cm depth) were taken in each one soil pit of 1.35 m length per

subplot (i.e. three per study site) that was dug with an excavator to 2 m depth (or to bedrock depth at the sites EG, DR and GW). Using a steel cylinder of 12.3 cm in diameter, each three soil samples were taken from the three walls of a pit at depth intervals of 20 cm, corresponding to a sample volume of ~ 2.4 L. Each sample was taken right under the sample of the next higher depth. In total, nine samples (three per soil pit, three pits) were extracted per soil depth and site, resulting in a total soil volume of ca. 22 L that was analyzed per depth layer. All samples were transferred to plastic bags and stored at 4 °C until being processed in the laboratory.

In the laboratory, the samples were gently washed over sieves of 0.25 mm mesh size to separate the roots from adhering soil particles. We soaked the sample remains in demineralized water and extracted all roots greater 10 mm length with tweezers for further examination; smaller root fractions were neglected in two out of three samples to keep the workload reasonable. Under the stereo-microscope, the larger rootlets >10 mm length were separated into live (biomass) and dead (necromass) roots, and subsequently into fine (≤2 mm in diameter) and coarse roots (> 2 mm in diameter). The distinction of live and dead roots was done based on the criteria root and periderm color, tissue elasticity, and cohesion of cortex, periderm and stele (Hertel et al. 2013). Even though the small root fragments < 10 mm in length were neglected, the procedure has been found to be suitable to collect the largest part of fine root biomass (> 95%) (Bauhus and Bartsch 1996; Leuschner et al. 2001). Fine root necromass, however, is considerably underestimated by the neglect of root fragments < 10 mm length. We used soil depth-specific regression equations to correct this error by extrapolating the necromass from precisely analyzed samples to those samples that were only partly analyzed. The regressions relate the mass of dead fine roots < 10 mm in length to the necromass particles ≥ 10 mm in length, established separately for every third sample. In these precisely investigated samples, the mass of small dead roots was quantified with a method introduced by van Praag et al. (1988) and modified by Hertel (1999). After the extraction of the large rootlets, the sample residue was evenly spread on a filter paper (730 $cm^2$), which was divided into 36 even-sized small quadrats. Six of the quadrats were randomly selected and even the finest necromass particles collected under the microscope. All live and dead root samples were dried at 70°C for 48 h and weighed.

### *Analysis of fine root morphology*

For determining specific root length (SRL, in cm g d.m.$^{-1}$), specific root surface area (SRA, in cm² g d.m.$^{-1}$), and the mean root diameter (MD, in mm) of the live fine root fraction < 2 mm, the fine roots of each sample were scanned (EPSON expression 1680, EPSON America Inc.) and analyzed using the WinRHIZO 2005c image analysis software (Régent Instruments Inc., Quebec, Canada). Fine root length index (RLI, in m root length m$^{-2}$ ground area) and fine root area index (RAI, in m$^2$ root area m$^{-2}$ ground area) were calculated by multiplying SRL or SRA with the fine root biomass of the respective depth layers and integrating fine root length or surface area over the whole soil profile. Root tip frequency (RTF, in n mg$^{-1}$ root d.m.) was determined by counting all turgescent tips of two live fine root strands per sample and relating the number to the respective root dry mass; root tip abundance (RTA, n m$^{-2}$ ground area) was calculated by multiplying RTA with the fine root biomass of the respective soil layer, root tip density (RTD, n L$^{-1}$) by relating to soil volume.

### *Statistical analyses*

Means and standard errors were calculated by averaging over the each three soil pits of a study site, while the each three samples taken in the same depth of a pit were treated as pseudo-replicates by averaging over them.

We used the SAS package, version 9.3 (Statistical Analyses System, SAS Institute Inc., Cary, NC, USA) for statistical analysis. A non-parametric Mann-Whitney (Wilcoxon) two-sample test was used to determine significant differences between the different soil layers at a site, and difference between the six sites for a given soil layer. Significance was determined at $P \leq 0.05$ throughout. Multivariate regression analyses were performed to analyze the influence of soil characteristics on fine root biomass, and of fine root biomass and soil characteristics on fine root morphological traits. We used the backward elimination procedure at the significance level $P \leq 0.05$. Vertical root mass distribution was modeled as $y = 1-\beta d$, where y is the cumulative root fraction from the soil surface to depth d and β is the extinction coefficient (Gale and Grigal 1987; Jackson et al. 1996). High β values correspond to a larger proportion of root mass in greater soil depth. We applied a Pearson correlation analysis to search for relationships between root

morphological traits and measures of fine root system size and structure, and edaphic and stand structural parameters. We conducted a Principal Components Analysis (PCA) to analyze relationships between fine root biomass, root morphological traits and soil properties (for a list of matrix factors see Table 3.7). The PCA was conducted with the package CANOCO, version 4.5 (Biometris, Wageningen, The Netherlands).

## 3.4 Results

### *Soil characteristics*

The six study sites represent a broad spectrum of bedrock types from silicate-poor Pleistocene sandy deposits and Triassic sandstone to volcanic basalt and Triassic limestone, which is most clearly mirrored in the base saturation of the subsoil (6 to 100 %) (Table 3.2). The base richness gradient in the topsoil (5-57 %) was less pronounced due to acidification, which was visible even at the limestone site. Soil texture varied from loamy sand (site GR) to silt (GW and RU sites), which is reflected in mass-specific cation exchange capacities that varied from around 10 µmolc $g^{-1}$ in the sandy substrates (GR, HM) to >200 µmolc $g^{-1}$ at the limestone site (GW). A much higher soil carbon content at the basalt and limestone sites (2.5-3.6 % vs. 1.0-1.6 % at the other sites) contributed to the CEC at the GW and DR sites, while the highest C/N ratios were observed at the GR site on Pleistocene sand (>25 in the topsoil); yet, no clear trend in C/N from base-poor to base-rich sites was observed. This was also true for topsoil pH ($CaCl_2$), which ranged between 3.5 and 4.3 at all six sites. Near-neutral pH values were found only at the limestone site in the subsoil (pH 6.6). All soil profiles were classified as Cambisols in different sub-types, ranging from dystric to chromic to eutric Cambisols. The profiles on sand, sandstone and loess had Leptomoders or Hemimors as humus forms, while the biologically more active forms Mullmoder and Vermimull were found on basalt and limestone with higher base saturation in the mineral soil. Relatively thick organic layers (>35 mm) occurred on sand and basalt, thinner layers (<20 mm) on loess, sandstone and limestone.

***Fine root biomass totals and vertical root distribution***

The profile totals of fine root biomass tended to be higher at the three sites with deep profiles (GR, HM, RU: 532-563 g $m^{-2}$) than at the shallow sites (EG, DR, GW: 308-390 g $m^{-2}$), but a significant difference existed only to the HM site on Tertiary sand (Table 3.3). Yet, the topsoil fine root biomass (0-20 cm of mineral soil plus organic layer) was on average not higher in the profiles on shallow soil than in the deeper profiles. As a consequence, half of the fine root biomass of the profiles at the shallow sites was located in the uppermost 12 to 21 cm, while half-biomass depth was reached only at 23 to 47 cm in the three deeper profiles (Table S3.2 in the Supplement). Only on Pleistocene sand (GR site), a significant proportion of the fine root biomass (67 g $m^{-2}$, i.e. 13 % of the profile total) was contained in the organic layer, while this fraction amounted to only 9-16 g $m^{-2}$ (less than 5 %) at the other five sites. The β coefficient, which characterizes the decrease in fine root biomass density with soil depth, was thus greater in the deeper profiles (0.971-0.982) than in the more shallow ones (0.948-0.964); however, the difference was not significant. In the three deep profiles, the bulk of fine root biomass (roughly 50 %) was located in the upper subsoil (20-110 cm), while it was the topsoil that contained most of the fine root biomass in the three shallow profiles (50-65 %) (Table 3.3). At all six sites, fine root density (mass per soil volume) reached its maximum in the organic layer and mineral topsoil (0-10 cm) with values between 0.5 and 1.5 g $L^{-1}$. At five of the six sites, density decreased to 0.2-0.4 g $L^{-1}$ at 60-80 cm and to <0.1 g $L^{-1}$ below 100 cm. The loess site RU was an exception with a markedly higher fine root density in the upper and lower subsoil (Fig. 1). Most profiles showed a secondary fine root density peak at 40-60 cm, the RU site also at 80-100 cm, where a clay layer existed.

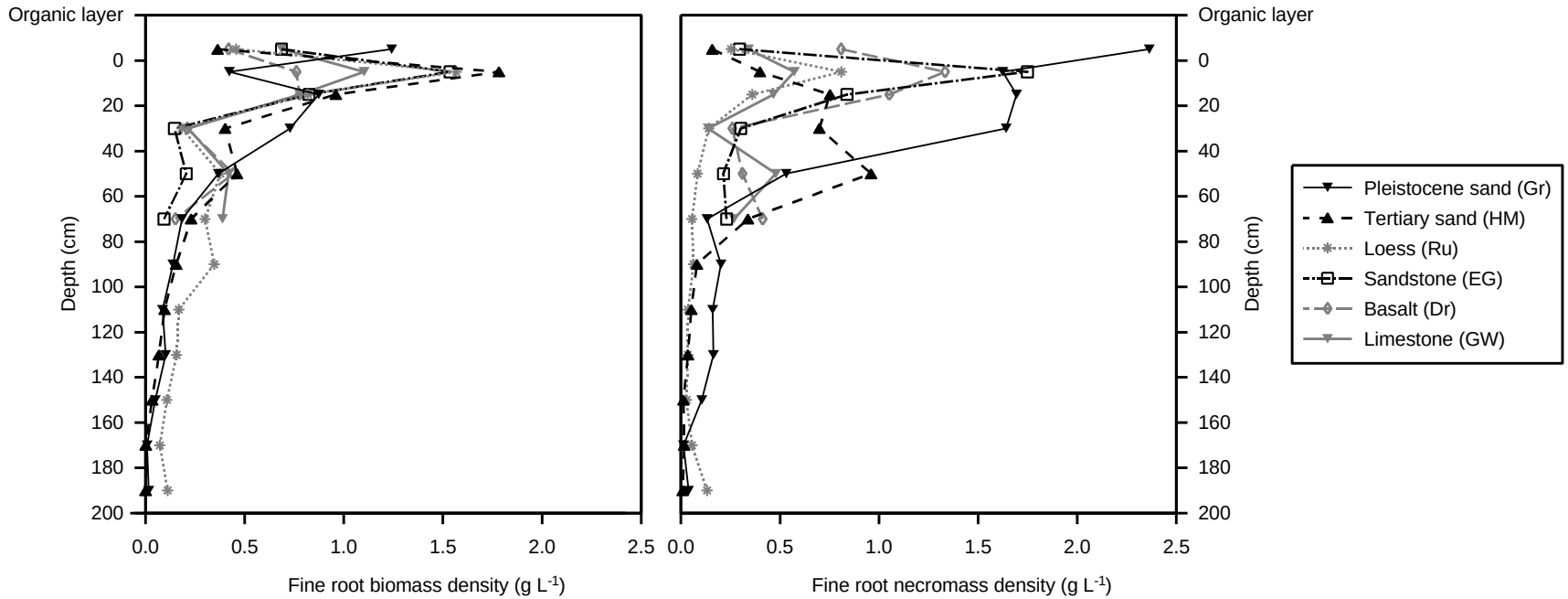


**FIGURE 3.1: Fine root biomass (left) and necromass (right) density (g $L^{-1}$) in the soil profiles of the six investigated mature beech forest stands. Values are means of three soil pits per field site.**

With profile totals of 559-708 g $m^{-2}$, fine root necromass was highest at the two sites on sand (GR: Pleistocene sand, HW: Tertiary sand) and significantly higher than at the four other sites (220-413 g $m^{-2}$; Table 3.3). Lowest necromass totals (~ a third of the values on sand) were recorded on limestone and loess (220 and 249 g $m^{-2}$). We found 5- to 10 times higher necromass densities in the organic layer and mineral topsoil (> 1.5 g $L^{-1}$) of the GR (Pleistocene sand) and EG (sandstone) sites than at the limestone (GW) and loess sites (RU) (Fig. 3.1). The decrease in fine root necromass density with soil depth resembled that of fine root biomass density (Fig. 3.1), as is reflected in similar β coefficients (Table 3.3). However, the Tertiary sand (HM) site deviated from this pattern with a necromass density peak at 40-60 cm, and not close to the surface. The fine root mass live:dead ratio varied between 0.73 and 2.12 (profile means) at the six sites with highest ratios at the loess and limestone sites (RU and GW: 2.12 and 1.56) and lowest at the Pleistocene sand and basalt sites (0.73 and 0.77) (Table 3.3). Three of the sites (HM, EG, GW) had particularly high live:dead ratios in the organic layer (up to 4.5), but an overall trend of decreasing live:dead ratios with increasing soil depth was not detected. With particularly low live-dead ratios occurring on sand and basalt, no clear relation between live:dead ratio and soil base saturation was visible.

**TABLE 3.3: Fine root biomass and necromass, and fine root live:dead ratio in the organic layer, mineral topsoil (0-20 cm), upper subsoil, and lower subsoil of the six investigated mature beech forests. 'Upper subsoil' stands for 20-110 cm soil depth at the GR, RU and HM sites with deep profiles, and 20-50 cm depth in the shallow profiles of the EG, DR and GW sites. 'Lower subsoil' stands for 110-200 cm soil depth at the GR, RU and HM sites, and 50-80 cm depth at the EG, DR and GW sites. Also given are ß-values, which characterize the depth distribution of root mass according to the expression: cumulative root mass y = 1-βd. Shown are means + SE of three soil pits per site. Different small letters indicate significant differences (P<0.05) between the stands, capital letters significant differences between the soil horizons.**

| | Deep profiles | | | | | | | | | Shallow profiles | | | | | | | | |
|---|---|---|---|---|---|---|---|---|---|---|---|---|---|---|---|---|---|---|
| Plot no. | 1 | | | 2 | | | 3 | | | 4 | | | 5 | | | 6 | | |
| Site code | GR | | | HM | | | RU | | | EG | | | DR | | | GW | | |
| Substrate type | Pleistocene sand | | | Tertiary sand | | | Loess | | | Sandstone | | | Basalt | | | Limestone | | |
| | **Fine root biomass (g m$^{-2}$)** | | | | | | | | | | | | | | | | | |
| Organic layer | 66.98 | aA | ± 18.15 | 8.96 | bB | ± 3.63 | 8.59 | bA | ± 2.07 | 13.08 | bB | ± 2.30 | 13.19 | bB | ± 6.19 | 15.76 | bC | ± 4.71 |
| Topsoil (0-20 cm) | 129.62 | abA | ± 44.55 | 267.44 | aA | ± 27.16 | 178.67 | abA | ± 44.21 | 251.52 | abA | ± 43.71 | 153.80 | bA | ± 22.57 | 188.02 | abA | ± 20.05 |
| Upper subsoil | 292.09 | aA | ± 89.65 | 256.54 | aA | ± 14.40 | 257.98 | aA | ± 100.45 | 71.31 | bB | ± 11.27 | 86.36 | bAB | ± 12.47 | 83.82 | bB | ± 6.88 |
| Lower subsoil | 43.51 | bcA | ± 22.14 | 30.04 | cB | ± 8.55 | 106.39 | bcA | ± 55.31 | 53.70 | bcB | ± 16.93 | 74.36 | bB | ± 13.26 | 119.53 | aB | ± 10.14 |
| Profile total | 532.21 | ab | ± 155.79 | 562.98 | a | ± 13.87 | 551.63 | ab | ± 177.63 | 389.61 | b | ± 43.07 | 307.60 | b | ± 37.49 | 327.46 | b | ± 42.55 |
| | **Fine root necromass (g m$^{-2}$)** | | | | | | | | | | | | | | | | | |
| Organic layer | 141.80 | aAB | ± 34.53 | 3.27 | bB | ± 2.02 | 6.13 | bB | ± 1.41 | 4.81 | bC | ± 0.47 | 21.53 | bC | ± 9.48 | 7.01 | bC | ± 3.49 |
| Topsoil (0-20 cm) | 199.02 | bAB | ± 5.94 | 115.16 | cB | ± 16.01 | 116.97 | cA | ± 33.55 | 258.74 | aA | ± 13.66 | 238.57 | aA | ± 13.05 | 103.93 | cA | ± 8.49 |
| Upper subsoil | 287.60 | bA | ± 55.58 | 420.71 | aA | ± 61.28 | 72.05 | cAB | ± 12.57 | 81.70 | cB | ± 6.50 | 82.95 | cB | ± 7.39 | 75.41 | cB | ± 4.45 |
| Lower subsoil | 79.94 | abcB | ± 34.58 | 19.84 | dB | ± 5.96 | 53.54 | cAB | ± 4.37 | 67.41 | cB | ± 5.52 | 113.47 | abA | ± 1.38 | 101.30 | bAB | ± 3.93 |
| Profile total | 708.35 | a | ± 69.23 | 558.98 | ab | ± 72.68 | 248.69 | c | ± 51.62 | 412.67 | b | ± 9.59 | 401.61 | b | ± 24.07 | 220.11 | c | ± 50.59 |
| | **Fine root live : dead ratio** | | | | | | | | | | | | | | | | | |
| Organic layer | 0.46 | bB | ± 0.05 | 4.54 | aA | ± 2.30 | 1.43 | aB | ± 0.18 | 2.81 | aA | ± 0.61 | 0.51 | bA | ± 0.16 | 2.86 | aA | ± 0.71 |
| Topsoil (0-20 cm) | 0.64 | bAB | ± 0.20 | 2.35 | aA | ± 0.12 | 1.64 | aAB | ± 0.48 | 0.97 | abB | ± 0.17 | 0.66 | bA | ± 0.12 | 1.84 | aA | ± 0.26 |
| Upper subsoil | 1.02 | bcA | ± 0.26 | 0.64 | cB | ± 0.11 | 3.34 | aA | ± 0.70 | 0.91 | bcB | ± 0.22 | 1.06 | bcA | ± 0.17 | 1.11 | bB | ± 0.06 |
| Lower subsoil | 0.42 | bB | ± 0.16 | 1.68 | aA | ± 0.55 | 1.85 | aAB | ± 0.83 | 0.84 | abB | ± 0.29 | 0.66 | bA | ± 0.12 | 1.18 | aB | ± 0.05 |
| Profile total | 0.73 | a | ± 0.14 | 1.04 | ab | ± 0.12 | 2.12 | c | ± 0.25 | 0.94 | a | ± 0.09 | 0.77 | a | ± 0.09 | 1.56 | bc | ± 0.16 |
| | **Fine root biomass** | | | | | | | | | | | | | | | | | |
| ß-value | 0.975 | a | ± 0.002 | 0.971 | a | ± 0.004 | 0.982 | a | ± 0.005 | 0.948 | a | ± 0.008 | 0.964 | a | ± 0.005 | 0.950 | a | ± 0.012 |
| | **Fine root necromass** | | | | | | | | | | | | | | | | | |
| ß-value | 0.974 | a | ± 0.003 | 0.979 | a | ± 0.001 | 0.984 | a | ± 0.002 | 0.953 | a | ± 0.005 | 0.953 | a | ± 0.007 | 0.957 | a | ± 0.015 |

**TABLE 3.4: N content, specific root length (SRL), specific root area (SRA), root tip frequency (tips per root mass), tip abundance (tips per ground area), of living fine roots in the organic layer, topsoil, upper subsoil, and lower subsoil of the six investigated mature beech forest stands. Upper subsoil: 20-110 cm soil depth in GR, RU, HM, 20-50 cm soil depth in EG, DR, GW, lower subsoil: 110-200 cm soil depth in GR, RU, HM, 50-80 cm soil depth in EG, DR, GW. Shown are means + SE of three soil pits per field site. Different small letters indicate significant differences (P<0.05) between the stands, capital letters significant differences between the soil horizons.**

| | Deep profiles | | | | | | Shallow profiles | | | | | | | | |
|---|---|---|---|---|---|---|---|---|---|---|---|---|---|---|---|
| Plot no. | 1 | | | 2 | | | 3 | | | 4 | | | 5 | | | 6 | | |
| Site code | GR | | | HM | | | RU | | | EG | | | DR | | | GW | | |
| Substrate type | Pleistocene sand | | | Tertiary sand | | | Loess | | | Sandstone | | | Basalt | | | Limestone | | |
| | **N content (%)** | | | | | | | | | | | | | | | | | |
| Organic layer | 1.35 | bB | ± 0.06 | 1.54 | abA | ± 0.12 | 1.78 | abA | ± 0.22 | 1.43 | bA | ± 0.01 | 1.51 | abA | ± 0.17 | 1.48 | abA | ± 0.20 |
| Topsoil (0-20 cm) | 1.14 | aB | ± 0.09 | 0.99 | abcB | ± 0.03 | 0.95 | bcdB | ± 0.06 | 0.90 | cdB | ± 0.03 | 1.08 | abB | ± 0.04 | 0.89 | dB | ± 0.02 |
| Upper subsoil | 1.88 | aA | ± 0.19 | 0.76 | bC | ± 0.09 | 0.75 | bBC | ± 0.06 | 0.62 | bC | ± 0.07 | 0.75 | bD | ± 0.03 | 0.68 | bcC | ± 0.02 |
| Lower subsoil | 1.57 | aAB | ± 0.22 | 0.61 | cC | ± 0.03 | 0.66 | cC | ± 0.03 | 0.76 | bcC | ± 0.05 | 0.85 | bC | ± 0.01 | 0.82 | bBC | ± 0.09 |
| | **Specific root length (cm $g^{-1}$)** | | | | | | | | | | | | | | | | | |
| Organic layer | 2320.2 | cA | ± 80.3 | 7073.2 | aA | ± 2818.1 | 6659.6 | aA | ± 3797.1 | 4003.5 | aA | ± 1141.7 | 2501.9 | bA | ± 0.8 | 3652.3 | aA | ± 244.4 |
| Topsoil (0-20) | 1638.7 | abAB | ± 362.3 | 1391.7 | bB | ± 68.4 | 1934.9 | aB | ± 245.4 | 1338.8 | bB | ± 36.8 | 1645.0 | abB | ± 192.6 | 1396.0 | bB | ± 34.4 |
| Upper subsoil | 1222.5 | abB | ± 437.9 | 849.5 | bBC | ± 308.2 | 2095.0 | aB | ± 257.7 | 1076.9 | bBC | ± 127.4 | 1032.4 | bC | ± 42.8 | 1434.5 | abBC | ± 334.5 |
| Lower subsoil | 2044.5 | aAB | ± 638.3 | 698.9 | cdC | ± 192.9 | 2497.1 | aB | ± 739.4 | 833.6 | cC | ± 60.7 | 613.8 | dD | ± 30.4 | 1046.8 | bC | ± 8.8 |
| | **Specific root area ($cm^2$ $g^{-1}$)** | | | | | | | | | | | | | | | | | |
| Organic layer | 342.4 | bA | ± 16.4 | 622.7 | abA | ± 155.7 | 832.0 | aA | ± 368.5 | 521.0 | bA | ± 138.4 | 378.3 | bA | ± 17.1 | 580.9 | aA | ± 29.8 |
| Topsoil (0-20 cm) | 255.6 | abAB | ± 41.7 | 197.3 | abB | ± 7.9 | 249.2 | abB | ± 33.4 | 200.9 | abB | ± 5.4 | 226.1 | aB | ± 16.7 | 189.9 | bB | ± 10.9 |
| Upper subsoil | 203.4 | abB | ± 45.8 | 140.2 | bBC | ± 31.6 | 240.6 | aB | ± 20.0 | 186.7 | abB | ± 40.0 | 160.2 | bC | ± 8.1 | 218.0 | abBC | ± 42.8 |
| Lower subsoil | 278.5 | aAB | ± 46.6 | 152.5 | bcC | ± 21.5 | 285.9 | aB | ± 54.2 | 126.8 | bcC | ± 2.9 | 116.5 | cD | ± 5.4 | 146.9 | bC | ± 9.1 |
| | **Root tip frequency ($10^3$n $g^{-1}$)** | | | | | | | | | | | | | | | | | |
| Organic layer | 19.65 | bAB | ± 2.96 | 25.36 | abAB | ± 5.78 | 50.39 | abAB | ± 29.44 | 30.75 | aA | ± 2.75 | 35.31 | abA | ± 8.15 | 33.87 | abB | ± 7.48 |
| Topsoil (0-20 cm) | 17.45 | abAB | ± 4.72 | 23.87 | aA | ± 1.86 | 20.52 | abB | ± 1.23 | 20.06 | abB | ± 2.53 | 17.16 | bB | ± 2.06 | 21.18 | abB | ± 5.19 |
| Upper subsoil | 7.05 | bB | ± 2.37 | 11.88 | abB | ± 1.98 | 21.95 | aB | ± 4.90 | 14.19 | abB | ± 4.31 | 13.00 | abB | ± 2.42 | 21.06 | aB | ± 4.36 |
| Lower subsoil | 36.32 | abA | ± 15.80 | 19.75 | abAB | ± 15.73 | 83.77 | aA | ± 27.40 | 13.79 | bAB | ± 7.45 | 5.48 | bC | ± 0.57 | 51.25 | aA | ± 0.11 |
| | **Root tip abundance ($10^6$ n $m^{-2}$)** | | | | | | | | | | | | | | | | | |
| Organic layer | 1.35 | aA | ± 0.43 | 0.74 | aC | ± 0.16 | 0.20 | bB | ± 0.06 | 0.49 | abB | ± 0.22 | 0.60 | abAB | ± 0.20 | 0.82 | aA | ± 0.33 |
| Topsoil (0-20 cm) | 1.75 | bA | ± 0.51 | 7.11 | aA | ± 1.49 | 3.43 | abA | ± 0.86 | 5.26 | abA | ± 1.45 | 2.73 | aC | ± 0.50 | 2.90 | aB | ± 0.54 |
| Upper subsoil | 2.55 | abA | ± 0.53 | 4.39 | abAB | ± 1.50 | 6.66 | aA | ± 2.74 | 0.57 | dB | ± 0.11 | 1.05 | cdB | ± 0.21 | 1.91 | cBC | ± 0.49 |
| Lower subsoil | 0.15 | cB | ± 0.13 | 1.32 | bcBC | ± 1.14 | 1.94 | bA | ± 1.14 | 0.73 | abA | ± 0.50 | 0.40 | aB | ± 0.11 | 4.76 | aA | ± 0.21 |
| Profile total | 5.79 | b | ± 1.54 | 13.56 | a | ± 3.51 | 12.22 | ab | ± 4.43 | 7.06 | ab | ± 0.97 | 4.69 | a | ± 0.74 | 7.21 | ab | ± 1.62 |

### *Fine root morphology and chemistry*

Fine root biomass N content was remarkably similar at all six sites with site means in the topsoil (0-20 cm) varying between 0.89 and 1.14 %, without a clear trend along the base-richness gradient among the sites (Table 3.4). At all sites except for GR, root N content was highest in the organic layer (>1.4 %) and significantly decreased toward the subsoil (< 0.9 %). At the GR site on Pleistocene sand, topsoil and subsoil roots (but not organic layer roots) were particularly rich in N, which resulted in higher root N contents in the subsoil.

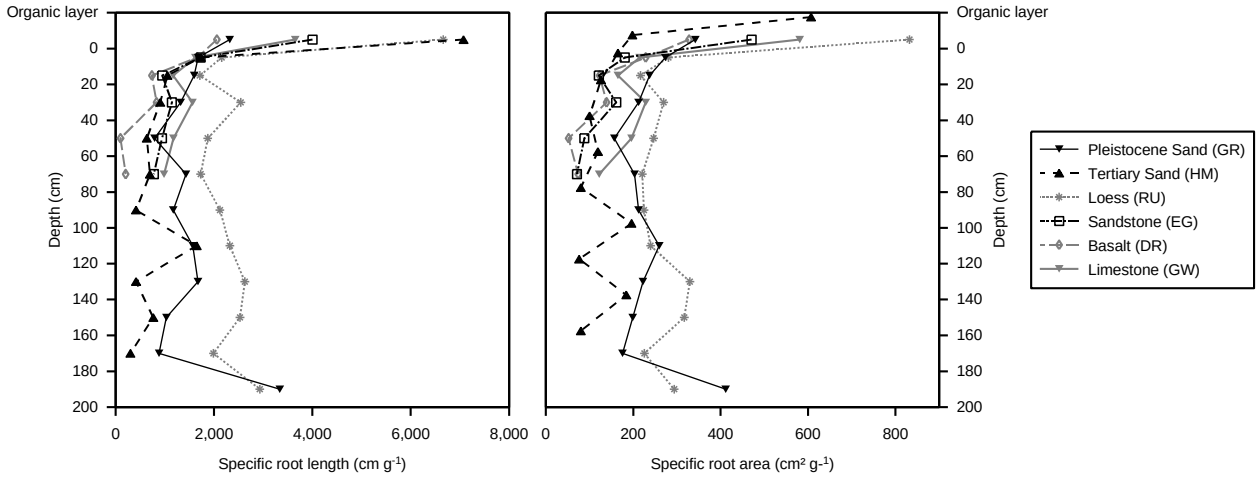


**FIGURE 3.2: Specific root length (cm $g^{-1}$) (left) and specific root area (right) ($cm^2$ $g^{-1}$) in the soil profiles of the six investigated mature beech forest stands. Values are means of three soil pits per field site.**

At all six sites, specific root length (SRL) and specific root area (SRA) were highest in the organic layer, exceeding the mineral topsoil by 40 to 400 percent (Table 3.4). Minimum SRL and SRA were reached in the upper subsoil (with higher values in the lower subsoil: GR and RU), or a more or less continuous decrease to the lower subsoil was detected (HM, EG, DR and GW; Figure 3.2, Table 3.4). Interestingly, SRL and SRA reached secondary peaks deep in the soil at 180-200 cm depth in the GR and RU profiles on Pleistocene sand and loess (Fig. 3.2). SRL and SRA varied by less than 50 % between the six sites in the topsoil (0-20 cm) (range of means: 1339-1935 cm $g^{-1}$, 190-256 $cm^2$ $g^{-1}$), whereas among-site variation was larger in the organic layer (2502-7072 cm $g^{-1}$, 342-832 $cm^2$ $g^{-1}$) and also in the lower subsoil (614-2497 cm $g^{-1}$, 117-286 $cm^2$ $g^{-1}$). While the Pleistocene sand site (GR) generally had relatively high SRL and SRA

values, this was also the case in the more base-rich loess site (RU), and no principal trend in fine root morphology from the acid, base-poor to the alkaline, base-rich sites emerged (Table 3.4).

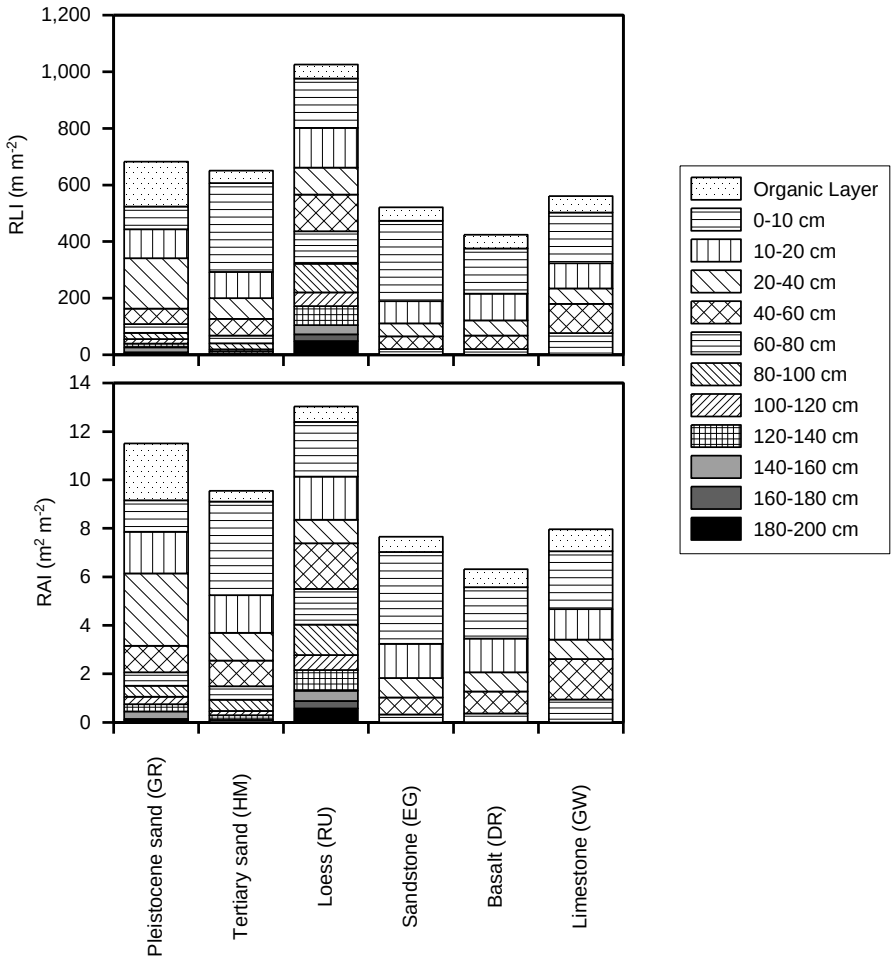


**FIGURE 3.3: Stack diagram of fine root length index (RLI, m $m^{-2}$) (left) and fine root area index (RLA, $m^2$ $m^{-2}$) (right) in the soil profiles of the six investigated mature beech forest stands. Values are means of three soil pits per field site.**

Average root diameter in the <2 mm-fraction varied between 0.32 and 0.84 mm without clear trends among the soil layers and along the base-richness gradient across sites (Table 3.5). Significant increases in mean fine root diameter with increasing soil depth were found at the HM and DR sites, but not at the other four sites.

At the stand level, root length index (RLI, in m $m^{-2}$ ground area integrated over the whole profile) and root surface area index (RAI, in $m^2$ $m^{-2}$) tended to be higher at the sites with acidic soil (GR, HM, EG) than at the base-richer basalt and limestone sites (DR and GW), but the highest indices were recorded at the relatively base-rich loess site (RU) (Fig. 3.3). This pattern is mainly caused by the greater profile depth at the GR, HM and RU sites and not by among-site differences in root length and area per layer.

Root tip frequency (RTF; tips per fine root mass) was highest in the organic layer and generally decreased toward the upper subsoil to about a half (Table 3.4). In three of the sites (GR, RU, GW), it increased again toward the lower subsoil to reach a maximum with values exceeding even the organic layer. Across the six sites, root tip frequency was similar in the mineral topsoils (17.2-23.9 · 103 $g^{-1}$), but differed considerably in the organic layers (19.7–50.4 · 103 $g^{-1}$) and especially in the lower subsoils (5.5-83.8 · 103 $g^{-1}$). A clear pattern with respect to the base-richness gradient did not emerge (Table 3.4). Root tip abundance, which is calculated from RTF, fine root density and profile depth, varied between 4.7 and 13.6 ·106 $m^{-2}$ at the six sites with a maximum at the loess site (RU) and minima at the basalt (DR) and Pleistocene sand sites (GR). A clear dependence on the base-richness gradient did not emerge, while the deeper profiles (HM and RU, but not GR) tended to have higher overall tip numbers. Most of the tips of the GR, HM, RU and GW sites were located in the upper or the lower subsoil and not in the organic layer. In contrast, the topsoil (0-20 cm) played a key role for tip abundance at the EG and DR sites. Only at the acidic GR site on Pleistocene sand, a considerable number of tips were located in the organic layer (~25 % of the profile total).

***Edaphic and stand structural drivers of fine root system size and fine root morphology***

A Pearson correlation analysis between various soil physical and chemical parameters (soil bulk density, clay content, organic layer thickness, soil C/N ratio, base saturation) and fine root morphological traits and parameters characterizing fine root system size and distribution revealed only very few significant relationships in our sample of six sites. While the FRB profile total was not dependent on soil pH, base saturation, soil C/N ratio or clay content, the volume density of both fine root biomass and root tips decreased with increasing soil bulk density ($r = -0.76$, and $r = -0.73$, respectively; $P \leq 0.01$; Table 3.5). The volume density of both fine root biomass and fine root necromass increased with soil C/N ratio ($r = 0.51$, and $r = 0.79$, respectively; $P \leq 0{,}05$, and $P \leq 0.001$, respectively). Live fine root N content was negatively correlated with soil clay content ($r = 0.60$, $P \leq 0.01$). We did not observe any significant relationships between profile totals of fine root biomass and soil physical and chemical parameters. We further tested whether fine root system size and fine root morphology vary with stand structural parameters, but neither for fine root abundance and distribution, nor for fine root morphological traits significant correlations with stem density and plot basal area appeared.

Additionally, we conducted multivariate regression analyses to detect whether soil chemical and physical parameters (soil C/N ratio, base saturation, clay content) are influencing the abundance of fine root biomass and fine root morphological traits (Table 3.6). Soil C/N ratio explained about a quarter to a third of the variation in fine root biomass in the topsoil ($r^2 = 0.31$) and the lower subsoil ($r^2 = 0.27$) at our sites, and about a quarter of the variation in case of the whole profile ($r^2 = 0.24$). With respect to fine root morphological traits, only soil base saturation showed a significant relation to average root diameter in the lower subsoil ($r^2 = 0.30$) and to root tip frequency in the upper subsoil ($r^2 = 0.27$). Neither soil C/N ratio and clay content, nor fine root biomass were significantly related to the studied fine root morphological traits. Correspondingly, a PCA arranged the six sites along the first axis, which correlated with clay content, base saturation and soil C/N (Table 3.7), while fine root diameter, and in opposite direction, fine root biomass and SRA differentiated the sampled sites and horizons on the second axis. Interestingly, most of the upper and lower subsoil horizons of the six sites were, irrespective of geology, located in the upper section of the PCA plot, thus in association with increasing fine root diameter, while most of the topsoil horizons were found in the lower plot section, coinciding with

high fine root biomass and SRA values. Root tip frequency was the only variable with highest loading on the third axis; it was negatively related to clay content and soil C/N ratio.

**TABLE 3.5: Coefficients of linear Pearson correlations between fine root and soil and stand characteristics. * indicates significance at ≤ 0.05, ** significance at ≤ 0.01, and *** significance at ≤ 0.001 error probability. (FRB – Fine root biomass. FRN – Fine root necromass. FR – Fine root. RTD – Root tip density. SRA – Specific root area. OL- Organic layer.)**

| | FRB density ($g\ L^{-1}$) | FRN density ($g\ L^{-1}$) | FRB ($g\ m^{-2}$) | FRN ($g\ m^{-2}$) | FR live:dead ratio | Live FR N content (%) | RTD ($n\ L^{-1}$) | SRA ($cm^2\ g^{-1}$) | Thickness of OL (mm) | Soil C:N ratio | Soil bulk density ($g\ cm^{-3}$) | pH ($CaCl_2$) | Soil base saturation (%) | Soil clay content (%) |
|---|---|---|---|---|---|---|---|---|---|---|---|---|---|---|
| **FRB density ($g\ L^{-1}$)** | | **0.60**** | 0.34 | 0.17 | 0.07 | 0.10 | **0.87***** | 0.08 | -0.10 | **0.51*** | **-0.76**** | -0.26 | -0.21 | 0.28 |
| **FRN density ($g\ L^{-1}$)** | | | 0.16 | 0.42 | -0.44 | 0.20 | 0.37 | -0.06 | 0.20 | **0.79***** | **-0.54*** | -0.28 | -0.35 | -0.24 |
| **FRB ($g\ m^{-2}$)** | | | | 0.74 | -0.07 | -0.22 | 0.12 | -0.51** | 0.06 | 0.33 | -0.24 | -0.20 | -0.31 | -0.03 |
| **FRN ($g\ m^{-2}$)** | | | | | -0.47 | -0.10 | -0.10 | -0.48 | 0.29 | 0.39 | -0.08 | -0.13 | -0.39 | -0.27 |
| **Fine root live:dead ratio** | | | | | | 0.12 | 0.36 | 0.47 | -0.10 | -0.23 | -0.07 | -0.15 | 0.09 | 0.27 |
| **Live FR N content (%)** | | | | | | | 0.18 | **0.70***** | 0.16 | 0.40 | 0.14 | -0.16 | -0.43 | **-0.60**** |
| **RTD ($n\ L^{-1}$)** | | | | | | | | 0.28 | -0.08 | 0.39 | **-0.73**** | -0.05 | -0.10 | 0.35 |
| **SRA ($cm^2\ g^{-1}$)** | | | | | | | | | -0.14 | 0.14 | 0.16 | -0.35 | -0.12 | -0.31 |
| **Thickness of OL (mm)** | | | | | | | | | | 0.39 | 0.18 | -0.29 | -0.47 | -0.45 |
| **Soil C:N ratio** | | | | | | | | | | | -0.43 | -0.15 | -0.32 | -0.26 |
| **Soil bulk density ($g\ cm^{-3}$)** | | | | | | | | | | | | 0.12 | 0.15 | -0.34 |
| **pH ($CaCl_2$)** | | | | | | | | | | | | | **0.72***** | 0.28 |
| **Soil base saturation (%)** | | | | | | | | | | | | | | 0.45 |
| **Soil clay content (%)** | | | | | | | | | | | | | | |

**TABLE 3.6: Results of multivariate regression analyses between fine root biomass and clay content (%), C/N ratio, and base saturation (BS, %), and between specific root area, average fine root diameter, and root tip frequency and clay content (%), C/N ratio, base saturation (BS, %), and fine root biomass (g $m^{-2}$). The regression analyses were conducted separately for the topsoil, upper subsoil and lower topsoil, and for all layers together. Shown are significant correlations with P < 0.05.**

| Variable | Unit | Depth | Regression function | $r^2$ |
|---|---|---|---|---|
| Fine root biomass | g $m^{-2}$ | Topsoil | y = 11.0641 x C/N + 27.0433 | 0.31 |
| | | Upper subsoil | | |
| | | Lower subsoil | y = 7.3188 x C/N + 8.5772 | 0.27 |
| | | All | y = 9.7370 x C/N + 16.3076 | 0.24 |
| Specific root area | $cm^2$ $g^{-1}$ | Topsoil | | |
| | | Upper subsoil | | |
| | | Lower subsoil | | |
| | | All | | |
| Average root diameter | mm | Topsoil | | |
| | | Upper subsoil | | |
| | | Lower subsoil | y = -0.0019 x BS + 0.6771 | 0.30 |
| | | All | y = -0.0010 x BS + 0.5762 | 0.08 |
| Root tip frequency | n $g^{-1}$ | Topsoil | | |
| | | Upper subsoil | y = 118.4406 x BS + 10309.5292 | 0.27 |
| | | Lower subsoil | | |
| | | All | y = 232.4285 x BS + 14386.4874 | 0.14 |

**TABLE 3.7. Results of the Principal Components Analysis with eigenvalues (EV) of the first for axes and loadings.**

| Variables | Axis 1 (EV 0.338) | Axis 2 (EV 0.288) | Axis 3 (EV 0.169) | Axis 4 (EV 0.100) |
|---|---|---|---|---|
| Clay content | **-0.742 (0.55)** | 0.018 (0.55) | -0.492 (0.79) | 0.239 (0.85) |
| Soil C/N | **0.779 (0.61)** | -0.171 (0.64) | -0.457 (0.84) | 0.181 (0.88) |
| Base saturation | **-0.863 (0.75)** | -0.029 (0.75) | -0.223 (0.80) | -0.025 (0.80) |
| Fine root biomass | 0.333 (0.11) | **-0.764 (0.69)** | -0.262 (0.76) | 0.400 (0.92) |
| SRA | 0.115 (0.01) | **-0.826 (0.70)** | 0.310 (0.79) | -0.348 (0.91) |
| Root tip frequency | -0.409 (0.17) | -0.365 (0.30) | **0.658 (0.73)** | 0.491 (0.98) |
| Root diameter | 0.418 (0.18) | **0.767 (0.76)** | 0.287 (0.85) | 0.292 (0.93) |

## 3.5 Discussion

***Does fine root biomass increase with decreasing soil pH, base saturation and soil fertility?***

In contrast to earlier studies on fine root biomass in temperate forests, we did not find FRB totals to be in all cases smaller in profiles with high base saturation, and higher in profiles with low base saturation. As expected, the FRB total at the base-rich limestone site was small (GW; 330 g $m^{-2}$) but high in two profiles with low base saturation (GR and HM; 530 – 560 g $m^{-2}$). However, the difference was only partly significant and the studied beech forest sample contains a site with high FRB despite high subsoil base saturation (RU), as well as a site with low base saturation but relatively low FRB (EG). Therefore, our data does neither support nor disprove the assumption of a dominant role of base saturation for the FRB total in *F. sylvatica* forests (hypothesis i). In contrast, FRB significantly increased with the soil C/N ratio in the topsoil and lower subsoil of the investigated profiles, pointing at higher FRB in soil horizons with low N supply. This suggests that N availability may be more influential than base richness or pH.

It further appears that profile depth is a more important determinant of FRB profile totals than base saturation in our 6-site sample (hypothesis iii). This factor is rarely explored in cross-site comparisons or meta-analyses of tree fine root biomass. Rather, a standard profile depth of 60, 70 or 100 cm is often used and shallow profiles are not included in the samples or do not occur. Studies controlling for profile depth did frequently report a negative relation between soil CEC, base saturation or pH, and stand FRB (e.g. Aber et al. 1985, Gower et al. 1992, Poorter and Nagel 2000, Le Goff and Ottorini 2001, Neatrour et al. 2005). With respect to *F. sylvatica*, inverse nutrient availability-FRB relationships have been reported by Schmid (2002) and Leuschner and Hertel (1998) and (2004), and they also appeared from the meta-analyses of Leuschner and Hertel (2003) and Finér et al. (2007). Assuming that the conventional definition of FRB with a diameter threshold of 2 mm represents a suitable proxy for the nutrient- and water-absorbing surface area of a tree root system, this relationship can be interpreted as an adaptive response to low supply of N, P or base cations (mostly Ca, K, Mg), being an element of a strategy to compensate low supply rates by a larger absorbing belowground surface. Given that stand leaf area (LAI) has been found to be remarkably constant in Central European *F. sylvatica* forests across soil fertility and pH/base saturation gradients (Leuschner et al. 2006), an inverse nutrient availability-FRB relation would indicate a growing ratio of belowground to aboveground resource-absorbing surfaces,

when soil resources become increasingly short in supply. The results of our study suggest that a limited exploitable soil volume can effectively reduce stand FRB. We interpret the smaller root area indices (5.8-7.7 $m^2$ $m^{-2}$) at the three shallow sites (60-80 cm profile depth) in comparison to the deep profiles (9.3-13.0 $m^2$ $m^{-2}$; see Fig. 3.3) as a hint that these stands would in deeper soils develop larger fine root biomasses, with putative positive effects on nutrient and water uptake. If this result is more generally valid, it indicates that beech fine root density does in general not exceed 1.5 (or more often 1.0) g $L^{-1}$ in the topsoil irrespective of profile depth, presumably to avoid self-competition between roots of the same individual. Correspondingly, we did not find evidence that the density of fine root tips (n per soil volume) is higher in the topsoil of shallow profiles than in deep profiles; density never exceeded 35,000 tips per L.

Although our sample (n = 6 sites) is smaller than in some other comparative root studies, the study is one of very few covering the subsoil to 2 m depth and we can thus refer to profile totals of FRB which is not possible in most other studies. Some authors doubt that fine root biomass (<2 mm in diameter) is a biologically meaningful parameter with relation to resource uptake capacity, since this fraction may contain both absorbing and non-absorbing root sections (e.g. Guo et al. 2008). This possible shortcoming is, however, less relevant for our study, as we consider a single tree species that showed relatively uniform fine root morphology across the studied edaphic gradient.

***Do vertical fine root distribution patterns and fine root live:dead ratios differ between base-poor and base-rich soils?***

In most forest soils, fine root biomass per soil volume has been found to decrease exponentially with soil depth, resulting in highest root mass densities in the mineral topsoil or the organic layer (e.g. Jackson et al. 1996; Hertel 1999; Jobbágy and Jackson 2001; Leuschner et al. 2004; Meier et al. 2017). Factors possibly driving this root biomass decline with soil depth are a downward decrease in leaf litter-derived N and P supply rate, the increase in soil bulk density, a reduction in soil biological activity (including mycorrhiza), and, at least locally, subsoil water logging in combination with low oxygen contents and putative metal toxicity (Jobbágy and Jackson 2000; Jentschke et al. 2001; Hodge 2004). In more acidic soils, the root biomass decrease may be more

pronounced, as soil biological activity is generally lower in the subsoil and the downward transport of litter-derived nutrients is less intense, and toxic elements in the subsoil (e.g. Al3+) may reach higher concentrations than in base-richer soils. Our results show a tendency for a steeper root biomass decrease (higher β-coefficient) in the deeper profiles, but the difference between base-poor and base-rich sites was not clear-cut (hypothesis ii). The principal similarity of β-coefficients for beech fine root systems in soils with low or high base saturation and soil biological activity suggests that the FRB peak close to the soil surface is mainly caused by the nutrient supply from decomposing leaf litter as well as the lower soil bulk density at the surface, whereas soil moisture (which is often more readily available in the subsoil), soil biological activity and toxic elements (which differ largely between sites) must be of secondary importance. In apparent contradiction to this finding, Braun et al. (2005) found a significant reduction in rooting depth of *F. sylvatica* at sites with low base saturation. Yet, other studies reported only weak influences of soil acidity or nutrient availability on vertical fine root distribution patterns in European beech forests (Leuschner et al. 2004, Mainiero and Kazda 2006). Based on the analysis of 302 root profiles in German forests, Hartmann and von Wilpert (2014) concluded that soil chemical properties are of minor importance as determinants of tree fine root vertical distribution. In our study, we did not observe any relation between the vertical distribution of FRB to the thickness and structure of the organic layer, which normally increases in thickness with the transition from mull to moder and mor humus along a soil base richness gradient. Thick moder-type organic layers on mineral soils of low biological activity (as the GR site on Pleistocene sand) represent attractive media for fine roots to explore, when they are sufficiently moist, even though the C/N ratio can be high and decomposition rate relatively low. Schenk and Jackson (2002) concluded from a global review that the fine root system in forests becomes the shallower the thicker the organic layer is, in apparent contradiction to our findings. A possible explanation for this discrepancy is that organic layer thickness increases in forests not only along soil acidity gradients, but also along temperature gradients. We assume from our results that decreasing temperature shapes the vertical fine root distribution much more than increasing acidity.

Various studies have shown that base-poor forest soils typically have a greater live-dead ratio of fine root mass than base-rich soils (e.g. Leuschner et al. 1998, Godbold et al. 2003, Leuschner and Hertel 2003, Leuschner et al. 2004, Braun et al. 2005), which may be explained by a higher

fine root mortality in acid, infertile soils, but alternatively could also result from a lower decomposition rate of fine root necromass due to reduced soil biological activity. We found high fine root necromass amounts in the acid profiles on sand (GR and HM), intermediate amounts on sandstone and basalt (EG and DR), and low ones on loess and limestone (RU and GW). Yet, no clear dependence of the live:dead ratio of fine root mass on base saturation was visible (hypothesis iv). In the absence of root turnover and decomposition measurements at our sites, we cannot decide what is driving the differences in necromass amounts. However, an earlier study in four *F. sylvatica* forests on different soils indicated that the site differences in fine root mortality were much greater than the differences in root decomposition rates (Hertel 1999), suggesting that nutrient shortage and soil acidity are reducing root longevity more than decomposer activity.

***Do fine roots alter their morphology in response to nutrient shortage and soil acidity?***

Plasticity in root morphology and root system structure is one strategy of trees to cope with belowground environmental heterogeneity and temporal change in physical and chemical conditions (Hodge 2006, Ostonen et al. 2007, Comas and Eissenstat 2009). For example, plants exposed to nutrient shortage or drought might produce finer, more branched rootlets with greater surface area in order to increase resource uptake and improve the cost/benefit ratio of root formation and maintenance (Eissenstat and Yanai 1997, Pregitzer et al. 2002, Ostonen et al. 2007). Our data show considerable variation in specific root length and specific root area across sites and soil layers, but no consistent change in root morphology along the gradient from more alkaline, base-rich to acidic, base-poor sites in the same soil layer (hypothesis v). Only in the lower subsoil, base saturation had a significant effect on average fine root diameter according to the multivariate regression analysis, explaining 30 percent of the variation. This matches with findings from a comparison of another six German *F. sylvatica* forests, where fine root morphological differences were small and no consistent relation between soil chemistry and SRA (and RAI) could be detected (Leuschner et al. 2004). In many comparative root studies with non-woody plants as well, no root morphological changes could be detected along gradients of soil acidity or base saturation (Hutchings and de Kroon 1994, Ryser 1998). In contrast to some earlier studies (e.g. Meyer 1967, Kottke and Agerer 1983, Hertel 1999, Leuschner et al. 2004), a relation between the frequency of root tips per root mass and base richness existed only in one horizon

(upper subsoil) but not in the others, and this relation was positive and not negative. This does not support hypothesis (vi). These findings suggest that, on the species level, fine root morphological adaptation to nutrient shortage apparently is not the rule in temperate trees. We have no information on root physiological changes or altered mycorrhizal associations in response to decreases in nutrient availability and soil pH; they could well increase the mass-specific nutrient uptake capacity of roots in infertile soils.

Much larger root morphological differences existed between the different soil layers within the same soil profile, i.e. among the roots of a single tree, providing evidence of large root morphological plasticity in *F. sylvatica*. In general, the fine roots of the organic layer had the largest SRL and SRA values and the highest root tip frequency, while mineral topsoil and subsoil differed less. However, at half of the sites (GR, RU, GW), root tip frequency reached its profile maximum in the lower subsoil and not in the organic layer, which we explain with relatively high subsoil nutrient concentrations at these sites. Average fine root diameter was in most profiles relatively invariant across the profile. The high branching intensity and surface development of the organic layer fine roots is likely caused by particularly high nutrient supply rates in conjunction with the low bulk density of the organic material, conditions that should favor the formation and maintenance of structurally complex fine root systems, given that soil moisture is sufficiently high. The decrease in root N content with increasing soil depth is thought to mirror N mineralization rates in the profile, which decrease with soil depth despite a reduction in soil C/N ratio (Runge 1983, Leuschner et al. 2014). The observed differences in the chemistry and morphology of topsoil and subsoil roots could also reflect a functional differentiation within the fine root system, with surface roots being mainly responsible for nutrient (N and P) uptake and subsoil roots primarily representing water-absorbing roots. This hypothesis has to be tested by physiological measurements under field conditions.

## 3.6 Conclusions

This comparative study in six beech forests on largely different bedrock explored the influence of base saturation and soil acidity on the fine root system size, fine root distribution, live:dead ratio, and fine root morphology of *F. sylvatica* stands. The influence of profile depth was addressed through a thorough study of subsoil rooting patterns. The results highlight the importance of subsoil for the fine root system of beech, even on soils with only 60-80 cm profile depth. Reduced profile depth was found to be an important determinant of overall fine root system size, which reduced the stand total of FRB significantly, when bedrock depth was 80 cm or less (hypothesis iii). Comparison of sites and soil layers evidences great plasticity in fine root system structure and also fine root morphology. This is interpreted as an adaptive belowground strategy of *F. sylvatica* to colonize a broad range of soil types, and it may explain why the species is able to grow on highly acidic and also alkaline soils, revealing the behavior of a calcifuge and a calcicole plant. Indeed, fine root system structure and fine root morphology differed less between stands on base-poor and base-rich sites (hypothesis v and vi) than between the topsoil and subsoil within a profile. Future fine root studies on soils differing in soil chemistry and nutrient availability should also investigate root branching patterns (notably the 1st- and 2nd-order fraction) and root functioning (root longevity and uptake activity) in order to deepen our understanding of tree belowground adaptation to variable edaphic conditions.

***Acknowledgements***

This study was supported by funding from the Deutsche Forschungsgemeinschaft (DFG) as part of the research unit FOR1806 "The Forgotten Part of Carbon Cycling: Organic Matter Storage and Turnover in Subsoils (SUBSOM)". The support is gratefully acknowledged.

# Supplementary Material

**TABLE S3.1: Fine root biomass (FRB) and necromass (FRN) in the organic layer and mineral top- and subsoil of the six investigated mature beech forests. Shown are means + SE of three soil pits per site.**

| Plot no. | 1 | | | | 2 | | | | 3 | | | |
|---|---|---|---|---|---|---|---|---|---|---|---|---|
| Site code | GR | | | | HM | | | | RU | | | |
| Substrate type | Pleistocene sand | | | | Tertiary sand | | | | Loess | | | |
| | FRB (g m$^{-2}$) | | FRN (g m$^{-2}$) | | FRB (g m$^{-2}$) | | FRN (g m$^{-2}$) | | FRB (g m$^{-2}$) | | FRN (g m$^{-2}$) | |
| Depth (cm) | | | | | | | | | | | | |
| Organic layer | 66.98 | ± 18.15 | 141.80 | ± 34.53 | 8.96 | ± 3.63 | 3.27 | ± 2.02 | 8.59 | ± 2.07 | 20.72 | ± 13.90 |
| 0-10 | 42.29 | ± 15.01 | 97.42 | ± 4.24 | 178.24 | ± 16.79 | 39.83 | ± 9.96 | 96.78 | ± 39.33 | 6.13 | ± 1.41 |
| 10-20 | 87.34 | ± 39.92 | 101.60 | ± 6.66 | 89.20 | ± 11.12 | 75.33 | ± 14.62 | 81.89 | ± 4.93 | 81.03 | ± 27.74 |
| 20-40 | 145.72 | ± 27.08 | 98.48 | ± 11.78 | 80.31 | ± 7.63 | 139.88 | ± 10.88 | 36.64 | ± 6.25 | 35.93 | ± 6.02 |
| 40-60 | 73.44 | ± 23.19 | 106.38 | ± 47.73 | 89.66 | ± 12.88 | 191.92 | ± 37.90 | 75.30 | ± 25.45 | 28.08 | ± 5.20 |
| 60-80 | 36.66 | ± 20.56 | 26.34 | ± 9.69 | 46.02 | ± 17.07 | 67.52 | ± 12.96 | 59.93 | ± 22.38 | 16.69 | ± 1.54 |
| 80-100 | 27.69 | ± 16.49 | 40.42 | ± 21.58 | 30.92 | ± 16.63 | 16.13 | ± 5.91 | 69.32 | ± 43.00 | 11.09 | ± 1.76 |
| 100-120 | 17.17 | ± 15.21 | 31.96 | ± 23.64 | 19.24 | ± 18.65 | 10.53 | ± 6.26 | 33.57 | ± 28.22 | 12.64 | ± 3.47 |
| 120-140 | 20.27 | ± 10.05 | 32.73 | ± 20.80 | 13.48 | ± 7.34 | 7.11 | ± 1.69 | 31.34 | ± 20.84 | 7.12 | ± 1.83 |
| 140-160 | 9.90 | ± 5.55 | 20.99 | ± 15.38 | 6.66 | ± 4.04 | 2.49 | ± 1.83 | 21.52 | ± 8.92 | 6.76 | ± 2.58 |
| 160-180 | 1.58 | ± 1.03 | 2.59 | ± 1.57 | 0.28 | ± 0.28 | 3.21 | ± 1.68 | 14.40 | ± 5.07 | 5.63 | ± 0.39 |
| 180-200 | 3.18 | ± 2.42 | 7.65 | ± 4.02 | 0.00 | ± 0.00 | 1.76 | ± 0.02 | 22.35 | ± 10.00 | 11.23 | ± 0.22 |
| Profile total | 532.21 | ± 155.79 | 708.35 | ± 69.23 | 562.98 | ± 13.87 | 558.98 | ± 72.68 | 551.63 | ± 177.63 | 248.69 | ± 51.62 |

| Plot no. | 4 | | | | 5 | | | | 6 | | | |
|---|---|---|---|---|---|---|---|---|---|---|---|---|
| Site code | EG | | | | DR | | | | GW | | | |
| Substrate type | Sandstone | | | | Basalt | | | | Limestone | | | |
| | FRB (g m$^{-2}$) | | FRN (g m$^{-2}$) | | FRB (g m$^{-2}$) | | FRN (g m$^{-2}$) | | FRB (g m$^{-2}$) | | FRN (g m$^{-2}$) | |
| Depth (cm) | | | | | | | | | | | | |
| Organic layer | 13.08 | ± 2.30 | 4.81 | ± 0.47 | 13.19 | ± 6.19 | 21.53 | ± 9.48 | 15.76 | ± 4.71 | 7.01 | ± 3.49 |
| 0-10 | 161.36 | ± 16.17 | 174.88 | ± 28.96 | 76.13 | ± 19.27 | 133.35 | ± 4.85 | 110.24 | ± 12.34 | 57.28 | ± 0.69 |
| 10-20 | 90.16 | ± 28.11 | 83.86 | ± 16.45 | 77.67 | ± 12.85 | 105.22 | ± 8.27 | 77.79 | ± 13.62 | 46.65 | ± 8.97 |
| 20-40 | 44.61 | ± 10.38 | 60.29 | ± 6.06 | 42.16 | ± 4.03 | 51.86 | ± 7.92 | 41.91 | ± 11.02 | 27.52 | ± 2.52 |
| 40-60 | 53.38 | ± 17.36 | 42.82 | ± 1.13 | 88.40 | ± 26.52 | 62.18 | ± 2.76 | 83.82 | ± 28.67 | 95.77 | ± 11.11 |
| 60-80 | 27.01 | ± 8.82 | 46.00 | ± 5.00 | 30.17 | ± | 82.38 | ± | 77.62 | ± | 53.42 | ± |
| 80-100 | | | | | | | | | | | | |
| 100-120 | | | | | | | | | | | | |
| 120-140 | | | | | | | | | | | | |
| 140-160 | | | | | | | | | | | | |
| 160-180 | | | | | | | | | | | | |
| 180-200 | | | | | | | | | | | | |
| Profile total | 389.61 | ± 43.07 | 412.67 | ± 9.59 | 307.60 | ± 37.49 | 401.61 | ± 24.07 | 327.46 | ± 42.55 | 220.11 | ± 50.59 |

**TABLE S3.2: Fine root biomass and necromass (fraction of profile average), coefficients of variation (CV) for fine root biomass and fine root necromass, fine root C/N ratio, and root tip density in the organic layer, mineral topsoil (0-20 cm), upper subsoil, and lower subsoil of the six investigated mature beech forests. 'Upper subsoil' stands for 20-110 cm soil depth at the GR, RU and HM sites with deep profiles, and 20-50 cm depth in the shallow profiles of the EG, DR and GW sites. 'Lower subsoil' stands for 110-200 cm soil depth at the GR, RU and HM sites, and 50-80 cm depth at the EG, DR and GW sites. Also given is the soil depth to which 50 or 90 %, of fine root biomass and necromass are found in the soil profile of the six investigated mature beech forests Shown are means + SE of three soil pits per site. Different small letters indicate significant differences (P<0.05) between the stands, capital letters significant differences between the soil horizons.**

| | Deep profiles | | | Shallow profiles | | |
|---|---|---|---|---|---|---|
| Plot no. | 1 | 2 | 3 | 4 | 5 | 6 |
| Site code | GR | HM | RU | EG | DR | GW |
| Substrate type | Pleistocene sand | Tertiary sand | Loess | Sandstone | Basalt | Limestone |
| | **Fine root biomass (fraction of profile average)** | | | | | |
| Organic layer | 0.13 a ± 0.04 | 0.02 bc ± 0.01 | 0.02 c ± 0.00 | 0.04 bc ± 0.01 | 0.04 bc ± 0.02 | 0.05 b ± 0.02 |
| Topsoil (0-20 cm) | 0.24 b ± 0.03 | 0.47 a ± 0.04 | 0.35 ab ± 0.09 | 0.64 a ± 0.07 | 0.50 a ± 0.03 | 0.59 a ± 0.09 |
| Upper subsoil | 0.56 a ± 0.09 | 0.46 a ± 0.03 | 0.45 a ± 0.04 | 0.18 c ± 0.02 | 0.28 b ± 0.04 | 0.25 bc ± 0.04 |
| Lower subsoil | 0.07 c ± 0.04 | 0.05 c ± 0.02 | 0.18 bc ± 0.05 | 0.14 bc ± 0.05 | 0.25 ab ± 0.04 | 0.31 a ± 0.02 |
| | **Fine root necromass (fraction of profile average)** | | | | | |
| Organic layer | 0.20 a ± 0.04 | 0.01 c ± 0.00 | 0.02 b ± 0.00 | 0.01 c ± 0.00 | 0.05 b ± 0.02 | 0.04 bc ± 0.03 |
| Topsoil (0-20 cm) | 0.28 c ± 0.02 | 0.21 d ± 0.01 | 0.46 b ± 0.03 | 0.63 a ± 0.03 | 0.60 a ± 0.07 | 0.51 ab ± 0.08 |
| Upper subsoil | 0.41 b ± 0.08 | 0.75 a ± 0.01 | 0.29 b ± 0.01 | 0.20 c ± 0.02 | 0.21 c ± 0.01 | 0.33 b ± 0.05 |
| Lower subsoil | 0.11 cd ± 0.04 | 0.04 d ± 0.02 | 0.23 b ± 0.03 | 0.16 c ± 0.01 | 0.26 b ± 0.01 | 0.36 a ± 0.01 |
| % of total | **Fine root biomass (g $m^{-2}$)** | | | | | |
| 50 | 29.0 a ± 3.8 | 22.6 a ± 3.7 | 47.4 a ± 16.2 | 12.1 b ± 0.9 | 19.9 a ± 3.9 | 21.0 ab ± 8.8 |
| 90 | 102.4 a ± 16.0 | 83.6 ab ± 13.9 | 120.4 a ± 15.3 | 50.9 c ± 7.5 | 56.4 bc ± 1.8 | 49.0 bc ± 11.3 |
| % of total | **Fine root necromass (g $m^{-2}$)** | | | | | |
| 50 | 24.2 bc ± 4.9 | 42.0 a ± 0.8 | 24.9 b ± 4.4 | 13.0 c ± 2.1 | 14.6 bc ± 1.7 | 24.3 abc ± 9.2 |
| 90 | 115.9 b ± 18.3 | 81.5 bc ± 9.6 | 178.6 a ± 6.2 | 61.7 c ± 1.6 | 54.6 cd ± 7.3 | 51.6 d ± 10.8 |
| | **$C_v$ Fine root biomass** | | | | | |
| Organic layer | 0.48 bB ± 0.08 | 1.49 aA ± 0.26 | 1.15 abA ± 0.61 | 1.18 aA ± 0.19 | 1.84 aA ± 0.31 | 1.57 aA ± 0.05 |
| Topsoil (0-20 cm) | 0.65 aB ± 0.05 | 0.45 bC ± 0.05 | 0.61 abA ± 0.09 | 0.69 aB ± 0.05 | 0.57 abB ± 0.11 | 0.82 aB ± 0.11 |
| Upper subsoil | 0.69 aB ± 0.21 | 0.82 aB ± 0.07 | 0.67 aA ± 0.05 | 0.74 aAB ± 0.09 | 0.63 aB ± 0.12 | 1.01 aB ± 0.16 |
| Lower subsoil | 1.25 bA ± 0.09 | 1.66 aA ± 0.07 | 0.85 cA ± 0.14 | 0.88 abcdAB ± 0.35 | 0.31 eC ± 0.05 | 0.47 dC ± 0.04 |
| | **$C_v$ Fine root necromass** | | | | | |
| Organic layer | 0.64 aAB ± 0.18 | 0.76 aA ± 0.25 | 0.70 aAB ± 0.14 | 0.69 aA ± 0.02 | 1.06 aA ± 0.46 | 0.99 aA ± 0.34 |
| Topsoil (0-20 cm) | 0.28 cC ± 0.02 | 0.52 bA ± 0.07 | 0.83 aA ± 0.13 | 0.47 bB ± 0.09 | 0.33 bcA ± 0.11 | 0.31 bcAB ± 0.15 |
| Upper subsoil | 0.59 aB ± 0.14 | 0.40 aA ± 0.06 | 0.56 aAB ± 0.14 | 0.33 aB ± 0.11 | 0.46 aA ± 0.12 | 0.41 aAB ± 0.14 |
| Lower subsoil | 1.02 aA ± 0.13 | 0.59 bA ± 0.10 | 0.32 bcB ± 0.12 | 0.73 abAB ± 0.37 | 0.23 cA ± 0.02 | 0.19 cB ± 0.08 |
| | **Fine root C/N ratio** | | | | | |
| Organic layer | 36.23 aA ± 1.89 | 30.95 aC ± 2.64 | 28.97 aC ± 3.86 | 33.89 aC ± 0.67 | 33.36 aD ± 4.13 | 34.30 aC ± 4.43 |
| Topsoil (0-20 cm) | 42.66 bA ± 3.56 | 47.44 abB ± 1.84 | 50.14 aB ± 2.39 | 53.26 aB ± 2.51 | 43.49 bC ± 1.51 | 52.71 aB ± 1.61 |
| Upper subsoil | 24.16 cB ± 2.55 | 63.44 abA ± 4.62 | 63.61 abAB ± 5.92 | 76.79 aA ± 8.83 | 61.35 bA ± 3.00 | 69.43 aA ± 2.16 |
| Lower subsoil | 30.37 cAB ± 4.16 | 74.91 aA ± 5.20 | 75.54 aA ± 3.69 | 62.34 abAB ± 5.62 | 53.09 bB ± 0.20 | 58.96 abAB ± 6.10 |
| | **Root tip density ($10^3$ n $L^{-1}$)** | | | | | |
| Organic layer | 26.23 aA ± 10.27 | 18.31 abAB ± 7.42 | 9.48 bA ± 0.60 | 28.28 abA ± 11.43 | 18.25 abA ± 6.10 | 19.51 abAB ± 6.41 |
| Topsoil (0-20 cm) | 8.74 cA ± 2.53 | 35.53 aA ± 7.45 | 25.45 abA ± 10.87 | 26.32 aA ± 7.25 | 13.66 cbA ± 2.50 | 19.27 bA ± 2.19 |
| Upper subsoil | 2.84 bcB ± 0.59 | 5.10 abB ± 1.69 | 7.40 aA ± 3.04 | 1.91 cB ± 0.36 | 3.18 bB ± 0.45 | 8.76 aB ± 3.50 |
| Lower subsoil | 0.73 cB ± 0.63 | 6.60 bcB ± 5.71 | 9.69 abA ± 5.71 | 2.44 cB ± 1.66 | 1.35 cC ± 0.37 | 15.85 aAB ± 0.69 |

**TABLE S3.3: Specific root length and specific root area for the organic layer and mineral top- and subsoil of the six investigated mature beech forests. Shown are means + SE of three soil pits per site.**

| Plot no. | 1 | 2 | 3 | 4 | 5 | 6 |
|---|---|---|---|---|---|---|
| Site code | GR | HM | RU | EG | DR | GW |
| Substrate type | Pleistocene sand | Tertiary sand | Loess | Sandstone | Basalt | Limestone |
| **SPECIFIC ROOT LENGTH (cm $g^{-1}$)** | | | | | | |
| Depth (cm) | | | | | | |
| Organic layer | 2320.2 ± 80.3 | 7073.2 ± 2818.1 | 6659.6 ± 3797.1 | 4003.5 ± 1141.7 | 2501.9 ± 0.8 | 3652.3 ± 244.4 |
| 0-10 | 1679.5 ± 401.2 | 1729.5 ± 174.1 | 2158.1 ± 455.1 | 1728.1 ± 195.7 | 2105.9 ± 278.6 | 1623.2 ± 48.2 |
| 10-20 | 1597.9 ± 474.3 | 1053.8 ± 55.2 | 1711.7 ± 65.6 | 949.4 ± 126.2 | 1184.1 ± 132.9 | 1168.7 ± 103.1 |
| 20-40 | 1322.4 ± 502.4 | 907.5 ± 193.1 | 2544.6 ± 451.8 | 1143.8 ± 258.7 | 1276.3 ± 37.2 | 1564.3 ± 491.9 |
| 40-60 | 791.4 ± 73.9 | 633.6 ± 136.6 | 1872.9 ± 525.3 | 943.1 ± 188.1 | 544.8 ± 91.3 | 1175.0 ± 37.4 |
| 60-80 | 1430.5 ± 779.5 | 697.7 ± 163.8 | 1728.8 ± 261.6 | 778.8 ± 98.8 | 648.3 | 982.7 |
| 80-100 | 1171.8 ± 374.3 | 414.8 ± 108.4 | 2119.5 ± 537.7 | | | |
| 100-120 | 1570.2 ± 494.6 | 1650.1 ± 1377.5 | 2323.4 ± 656.3 | | | |
| 120-140 | 1675.1 ± 1033.5 | 416.7 ± 0.5 | 2627.0 ± 416.7 | | | |
| 140-160 | 1033.6 ± 300.4 | 766.0 ± 172.8 | 2528.6 ± 1295.6 | | | |
| 160-180 | 884.0 ± 81.0 | 301.4 | 1988.8 ± 421.6 | | | |
| 180-200 | 3337.4 ± 882.9 | | 2930.7 ± 1059.4 | | | |
| **SPECIFIC ROOT AREA ($cm^2$ $g^{-1}$)** | | | | | | |
| Depth (cm) | | | | | | |
| Organic layer | 342.4 ± 16.4 | 622.7 ± 155.7 | 832.0 ± 368.5 | 521.0 ± 138.4 | 378.3 ± 17.1 | 580.9 ± 29.8 |
| 0-10 | 273.7 ± 52.5 | 214.1 ± 11.2 | 281.1 ± 58.8 | 230.6 ± 19.0 | 278.8 ± 17.8 | 214.7 ± 10.9 |
| 10-20 | 237.5 ± 45.9 | 180.5 ± 24.3 | 217.2 ± 24.9 | 171.2 ± 26.6 | 173.4 ± 15.8 | 165.1 ± 17.5 |
| 20-40 | 212.6 ± 60.5 | 142.3 ± 18.1 | 270.5 ± 40.1 | 210.9 ± 66.1 | 189.3 ± 14.3 | 228.9 ± 74.8 |
| 40-60 | 156.8 ± 11.4 | 116.2 ± 13.0 | 247.3 ± 38.2 | 138.1 ± 13.2 | 102.1 ± 16.1 | 196.1 ± 38.6 |
| 60-80 | 203.3 ± 61.3 | 135.5 ± 23.9 | 220.6 ± 37.4 | 121.2 ± 3.9 | 123.7 | 122.4 |
| 80-100 | 212.5 ± 48.4 | 95.6 ± 16.7 | 224.6 ± 35.4 | | | |
| 100-120 | 259.9 ± 53.9 | 212.1 ± 134.1 | 239.8 ± 49.0 | | | |
| 120-140 | 222.5 ± 83.6 | 92.1 ± 0.8 | 329.9 ± 51.8 | | | |
| 140-160 | 198.9 ± 24.1 | 199.7 ± 60.3 | 316.6 ± 154.2 | | | |
| 160-180 | 175.4 ± 10.7 | 95.6 | 226.3 ± 13.5 | | | |
| 180-200 | 411.7 ± 75.2 | | 294.0 ± 65.2 | | | |
| 180-200 | 3337.4 ± 882.9 | | 2930.7 ± 1059.4 | | | |

**TABLE S3.4: Average fine root diameter and root tip frequency for the organic layer and mineral top- and subsoil of the six investigated mature beech forests. Shown are means + SE of three soil pits per site.**

| Plot no. | 1 | 2 | 3 | 4 | 5 | 6 |
|---|---|---|---|---|---|---|
| Site code | GR | HM | RU | EG | DR | GW |
| Substrate type | Pleistocene sand | Tertiary sand | Loess | Sandstone | Basalt | Limestone |
| **AVERAGE ROOT DIAMETER (mm)** | | | | | | |
| Depth (cm) | | | | | | |
| Organic layer | 0.55 ± 0.06 | 0.32 ± 0.05 | 0.47 ± 0.05 | 0.47 ± 0.02 | 0.48 ± 0.02 | 0.56 ± 0.03 |
| 0-10 | 0.52 ± 0.06 | 0.41 ± 0.02 | 0.43 ± 0.03 | 0.45 ± 0.02 | 0.45 ± 0.03 | 0.44 ± 0.02 |
| 10-20 | 0.57 ± 0.09 | 0.62 ± 0.08 | 0.46 ± 0.07 | 0.60 ± 0.05 | 0.51 ± 0.05 | 0.47 ± 0.01 |
| 20-40 | 0.56 ± 0.07 | 0.58 ± 0.06 | 0.38 ± 0.05 | 0.63 ± 0.03 | 0.51 ± 0.03 | 0.49 ± 0.01 |
| 40-60 | 0.62 ± 0.03 | 0.61 ± 0.08 | 0.42 ± 0.05 | 0.51 ± 0.06 | 0.62 ± 0.02 | 0.49 ± 0.08 |
| 60-80 | 0.64 ± 0.08 | 0.65 ± 0.02 | 0.48 ± 0.08 | 0.51 ± 0.05 | 0.61 | 0.45 |
| 80-100 | 0.61 ± 0.08 | 0.82 ± 0.07 | 0.38 ± 0.05 | | | |
| 100-120 | 0.58 ± 0.07 | 0.77 ± 0.23 | 0.37 ± 0.05 | | | |
| 120-140 | 0.60 ± 0.14 | 0.72 ± 0.01 | 0.42 ± 0.06 | | | |
| 140-160 | 0.68 ± 0.11 | 0.82 ± 0.10 | 0.41 ± 0.04 | | | |
| 160-180 | 0.65 ± 0.02 | 1.01 | 0.42 ± 0.10 | | | |
| 180-200 | 0.43 ± 0.06 | | 0.40 ± 0.06 | | | |
| **ROOT TIP FREQUENCY (n $g^{-1}$)** | | | | | | |
| Depth (cm) | | | | | | |
| Organic layer | 19647 ± 2957 | 25355 ± 5777 | 50395 ± 29441 | 30748 ± 2750 | 35306 ± 8147 | 33873 ± 7477 |
| 0-10 | 21317 ± 6290 | 27466 ± 6289 | 21250 ± 511 | 23216 ± 2862 | 20534 ± 2809 | 27916 ± 10838 |
| 10-20 | 13580 ± 3540 | 20280 ± 5037 | 19797 ± 1998 | 16911 ± 2456 | 13791 ± 1515 | 14451 ± 2985 |
| 20-40 | 14407 ± 4666 | 15488 ± 5128 | 25153 ± 1966 | 15517 ± 5393 | 16465 ± 2800 | 22691 ± 6703 |
| 40-60 | 7696 ± 4333 | 24932 ± 11865 | 28754 ± 9068 | 11523 ± 7076 | 6062 ± 1721 | 17805 ± 456 |
| 60-80 | 5085 ± 1075 | 4483 ± 1903 | 16685 ± 6197 | 14925 ± 12885 | 5196 | 67972 |
| 80-100 | 2997 ± 1191 | 6896 ± 1885 | 15481 ± 3107 | | | |
| 100-120 | 6472 ± 4101 | 5029 ± 133 | 25419 ± 4676 | | | |
| 120-140 | 6840 ± 4624 | 24544 ± 18614 | 10443 ± 2607 | | | |
| 140-160 | 9390 ± 6380 | 2561 ± 1048 | 13164 ± 2974 | | | |
| 160-180 | 12389 ± 9062 | | 13322 ± 2157 | | | |
| 180-200 | 17589 ± 5613 | | 34133 ± 18197 | | | |

**TABLE S3.5: Root length index (RLI) and root area index (RAI) for the organic layer and mineral top- and subsoil of the six investigated mature beech forests. Shown are means + SE of three soil pits per site.**

| Plot no. | 1 | 2 | 3 | 4 | 5 | 6 |
|---|---|---|---|---|---|---|
| Site code | GR | HM | RU | EG | DR | GW |
| Substrate type | Pleistocene sand | Tertiary sand | Loess | Sandstone | Basalt | Limestone |
| **RLI (cm m$^{-2}$)** | | | | | | |
| Depth (cm) | | | | | | |
| Organic layer | 158095 ± 45710 | 43900 ± 4143 | 49956 ± 23211 | 47659 ± 5359 | 48471 ± 918 | 58208 ± 18245 |
| 0-10 | 80831 ± 42450 | 313913 ± 59886 | 174378 ± 61265 | 284711 ± 55799 | 160130 ± 42339 | 178661 ± 20076 |
| 10-20 | 101900 ± 6251 | 92777 ± 7405 | 139918 ± 8326 | 78546 ± 17693 | 94326 ± 25028 | 89452 ± 14770 |
| 20-40 | 178738 ± 52601 | 72474 ± 15723 | 95892 ± 29807 | 45708 ± 2224 | 53931 ± 5969 | 54757 ± 4431 |
| 40-60 | 54707 ± 14464 | 59169 ± 19794 | 129151 ± 34887 | 44561 ± 11954 | 47477 ± 17953 | 103349 ± 13578 |
| 60-80 | 30206 ± 8199 | 27999 ± 7618 | 115027 ± 59930 | 20345 ± 6065 | 19557 | 76276 |
| 80-100 | 22678 ± 12576 | 20660 ± 8728 | 101378 ± 31687 | | | |
| 100-120 | 15591 ± 12581 | 7048 ± 6773 | 48143 ± 33227 | | | |
| 120-140 | 13504 ± 7276 | 8431 ± 1724 | 67360 ± 35403 | | | |
| 140-160 | 16948 ± 8134 | 3804 ± 1661 | 32073 ± 7772 | | | |
| 160-180 | 1974 ± 644 | 254 | 24537 ± 5197 | | | |
| 180-200 | 7035 ± 3875 | | 48160 ± 15396 | | | |
| Profile total | 675901 ± 140324 | 640562 ± 90536 | 1025974 ± 248209 | 521530 ± 68783 | 394697 ± 94114 | 475402 ± 53626 |
| **RAI (cm$^2$ m$^{-2}$)** | | | | | | |
| Depth (cm) | | | | | | |
| Organic layer | 23402 ± 6944 | 4451 ± 966 | 6405 ± 2170 | 6272 ± 761 | 7340 ± 473 | 9032 ± 2437 |
| 0-10 | 13031 ± 6244 | 38528 ± 5561 | 22586 ± 7596 | 37812 ± 6469 | 21232 ± 5277 | 23887 ± 3723 |
| 10-20 | 17144 ± 3815 | 15563 ± 235 | 17799 ± 2457 | 14099 ± 3394 | 13859 ± 3634 | 12582 ± 2060 |
| 20-40 | 29813 ± 7019 | 11368 ± 1597 | 9704 ± 1617 | 8064 ± 243 | 7954 ± 915 | 7946 ± 258 |
| 40-60 | 10983 ± 3030 | 10597 ± 2433 | 18883 ± 7265 | 7028 ± 2078 | 9002 ± 3446 | 16659 ± 1663 |
| 60-80 | 5478 ± 2033 | 5634 ± 1662 | 14647 ± 7463 | 3251 ± 1017 | 3730 | 9498 |
| 80-100 | 4529 ± 2475 | 4648 ± 1627 | 12564 ± 5728 | | | |
| 100-120 | 3153 ± 2642 | 1738 ± 1682 | 6150 ± 4717 | | | |
| 120-140 | 2921 ± 1601 | 1867 ± 394 | 8546 ± 4801 | | | |
| 140-160 | 3082 ± 1065 | 983 ± 482 | 4203 ± 1268 | | | |
| 160-180 | 399 ± 141 | 80 | 3124 ± 964 | | | |
| 180-200 | 1066 ± 673 | | 5750 ± 2557 | | | |
| Profile total | 113842 ± 26627 | 93231 ± 7056 | 130362 ± 41818 | 76525 ± 7787 | 58185 ± 12027 | 67719 ± 9013 |

## 3.7 References

Aber, J.D., Melillo, J.M., Nadelhoffer, K.J., McClaugherty, C.A., and Pastor, J. (1985) Fine root turnover in forest ecosystems in relation to quantity and form of nitrogen availability: a comparison of two methods. Oecologia 66:317–321.

Bauhus, J., and Bartsch, N. (1996) Fine-root growth in beech (*Fagus sylvatica*) forest gaps. Canadian Journal of Forest Research 26(12):2153-2159.

Bradshaw, A.D. (1965) Evolutionary significance of phenotypic plasticity in plants. Advances in Genetics 13:115–155.

Braun, S., Cantaluppi, L., and Flückiger, W. (2005) Fine roots in stands of *Fagus sylvatica* and *Picea abies* along a gradient of soil acidification. Environmental Pollution 137:574-579.

Campbell, B.D., Grime, J.P., and Mackey, J.M.L. (1991) A trade-off between scale and precision in resource foraging. Oecologia,87:532–538.

Canadell, J., Jackson, R.B., Ehleringer, J.R., Mooney, H.A., Sala, O.E., and Schulze, E.-D. (1996) Maximum rooting depth of vegetation types at the global scale. Oecologia 108:583-595.

Comas, L.H., and Eissenstat, D.M. 2009. Patterns in root trait variation among 25 co-existing North American forest species. New Phytologist 182:919–928.

Eissenstat, D.M., and Yanai, R.D. (1997) The ecology of root lifespan. Advances in Ecological Research 27:1–60.

Farley, R.A., and Fitter, A.H. (1999) The responses of seven co-occurring woodland herbaceous perennials to localized nutrient-rich patches. Ecology 87:849–859.

Finér, L., Helmisaari, H.-S., Lõhmus, K., Majdi, H., Brunner, I., Børja, I., Eldhuset, T., Godbold, D., Grebenc, T., Konôpka, B., Kraigher, H., Möttönen, M.-R., Ohashi, M., Oleksyn, J., Ostonen, I., Uri, V., and Vanguelova, E. (2007) Variation in fine root biomass of three European tree species: Beech (*Fagus sylvatica* L.), Norway spruce (*Picea abies* L. Karst.), and Scots pine (*Pinus sylvestris* L.). Plant Biosystems 141:394–405.

Fitter, A.H. (1994) Architecture and biomass allocation as components of the plastic response of root systems to soil heterogeneity. In: Caldwell, M.M., and Pearcy, R.W. (eds.) Exploitation of environmental heterogeneity by plants, Academic Press, San Diego, USA, 305–323.

Fogel, R. (1985) Roots as primary producers in below-ground ecosystems. In: Fitter, A.H., Atkinson, D., Read, D.J., and Usher, M.B. (eds.) Ecological Interactions in Soil: Plants Microbes and Animals, Special Publication No. 4 of the British Ecological Society, Blackwell Scientific Publications, Oxford, UK, 23–36.

Fogel, R., and Hunt, G. (1983) Contribution of mycorrhizae and soil fungi to nutrient cycling in a Douglas-fir ecosystem. Canadian Journal of Forest Research 13:219–232.

Forde, B., and Lorenzo, H. (2001) The nutritional control of root development. Plant and soil 232(1-2):51-68.

Gale, M.R., and Grigal, D.F. (1987) Vertical root distributions of northern tree species in relation to successional status. Canadian Journal of Forest Research 17(8):829-834.

Gill, R.A., Burke, I.C. (2002) Influence of soil depth on the decomposition of Bouteloua gracilis roots in the shortgrass step. Plant Soil 241:233-242.

Gill, R.A., and Jackson, R.B. (2000) Global patterns of root turnover for terrestrial ecosystems. New Phytologist 147:13–31.

Godbold, D.L., Fritz, H.W., Jentschke, G., Meesenburg, H., and Rademacher, P. (2003) Root turnover and root necromass accumulation of Norway spruce (Picea abies) are affected by soil acidity. Tree Physiology 23:915-921.

Gower, S.T., Vogt, K.A., and Grier, C.C. (1992) Carbon dynamics of Rocky Mountain Douglas-fir: influence of water and nutrient availability. Ecological Monographs 62:43-65.

Guo, D.L., Xia, M.X., Wie, X., Chang, W.J., Liu, Y., and Wang, Z.Q. (2008) Anatomical traits associated with absorption and mycorrhizal colonization are linked to root branch order in twenty-three Chinese temperate tree species. New Phytol 180:673–683. https://doi.org/10.1111/j.1469-8137.2008.02573.x

Harper, R.J., and Tibbett, M. (2013) The hidden organic carbon in deep mineral soils. Plant Soil 368:641–648. doi: 10.1007/s11104-013-1600-9.

Harrison, R., Footen, P., and Strahm, B. (2011) Deep soil horizons: contribution and importance to soil carbon pools and in assessing whole-ecosystem response to management and global change. For Sci 57:67–76.

Hartmann, P., and von Wilpert, K. (2014) Fine-root distributions of Central European forest soils and their interaction with site and soil properties. Can J For Res 44:71-81.

Hendrick, R.L., and Pregitzer, K.S. (1997) The relationship between fine root demography and the soil environment in northern hardwood forests. Ecoscience 4(1):99-105.

Hertel, D. (1999) Das Feinwurzelsystem von Rein-und Mischbeständen der-Rotbuche: Struktur, Dynamik und interspezifische Konkurrenz. Dissertationes Botanicae 317, J. Cramer, Berlin, Stuttgart.

Hertel, D., Strecker, T., Müller-Haubold, H., and Leuschner, C. (2013) Fine root biomass and dynamics in beech forests across a precipitation gradient – is optimal resource partitioning theory applicable to water-limited mature trees? Journal of Ecology 101:1183–1200.

Hodge, A. (2004) The plastic plant: root responses to heterogeneous supplies of nutrients. New Phytologist 162:9–24.

Hodge, A. (2006) Plastic plants and patchy soils. Journal of Experimental Botany 57(2):401–411.

Hutchings, M.J., and de Kroon, H. (1994) Foraging in plants: the role of morphological plasticity in resource acquisition. Adv Ecol Res 25:159–238.

Jackson, R.B., Canadell, J., Ehleringer, J.R., Mooney, H.A., Sala, O.E., and Schulze, E.D. (1996) A global analysis of root distributions for terrestrial biomes. Oecologia 108:389-411.

Jackson, R.B., Mooney, H.A., and Schulze, E.D. (1997) A global budget for fine root biomass, surface area, and nutrient contents. Proceedings of the National Academy of Sciences United States of America 94:7362–7366.

Jentschke, G., Drexhage, M., Fritz, H.-W., Fritz, E., Schella, B., and Lee, D.-H. (2001) Does soil acidity reduce subsoil rooting in Norway spruce (Picea abies)? Plant Soil 237:91–108.

Jobbágy, E.G., and Jackson, R.B. (2000) The vertical distribution of soil organic carbon and its relation to climate and vegetation. Ecological applications 10(2):423-436.

Jobbágy, E.G., and Jackson, R.B. (2001) The distribution of soil nutrients with depth: global patterns and the imprint of plants. Biogeochemistry 53(1):51-77.

Keyes, M.R., and Grier, C.C. (1981) Above- and below-ground net production in 40-year-old Douglas-fir stands on low and high productivity sites. Canadian Journal of Forest Research 11:599-605.

Koarashi, J., Hockaday, W.C., Masiello, C.A., and Trumbore, S.E. (2012) Dynamics of decadally cycling carbon in subsurface soils. J Geophys 117:G03033. doi: 10.1029/2012JG002034.

Kottke, I., and Agerer, R. (1983) Untersuchungen zur Bedeutung der Mykorrhiza in älteren Laub- und Nadelwaldbeständen des südwestlichen Keuperberglandes. Mitt Ver Forstl Standortsk Forstpflanzenzüchtung, Bundesrepublik Deutschl 30:30–39.

Le Goff, N., and Ottorini, J.-M. (2001) Root biomass and biomass increment in a beech (*Fagus sylvatica* L.) stand in North-East France. Ann For Sci 58:1–13.

Lehmann, J. (2003) Subsoil root activity in tree-based cropping systems. Plant and Soil 255:319–331.

Leuschner, C., and Hertel, D. (2003) Fine Root Biomass of Temperate Forests in Relation to Soil Acidity and Fertility, Climate, Age and Species. Progress in Botany 64:405-438.

Leuschner, C., Hertel, D., Coners, H., and Büttner, V. (2001) Root competition between beech and oak: a hypothesis. Oecologia 126:276–284.

Leuschner, C., Hertel, D., Muhs, A., and Schmid, I. (1998) Feinwurzel-Bestandesmassen der Rotbuche an verschiedenen Standorten innerhalb ihrer ökologischen Amplitude in Nordwest- und Mitteldeutschland. Verhandlungen der Gesellschaft für Ökologie 28:429-434.

Leuschner, C., Hertel, D., Schmid, I., Koch, O., Muhs, A., and Hölscher, D. (2004) Stand fine root biomass and fine root morphology in old-growth beech forests as a function of precipitation and soil fertility. Plant and Soil 258:43–56.

Leuschner, C., Voss, S., Foetzki, A., and Clases, Y. (2006) Variation in leaf area index and stand leaf mass of European beech (*Fagus sylvatica* L.) across gradients of soil acidity and precipitation. Plant Ecology 186:247-258.

Leuschner, C., Wulf, M., Bäuchler, P., and Hertel, D. (2014) Forest continuity as a key determinant of soil carbon and nutrient storage in beech forests on sandy soils in Northern Germany. Ecosystems 17:497-511.

Leuschner, C., and Ellenberg, H. (2017) Ecology of Central European Forests. Vegetation Ecology of Central Europe, Vol I, Springer Nature, Cham, Switzerland.

Maeght, J.-L., Rewald, B., Pierret, A. (2013) How to study deep roots — and why it matters. Frontiers in plant science 4:1-14.

Mainiero, R., and Kazda, M. (2006) Depth-related fine root dynamics of *Fagus sylvatica* during exceptional drought. Forest Ecology and Management 237:135–142.

McCormack, M.L., Dickie, I.A., Eissenstat, D.M., Fahey, T.J., Fernandez, C.W., Guo, D., Helmisaari, H.-S., Hobbie, E.A., Iversen, C.M., Jackson, R.B., Leppälammi-Kujansuu, J., Norby, R.J., Phillips, R.P., Pregitzer, K.S., Pritchard, S.G., Rewald, B., and Zadworny, M. (2015) Redefining fine roots improves understanding of below-ground contributions to terrestrial biosphere processes. New Phytologist 207:505–518.

Meier, I.C., Knutzen, F., Eder, L.M., Müller-Haubold, H., Goebel, M.O., Bachmann, J., Hertel, D., and Leuschner, C. (2017) The Deep Root System of *Fagus sylvatica* on Sandy Soil: Structure and Variation Across a Precipitation Gradient. Ecosystems 21(2):280-296. doi:10.1007/s10021-017-0148-6.

Meyer, F.H. (1967) Feinwurzelverteilung bei Waldbäumen in Abhängigkeit vom Substrat. Forstarchiv 38:286-290.

Neatrour, M.A., Jones, R.H., and Golladay, S.W. (2005) Correlations between soil nutrient availability and fine-root biomass at two spatial scales in forested wetlands with contrasting hydrological regimes. Canadian Journal of Forest Research 35(12):2934-2941.

Ostonen, I., Püttsepp, Ü., Biel, C., Alberton, O., Bakker, M.R., Lõhmus, K., Majdi, H., Metcalfe, D., Olsthoorn, A.F.M., Pronk, A., Vanguelova, E., Weih, M., and Brunner, I. (2007) Specific root length as an indicator of environmental change. Plant Biosystems - An International Journal Dealing with all Aspects of Plant Biology 141(3):426-442. DOI: 10.1080/11263500701626069.

Pierret, A., Doussan, C., Capowiez, Y., Bastardie, F., and Pagès, L. (2007) Root Functional Architecture: A Framework for Modeling the Interplay between Roots and Soil. Vadose Zone Journal 6(2):269-281.

Poorter, H., and Nagel, O. (2000) The role of biomass allocation in the growth response of plants to different levels of light, $CO_2$, nutrients and water: a quantitative review. Australian Journal of Plant Physiology 27:595–607.

Pregitzer, K.S., DeForest, J.L., Burton, A.J., Allen, M.F., Ruess, R.W., and Hendrick, R.L. (2002) Fine root architecture of nine North American trees. Ecological Monographs 72:293–309.

Rasse, D.P., Rumpel, C., and Dignac, M.-F. (2005) Is soil carbon mostly root carbon? Mechanisms for a specific stabilization. Plant and Soil 269:341-356.

Runge, M. (1983) Physiology and ecology of nitrogen nutrition. In: Lange, O.L., Nobel, P.S., Osmond, C.B., and Ziegler, H. (eds.) Encyclopedia of Plant Physiology, New Series, Physiological Ecology III, Springer, Berlin, 163-200.

Ryser, P. (1998) Intra- and interspecific variation in root length, root turnover and the underlying parameters. In: Lambers, H., Poorter, H., and VanVuuren, M. (eds.) Inherent variation in plant growth: Physiological mechanisms and ecological consequences, Backhuys, Leiden, Netherlands, 441–465.

Santner, A., Calderon-Villalobos, L.I.A., and Estelle, M. (2009) Plant hormones are versatile chemical regulators of plant growth. Nat Chem Biol 5:301–307. doi: 10.1038/nchembio.165.

Schenk, H.J., and Jackson, R.B. (2002) The global biogeography of roots. Ecological Monographs 72:311–328.

Schenk, H.J., and Jackson, R.B. (2005) Mapping the global distribution of deep roots in relation to climate and soil characteristics. Geoderma 126:129-140.

Schmid, I. (2002) The influence of soil type and interspecific competition on the fine root system of Norway spruce and European beech. Basic Appl Ecol 3:339–346.

Stone, E.L., and Kalisz, P.J. (1991) On the maximum extent of tree roots. Forest Ecology and Management 46:59-102.

Van Praag, H.J., Sougnez-Remy, S., Weissen, F., and Carletti, G. (1988) Root turnover in a beech and a spruce stand of the Belgian Ardennes. Plant and soil 105(1):87-103.

Vogt, K.A., Vogt, D.J., Palmiotto, P.A., Boon, B., O´Hara, J., and Asbjornsen, H. (1996) Review of root dynamics in forest ecosystems grouped by climate, climatic forest type and species. Plant Soil 187:159-219.

World Clim: Global Climate Data Model http://www.worldclim.org/download, Access date: 3 February 2016

Yanai, R.D., Fahey, T.J., and Miller, S.L. (1995) Efficiency of nutrient acquisition by fine roots and mycorrhizae. In: Smith, W.K., and Hinkley, T.M. (eds.) Resource Physiology of Conifers, Academic Press, New York, 75-103.

Yuan, Z.Y., and Chen, Y.H. (2010) Fine root biomass, production, turnover rates, and nutrient contents in boreal forest ecosystems in relation to species, climate, fertility, and stand age: literature review and meta-analyses. Critical Rev Plant Sci 29:204-221.

# CHAPTER 4

# Influence of Root Diameter and Soil Depth on the Xylem Anatomy of Fine- to Medium-Sized Roots of Mature Beech Trees in the Top- and Subsoil

Kristina KIRFEL, Christoph LEUSCHNER, Dietrich HERTEL and Bernhard SCHULDT

FRONTIERS IN PLANT SCIENCE, 2017, 8:1194. DOI: 10.3389/fpls.2017.01194.

## 4.1 Abstract

Despite their importance for water uptake and transport, the xylem anatomical and hydraulic properties of tree roots have only rarely been studied in the field. We measured mean vessel diameter (*D*), vessel density (VD), relative vessel lumen area (lumen area per xylem area) and derived potential hydraulic conductivity ($K_p$) in the xylem of 197 fine- to medium-diameter roots (1–10 mm) in the topsoil and subsoil (0–200 cm) of a mature European beech forest on sandy soil for examining the influence of root diameter and soil depth on xylem anatomical and derived hydraulic traits. All anatomical and functional traits showed strong dependence on root diameter and thus root age but no significant relation to soil depth. Averaged over topsoil and deep soil and variable flow path lengths in the roots, *D* increased linearly with root diameter from ~50 µm in the smallest diameter class (1–2 mm) to ~70 µm in 6–7 mm roots (corresponding to a mean root age of ~12 years), but remained invariant in roots >7 mm. *D* never exceeded ~82 µm in the 1–10 mm roots, probably in order to control the risk of frost- or drought-induced cavitation. This pattern was overlain by a high variability in xylem anatomy among similar-sized roots with $K_p$ showing a higher variance component within than between root diameter classes. With 8% of the roots exceeding average $K_p$ in their diameter class by 50–700%, we obtained evidence of the existence of 'high-conductivity roots' indicating functional differentiation among similar-sized roots. We conclude that the hydraulic properties of small to medium diameter roots of beech are mainly determined by root age, rendering root diameter a suitable predictor of hydraulic functioning, while soil depth – without referring to path length – had a negligible effect.

**Keywords:** cambial aging, deep roots, *Fagus sylvatica*, hydraulic conductivity, high-conductivity roots, vascular differentiation, vessel diameter

## 4.2 Introduction

Water uptake and transport is a key function of the root system and essential for plant growth. and survival. Despite their decisive role for the provision of water to the shoot, the anatomical and hydraulic properties of the root system have only rarely been studied in comparison to the hydraulic system of aboveground organs (e.g., Brunner et al. 2015). This particularly applies to deep roots (McElrone et al. 2004; Gebauer and Volařík 2013; Maeght et al. 2013), although their importance for water uptake especially in dry periods is well recognized (Stone and Kalisz 1991; Domec et al. 2004; Bleby et al. 2010; David et al. 2013).

The function of a tree's hydraulic system is largely determined by the number, diameter, and length of xylem conduits within the network of conducting elements from roots to leaves (Lintunen and Kalliokoski 2010; Schuldt et al. 2013; Kotowska et al. 2015). Different xylem anatomical designs represent functional adaptations to variation in water availability among other environmental factors (Tyree et al. 1994a). High hydraulic conductance facilitates high rates of water movement and tree growth, but may imply high vulnerability to cavitation and xylem dysfunction induced by frost and drought (Tyree 2003a; Hajek et al. 2014). The hydraulic architecture of trees therefore results from a trade-off between mechanical requirements, hydraulic safety, and hydraulic efficiency, with the latter being most effectively provided by large conduit diameters according to the Hagen–Poiseuille law, since increases in conduit diameter exponentially enhance hydraulic conductivity (Tyree and Zimmermann 2002).

The anatomy of the xylem is highly heterogeneous at the interspecific level but also within a species or even a single tree (Sperry and Saliendra 1994; Sperry et al. 2006; Lachenbruch.et al. 2011; Schuldt et al. 2013; Chenlemuge et al. 2015; Kotowska et al. 2015). As one general structural principle of the hydraulic architecture of trees, a pattern of radial variation.in xylem anatomy and hence in hydraulic performance from pith to bark has frequently been observed in the stems of both angiosperm and gymnosperm trees: in general, the density of tracheids and vessels decreases in radial direction, while conduit length and diameter increase (Gartner 1995; Tyree 2003b; Christensen-Dalsgaard et al. 2008; Fan et al. 2009). This radial gradient in anatomical structure is thought to be caused by the process of cambial aging, and is generated, depending on the species, most pronouncedly in the first 5 to 40 years of a tree organ's lifespan (Fan et al. 2009; Lachenbruch et al. 2011). However, addressing cambial maturation does not

provide a mechanistic explanation and solely describes a developmental process that results in a change in the dimensions of cambial initials over time, which in turn affects the dimensions of xylem cells produced by the cambium (Spicer and Gartner 2001).

While the phenomenon of basipetal and radial conduit widening has often been recognized in tree stems, studies investigating radial patterns of xylem anatomy in tree roots are scarce. For the roots of Douglas-fir trees, the pattern could partly be confirmed by one study (Peterson et al. 2007), while Dunham et al. (2007), in contrast, reported a decrease in tracheid diameter and length, and specific conductivity with cambial age. Lintunen and Kalliokoski (2010) observed a generally large intra- and interspecific variation in radial xylem anatomical patterns.in the roots of three different tree species. Opposite to a trend towards smaller but more numerous conduits from pith to bark in the roots of Pinus sylvestris, in the roots of Betula pendula and Picea abies, conduit frequency decreased and mean conduit size increased from the pith to the bark in agreement with observations at the stem base. Apart from such radial gradients of root hydraulic architecture, most.studies.recognized.a.successive.increase.in the diameter of xylem conduits from the terminal branches to the stem, and further to the roots (Aloni 1987; Tyree and Zimmermann 2002; Hacke et al. 2016).

Soil depth-dependent changes in xylem architecture and hydraulic performance of roots have as well only rarely been the object of scientific study (e.g., Gebauer and Volařík 2013; Maeght et al., 2013; Wang et al. 2015; Pierret et al. 2016).. The results of the few existing studies indicate a gradient in root axial hydraulic conductivity as a result of xylem anatomical adaptations with increasing soil depth (Tyree 2003b). McElrone et al. (2004) reported decreasing conduit radii from the most distant 20 m deep-reaching roots to the shallow surface roots, and to the stem wood in four tree species of different systematic position and growth habit (evergreen vs. deciduous, angiosperm vs. gymnosperm). Correspondingly, Pate et al. (1995) observed a progressive increase in mean xylem conduit diameter and specific hydraulic conductivity (30- to 150-fold) from the stem to the lateral roots and with soil depth in the sinker roots of different Proteaceae species. Investigating xylem anatomical and hydraulic properties in small roots of two different oak species at different soil depths, Gebauer and Volařík (2013) found a higher specific hydraulic conductivity due to larger vessel diameters in roots in 50 cm depth than at the surface, but no further increase in these traits from 50 to 100 cm depth. They assumed that vessel

diameters in roots at the soil surface are limited in order to avoid cavitation due to freeze-thaw cycles. In three temperate hardwood tree species, a depth-dependent increase in specific hydraulic conductivity was observed in the tree fine root system: first-order roots exhibited 78 to 217% greater specific hydraulic conductivities in the subsurface (20–30 cm soil depth) than in the surface layer (0–10 cm soil depth) in the same species (Wang et al. 2015). In this case, the higher hydraulic efficiency appeared to be not solely a function of wider maximum conduit diameters, but also to result from a higher conduit frequency and greater xylem to cross-sectional area ratio.

Systematic influences of position in the conductive system and cambial age on the xylem anatomy and hydraulic architecture of roots may be masked by a great anatomical variation across roots of the same soil depth and age (Rewald et al. 2011; Köcher et al. 2012; Hajek et al. 2014). These authors observed an anatomically deviating form of roots which they termed 'high-conductivity roots' with an up to 10-fold higher specific hydraulic conductivity compared to the mean of roots. Such specialized roots were found in mature trees of several deciduous species including *Fagus sylvatica*. The high hydraulic conductivity of these roots was in most cases caused by the existence of a few very large vessels, but in others also by a large increase in vessel density, or by a combination of both anatomical adaptations. It is not well understood how frequent such 'high-conductivity roots' are and in which part of the root system they are occurring.

In this study, we analyzed the intraspecific variability in xylem anatomical and derived hydraulic traits of small- and medium-sized roots (1–10 mm in diameter) in the top- and subsoil down to a depth of 200 cm in a mature *F. sylvatica* L. (European beech) forest stand in Northern Germany. We hypothesized that (i) vessel diameter and hydraulic conductivity is a function of root diameter and, thus, of root age, (ii) the variability in xylem anatomical and hydraulic traits in similar-sized roots is high at a given soil depth with some roots exhibiting characteristics of 'high-conductivity roots,' and (iii) vessel diameter and consequently hydraulic conductivity increase with increasing soil depth.

## 4.3 Material and Methods

### *Study Site and Field Sampling*

The study site is located in the Grinderwald in the Pleistocene lowlands of Lower Saxony, Germany, 33 km northwest of Hannover (52° 34’ 22,115 North, 9° 18’ 49,762 East), 106 m above sea level. The climate is cool-temperate with a mean annual temperature of 8.7°C, and a mean annual precipitation of 718 mm. The even-aged mature forest stand was established in 1914 and is dominated by *F. sylvatica* L. with admixture of single trees of other species. Mean stem density is 407 stems $ha^{-1}$, mean diameter at breast height is 26.3 cm, and mean basal area 27.1 $m^2$ $ha^{-1}$. The predominant soil type at the study site is an acid (pH 3.4–4.5), sandy Dystric Cambisol which developed from Pleistocene fluvial and aeolian sandy deposits from the penultimate (Saale) glaciation.

In order to analyze the soil depth influence on the wood anatomical and derived hydraulic properties of the roots, fine-, small- and medium-sized (Supplementary Table S4.1) beech root segments were collected in autumn 2013 in three soil pits that were dug to 200 cm depth in the stand. Root segments of ~10 cm length originating from the neighboring trees were sampled on the 200 cm-wide profile walls at 7 soil depths from 0–20 to 160–200 cm. In each soil pit and soil depth, 6–10 root segments were selected covering all root diameters between 1 and 10 mm, yielding 197 analyzed root segments in total (Supplementary Table S4.1). The sampled root segments were cleaned from soil residues and immediately transferred to 70% ethanol for storage.

Since we assumed a generally high variability in xylem anatomical and hydraulic traits for similar-sized roots, we additionally investigated the effect of root age on root xylem characteristics and hydraulic properties in individual root strands for being able to separate age effects on root anatomy from possible depth-dependent and flow-path length induced changes in these traits. Therefore, we additionally excavated four complete root strands (root individuals with their main axes and appending secondary and higher-order branch roots) belonging to three different tree individuals located in the organic and topsoil layer. From each strand, 6–10 segments covering as many root diameter classes between 2 and 10 mm as possible were processed, yielding 42 analyzed segments in total.

***Xylem Anatomical and Derived Hydraulic Properties of Beech Roots***

All root samples were stained with safranin (1% in 50% ethanol, Merck, Darmstadt, Germany) and washed with 70% ethanol prior to cutting. Subsequently, 10–20 mm semi-thin transverse sections were cut using a sliding microtome (G.S.L.1, WSL Birmensdorf, Switzerland). We processed and analyzed images of each cross-sectional transverse section taken with a stereo-microscope equipped with an automatic stage and a digital camera (SteREOV20, Carl Zeiss MicroImaging GmbH, Göttingen, Germany) at 100× magnification using Adobe Photoshop CS6 (version 13.0 x 64, Adobe Systems Incorporated, United States) and the particle analysis function from ImageJ (version 1.49 v).

Root age (years) was determined by counting growth rings in each sample. However, contrary to stems and branches, growth rings in roots are sometimes difficult to identify and false rings might have been counted in certain roots. Consequently, our root age determination may partly over- or underestimate real age. The complete cross-section was analyzed (mean SE of analyzed root xylem area: 15.69 ± 0.95 $mm^2$), yielding 116 to 5,871 measured vessels per sample, and 319,293 analyzed vessels in total. For the complete xylem cross-sectional area ($A_{xylem}$, $mm^2$) without bark, we determined vessel density (VD, n $mm^{-2}$) and calculated the relative vessel lumen area ($A_{lumen}$:$A_{xylem}$, %), i.e., the relative proportion of cumulative vessel lumen area ($A_{lumen}$, $mm^2$) in percent of $A_{xylem}$. The idealized mean vessel diameter ($D$, mm) was obtained from major (a) and minor (b) vessel radii according to the equation given by Lewis and Boose (1995) as $D = ((32 \times (a \times b)^3) / (a^2 + b^2))^{1/4}$. In addition to $D$, the maximum vessel diameter of a given root sample is given ($D_{max}$, mm). The hydraulically weighted vessel diameter ($D_h$, mm), in which each vessel is weighted proportionally to its contribution to total hydraulic conductance, was calculated from single vessel diameters ($D$) according to Sperry et al. (1994) as $D_h = \Sigma D^5 / \Sigma D^4$. Potential hydraulic conductivity ($K_p$, kg $m^{-1}$ $MPa^{-1}$ $s^{-1}$) was calculated according to the Hagen–Poiseuille equation as $K_p = (((\pi \times \Sigma r^4) / 8\eta) \times \rho) / A_{xylem}$, where $\eta$ is the viscosity of water (1.002 $10^{-9}$ MPa s), $\rho$ the density of water (998.2 kg $m^{-3}$), both at 20 °C, and $A_{xylem}$ ($m^2$) the corresponding xylem area.

### *Statistical Analyses*

Statistical analyses were performed with the software package R (R Core Team, 2013, version 3.4.0) except for linear regression analyses which were executed with the software XACT 8.03 (SciLab, Hamburg, Germany). During the analysis, normal distribution of the residuals and homogeneity of variance were assessed visually using residual diagnostics and quantile-quantile plots; if the assumption of normality was not met data were log-transformed. Linear mixed effect (LME) models with soil depth, root diameter and their interaction as fixed continuous variables were applied to analyze their influence on the xylem anatomical and derived hydraulic properties with the '*lme*' routine of the '*nlme*' package. We assumed non-independence of the three soil pits in the stand by adding soil pit as random effect. Additionally, we accounted for deviations from the assumed linear trend with soil depth resulting from spatial dependence in root samples by adding a random effect for a given soil depth as distinct variable nested in soil pit.

In order to estimate the variability in xylem anatomical and hydraulic traits in similar-sized roots, we divided the dataset into 9 different root diameter classes (1–2, 2–3 mm, and so on). The ratio of diameter class variance component to total variance was calculated using the R package '*varComp*' according to a variance component analysis with the program '*lme*' to calculate the proportion of total variance explained by the variability between root diameter classes ($\sigma^2_{inter}$) and residual variance within root diameter classes ($\sigma^2_{intra}$). Variance component between root diameter classes ($VC_{inter}$) was calculated according to $VC_{inter} = (\sigma^2_{inter} / (\sigma^2_{inter} + \sigma^2_{intra})) \times 100$ and variance component within root diameter classes ($VC_{intra}$) as $VC_{intra} = (\sigma^2_{intra} / (\sigma^2_{intra} + \sigma^2_{inter})) \times 100$, all in percentage. We additionally calculated $VC_{inter}$ and $VC_{intra}$ for the variability between and within the seven investigated soil depth classes.

## 4.4 Results

***Effect of Root Diameter on Xylem Anatomical and Derived Hydraulic Traits***

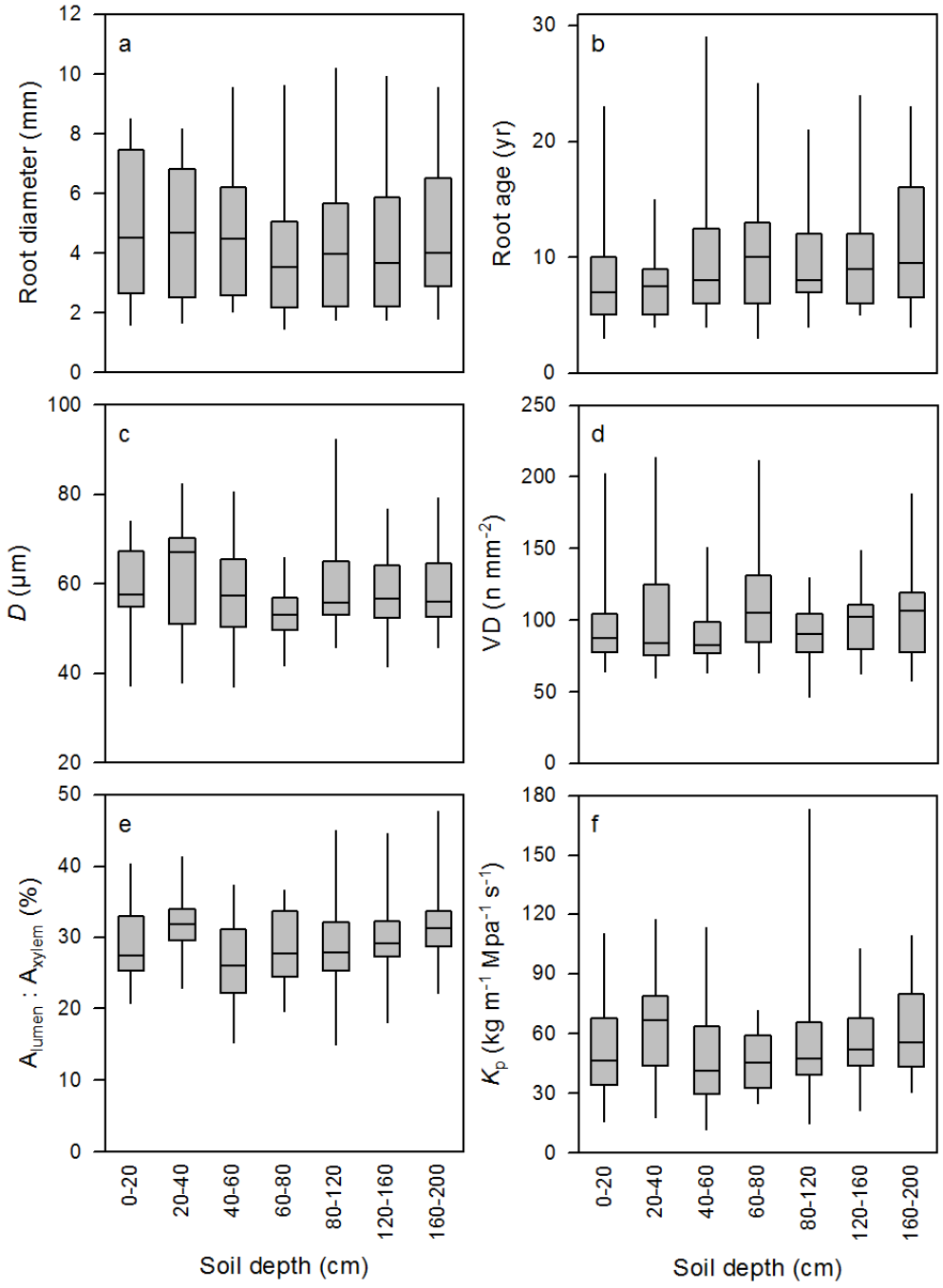


**FIGURE 4.1: Box-whisker plots (with median, 25 and 75% quantiles and extreme values) for the variation in root diameter (A), root age (B), mean vessel diameter (C, *D*), vessel density (D, VD), relative vessel lumen area (E, $A_{lumen}$: $A_{xylem}$), and potential hydraulic conductivity (F, $K_p$) in seven different soil depth classes.**

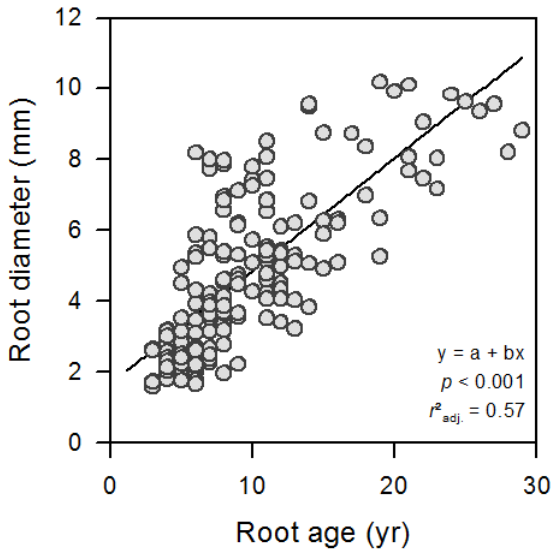


**FIGURE 4.2: Root diameter in relation to root age in the sample of 197 roots.**

The results of the LME model covering roots of all diameter classes from all seven soil depth classes down to a depth of 200 cm (see Supplementary Table S4.1 and Figure 4.1A) showed a significant influence of root diameter on all studied xylem anatomical and hydraulic traits (Table 4.1). Although root diameter varied considerably among the roots of a given root age, both parameters were tightly linked to each other ($P < 0.001$; $r^2 = 0.57$; Figure 4.2). The regression analyses exhibited a strong linear positive relationship between root diameter and mean vessel diameter ($D$) and potential hydraulic conductivity ($K_p$) up to the diameter class 6–7 mm, followed by a slight decrease in $D$ (from ~69 to ~66 mm) and $K_p$ for larger roots (Figures 4.3A,D). The mean $K_p$ values were 42.6, 59.0 and 60.2 kg $m^{-1}$ $MPa^{-1}$ $s^{-1}$ for roots of 2–3, 4–5, and 5–6 mm in diameter, respectively (Figure 4.3D). Inversely, mean vessel density (VD) significantly declined with increasing root diameter up to the diameter class 6–7 mm (Figure 4.3B). Since the hydraulically weighted vessel diameter ($D_h$) exhibited the same relationships to the analyzed parameters as D, we refrain from discussing this parameter further in order to avoid redundancies.

Despite the significant correlation between root diameter and xylem anatomical and hydraulic parameters, we found a high variability in these traits for similar-sized roots. Within a root diameter class, $D$ varied between the extremes by 54–80% and $K_p$ by 210–720% (average variation of $D$ and $K_p$ by ~39 and ~76%, respectively). Accordingly, the variance component of both traits within a diameter class is similar to, or larger than that between diameter classes (Table 4.1).

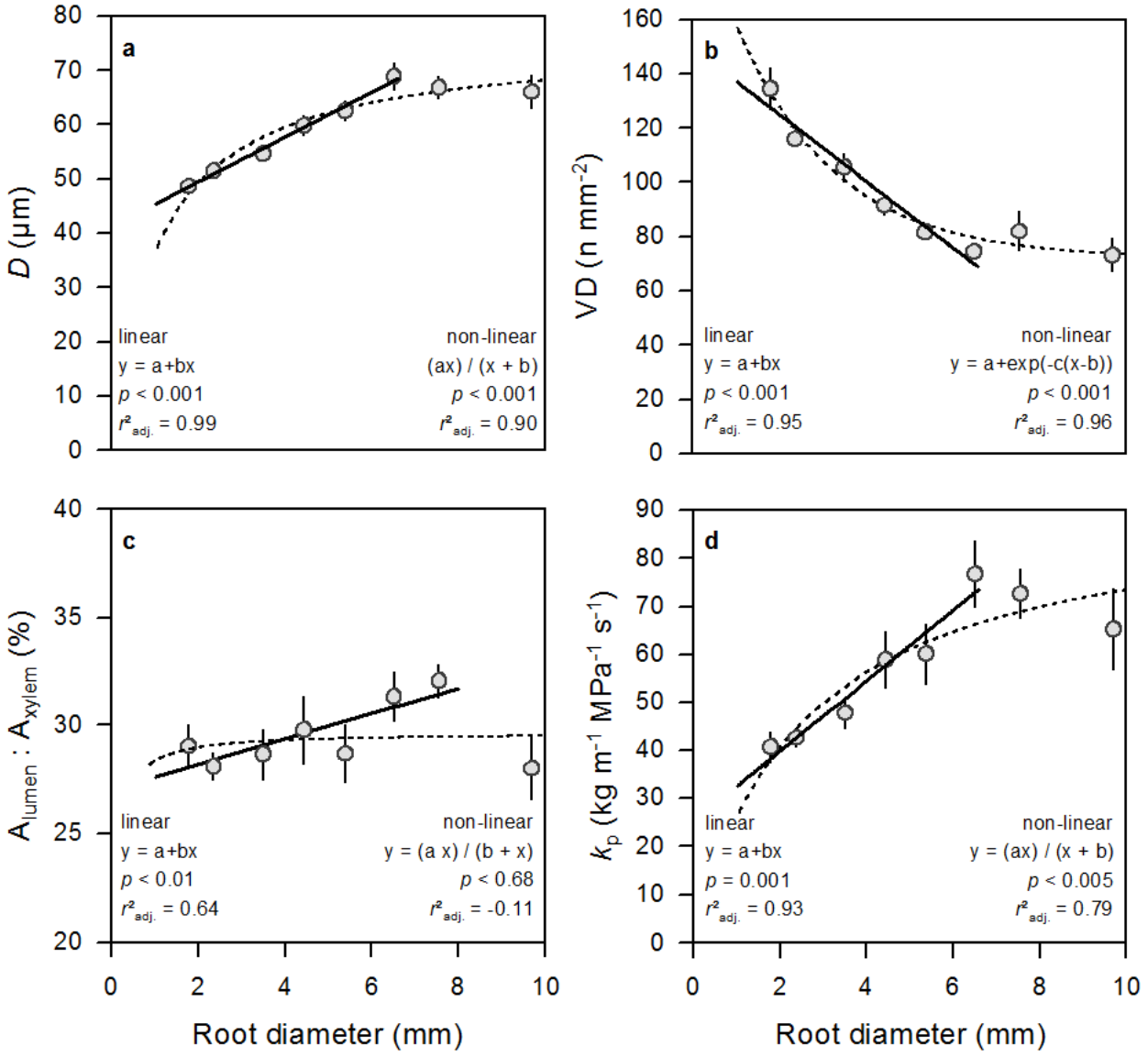


**FIGURE 4.3: Root diameter in relation to mean vessel diameter (A, *D*), vessel density (B, VD), relative vessel lumen area (C, $A_{lumen}$: $A_{xylem}$), and potential hydraulic conductivity (D, $K_p$). Values are means ±1 SE.**

**Table 4.1: Results of linear mixed effects models on the influence of soil depth and root diameter as fixed continuous variables on eight wood anatomical variables in roots of European beech (*Fagus sylvatica*) (n = 197), and the interaction of both factors. Studied traits are root age (age, yr), cross-sectional xylem area ($A_{xylem}$, mm$^2$), relative vessel lumen area ($A_{lumen}$: $A_{xylem}$, %), vessel density (VD, n mm$^{-2}$), vessel diameter ($D$, µm), maximal vessel diameter ($D_{max}$, µm), hydraulically-weighted vessel diameter ($D_h$, µm) and potential hydraulic conductivity ($K_p$, kg m$^{-1}$ MPa$^{-1}$ s$^{-1}$). Also expressed is the variation of the traits (variance component, VC in %) within ($VC_{intra}$) and between ($VC_{inter}$) different root diameter classes (n = 9) and soil depth classes (n = 7). Given are the delta Akaike information criterion (Δi), the likelihood ratio (LR) and probability of error (*P*-value). Significant correlations ($P$<0.05) are shown in bold.**

| Variable | Soil depth | | | Root diameter | | | Soil depth : root diameter | | | $VC_{intra}$ | $VC_{inter}$ | $VC_{intra}$ | $VC_{inter}$ |
|---|---|---|---|---|---|---|---|---|---|---|---|---|---|
| | $\Delta_i$ | LR | *P* | $\Delta_i$ | LR | *P* | $\Delta_i$ | LR | *P* | root diameter class | | soil depth class | |
| Age | 0.27 | 2.27 | 0.13 | 96.86 | 98.86 | **<0.001** | 1.82 | 0.18 | 0.67 | 31.40 | 68.60 | 96.08 | 3.92 |
| $A_{xylem}$ | 1.18 | 0.82 | 0.37 | 406.85 | 408.85 | **<0.001** | 0.57 | 2.57 | 0.11 | 5.27 | 94.73 | 99.53 | 0.47 |
| $A_{lumen} : A_{xylem}$ | 1.24 | 3.24 | 0.07 | 6.40 | 8.40 | **0.004** | 2.22 | 4.22 | **0.04** | 98.46 | 1.54 | 91.10 | 8.90 |
| VD | 1.55 | 0.45 | 0.50 | 64.95 | 66.95 | **<0.001** | 1.70 | 0.30 | 0.58 | 51.38 | 48.62 | 97.52 | 2.48 |
| $D$ | 1.97 | 0.03 | 0.86 | 53.44 | 55.44 | **<0.001** | 1.92 | 0.08 | 0.78 | 50.35 | 49.65 | 96.13 | 3.87 |
| $D_{max}$ | 0.13 | 1.87 | 0.17 | 77.39 | 79.39 | **<0.001** | 1.68 | 0.32 | 0.57 | 45.04 | 54.96 | 97.43 | 2.57 |
| $D_h$ | 1.35 | 0.65 | 0.42 | 36.46 | 38.46 | **<0.001** | 1.98 | 0.02 | 0.90 | 62.92 | 37.08 | 98.24 | 1.76 |
| $K_P$ | 0.61 | 2.61 | 0.11 | 27.59 | 29.59 | **<0.001** | 0.53 | 1.47 | 0.23 | 74.95 | 25.05 | 95.88 | 4.12 |

### *Existence of 'High-Conductivity Roots'*

In our sample of 197 studied roots, we found 16 roots with a large number of vessels >100 mm diameter and therefore particularly high axial conductivity. We termed roots with at least 50% higher $K_p$ values than the average of its diameter class 'high-conductivity roots' and roots with only 50% or less of average $K_p$ 'low-conductivity roots.' Figure 4.4 presents microscopic pictures of the anatomy and the vessel size distribution for pairs of high- and low-conductivity roots in three different root diameter classes. The existence of roots with particularly high potential hydraulic conductivity appears to be independent of soil depth. Unlike similar-sized roots with lower $K_p$ values, which typically are characterized by left-skewed vessel size distributions, high-conductivity roots possess a large proportion of vessels with medium or large diameters and tend more to a right-skewed distribution. In analogy to the dependence of vessel size and hydraulic conductivity on root diameter in the whole data set (Figure 4.3), mean $D$ and $K_p$ of high-conductivity roots linearly increased to a maximum value at root diameters of 6–7 or 5–6 mm, respectively, and then leveled off in roots of larger diameters (data not shown). In the high-conductivity roots of this beech stand, mean $D$ did not exceed a value of ~82 mm.

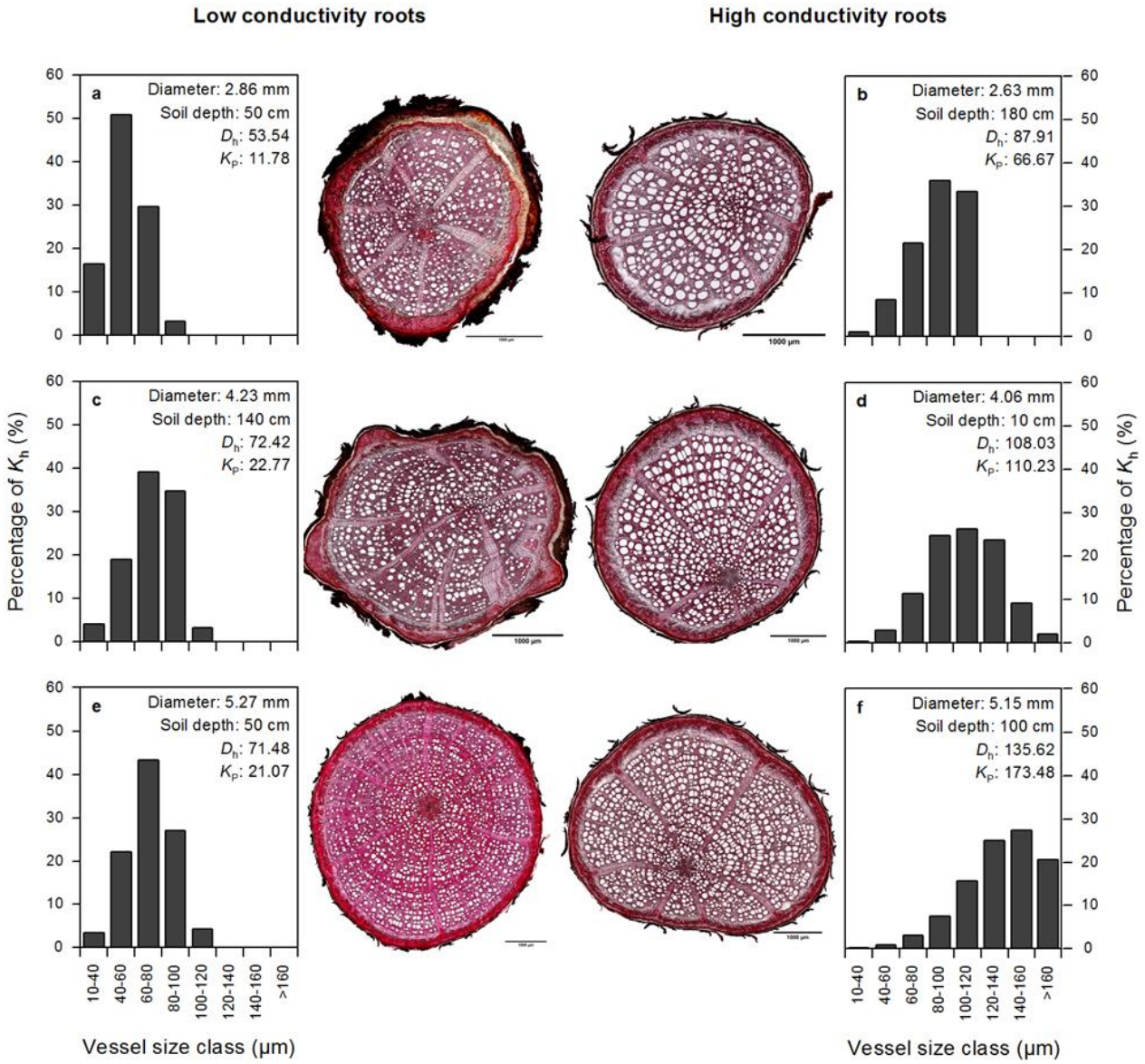


**FIGURE 4.4: Cross-sections at 100× magnification for three pairs of roots of each similar diameter (A,B: 2.7 mm; C,D: 4.1 mm; E,F: 5.2 mm) displaying typical 'low conductivity' (left) and 'high conductivity' (right) characteristics, and relative contribution of eight vessel size classes to theoretical hydraulic conductivity ($K_h$). The depicted scale bars represent 1 mm.**

### *Effect of Soil Depth on Xylem Anatomical and Derived Hydraulic Traits*

The results of the LME model revealed no significant influence of soil depth on the studied xylem anatomical and hydraulic characteristics (Table 4.1). Even when the relationship is analyzed separately within the nine root diameter classes, no clear pattern of a soil depth

influence on D emerged although vessels declined in size with depth in the root diameter class 4–5 mm, but they increased in size in the root diameter class 9–10 mm (Supplementary Figure S4.1). Likewise, maximum vessel diameter ($D_{max}$) did not increase with soil depth but remained more or less unaltered around 126.15 ± 1.75 mm (mean ± SE, $n$ = 7) across the vertical profile (Supplementary Figure S4.2).

Similarly, comparison of the studied root traits in different soil depth classes did not show significant vertical gradients in $D$, VD, $K_p$, root age and relative vessel lumen area ($A_{lumen}$: $A_{xylem}$) (Figures 4.1B–F). Accordingly, the variance component of all variables tested was larger within a given soil depth class than that between depth classes (Table 4.1).

***Detailed Analysis of Individual Root Strands***

In order to investigate the diameter dependence of the seven studied root traits independent of possible path-length induced or depth-dependent changes in these variables, we conducted a detailed study in four selected root strands from the topsoil, complementing our main analysis of 197 segments from a large number of roots. In three of the four roots, $D$ was hyperbolically related to root diameter and turned to an asymptote at root diameters of 6–8 mm, never exceeding maximum $D$-values of 51 mm (Figure 4.5A and Table 4.2). This corresponds to the results of the regression analysis between root and vessel diameter in the main analysis (Figure 4.3). This pattern was not found in root #4, probably because small-diameter segments with most rapid vessel diameter increase were not present in this strand. This root further showed a linear, and not an exponential, decrease of VD with increasing root diameter, contrary to the pattern observed in root #1 and #2 (Figure 4.5B and Table 4.2).

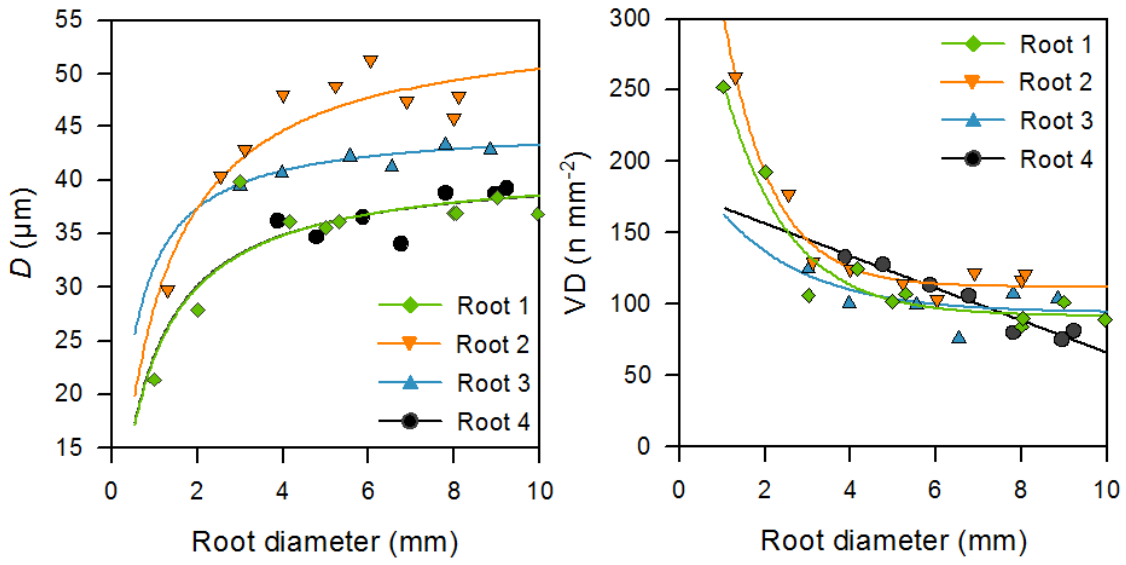


**FIGURE 4.5: Root diameter of single root strands in relation to mean vessel diameter (A, *D*) and vessel density (B, VD). Regression functions, adjusted coefficients of determination ($r^2_{adj.}$) and probability of error (*P*-value) are given in Table 4.2.**

**TABLE 4.2: Results of regression analyses between the diameter of single root strands and the corresponding mean vessel diameter (*D*, µm), vessel density (VD, n mm-2) (shown in Figure 4.5) and potential hydraulic conductivity ($K_p$, kg $m^{-1}$ $MPa^{-1}$ $s^{-1}$) at the cross-section. Given are the number of observed segments along the individual root, the adjusted coefficient of determination ($r^2_{adj.}$), and the probability of error (*P*-value). Significant correlations (*P*<0.05) are shown in bold.**

| Variable | Unit | Root no. | Regression function | $r^2_{adj.}$ | *P* |
|---|---|---|---|---|---|
| *D* | µm | 1 | y = (41.5130 * x) / (x + 0.7698) | 0.76 | **<0.001** |
| | | 2 | y = (55.2948 * x) / (x + 0.9587) | 0.83 | **<0.001** |
| | | 3 | y = (45.0381 * x) / (x + 0.4087) | 0.80 | **<0.050** |
| | | 4 | y = (45.0381 * x) / (x + 0.4087) | 0.26 | 0.135 |
| VD | n $mm^{-2}$ | 1 | y = 91.3833 + exp (-0.6727 (x - 8.5868)) | 0.93 | **<0.001** |
| | | 2 | y = 111.9291 + exp (-0.8945 (x - 6.8872) | 0.95 | **<0.001** |
| | | 3 | y = 93.7398 + exp (-0.4910 (x - 9.6527)) | -0.07 | 0.284 |
| | | 4 | y = 178.6284 - 11.2725x | 0.93 | **<0.001** |
| $K_p$ | kg $m^{-1}$ $MPa^{-1}$ $s^{-1}$ | 1 | y = 5.2304 + 0.1774x | -0.04 | 0.219 |
| | | 2 | y = (37.1319 * x) / (x + 2.5028) | 0.53 | **<0.050** |
| | | 3 | y = 8.1632 + 0.5034x | 0.08 | 0.149 |
| | | 4 | y = 8.5599 - 0.2249x | 0.01 | 0.178 |

## 4.5 Discussion

### *Effects of Root Diameter and Root Age on Wood Anatomical and Hydraulic Properties*

In agreement with our first hypothesis, we could confirm that mean vessel diameter (*D*) and potential hydraulic conductivity ($K_p$) in beech roots are a function of root diameter and thus of root age. We found *D* and $K_p$, analogously, to increase linearly from the root tip in proximal direction to a maximum of ~70 mm and ~77 kg $m^{-1}$ $MPa^{-1}$ $s^{-1}$, respectively, in medium-sized roots at a diameter of 6–7 mm, corresponding to a mean root age of ~12 years. In thicker roots, *D* remained constant at this vessel diameter level while $K_p$ decreased to a level of ~65 kg $m^{-1}$ $MPa^{-1}$ $s^{-1}$ in the root diameter class from 8 to 10 mm. The inverse pattern was found for the relationship between root diameter and vessel density (VD). The longitudinal diameter-dependent patterns in *D* and VD were characteristic for the majority of investigated root strands and were also present in the 'high-conductivity roots.' However, *D* remained constant at a value of ~82 mm in the latter and already at ~51 mm in the other ('normal' or low-conductivity) root strands. This observation may suggest that maximum vessel diameter is restricted already in medium-sized beech roots (Ø 5–10 mm), perhaps for avoiding drought- or frost-induced cavitation. Larger conduit sizes greatly increase the risk of freeze-thaw (Mayr et al. 2006; Pittermann and Sperry 2006; Christensen-Dalsgaard and Tyree 2014) and drought-induced embolism (Hargrave et al. 1994; Tyree et al. 1994a, b; Hajek et al. 2014), presumably because wider vessels may have thinner and more porous pit membranes compared to narrower ones (Hacke et al. 2016). Already 30 years ago, Tyree and Sperry (1989) speculated that the development of frost- or drought-induced embolism is not directly influenced by conduit size but rather indirectly by pit properties, a hypothesis recently confirmed by Li et al. (2016). The authors identified pit membrane thickness as key determinant of embolism resistance across a broad range of woody angiosperm species. However, independent of the mechanisms underlying the increased risk of cavitation in wider vessels, maximum vessel size may well be limited to balance all of these requirements, since conduit size is thought to display a trade-off between hydraulic efficiency and safety, as well as mechanical requirements. As a general structural principle of the hydraulic architecture of trees, it is assumed that conduit diameters increase with increasing distance from the apex in order to maintain a constant flow rate along the entire path from the roots to the leaves (West et al. 1999; Zaehle 2005). This architectural principle has been confirmed by a number of studies in the stems and

branches of trees (e.g., Anfodillo et al. 2006; Petit et al. 2008; Petit and Anfodillo 2009), but our knowledge on the belowground scaling of xylem conduits is very limited (e.g., Petit et al. 2009; Wang et al. 2015). For the long conducting lateral roots of dicotyledonous and monocotyledonous plants, Aloni (1987) suggested from a comprehensive review on vascular differentiation a universal pattern of continuous vessel diameter increase with increasing distance to the stem base. Petit et al. (2009) confirmed continuous tapering in the roots of small coniferous trees with increasing proximity to the stem base. Contrary to the findings of these authors, our observation of conduit widening with increasing diameter from small- to medium-sized roots seems to be at odds with the concept of conduit tapering which predicts that mean vessel size should decline along the flow path from the distal roots tips to the stem base as observed by Petit et al. (2009). While we do not know the path length of the studied root individuals, we can certainly infer that vessel diameters initially widen at least along the first part of the flow path from the root tip until the roots reach diameters of ~7 mm in our investigated beech root sample. Vessel tapering may well occur, when roots grow thicker than 10 mm, but this was not studied here. Hence, the question whether conduit tapering is playing a similarly important role in the xylem of tree root systems as it seems to do in the crown remains unanswered at this point.

In support of our first hypothesis, our results prove that vessel diameter increases with increasing root diameter and thus with root age, suggesting, that in this root diameter range, vessel diameter is predictable by organ diameter. Similarly, a vessel diameter–stem diameter relation has been observed by various other authors (e.g., Coomes et al. 2007; Olson and Rosell 2013; Olson et al. 2014; Pfautsch 2016; Rosell et al. 2017). This finding matches the frequent observation of a radial increase in conduit diameter from the pith to the bark in the stem of angiosperm and gymnosperm trees (Gartner 1995; Lachenbruch et al. 2011). However, information on radial variation in root xylem anatomical and hydraulic properties is yet very limited. Several studies separating root branching orders showed that conduit diameter tends to increase toward higher root orders, in agreement with our findings (Valenzuela-Estrada et al. 2008; Huang et al. 2010; Long et al. 2013; Gu et al. 2014), while others, however, failed to detect a radial conduit widening from the pith to the bark in roots (Dunham et al. 2007; Peterson et al. 2007; Lintunen and Kalliokoski 2010). This may suggest that the radial pattern of xylem anatomy in woody roots

is often overlain by adaptive responses to locally varying mechanical requirements (Christensen-Dalsgaard et al. 2008).

### *Drivers of Vessel Development*

Gradual radial change in xylem anatomy is commonly assigned to the process of cambial maturation, addressing the aging of cambial initial cells over time, which is thought to cause changes in the dimension of xylem cells formed (Spicer and Gartner 2001). In the first years of growth when trees produce juvenile wood, the cambial initials undergo rapid change and the size of conduits formed typically increases. After 5–40 years, depending on species, the increase in conduit diameter levels off and mature wood with more uniform xylem anatomical properties is produced (Spicer and Gartner 2001; Mäkinen et al. 2007; Christensen-Dalsgaard et al. 2008; Fan et al. 2009). This gradual increase in conduit diameter exponentially increases hydraulic efficiency because flow in capillary systems increases with diameter raised to the fourth power according to the Hagen–Poiseuille law. However, the mechanisms underlying the process of cambial maturation are not well understood.

Some evidence suggests that age-related differences in xylem differentiation result from a complex interplay between plant hormones, gene expression, and environmental influences (Li et al. 2012). It is well established that the plant hormone auxin – in concert with further plant hormones such as gibberellins, cytokinins and ethylene – is a key regulator in plant vascular development (Nilsson et al. 2008; Aloni 2015). Auxin is synthesized in the developing leaves, resulting in a longitudinal gradient in auxin concentration along the flow path from the apex to the roots (Aloni and Zimmermann 1983; Uggla et al. 1998; Aloni 2015; Hacke et al. 2016; Pfautsch 2016). However, auxins are also synthesized in the roots with concentrations decreasing from the tip to more proximal root sections, as shown for Arabidopsis (Ljung et al. 2005; Teale et al. 2006; Petersson et al. 2009). Although it is not fully understood how auxin modulates vessel size patterns (Teale et al. 2006; Anfodillo et al. 2012), its involvement in turgor-driven cell growth suggests that auxin plays a role in determining vessel diameters (Hacke et al. 2016). Frequent observations of vertical vessel widening from the apex to the stem base, and radially from the pith to the cambium, have led to the hypothesis that gradients in auxin concentration are

responsible for this vascular modification with flow path length or cambial age (Aloni and Zimmermann 1983; Lachenbruch et al. 2011; Anfodillo et al. 2013). Applied to our data, a decreasing auxin concentration with distance from the root tip in parallel to the observed larger vessel diameters with increasing root diameters could well explain the vessel widening with increasing root diameter. However, a consistent relationship between auxin concentration and variation in xylem differentiation has not always been demonstrated (Zajaczkowski 1973; Sundberg et al. 1993; Little and Pharis 1995; Uggla et al. 1998). While it is undisputed that auxin is a key regulator in secondary xylem development, differences in the responsiveness of cambial cells to different auxin levels may be a cause of variation in xylem anatomical traits (Nilsson et al. 2008).

Investigations on the molecular level offer clues on the mechanisms underlying the phenomena ascribed to cambial maturation suggesting that xylem differentiation differs with age in dependence of ontogenetic change in gene expression (Lenz et al. 2010; Li et al. 2012). Comparing the regulation of xylem candidate genes at different tree ages, Li et al. (2010) observed that many of the relevant genes are preferentially expressed in certain development phases or tree ages, resulting in variations in transcript abundance at different stages of cambial maturity. For example, the expression of cell wall related genes generally decreased with cambial age. It is evident that our understanding of genetic regulation of cambial aging is still rudimentary and needs further intensive study (Li et al. 2010).

### *Variability in Xylem Anatomical and Hydraulic Traits among Similar-Sized Roots*

Another main result of this study is the high plasticity in xylem anatomy and related hydraulic properties in beech roots of similar size co-occurring at the same soil depth. Despite the relative scarcity of information about xylem anatomical and hydraulic properties of tree roots, a growing number of studies provide evidence of a generally high heterogeneity in these traits, as evidenced in the studies of, e.g., Leuschner et al. (2004) and Rewald (2008) for temperate hardwoods. This suggests that morphologically and anatomically different roots in the same soil horizon may also serve different functions, for example predominantly nutrient absorption, or alternatively water uptake and conduction. Functional specialization may develop in response to gradients in nutrient

and water availability, as has been indicated by a number of studies (Pierret et al. 2007; Rewald et al. 2011; Köcher et al. 2012; Hajek et al. 2014).

Thus, the observed high variability in the wood anatomical and derived hydraulic properties of the beech roots in this soil is presumably a consequence of the considerable heterogeneity in soil texture and soil water content at the site (Supplementary Table S4.2). We speculate that high-conductivity roots have contact to soil patches where water is, or was, more easily available stimulating vessel diameter growth, in contrast to other roots which may predominantly be responsible for nutrient uptake (Pierret et al. 2007). In general, the marked anatomical and functional plasticity in secondary vascular elements is considered to be of high adaptive significance in response to climatic conditions and other external factors (Carlquist 2001; Spicer and Groover 2010). Alternatively, the wide vessels in high-conductivity roots could also result from greater pathway length, i.e., longer distal fine root strands than in the average of roots in that diameter class. The higher conductivity of the more proximal root segment would then simply balance the higher cumulative resistance in the longer distal flow path.

We found 'high-conductivity roots' in six of seven soil depth classes between the surface and 200 cm depth. Seventy-five percent of these roots were found in the subsoil below 60 cm depth. We observed 'high-conductivity roots' in all studied diameter classes from fine to medium roots (1–10 mm in diameter). Their particularly high hydraulic conductivity is mainly a result of larger mean vessel diameters and not higher vessel density. This is in accordance with conclusions from earlier work that conduit diameter is the main determinant of axial conductivity in roots (McElrone et al. 2004; Köcher et al. 2012; Gebauer and Volařík 2013; Hajek et al. 2014), since an increase in conduit radius scales the flow in capillary systems exponentially by a fourth-power relationship (Tyree and Zimmermann 2002). In comparison, the plasticity of the branch hydraulic system seems to be lower in temperate broad-leaved trees: vessel size distribution was found to be more balanced than in roots with no indication of 'high-conductivity branches' (Hajek et al. 2014).

### *Influence of Soil Depth on Xylem Anatomical and Related Hydraulic Properties*

Our study did not produce evidence for increases in vessel diameter and potential hydraulic conductivity with increasing soil depth in mature beech trees. In contrast to our findings, Pate et al. (1995) found a progressive increase in mean xylem conduit diameter and specific hydraulic conductivity down to 1.3 m depth for sinker roots of various Proteaceae species. Likewise, McElrone et al. (2004) observed increases in mean *D* and hydraulic efficiency from shallow to deep roots (7–20 m soil depth) for several tree species.

Several factors may be responsible for the apparent discrepancy between the reported soil-depth effects on xylem anatomy and our results. First, it may be that the depth-dependent gradients in xylem anatomical and hydraulic traits reported in the cited studies are reflecting differences in path length between the investigated root sections, while we were not able to measure root length and thus path length to the stem base and the related position of the segment in the flow path. This is the reason why we refer to soil depth, and this could explain differences to the above-mentioned studies. Second, the few existing studies on conduit scaling in roots indicate that the rooting system is much more responsive to external factors (Nardini et al. 2002; Christensen-Dalsgaard et al. 2008) like freeze-thaw events (Gebauer and Volařík 2013) or water availability (Rewald et al. 2011; Köcher et al. 2012), and mechanical demands (Dunham et al. 2007; Lintunen and Kalliokoski 2010) than the crown. Gebauer and Volařík (2013) found an increase in mean vessel diameter and specific hydraulic conductivity from 0 to 50 cm in the roots of two temperate oak species, but no further scaling in these traits from 50 to 100 cm soil depth, concluding that vessel size in the upper soil layer is restricted in order to avoid freeze-thaw-induced embolism formation. In contrast to McElrone et al. (2004), Lintunen and Kalliokoski (2010) reported a tendency for sinker roots to have smaller conduit radii than shallow roots of the same species, concluding that hydraulic conductivity of sinker roots might be traded off against the mechanical demand of anchoring the tree firmly to the soil under conditions of ample moistures.

## 4.6 Conclusion

We found key anatomical and hydraulic traits of beech roots to scale with root diameter in roots of ~7 mm in diameter, pointing at a dominant root age effect on belowground hydraulic properties. In the first months to years of their life beech roots grow in diameter to 6–7 mm and *D* increases to a threshold value of 70–80 mm. As a result, the capacity for water conduction doubles and activity shifts from resource uptake to transport and storage functions. The threshold *D* level may be defined by safety requirements to avoid embolism.

From the observed large variability in anatomical properties among similar-sized neighboring roots it is evident that the age-related pattern is overlain by a high xylem architectural plasticity of the root system. This heterogeneity might either be attributable to spatial variation in the influence of external factors or to differences in flow path length from the distal root to the stem base. It appears that different functional types of roots with respect to water uptake and conduction do exist in the root system of beech trees, which deserve more detailed study.

To separate between the influential factors, future studies on root vascular anatomy adjustment in soil profiles should account for path length effects in the root strands. This would require excavating larger parts of the tree root system instead of sampling individual root sections only, and thus is very labor-intensive and destructive, when done in mature forests.

***Acknowledgements***

This study was supported by funding from the Deutsche Forschungsgemeinschaft (DFG) in the context of the research unit FOR1806 ‘The Forgotten Part of Carbon Cycling: Organic Matter Storage and Turnover in Subsoils (SUBSOM).’ The support is gratefully acknowledged. We thank Roman Link for statistical advice, and further acknowledge the support by the Open Access Publication Funds of the University of Göttingen.

## Supplementary Material

**TABLE S4.1: Root classification according to diameter after Sutton and Tinus (1983) and number of observations (n) per root class and soil depth (cm) across the three excavated soil pits.**

| Root diameter | Classification | Soil depth (cm) | | | | | | |
|---|---|---|---|---|---|---|---|---|
| | | 0 - 20 | 20 - 40 | 40- 60 | 60 - 80 | 80 - 120 | 120 - 160 | 160 - 200 |
| Ø 1-5 mm | fine and small roots | 16 | 15 | 15 | 19 | 18 | 18 | 19 |
| Ø 5-10 mm | medium roots | 14 | 11 | 13 | 7 | 10 | 11 | 11 |
| Ø 1-2 mm | | 2 | 4 | 0 | 4 | 4 | 5 | 1 |
| Ø 2-3 mm | | 7 | 3 | 9 | 6 | 9 | 6 | 7 |
| Ø 3-4 mm | | 3 | 3 | 4 | 7 | 3 | 4 | 7 |
| Ø 4-5 mm | | 4 | 5 | 2 | 2 | 4 | 3 | 4 |
| Ø 5-6 mm | | 4 | 1 | 5 | 5 | 4 | 4 | 2 |
| Ø 6-7 mm | | 1 | 5 | 4 | 0 | 2 | 1 | 3 |
| Ø 7-8 mm | | 4 | 4 | 0 | 1 | 1 | 0 | 3 |
| Ø 8-9 mm | | 5 | 1 | 2 | 0 | 0 | 3 | 1 |
| Ø 9-10 mm | | 0 | 0 | 2 | 1 | 1 | 3 | 2 |

**TABLE S4.2: Physical and chemical soil characteristics at different soil depths in the Grinderwald forest (June 2013). Classification of soil horizons according to FAO - WRB 2014.**

| Soil depth (cm) | Soil horizon | pH ($CaCl_2$) | SOC (g $kg^{-1}$) | Sand (%) | Silt (%) | Clay (%) |
|---|---|---|---|---|---|---|
| 0-2 | AE | 3.3 | 27.0 | 70.0 | 26.0 | 4.0 |
| 2-12 | Bsw | 3.4 | 17.0 | 65.0 | 30.0 | 5.0 |
| 12-36 | Bw | 4.4 | 7.0 | 67.0 | 29.0 | 4.0 |
| 36-65 | BwC | 4.5 | 3.0 | 73.0 | 24.0 | 3.0 |
| 65-125 | C | 4.4 | 0.4 | 95.0 | 4.0 | 1.0 |
| 125-150 | 2C | 4.1 | 0.1 | 81.0 | 11.0 | 8.0 |
| 150-180 | 2Cg | 4.2 | 0.8 | 72.0 | 19.0 | 9.0 |
| 180+ | 3C | 4.2 | <0.1 | 95.0 | 4.0 | 1.0 |

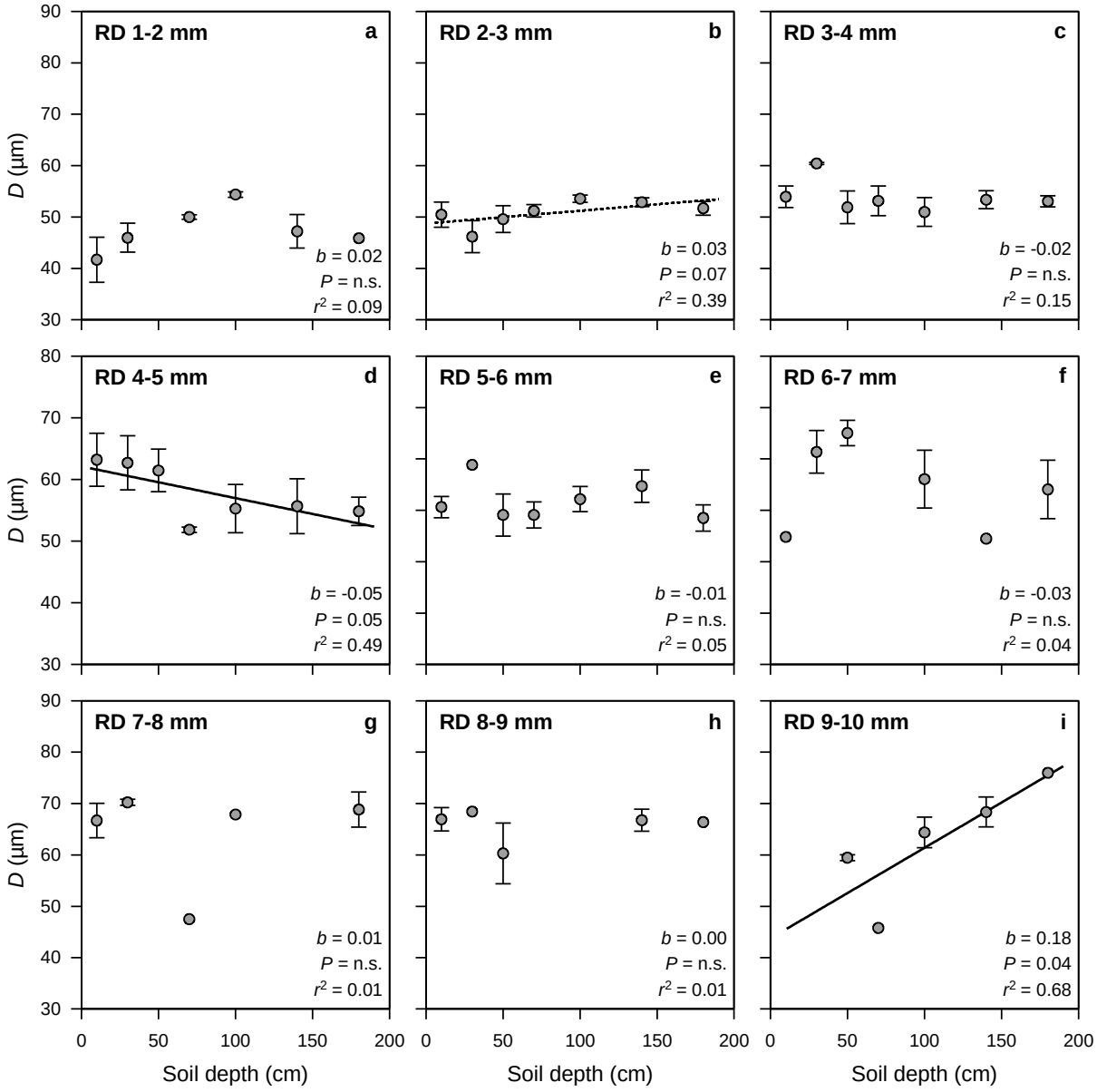


**FIGURE S4.1: Influence of soil depth on mean vessel diameter (*D*) for nine different root diameter classes (RD). For each root diameter class, 9-44 samples were available, which subsequently were averaged for each soil depth class. For number of replicates per root diameter class see Table S1. Values are means ± SE; the slope (*b*), coefficient of determination ($r^2$) and probability of error (*P*-value) of the linear regressions are given.**

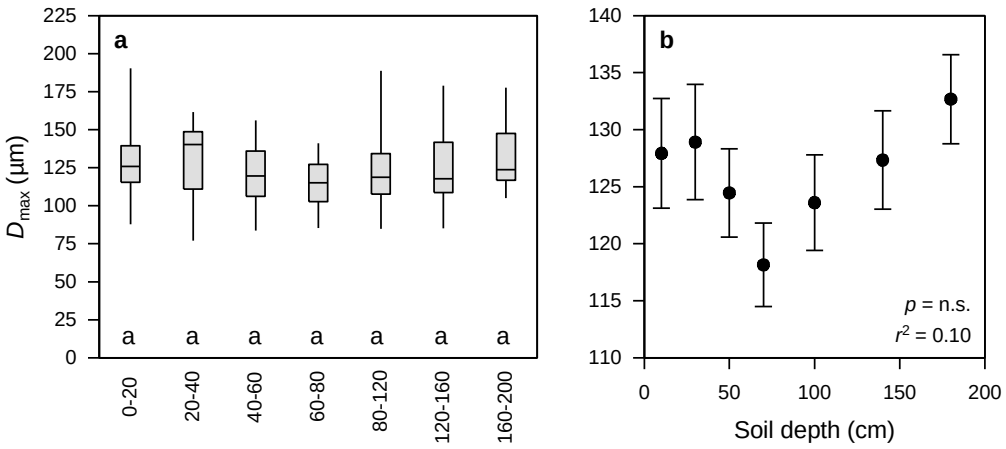


**FIGURE S4.2: Box-whisker plots with median values for the variation in maximum vessel diameter ($D_{max}$) in seven soil depth classes (a); small letters indicate significant differences between depth classes. Additionally given is the relation between soil depth and mean values ± SE for $D_{max}$ (b). Please note the different scaling of the y-axis.**

## 4.7 References

Aloni, R. (1987) Differentiation of vascular tissues. Annu. Rev. Plant Physiol. 38: 179–204. doi: 10.1146/annurev.pp.38.060187.001143

Aloni, R. (2015) Ecophysiological implications of vascular differentiation and plant evolution. Trees Struct. Funct. 29: 1–16. doi: 10.1007/s00468-014- 1070-6

Aloni, R., and Zimmermann, M. H. (1983) The control of vessel size and density along the plant axis: a new hypothesis. Differentiation 24: 203–208. doi: 10.1111/ j.1432-0436.1983.tb01320.x

Anfodillo, T., Carraro, V., Carrer, M., Fior, C., and Rossi, S. (2006) Convergent tapering of xylem conduits in different woody species. New Phytol. 169: 279–290. doi: 10.1111/j.1469-8137.2005.01587.x

Anfodillo, T., Deslauriers, A., Menardi, R., Tedoldi, L., Petit, G., and Rossi, S. (2012) Widening of xylem conduits in a conifer tree depends on the longer time of cell expansion downwards along the stem. J. Exp. Bot. 63 837–845. doi: 10.1093/jxb/err309

Anfodillo, T., Petit, G., and Crivellaro, A. (2013). Axial conduit widening in woody species: a still neglected anatomical pattern. IAWA J. 34: 352–364. doi: 10.1163/ 22941932-00000030

Bleby, T. M., McElrone, A. J., and Jackson, R. B. (2010) Water uptake and hydraulic redistribution across large woody root systems to 20 m depth. Plant Cell Environ. 33: 2132–2148. doi: 10.1111/j.1365-3040.2010. 02212.x

Brunner, I., Herzog, C., Dawes, M. A., Arend, M., and Sperisen, C. (2015) How tree roots respond to drought. Front. Plant Sci. 6:547. doi: 10.3389/fpls.2015. 00547

Carlquist, S. (2001) Comparative Wood Anatomy: Systematic, Ecological, and Evolutionary Aspects of Dicotyledon Wood. Berlin: Springer-Verlag. doi: 10.1007/978-3-662-04578-7

Chenlemuge, T., Schuldt, B., Dulamsuren, C., Hertel, D., Leuschner, C., and Hauck, M. (2015) Stem increment and hydraulic architecture of a boreal conifer (Larix sibirica) under contrasting macroclimates. Trees 29: 623–636. doi: 10.1007/s00468-014-1131-x

Christensen-Dalsgaard, K. K., Ennos, A. R., and Fournier, M. (2008) Are radial changes in vascular anatomy mechanically induced or an ageing process? Evidence from observations on buttressed tree root systems. Trees 22: 543–550. doi: 10.1007/s00468-008-0214-y

Christensen-Dalsgaard, K. K., and Tyree, M. T. (2014) Frost fatigue and spring recovery of xylem vessels in three diffuse-porous trees in situ. Plant Cell Environ. 37: 1074–1085. doi: 10.1111/pce.12216

Coomes, D. A., Jenkins, K. L., and Cole, L. E. S. (2007) Scaling of tree vascular transport systems along gradients of nutrient supply and altitude. Biol. Lett. 3: 86–89. doi: 10.1098/rsbl.2006.0551

David, T. S., Pinto, C. A., Nadezhdina, N., Kurz-Besson, C., Henriques, M. O., Quilhó, T., et al. (2013) Root functioning, tree water use and hydraulic redistribution in Quercus suber trees: a modeling approach based on root sap flow. For. Ecol. Manage. 307: 136–146. doi: 10.1016/j.foreco.2013.07.012

Domec, J. C., Warren, J. M., Meinzer, F. C., Brooks, J. R., and Coulombe, R. (2004) Native root xylem embolism and stomatal closure in stands of Douglas-fir and ponderosa pine: mitigation by hydraulic redistribution. Oecologia 141: 7–16. doi: 10.1007/s00442-004-1621-4

Dunham, S. M., Lachenbruch, B., and Ganio, L. M. (2007) Bayesian analysis of Douglas-fir hydraulic architecture at multiple scales. Trees 21: 65–78. doi: 10.1007/s00468-006-0097-8

Fan, Z. X., Cao, K. F., and Becker, P. (2009) Axial and radial variations in xylem anatomy of angiosperm and conifer trees in Yunnan, China. IAWA J. 30: 1–13. doi: 10.1163/22941932-90000198

FAO (2014) World reference base for soil resources 2014. International soil classification system for naming soils and creating legends for soil maps. World Soil Resource Reports 106. Food and Agriculture Organization of the United Nations, Rome, Italy.

Gartner, B. L. (1995) Patterns of xylem variation within a tree and their hydraulic and mechanical consequences. In Gartner, B. (ed.) Plant Stems: Physiology and Functional Morphology. Academic Press, San Diego, CA, 125–149.

Gebauer, R., and Volařík, D. (2013) Root hydraulic conductivity and vessel structure modification with increasing soil depth of two oak species: Quercus pubescens and Quercus robur. Trees 27: 523–531. doi: 10.1007/s00468-012- 0805-5

Gu, J., Xu, Y., Dong, X., Wang, H., and Wang, Z. (2014) Root diameter variations explained by anatomy and phylogeny of 50 tropical and temperate tree species. Tree Physiol. 34: 415–425. doi: 10.1093/treephys/tpu019

Hacke, U. G., Spicer, R., Schreiber, S. G., and Plavcová, L. (2016) An ecophysiological and developmental perspective on variation in vessel diameter. Plant Cell Environ. 40: 831–845. doi: 10.1111/pce.12777

Hajek, P., Leuschner, C., Herte, I. D., Delzon, S., and Schuldt, B. (2014) Trade-offs between xylem hydraulic properties, wood anatomy and yield in Populus. Tree Physiol. 34, 744–756. doi: 10.1093/treephys/tpu048

Hargrave, K. R., Kolb, K. J., Ewers, F. W., and Davis, S. D. (1994). Conduit diameter and drought-induced embolism in Salvia mellifera Greene (Labiatae). New Phytol. 126: 695–705. doi: 10.1111/j.1469-8137.1994.tb02964.x

Huang, G., Zhao, X.-Y., Zhao, H.-L., Huang, Y.-X., and Zuo, X.-A. (2010) Linking root morphology, longevity and function to root branch order: a case study in three shrubs. Plant Soil 336: 197–208. doi: 10.1007/s11104-010-0466-3

Köcher, P., Horna, V., Beckmeyer, I., and Leuschner, C. (2012) Hydraulic properties and embolism in small-diameter roots of five temperate broad-leaved tree species with contrasting drought tolerance. Ann. For. Sci. 69: 693–703. doi: 10.1007/s13595-012-0189-0

Kotowska, M. M., Hertel, D., Rajab, Y. A., Barus, H., and Schuldt, B. (2015) Patterns in hydraulic architecture from roots to branches in six tropical tree species from cacao agroforestry and their relation to wood density and stem growth. Front. Plant Sci. 6:191. doi: 10.3389/fpls.2015.00191

Lachenbruch, B., Moore, J. R., and Evans, R. (2011) Radial variation in wood structure and function in woody plants, and hypotheses for its occurrence. In: Meinzer, C., Lachenbruch, B., and Dawson, T. E. (eds.) Size-and Age-Related Changes in Tree Structure and Function. Springer, Dordrecht, 121–164.

Lenz, P., Cloutier, A., MacKay, J., and Beaulieu, J. (2010) Genetic control of wood properties in Picea glauca—an analysis of trends with cambial age. Can. J. For. Res. 40: 703–715. doi: 10.1139/X10-014

Leuschner, C., Hertel, D., Schmid, I., Koch, O., Muhs, A., and Hölscher, D. (2004) Stand fine root biomass and fine root morphology in old-growth beech forests as a function of precipitation and soil fertility. Plant Soil 258: 43–56. doi: 10.1023/B:PLSO.0000016508.20173.80

Lewis, A. M., and Boose, E. R. (1995) Estimating volume flow rates through xylem conduits. Am. J. Bot. 82:1112–1116. doi: 10.2307/2446063

Li, S., Lens, F., Espino, S., Karimi, Z., Klepsch, M., Schenk, H. J., et al. (2016) Intervessel pit membrane thickness as a key determinant of embolism resistance in angiosperm xylem. IAWA J. 37: 152–171. doi: 10.1163/22941932-20160128

Li, X., Liang, E., Grièar, J., Prislan, P., Rossi, S., and Èufar, K. (2012) Age dependence of xylogenesis and its climatic sensitivity in Smith fir on the south-eastern Tibetan Plateau. Tree Physiol. 33: 48–56. doi: 10.1093/treephys/ tps113

Li, X., Wu, H. X., and Southerton, S. G. (2010) Seasonal reorganization of the xylem transcriptome at different tree ages reveals novel insights into wood formation in Pinus radiata. New Phytol. 187: 764–776. doi: 10.1111/j.1469-8137. 2010.03333.x

Lintunen, A., and Kalliokoski, T. (2010) The effect of tree architecture on conduit diameter and frequency from small distal roots to branch tips in Betula pendula, Picea abies and Pinus sylvestris. Tree Physiol. 30: 1433–1447. doi: 10.1093/ treephys/tpq085

Little, C. H. A., and Pharis, R. P. (1995) Hormonal control of radial and longitudinal growth in the tree stem. In Gartner, B. L. (ed.) Plant Stems: Physiology and Functional Morphology. Academic Press, San Diego, CA, 281–319.

Ljung, K., Hull, A. K., Celenza, J., Yamada, M., Estelle, M., Normanly, J., et al. (2005) Sites and regulation of auxin biosynthesis in Arabidopsis roots. Plant Cell 17: 1090–1104. doi: 10.1105/tpc.104.029272

Long, Y., Kong, D., Chen, Z., and Zeng, H. (2013) Variation of the linkage of root function with root branch order. PLoS ONE 8:e57153. doi: 10.1371/journal. pone.0057153

Maeght, J. L., Rewald, B., and Pierret, A. (2013) How to study deep roots—and why it matters. Front. Plant Sci. 4:299. doi: 10.3389/fpls.2013.00299

Mäkinen, H., Jaakkola, T., Piispanen, R., and Saranpää, P. (2007) Predicting wood and tracheid properties of Norway spruce. For. Ecol. Manage. 241: 175–188. doi: 10.1093/treephys/tpp099

Mayr, S., Hacke, U., Schmid, P., Schwienbacher, F., and Gruber, A. (2006) Frost drought in conifers at the alpine timberline: xylem dysfunction and adaptations. Ecology 87: 3175–3185. doi: 10.1890/0012-9658(2006)87[3175:FDICAT]2.0. CO;2

McElrone, A. J., Pockman, W. T., Martínez-Vilalta, J., and Jackson, R. B. (2004) Variation in xylem structure and function in stems and roots of trees to 20 m depth. New Phytol. 163: 507–517. doi: 10.1111/j.1469-8137.2004.01127.x

Nardini, A., Salleo, S., and Tyree, M. T. (2002) Ecological aspects of water permeability of roots. In Waisel, Y., Eshel, A., and Kafkafi, U. (eds.) Plant Roots: The Hidden Half. Marcel Dekker Inc., New York, NY, 683–698.

Nilsson, J., Karlberg, A., Antt, H., Lopez-Vernaza, M., Mellerowicz, E., Perrot-Rechenmann, C., et al. (2008) Dissecting the molecular basis of the regulation of wood formation by auxin in hybrid aspen. Plant Cell 20: 843–855. doi: 10.1105/tpc.107.055798

Olson, M. E., Anfodillo, T., Rosell, J. A., Petit, G., Crivellaro, A., Isnard, S., et al. (2014) Universal hydraulics of the flowering plants: vessel diameter scales with stem length across angiosperm lineages, habits and climates. Ecol. Lett. 17: 988–997. doi: 10.1111/ele.12302

Olson, M. E., and Rosell, J. A. (2013) Vessel diameter–stem diameter scaling across woody angiosperms and the ecological causes of xylem vessel diameter variation. New Phytol. 197: 1204–1213. doi: 10.1111/nph.12097

Pate, J. S., Jeschke, W. D., and Aylward, M. J. (1995) Hydraulic architecture and xylem structure of the dimorphic root systems of South-West Australian species of Proteaceae. J. Exp. Bot. 46: 907–915. doi: 10.1093/jxb/46.8.907

Peterson, M. G., Dietterich, H. R., and Lachenbruch, B. (2007) Do Douglas-fir branches and roots have juvenile wood? Wood Fiber Sci. 39: 651–660.

Petersson, S. V., Johansson, A. I., Kowalczyk, M., Makoveychuk, A., Wang, J. Y., Moritz, T., et al. (2009) An auxin gradient and maximum in the Arabidopsis root apex shown by high-resolution cell-specific analysis of IAA distribution and synthesis. Plant Cell 21: 1659–1668. doi: 10.1105/tpc.109.066480

Petit, G., and Anfodillo, T. (2009) Plant physiology in theory and practice: an analysis of the WBE model for vascular plants. J. Theor. Biol. 259: 1–4. doi: 10.1016/j.jtbi.2009.03.007

Petit, G., Anfodillo, T., and De Zan, C. (2009) Degree of tapering of xylem conduits in stems and roots of small Pinus cembra and Larix decidua trees. Botany 87: 501–508. doi: 10.1139/B09-025

Petit, G., Anfodillo, T., and Mencuccini, M. (2008) Tapering of xylem conduits and hydraulic limitations in sycamore (Acer pseudoplatanus) trees. New Phytol. 177: 653–664. doi: 10.1111/j.1469-8137.2007.02291.x

Pfautsch, S. (2016) Hydraulic anatomy and function of trees—basics and critical developments. Curr. For. Rep. 2: 236–248. doi: 10.1007/s40725-016- 0046-8

Pierret, A., Doussan, C., Capowiez, Y., Bastardie, F., and Pagès, L. (2007) Root functional architecture: a framework for modeling the interplay between roots and soil. Vadose Zone J. 6: 269–281. doi: 10.2136/vzj2006.0067

Pierret, A., Maeght, J.-L., Clément, C., Montoroi, J.-P., Hartmann, C., and Gonkhamdee, S. (2016) Understanding deep roots and their functions in ecosystems: an advocacy for more unconventional research. Ann. Bot. 118: 621–635. doi: 10.1093/aob/mcw130

Pittermann, J., and Sperry, J. S. (2006) Analysis of freeze-thaw embolism in conifers. The interaction between cavitation pressure and tracheid size. Plant Physiol. 140: 374–382. doi: 10.1104/pp.105.067900

R Core Team (2013) R: A Language and Environment for Statistical Computing. Vienna: R Foundation for Statistical Computing. Available at: http://www.Rproject.org/

Rewald, B. (2008) Impact of Climate Change-Induced Drought on Tree Root Hydraulic Properties and Competition Belowground. Ph.D. thesis, University of Göttingen, Göttingen.

Rewald, B., Leuschner, C., Wiesman, Z., and Ephrath, J. E. (2011) Influence of salinity on root hydraulic properties of three olive varieties. Plant Biosyst. 145: 12–22. doi: 10.1080/11263504.2010.514130

Rosell, J. A., Olson, M. E., and Anfodillo, T. (2017) Scaling of xylem vessel diameter with plant size: causes, predictions, and outstanding questions. Curr. For. Rep. 3: 46–59. doi: 10.1007/s40725-017-0049-0

Schuldt, B., Leuschner, C., Brock, N., and Horna, V. (2013) Changes in wood density, wood anatomy and hydraulic properties of the xylem along the root-to-shoot flow path in tropical rainforest trees. Tree Physiol. 33: 161–174. doi: 10.1093/treephys/tps122

Sperry, J. S., Hacke, U. G., and Pittermann, J. (2006) Size and function in conifer tracheids and angiosperm vessels. Am. J. Bot. 93: 1490–1500. doi: 10.3732/ajb.93.10.1490

Sperry, J. S., Nichols, K. L., Sullivan, J. E. M., and Eastlack, S. E. (1994) Xylem embolism in ring-porous, diffuse-porous, and coniferous trees of Northern Utah and interior Alaska. Ecology 75: 1736–1752. doi: 10.2307/1939633

Sperry, J. S., and Saliendra, N. Z. (1994) Intra-and inter-plant variation in xylem cavitation in Betula occidentalis. Plant Cell Environ. 17: 1233–1241. doi: 10.1111/j.1365-3040.1994.tb02021.x

Spicer, R., and Gartner, B. L. (2001) The effects of cambial age and position within the stem on specific conductivity in Douglas-fir (Pseudotsuga menziesii) xylem. Trees 15: 222–229. doi: 10.1007/s004680100093

Spicer, R., and Groover, A. (2010) Evolution of development of vascular cambia and secondary growth. New Phytol. 186: 577–592. doi: 10.1111/j.1469-8137.2010.03236.x

Stone, E. L., and Kalisz, P. J. (1991) On the maximum extent of tree roots. For. Ecol. Manage. 46: 59–102. doi: 10.1016/0378-1127(91)90245-Q

Sundberg, B., Ericsson, A., Little, C. H. A., Näsholm, T., and Gref, R. (1993) The relationship between crown size and ring width in Pinus sylvestris L. stems: dependence on indole-3-acetic acid, carbohydrates and nitrogen in the cambial region. Tree Physiol. 12: 347–362. doi: 10.1093/treephys/12.4.347

Sutton, R. F., & Tinus, R. W. (1983) Root and root system terminology. Forest Science, 29(suppl_1) : a0001-z0001.

Teale, W. D., Paponov, I. A., and Palme, K. (2006) Auxin in action: signaling, transport and the control of plant growth and development. Nat. Rev. Mol. Cell Biol. 7: 847–859. doi: 10.1038/nrm2020

Tyree, M. T. (2003a) Hydraulic limits on tree performance: transpiration, carbon gain and growth of trees. Trees 17: 95–100.

Tyree, M. T. (2003b) Hydraulic properties of roots. In: de Kroon, H.and Visser, E. J. W. (eds.) Root Ecology. Springer, Berlin, 125–150.

Tyree, M. T., Davis, S. D., and Cochard, H. (1994a) Biophysical perspectives of xylem evolution: Is there a tradeoff of hydraulic efficiency for vulnerability to dysfunction? IAWA J. 15: 335–360. doi: 10.1163/22941932-90001369

Tyree, M. T., Kolb, K. J., Rood, S. B., and Patiño, S. (1994b) Vulnerability to drought-induced cavitation of riparian cottonwoods in Alberta: a possible factor in the decline of the ecosystem? Tree Physiol. 14:455–466.

Tyree, M. T., and Sperry, J. S. (1989) Vulnerability of xylem to cavitation and embolism. Annu. Rev. Plant Physiol. Plant Mol. Biol. 40:19–38. doi: 10.1146/annurev.pp.40.060189.000315

Tyree, M. T., and Zimmermann, M. H. (2002) Xylem Structure and the Ascent of Sap. Berlin: Springer Science & Business Media. doi: 10.1007/978-3-662-04931-0

Uggla, C., Mellerowicz, E. J., and Sundberg, B. (1998) Indole-3-acetic acid controls cambial growth in Scots pine by positional signaling. Plant Physiol. 117:113–121. doi: 10.1104/pp.117.1.113

Valenzuela-Estrada, L. R., Vera-Caraballo, V., Ruth, L. E., and Eissenstat, D. M. (2008) Root anatomy, morphology, and longevity among root orders in Vaccinium corymbosum (Ericaceae). Am. J. Bot. 95:1506–1514. doi: 10.3732/ajb.0800092

Wang, Y., Dong, X., Wang, H., Wang, Z., and Gu, J. (2015) Root tip morphology, anatomy, chemistry and potential hydraulic conductivity vary with soil depth in three temperate hardwood species. Tree Physiol. 36:99–108. doi: 10.1093/treephys/tpv094

West, G. B., Brown, J. H., and Enquist, B. J. (1999) The fourth dimension of life: fractal geometry and allometric scaling of organisms. Science 284:1677–1679. doi: 10.1126/science.284.5420.1677

Zaehle, S. (2005) Effect of height on tree hydraulic conductance incompletely compensated by xylem tapering. Funct. Ecol. 19:359–364. doi: 10.1111/j.0269-8463.2005.00953.x

Zajaczkowski, S. (1973) Auxin stimulation of cambial activity in Pinus silvestris. I. The differential cambial response. Physiol. Plant 29:281–287. doi: 10.1111/j.1399-3054.1973.tb04826.x

# CHAPTER 5

# Factors controlling the variability of organic matter in the top- and subsoil of a sandy Dystric Cambisol under beech forest

Stefanie HEINZE, Bernard LUDWIG, Hans-Peter PIEPHO, Robert MIKUTTA, Axel DON, Patrick WORDELL-DIETRICH, Mirjam HELFRICH, Dietrich HERTEL, Christoph LEUSCHNER, Kristina KIRFEL, Ellen KANDELER, Sebastian PREUSSER, Georg GUGGENBERGER, Timo LEINEMANN, and Bernd MARSCHNER

GEODERMA, 2018, VOLUME 311, PAGES 37-44. DOI: 10.1016/j.geoderma.2017.09.028

## 5.1 Abstract

Organic carbon in subsoils amounts to 40–60% of the global soil carbon pool and is generally characterized by apparent turnover times of hundreds to thousands of years and an increasing spatial variability with depth. The objective of this study was to analyze the amounts and distribution of SOC and to elucidate the turnover and storage mechanisms throughout deep soil profiles of a sandy Dystric Cambisol on Pleistocene glacial deposits under beech forest in northern Germany. The soil was sampled within a grid design at three replicated profiles, each at 8 sampling depths (10, 35, 60, 85, 110, 135, 160, 185 cm) and 8 horizontal sampling points. 192 samples were analyzed for bulk density, texture, pH, SOC, total N, $^{13}$C-SOC, oxalate- and dithionite-extractable Fe and Al, root bio- and necromass, and microbial biomass C. For each sampling depth, a multi-effect model analysis was performed to identify the parameters explaining SOC variability. While SOC in the topsoil is only related to pH and dithionite-extractable Al, SOC in the subsoil is always related to root bio- and necromass and to Fe oxides and/or silt content. The comparison of SOC within rooted and root-free subsoil samples showed an up to 10 times higher SOC content in the rooted soil samples in comparison to the root-free samples. While the SOC content in the root-free soil declined with increasing depth the rooted soil samples showed no stratification with depth but were characterized by a higher spatial variability of SOC. At the same time, SOC in rooted soil samples has the same $\delta^{13}$C values as in root-free samples, indicating a similar degree of microbial processing. Microbial biomass C ($C_{mic}$) was not different between rooted and root-free samples, resulting in much higher $C_{mic}$:SOC ratios in the root-free soil. Since rooted soil samples are characterized by significantly higher silt and oxalate-extractable Fe ($Fe_o$) contents, it appears that roots preferentially grow into these chemically and physically slightly more favorable zones. At the same time, these higher inputs were apparently better stabilized through sorption to silt and metal oxyhydroxides, thus leading to the longer-term SOC sequestration in these hot-spots enhancing the spatial variability of SOC in subsoils.

***Keywords:*** subsoil, carbon storage, metal-oxyhydroxides, root biomass, variability

## 5.2 Introduction

Soils store large amounts of organic carbon (OC), generally exceeding that in the phytomass. Estimates of global organic carbon pools in terrestrial soils vary greatly, ranging from 500 to 3000 Pg in the top 1 m, with a median value of about 1460 Pg (Scharlemann et al. 2014). Still, the global carbon stocks in soils may be highly underestimated. Considering the second meter of soil, the carbon pool is estimated to increase by about 490 Pg while including the profile down to three meters depth (200–300 cm), the SOC pools would even increase by about 840 Pg in comparison to the pool within the top meter (Jobaggy and Jackson 2000; Batjes 1996). Especially forests soils store high amounts of organic carbon. Although subsoils store between 30 and 60% of global SOC the storage mechanisms and degradation processes are still poorly understood (Chabbi et al. 2009). Former studies on carbon storage and turnover focused mainly on processes in the top 30 cm where root density and SOC content are highest (Rumpel et al. 2012; Trumbore 2009; Chabbi et al. 2009). Recently, there is an arising interest in OC distribution, storage, and turnover in subsoils to assess the SOC behavior in deeper soil regions as a potential $CO_2$ source due to climate or management changes (Rumpel and Kögel-Knabner 2011).

Another distinct property of subsoil organic matter is its high apparent $^{14}C$ age which generally increases below 30 cm continuously indicating mean residence times of several 103 to 104 years (Rethemeyer et al. 2005; Mikutta et al. 2006; Jenkinson et al. 2008; Kögel-Knabner et al. 2008; Trumbore 2009). Large pool size and high radiocarbon age suggest that subsoil organic matter (OM) has accumulated at very low rates over very long time periods and therefore appears to be very stable. Consequently, subsoil OM was generally not considered to be relevant for the global C cycle due to its low sequestration potential and a low risk for destabilization.

However, some recent studies suggest that subsoil C pools are more dynamic than previously assumed since they appear to be affected by environmental and management changes on an annual to decadal basis (Baisden and Parfitt 2007; Leuschner et al. 2014; Mobley et al. 2015; Steinmann et al. 2016). This may be due to changes of input fluxes with roots and DOC or changes in their turnover times. Nevertheless, the underlying processes are only poorly understood (Preusser et al. 2017). There is some evidence that geogenic carbon “inherited” from the parent material may contribute to subsoil OC pools and thus partly explain the apparent old $^{14}C$ age (Rethemeyer, personal communication, Paul et al. 2001, Helfrich et al. 2007). Some

studies suggest that OC in subsoils is a highly processed residue of microbial degradation, making it recalcitrant to further microbial degradation (Lomander et al. 1998; Coleman et al. 1997; Stevenson 1994). However, recent studies found high amounts of easily degradable soil organic matter components in subsoils such as simple microbial carbohydrates or amino sugars (Krull and Skjemstad 2003; Liang and Balser 2008; Salomé et al. 2010) which apparently resist over long time periods (Rumpel et al. 2010). The persistence of such easily degradable compounds might be explained by their spatial separation from the microbial consumers (Rumpel et al. 2012, Salomé et al. 2010) as evidenced by the increasingly patchy distribution of SOC with increasing depth (Don et al. 2007) resulting in an enhanced inaccessibility of organic carbon for microorganisms (Lützow et al. 2006).

In addition, the association of OC with metal oxyhydroxides and clay minerals is considered as an important stabilization mechanism (Kleber et al. 2015; Porras et al. 2017) that may be more relevant in subsoils where the density of fresh sorption sites is higher as compared to topsoil horizons (Kaiser and Guggenberger 2003). Typically this is mirrored by the increasing contribution of mineral-associated SOC with soil depth (Eusterhues et al. 2007; Lorenz et al. 2011). Apart from minerals of the clay fraction (Kögel-Knabner et al. 2008; Eusterhues et al. 2005), the silt fraction may even contribute to SOC sorption to a higher extent than the clay fraction but with lower mean residence times than clay bound SOC, as shown by Curtin (2002) for Ap-horizons. Other authors consider aluminum (Al) and iron (Fe) oxyhydroxides as key factors for SOC stabilization in soil (Percival et al. 2000; Mikutta et al. 2009; Porras et al. 2017). Especially, Al-organic complexes can increase the stabilization capacity for SOC in comparison to Fe complexes, whereas the reactivity of crystalline Fe oxides for SOC stabilization can be enhanced through Al substitution (Kleber et al. 2015; Barthés et al. 2008).

Although the variability of SOC content generally increases with soil depth, little is known about the factors controlling the SOC distribution in subsoils. To elucidate the SOC distribution and the reasons for a suggested higher heterogenic allocation we applied a grid mapping approach of soil and SOC properties within a sandy Dystric Cambisol (FAO-WRB 2014) developed on Pleistocene glacio-fluviatile deposits. The study was carried out to better understand the mechanisms that engender the greater variability of subsoil OC as this will 1) allow a better

estimation of OC contents in subsoil, and 2) help to guide future management strategies for increasing subsoil OC stocks.

## 5.3 Materials and Methods

### *Study site*

The study site is located in a managed beech forest (*Fagus sylvatica*) established in 1916, 40 km north-west of Hannover (N 52°34′21,446″ E 9°18′53,039″), Lower Saxony, Germany at 74 m a.s.l. The trees are even-aged with a mean breast height diameter of 26.3 cm (Angst et al. 2016a). The climate is a moderate temperate climate with mean annual precipitation of 718 mm and mean annual temperature of 8.7 °C (WorldClim Model). The soil, developed on sandy glacio-fluviatile deposits from the Saale glaciation (Bundesanstalt für Bodenforschung 1973), is a Dystric Cambisol (FAO-WRB 2014) with varying clay contents between 1 and 9%, silt contents of 3 to 40% and differing sand contents of 65 to 95% in the whole soil profile down to 185 cm (Table 5.1). The clay fraction of individual horizons was mainly composed of illite and kaolinite with smectite minerals being virtually absent. The horizons of the profile were classified as follows: AE (0–2 cm) – Bsw (2–12 cm) – Bw (12–36 cm) – BwC (36–65 cm) – C (65–125 cm) – 2C (125–150 cm) – 2Cg (150–180 cm) – 3C (+ 180 cm). The forest floor shows variable thickness (between 4.0 and 9.5 cm) and was classified as a typical mor. The mean accumulation of litterfall estimated for 2013 was 366 g dry matter $m^{-2}$ resulting in a carbon input of 178 g C $m^{-3}$ on top of the soil (data not shown). The soil is low in OC and total nitrogen, with concentrations ranging from 27 g OC $kg^{-1}$ and 1.0 mg N in the topsoil to < 0.1 g OC $kg^{-1}$ and 0.002 mg N $kg^{-1}$ below 50 cm depth. The apparent $^{14}$C-age of bulk soil OC increased with increasing depth, with the upper soil showing modern ages (later than 1950) and OC in deeper soil regions showing ages ranging from 2650 to 3860 years (Angst et al. 2016b).

**TABLE 5.1: Mean bulk density (BD), pH (0.01 M $CaCl_2$), texture, root biomass, root necromass, dithionite- and oxalate-extractable Fe ($Fe_d$; $Fe_o$) and aluminum ($Al_d$, $Al_o$), Fe in crystalline Fe oxides ($Fe_{(d-o)}$) of soil samples originating from three transects at the Grinderwald site at different depth (n = 24 for each depth). Numbers in brackets show coefficient of variation in % of the respective depth over three transects (n = 24).**

| Depth (cm) | BD ($g\ cm^{-3}$) | pH ($CaCl_2$) | Clay | Silt | Sand | Root biomass | Root necromass | $Fe_d$ | $Fe_o$ | $Fe_{(d-o)}$ | $Al_d$ | $Al_o$ |
|---|---|---|---|---|---|---|---|---|---|---|---|---|
| | | | | (%) | | ($g\ l^{-1}$) | | | | ($mg\ g^{-1}$) | | |
| **10** | 1.19 (13) | 3.51 (10) | 2.96 (25) | 30.89 (27) | 64.81 (14) | 0.82 (67) | 1.17 (31) | 3.03 (15) | 0.82 (49) | 2.21 (33) | 0.74 (49) | 0.25 (79) |
| **35** | 1.32 (13) | 4.20 (2.6) | 3.98 (36) | 34.53 (25) | 61.49 (16) | 0.58 (70) | 0.74 (50) | 2.36 (18) | 1.63 (32) | 0.73 (64) | 1.32 (27) | 0.50 (56) |
| **60** | 1.54 (15) | 4.16 (3.8) | 2.82 (58) | 25.11 (38) | 72.06 (15) | 0.14 (144) | 0.15 (53) | 1.68 (30) | 0.70 (37) | 0.97 (52) | 0.55 (30) | 0.22 (77) |
| **85** | 1.54 (11) | 4.02 (2.9) | 1.73 (53) | 11.64 (75) | 86.61 (11) | 0.01 (336) | 0.01 (465) | 1.48 (46) | 0.35 (59) | 1.19 (43) | 0.29 (43) | 0.11 (181) |
| **110** | 1.49 (11) | 3.94 (3.3) | 2.02 (58) | 13.12 (84) | 84.86 (14) | 0.04 (188) | 0.03 (192) | 1.61 (54) | 0.32 (48) | 1.29 (57) | 0.28 (43) | 0.08 (80) |
| **135** | 1.50 (7.5) | 3.91 (5.4) | 2.97 (105) | 21.56 (124) | 75.47 (40) | 0.11 (188) | 0.03 (173) | 3.35 (94) | 0.52 (114) | 2.83 (91) | 0.47 (110) | 0.19 (181) |
| **160** | 1.52 (7.7) | 3.95 (5.4) | 1.87 (114) | 15.36 (160) | 82.80 (32) | 0.13 (232) | 0.03 (288) | 2.51 (118) | 0.38 (120) | 2.13 (118) | 0.34 (120) | 0.14 (161) |
| **185** | 1.49 (6.4) | 3.97 (4.2) | 1.52 (102) | 10.45 (139) | 88.02 (18) | 0.09 (303) | 0.03 (272) | 1.57 (83) | 0.26 (86) | 1.30 (85) | 0.23 (78) | 0.09 (144) |

### *Sampling and investigation design*

Soil sampling was conducted at the site on June 10th and 11th, 2013 along three randomly distributed transects with a minimal distance of 10 m from each other, each aligned towards a main tree to analyze the root effects on SOC distribution. The 330 cm long transects were excavated to 200 cm depth. The sampling scheme was designed as a regular grid with vertical and horizontal dimensions of 185 and 315 cm, respectively (Angst et al. 2016a). The regular grid started close (10–50 cm) to a main tree (*Fagus sylvatica* L.) and extended in 45 cm horizontal intervals and downwards in 25 cm steps. Soil samples were taken at each grid intersection with a round steel core sampler (diameter: 8.5 cm, height: 6 cm) at: 10, 35, 60, 85, 110, 135, 160, and 185 cm depth and 0, 45, 90, 135, 180, 225, 270, 315 cm horizontal dimension. Thus, a total of 64 soil samples were taken at each transect resulting in a total sum of 192 samples for the whole site. Immediately after sampling, the fresh soil samples were sieved (< 2 mm) to remove stones and roots. After sieving the soil samples were stored in polyethylene bags at 4 °C. The coarse (> 2 mm) material was filled into polyethylene bags, stored at 4 °C for weighing and determination of root biomass.

### *Analysis of soil properties*

#### *SOC, $N_t$ and isotope ratios*

Prior to the analysis of soil organic carbon and total nitrogen ($N_t$) by using a Vario EL analyzer (Elementar, Hanau, Germany) the soil was dried for 3 days at 50 °C and ground by a planet micromill (Fritsch Pulverisette 7). The $^{13}C/^{12}C$ isotope ratios of the soil samples were determined by isotope ratio mass spectrometer (Thermo Fisher Scientific Delta plus, Bremen, Germany) coupled to an elemental analyzer (CE Instruments FLASH EA 1112NA 1500, Wigan, UK).

#### *pH and texture*

The pH of all 192 soil samples was measured in 0.01 M $CaCl_2$ with a ratio of soil to solution of 1:2.5. Texture was analyzed with a laser particle sizer (Analysette 22, Fritsch, Idar-Oberstein, Germany). For this, soil samples with SOC contents above 1.2% were treated with $H_2O_2$ before analysis to destroy organic matter. Since all soil samples were acidic, no carbonate dissolution was necessary. Further, at the beginning of the measurement 5 ml of $Na_4P_2O_7$ peptisator were

added to the sample as dispersing agent. In addition, two droplets of the detergent Dusazin 9.0.1 were added to reduce surface tension of the water in the measurement chamber to ensure that all particles sink into the water for the laser detection. To increase the accuracy of the determination the samples were separated into two size fractions (> 0.2 and < 0.2 mm) with a 0.2 mm sieve and each fraction was measured separately.

***Root biomass***

Roots of each soil sample were picked from the sieving residual material (> 2 mm). To separate the roots from adhering soil particles, each sample was washed with deionized water using a sieve of 0.25 mm mesh size. The separated root samples were soaked in distilled water and all roots larger than 10 mm in length were picked out for further examination. Smaller root fractions were neglected during this first step. Under the stereo microscope, the larger rootlets > 10-mm length were separated, firstly into living (biomass) and dead (necromass) roots, and secondly into fine (≤ 2 mm in diameter) and coarse (> 2 mm in diameter) roots. The distinction of living and dead roots was made following the criteria root and periderm color, tissue elasticity, and cohesion of cortex, periderm and stele (Hertel et al., 2013). All roots were dried at 70 °C for 48 h and weighed. Although fine root fragments < 10 mm in length were not considered, the majority of fine root biomass (> 95%) is captured with this approach (Bauhus and Bartsch 1996; Leuschner et al. 2001). This leads to an underestimation of the fine root necromass which has therefore to be corrected for the small root fraction (< 10 mm length). The correction was made by extrapolation using soil depth-specific regression equations. These regression equations, relating the mass of dead fine roots < 10 mm to dead fine roots ≥ 10-mm length, were established for other samples from the same plot, for which the mass of small dead roots was quantified using a method introduced by Van Praag et al. (1988) and modified by Hertel (1999).

***Pedogenic Fe and Al fractions***

Dithionite-citrate-extractable Fe and Al ($Fe_d$, $Al_d$) were determined according to Blakemore et al. (1987) where 1 g air-dry soil in presence of 1 g sodium dithionite was extracted by 20 ml 22% sodium citrate. After shaking for 16 h and addition of 5 ml of 5 mM $MgSO_4$, samples were

centrifuged for 20 min at 500g and filtered through 0.1-µm polyethersulfone membranes. The filtrate was analyzed for dissolved Fe and Al by inductively coupled plasma optical emission spectroscopy (ICP-OES; Varian 725-ES, Varian Australia Pty Ltd., Mulgrave, Australia). Oxalate-extractable Fe and Al were determined after extraction of 1 g air-dry soil by 40 ml 0.2 M oxalic oxalate (pH 3) for 4 h in the dark (Ross and Wang, 1993). After centrifugation (500g, 20 min) the filtered extract (0.1-µm polyethersulfone) was analyzed for dissolved Fe and Al by ICP-OES. Dithionite-citrate-extractable Fe ($Fe_d$) represents the amount of pedogenetically formed Fe within oxyhydroxides as well as in organic complexes while dithionite-citrate-extractable Al ($Al_d$) characterizes an Al fraction potentially substituted in Fe oxides, as well as free aluminum and aluminum in metal-organic complexes (Dahlgren and Saigusa 1994). Oxalate-extractable Fe ($Fe_o$) and Al ($Al_o$) derive from poorly crystalline aluminosilicates, ferrihydrite, Al-gels, and Al- and Fe-organic complexes. The difference of dithionite-citrate-extractable and oxalate-extractable Fe ($Fe_d$-$Fe_o$) is taken as a measure of crystalline Fe oxides.

***Microbial biomass C***

The chloroform fumigation extraction (CFE) method (Vance et al. 1987) was used to determine microbial biomass carbon. Chloroform fumigated (24 h) and non-fumigated samples (sieved to < 2 mm) with a fresh soil weight of 10 g were extracted with 40 ml of 0.05 M $K_2SO_4$ on a horizontal shaker at 250 rpm for 30 min and then centrifuged at 4400g for 30 min. C concentrations of 1:4 dilutions of the supernatants were measured using a TOC-TNb Analyzer Multi-N/C 2100S (Analytik Jena, Jena, Germany). 200 µl of 1 M HCl was added to the dilutions to remove inorganic C. Microbial biomass C was calculated as $E_C$ / $k_{EC}$, where $E_C$ = (organic C extracted from fumigated soil) − (organic C extracted from non-fumigated soil) and $k_{EC}$ = 0.45 (Wu et al., 1990).

***Statistical analysis***

To study the effects of pH, silt, clay, root biomass, root necromass, oxalate-extractable Fe, Fe in crystalline oxides, oxalate-extractable Al, dithionite-citrate-extractable Al (fixed effects) and transect (random effect) on the content of SOC in each soil depth down to 135 cm, a multiple

linear regression model with spatially correlated errors was fitted with SAS version 9.4 (SAS Institute Inc., 2015). The model for spatial covariance among observations at the same depth and different distances from the tree was exponential. The estimation procedure was restricted to maximum likelihood and the denominator degrees of freedom were estimated using the Kenward-Roger method. Only factors with significant contributions ($p \leq 0.05$) were considered and the models with the lowest value of the Akaike information criterion (AIC) were chosen. The effect of the transect was not significant in the models for all depths, except for the model for 110 cm, where three transect-specific intercepts were thus obtained. For each final model, we tested whether the slopes between the three transects were significantly different by inspecting the interactions between transects and covariates. Studentized residuals were inspected for homoscedasticity and normality.

In one case (135 cm) the response variable was log-transformed to achieve normality and homoscedasticity. For two depths, the models with the lowest AIC were implausible: in 85 cm a negative contribution of crystalline Fe was obtained and in 135 cm negative contributions of dithionite-extractable Al und crystalline Fe. In these cases, the backward elimination was subsequently done without these factors.

Measured SOC contents were plotted against modeled ones. In cases of normality (35 and 60 cm), Pearson Product moment correlation coefficients were reported. Otherwise, Spearman rank correlation coefficients were shown (Fig. 5.2).

For the analysis of root effects on SOC content, data from each sampling depth were separated into two groups, one where roots had been found (“rooted soil”) and one without roots (“root-free soil”).

## 5.4 Results

### *Soil physical and chemical properties*

The bulk density of the soils collected from all three transects ranged between 1.19 and 1.54 g $cm^{-3}$ and showed the lowest value in 10 cm depth and increased with increasing depth until 60 cm (Table 5.1). Below 60 cm depth, bulk density varied moderately between 1.49 and 1.54 g $cm^{-3}$ with low depth-specific variability.

The texture of the soil was mainly built up by the sand fraction. Over all depths in the three transects, the sand content always accounted for > 60% of the texture class but varied between 61 and 88% (Table 5.1). As a result, the silt and clay fractions which can act as potential SOC stabilizing components varied strongly within the profile and within single sampling depths (Table 5.1). Silt contents were highest with > 30% in the topmost samples (10 and 35 cm) and mean values never fell below 10% in the whole profile. But the variability of this textural class was highest among all three fractions in the lower subsoil (135 to 185 cm). Clay was present only to a minor extent with a range of mean values between 1.52 and 3.98% and no pronounced depth gradient (Table 5.1). Still, similar to silt, the variability of clay content was highest in 135 to 185 cm.

The soil pH of the whole profile was in the acidic range and did not change distinctively with depth. The lowest value of 3.51 was found in 10 cm depth with slightly increased mean values of 4.20 and 4.16 in depth 35 and 60, respectively. The soil below 60 cm showed mean pH values around 3.94 (± 0.03). The variability of pH values among the three transects was low and showed the highest variation of 10% in 10 cm depth (Table 5.1).

The dithionite-citrate-extractable Fe as an indicator for pedogenic Fe oxyhydroxides in soil ranged between 1.48 and 3.35 mg $g^{-1}$ with the highest values found in 10 and 135 cm depth (Table 5.1). In contrast, dithionite-citrate-extractable Al, oxalate-soluble Fe and Al showed the highest values in 35 cm followed by a continuous decrease down to 110 cm, with a small maximum in 135 cm. Iron in crystalline oxides ($Fe_{d-o}$) amounted to 2.21 mg $g^{-1}$ in 10 cm depth and decreased strongly in 35 cm. Below 35 cm the values increased up to a maximum of 2.83 mg $g^{-1}$ in 135 cm depth (Table 5.1).

### *SOC and isotopic composition*

The highest SOC contents of 1.15% were found in 10 cm depth followed by a steep decline down to 0.12% in 60 cm (Fig. 5.1a and Supplementary material, Table S5.1). Below 60 cm, the mean SOC contents varied around 0.05% down to 185 cm with some single samples with contents of up to 0.4% (Fig. 5.1a). Due to the very low SOC contents in the subsoil and spotty distribution of SOC, the variability increased with increasing depth as underlined by the highest coefficient of variation of 153% in 160 cm depth, compared to 28–40% in the samples from 10 to 85 cm depth (Supplementary material Table S5.1).

The $\delta^{13}C$ values of SOC also showed a depth gradient down to 60 cm, with mean values increasing from − 27.9‰ in 10 cm to − 26.1‰ in 60 cm (Fig. 5.1b). Below this depth, the $\delta^{13}C$ values were relatively stable, with a slight decreasing trend from 110 cm (− 26.31‰) to 185 cm (− 26.49‰). The distribution of data showed a higher variability of $\delta^{13}C$ values in 160 cm and 185 cm depth compared to the upper soil (Fig. 5.1b).

### *Root biomass and necromass*

Root biomass (Table 5.1, Fig. 5.1c) and necromass (Table 5.1) strongly decreased with increasing depth. Assuming a mean C-content of 45% in roots (Hertel, pers. comm.), the mean root-C:SOC ratio was 0.07 to 0.10 in the three top depths (10, 35, 60 cm) and much lower in the deeper subsoil (0.01 to 0.06). Despite the strong decrease with depth, roots were abundant in the whole profile, but the distribution was patchier in deep soil regions. The variation of root biomass distribution increased with increasing depth which was indicated by the small number of sampling points containing roots (Fig. 5.2). In 10 and 35 cm depth roots were present in 23 out of 24 samples, whereas below 60 cm roots were only found in 4–13 out of 24 samples (Fig. 5.2). Through this patchy distribution with increasing depth, the coefficient of variation for root biomass increased from around 70% (10 and 35 cm) to 144–336% in the deeper soil (Table 5.1). Similarly, root necromass decreased with depth, while variability increased (Table 5.1). The root biomass to necromass ratio increased with depth ranging from 0.74 in 10 cm depth to maximum 25 in 160 cm, but without a clear depth gradient (whereas the coefficient of variation of these ratios strongly increased with increasing depth (Supplementary material, Table S5.1).

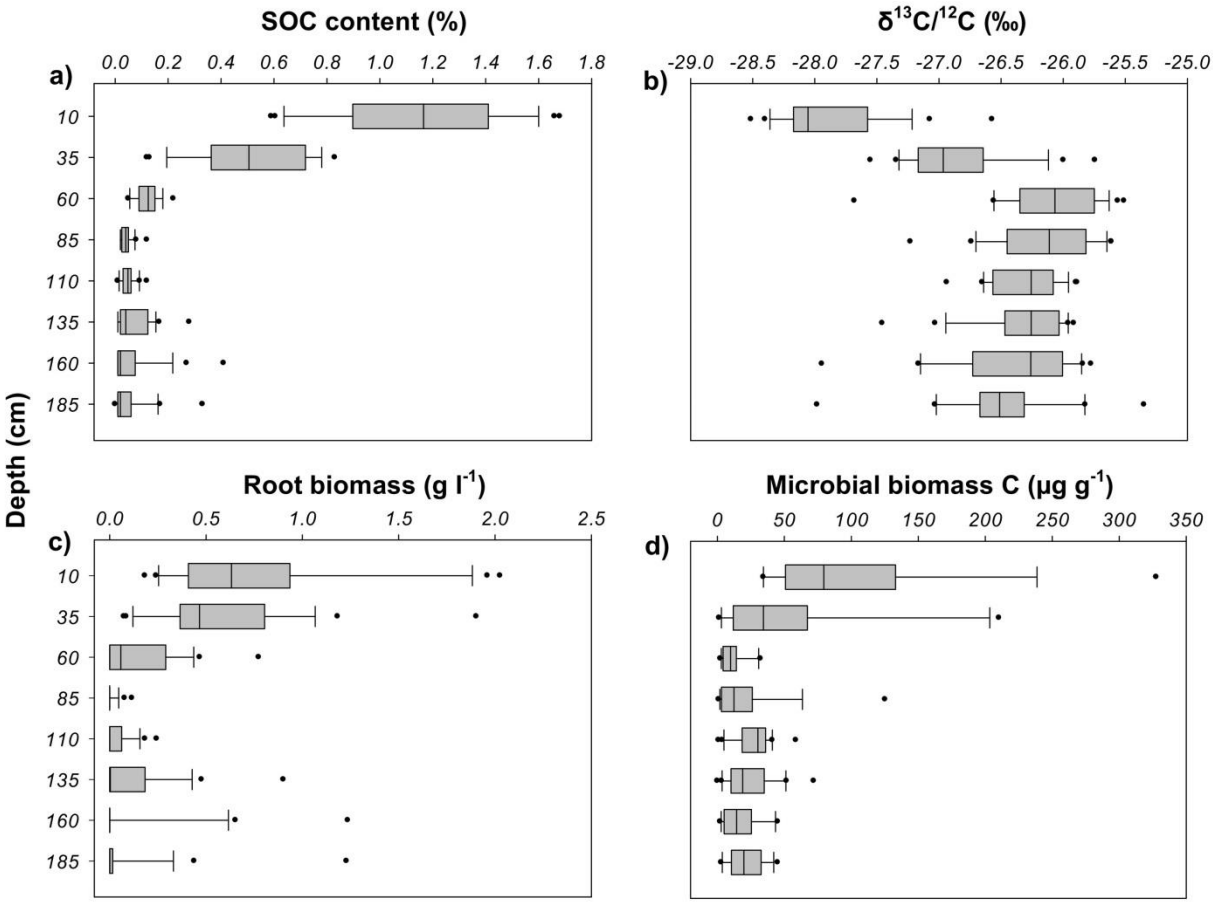


**FIGURE 5.1: Boxplots of a) SOC content (%), b) $\delta^{13}C/^{12}C$ (‰), c) root biomass (g $l^{-1}$) and d) microbial biomass C ($C_{mic}$, µg $g^{-1}$) within the soil profiles in different depth.**

### *Microbial biomass C*

Similar to the SOC content, $C_{mic}$ showed a strong decrease down to 60 cm depth. The highest Cmic values were determined in the upper soil with maximum values of 328 µg $g^{-1}$ and a mean value of 105 µg $g^{-1}$ in 10 cm (Fig. 5.1d, Supplementary material, Table S5.1). This was followed by a 47% reduction of Cmic in the second depth (35 cm) and a further 80% decrease in 60 cm. Below 60 cm, $C_{mic}$ varied around a mean of 24 µg $g^{-1}$ (± 3 µg g− 1) down to 185 cm. Interestingly, taking the whole data set, $C_{mic}$ was not correlated to SOC and in 10 cm depth only poorly correlated to SOC (Pearson correlation coefficient: r = 0.61; data not shown).

***Controls of SOC distribution analyzed with mixed effect model***

To further elucidate the soil parameters influencing SOC contents, a mixed effect model analysis was conducted for the depths 10 to 135 cm (Table 5.2). Interestingly, the presence of roots (live or dead) influenced SOC content in all sampling depths, except in 10 cm (Table 5.2). Among the textural parameters, only silt and not clay content was extracted as a relevant parameter in three out of four soil depths below 35 cm. In all depths, except 135 cm, SOC was related to some measure of metal oxide content. In 35, 85, and 110 cm this was $Fe_o$, indicative for less crystalline Fe oxyhydroxides such as ferrihydrite or nanocrystalline goethite. In 10 and 60 cm, SOC is related to $Al_d$, and in 35 cm, Fe in crystalline Fe oxides were also extracted as explanatory variable by the model (Table 5.2).

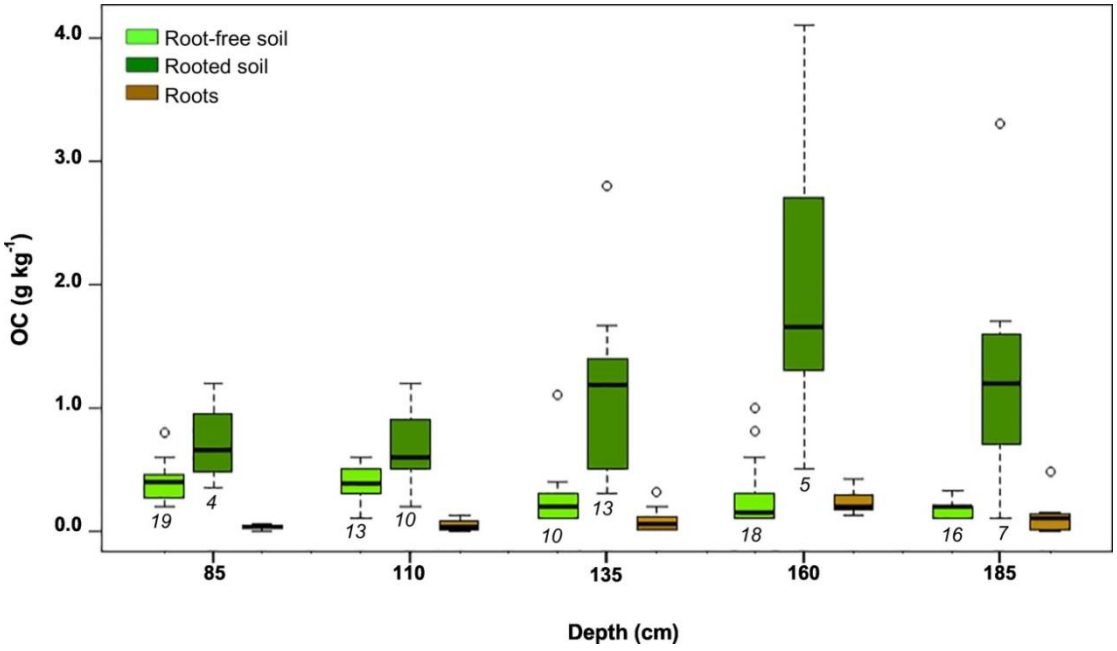


**FIGURE 5.2: Boxplot of OC-contents (g $kg^{-1}$) of roots, root-free and rooted soil in subsoil (85, 110, 135, 160, 185 cm). Italic numbers below the boxplot represent the number (n) of samples considered; number of root samples are conform to the number of rooted-soil samples.**

**TABLE 5.2: Results (intercepts and regression coefficients) of the mixed effects models for the SOC content (%) or its natural logarithm (log) with different factors (n = 23 for each depth due to missing data for one of the factors). $Al_d$: dithionite-extractable Al, $Fe_o$: oxalate-extractable Fe, $Fe_{(d-o)}$: Fe in crystalline Fe oxides. Bold words represent significant parameters influencing SOC contents.**

| Depth (cm) | Response variable | Intercept | Regression terms |
|---|---|---|---|
| **10** | SOC | 5.24% | $-1.26\% * \mathbf{pH} + 0.439$ g/mg % $* \mathbf{Al_d}$ |
| **35** | SOC | −0.350% | 0.312 l/g % $*$ **root biomass** + 0.410 g/mg % $* \mathbf{Fe_o} + 0.183$ g/mg % $* \mathbf{Fe_{(d-o)}}$ |
| **60** | SOC | −0.0243% | $2.00 * 10^{-3} * \mathbf{silt} + 0.813$ l/g % $*$ **root necromass** + 0.152 g/mg % $* \mathbf{Al_d}$ |
| **85** | SOC | $6.47 * 10^{-3}$% | 0.505 l/g % $*$ **root biomass** + 0.0999 g/mg % $* \mathbf{Fe_o}$ |
| **110** | SOC | Transect 1: $5.40 * 10-3$%<br>Transect 2: −0.0144%<br>Transect 3: $-2.23 * 10^{-3}$% | $8.84 * 10^{-4} * \mathbf{silt} + 1.04$ l/g % $*$ **root necromass** + 0.111 g/mg % $* \mathbf{Fe_o}$ |
| **135** | Log-SOC | −3.89 | $0.0311\%^{-1} * \mathbf{silt} + 32.5$ l/g $*$ **root necromass** |

The quality of the mixed effect models was very high for all depths (correlation coefficients between 0.87 and 0.96) and the distribution of values was generally satisfactorily even (Supplementary material, Fig. S5.1). The strongest correlation of modeled and measured SOC was found for 110 cm soil depth (r = 0.96) the only case where intercepts were calculated separately for each transect (Supplementary material, Fig. S5.1).

Since the mixed model analysis showed that the presence of roots had a strong effect on SOC content in the subsoil, this was investigated further, by separating all depth sample sets into root-free samples and samples with roots (Table 5.3). Since down to 60 cm depth, no root-free samples existed, this separation was only possible from 85 cm on downwards. In Fig. 5.2, the mean SOC content of rooted vs. root-free samples together with the root C-content of the rooted samples is presented for all five subsoil depths. Generally, more root-free than rooted samples were found in these depths, except for 135 cm. In the root-free samples, mean SOC content declined with depth, from 0.38 g $kg^{-1}$ in 85 cm to 0.16 g $kg^{-1}$ in 185 cm depth (Table 5.3, Fig. 5.2). The rooted samples did not show such a depth gradient and their SOC content was much more variable and showed up to 10 times higher median values than in the root-free samples.

Clearly, rooted samples, from which all visible roots had been removed, still contained substantially more SOC than root-free samples. Even if it is assumed that about 10–30% of the root biomass can remain as microscopic fragments in the sample (Hertel, pers. comm.), such fragments would contribute only 3–5% to the total SOC and thus cannot explain the large differences. If the higher SOC content in rooted samples were due to fresh root-borne C-inputs such as root hairs or exudates, this should be reflected in $\delta^{13}C$ values closer to that of the roots analyzed from the site (− 30.1 to − 28.2‰, unpublished). Instead, the mean $\delta^{13}C$ values of rooted soil samples were very similar to those in root-free samples, in two depths even slightly higher (Table 5.3).

Despite the much higher SOC content of the rooted samples and the assumed higher availability of fresh substrates, $C_{mic}$ showed no systematic differences between rooted and root-free samples (Table 5.3). As a consequence, the $C_{mic}$:SOC ratios in the rooted samples were generally much lower than in the root-free samples (Table 5.3) and similar to the ratios found in the rooted samples from the top 60 cm (data not shown). Interestingly, the rooted subsoil samples are generally also characterized by higher contents in clay, silt, $Fe_o$ and $Al_o$ and lower pH than the respective root-free samples (Table 5.3).

**TABLE 5.3: Mean soil properties in rooted and root-free soil in 85, 110, 135, and 185 cm depth and the mean variation shown as coefficient of variation (CV) in %. Numbers of samples are given in Fig. 5.2, respectively to each depth and soil sample.**

| Soil | 85 cm | | 110 cm | | 135 cm | | 160 cm | | 185 cm | |
|---|---|---|---|---|---|---|---|---|---|---|
| properties | Root-free | Rooted | Root-free | Rooted | Root-free | Rooted | Root-free | Rooted | Root-free | Rooted |
| **BD (g $cm^{-3}$)** | 1.47 | 1.5 | 1.54 | 1.47 | 1.55 | 1.42 | 1.55 | 1.55 | 1.55 | 1.51 |
| **CV (%)** | *11* | *14* | *11* | *13* | *4.6* | *8.9* | *6.6* | *8.4* | *6* | *7.8* |
| **$\delta^{13}C$ (‰)** | − 26.35 | − 26.30 | − 26.25 | − 26.42 | − 26.37 | − 26.80 | − 26.45 | − 26.67 | − 26.24 | − 25.88 |
| **CV (%)** | *1.6* | *0.64* | *1.1* | *0.91* | *0.84* | *1.7* | *1.6* | *2.9* | *1.2* | *3* |
| **SOC (g $kg^{-1}$)** | 0.04 | 0.07 | 0.03 | 0.11 | 0.03 | 0.2 | 0.02 | 0.13 | 0.04 | 0.07 |
| **CV (%)** | *44* | *50* | *46* | *51* | *103* | *66* | *102* | *68* | *51* | *79* |
| **pH** | 4 | 3.9 | 4 | 3.8 | 4 | 3.7 | 4 | 3.8 | 4 | 3.9 |
| **CV (%)** | *2.8* | *3.8* | *2.8* | *4* | *4.1* | *5.1* | *4* | *6.8* | *2.8* | *5* |
| **Clay (%)** | 2 | 2.1 | 1.6 | 4.2 | 1.3 | 4.1 | 0.84 | 3.1 | 1.7 | 2.2 |
| **CV (%)** | *52* | *57* | *43* | *88* | *126* | *83* | *99* | *78* | *56* | *66* |
| **Silt (%)** | 11 | 16 | 8.7 | 33 | 8.6 | 42 | 4.3 | 26 | 10 | 20 |
| **CV (%)** | *64* | *75* | *54* | *109* | *193* | *89* | *164* | *91* | *164* | *79* |
| **$Fe_d$ (mg $g^{-1}$)** | 1.6 | 1.7 | 2.7 | 4 | 1.6 | 6.2 | 0.94 | 2.9 | 1.4 | 1.8 |
| **CV (%)** | *51* | *22* | *42* | *72* | *87* | *91* | *90* | *73* | *41* | *58* |
| **$Fe_o$ (mg $g^{-1}$)** | 0.29 | 0.38 | 0.29 | 0.73 | 0.24 | 0.92 | 0.15 | 0.52 | 0.32 | 0.53 |
| **CV (%)** | *59* | *69* | *38* | *57* | *138* | *92* | *98* | *74* | *65* | *54* |
| **$Fe_{(d-o)}$ (mg $g^{-1}$)** | 1.3 | 1.4 | 2.4 | 3.3 | 1.3 | 5.3 | 0.78 | 2.4 | 1.1 | 1.2 |
| **CV (%)** | *56* | *37* | *43* | *79* | *84* | *92* | *90* | *73* | *47* | *59* |
| **$Al_d$ (mg $g^{-1}$)** | 0.27 | 0.31 | 0.31 | 0.63 | 0.21 | 0.84 | 0.13 | 0.44 | 0.27 | 0.37 |
| **CV (%)** | *45* | *91* | *35* | *54* | *119* | *95* | *89* | *76* | *36* | *48* |
| **$Al_o$ (mg $g^{-1}$)** | 0.06 | 0.11 | 0.05 | 0.32 | 0.12 | 0.23 | 0.08 | 0.11 | 0.07 | 0.3 |
| **CV (%)** | *59* | *156* | *50* | *89* | *65* | *140* | *198* | *86* | *182* | *54* |
| **$C_{mic}$ (µg $g^{-1}$)** | 22 | 31 | 17 | 27 | 30 | 18 | 21 | 27 | 20 | 18 |
| **CV (%)** | *143* | *29* | *63* | *33* | *93* | *65* | *90* | *59* | *84* | *33* |
| **$C_{mic}$/SOC (mg $g^{-1}$)** | 56 | 26 | 58 | 59 | 98 | 32 | 114 | 18 | 115 | 26 |
| **CV (%)** | *126* | *24* | *61* | *54* | *114* | *85* | *138* | *84* | *59* | *73* |

## 5.5 Discussion

In the Grinderwald forest located on Pleistocene glacio-fluviatile sandy deposits a Dystric Cambisol (FAO-WRB 2014) developed, low in SOC and $N_t$ with low pH values. As found in numerous other studies, SOC strongly decreases with depth (Rumpel and Kögel-Knabner 2011; Salomé et al. 2010; Rumpel et al. 2004). A striking feature of this SOC depth gradient is its increasing spatial variability with depth, indicating the existence of SOC hotspots formed by either localized inputs from roots or by DOC along preferential flow paths (Leinemann et al. 2016; Hafner et al. 2014; Tefs and Gleixner 2012; Syswerda et al. 2011; Salomé et al. 2010; Chabbi et al. 2009; Bundt et al. 2001). Angst et al. (2016b) have shown for the same site that lipid biomarkers from above-ground litter inputs were only found down to 35 cm depth, while SOC in greater depths was free of litter markers (Angst et al. 2016b). Therefore the main input of organic matter into the subsoil appears to originate from roots or root-rhizosphere interactions (Vancampenhout et al. 2012; Rumpel and Kögel-Knabner 2011; Lützow et al. 2006; Kögel-Knabner 2002; Gleixner 2003). Subsoil SOC hotspots may thus simply reflect the heterogeneous distribution of stabilizing agents such as metal oxyhydroxides and soil minerals (Eusterhues et al. 2005; Wiseman and Püttmann 2006; Kögel-Knabner et al. 2008). Don et al. (2007) found SOC variability to increase with soil depth and attributed this to variability in texture.

In the topsoil (10 cm), SOC content is adequately modeled with only pH and $Al_d$, suggesting that SOC accumulation is largely due to a pH-dependent reduced decomposition. In the subsoil below 10 cm, the oxalate-soluble Fe oxides ($Fe_o$) and/or silt contributed to explaining SOC contents in the mixed model analysis. An increasing importance of the fine texture class for SOC stabilization in deeper soil regions was also found by Rumpel et al. (2004), who showed a strong association of OC with the clay fraction (< 0.63 μm). On the other hand, Kalbitz and Kaiser (2008) showed that the mean residence time of SOC stabilized by Fe- and Al oxyhydroxides is higher in comparison to that sorbed to clay minerals. At the Grinderwald site, the silt fraction seemed to be more important for SOC stabilization than the clay fraction. However, this may simply be an artefact of the statistical analysis since silt and clay content were highly correlated in all depths.

But the most interesting result of this data analysis was that root inputs, appeared to play an important role in explaining the high variability of SOC content in the lower subsoil. The mixed

effect model showed that densities of dead or living roots were important independent variables describing SOC contents in all depths between 35 and 135 cm.

The importance of root inputs as source for subsoil SOC is further supported by the large SOC differences between rooted and root-free samples in the subsoil (Fig. 5.2). Since all visible root fragments had been removed from the rooted soil samples prior to SOC analysis and their C contribution to the elevated SOC content was negligible, the higher SOC content of the rooted soil samples cannot be explained by C inputs from the current roots, alone. Annual subsoil root exudation rates at the site were estimated by Tueckmantel et al. (2017) to be in the range of 80–212 mg C $g^{-1}$ root, which would thus also be far too low to explain the observed SOC differences. Furthermore, the similarity in $\delta^{13}C$ values in rooted and root-free subsoil samples indicates that SOC has undergone similar microbial processing in all samples and therefore cannot be attributed to fresh root-derived residues but originated from previous C inputs which had accumulated in the past. Unfortunately, only a very limited number of $^{14}C$ analyses was available for this sample set (n = 3–9 for each depth), but the values indicated that rooted soil samples generally were much more enriched in $^{14}C$ (i.e. apparently younger) than root-free soil samples (Rethemeyer, personal communication).

A possible explanation is that the current roots were already present at the sampling location since several years and have supplied root-derived C through exudation, the shedding of dead root tissue, mucilage production or turnover of mycorrhizal biomass. $^{14}C$ data gave approximate root ages of 3 to 13 years for roots of 2–5 mm in diameter for the subsoil of the studied profiles (Kirfel, Hertel, Leuschner, in preparation), indicating that rhizodeposition is a process with continuity of a decade or more in beech root systems, except for the fine and finest root fraction which are turned over usually in time spans between 3 months and 3 years (Kubisch et al. 2016). Roots have also been found to grow preferentially in old root channels because the penetration resistance is lower, water flows preferentially here, or roots are foraging for nutrients released from dying roots (Rasse and Smucker 1998). Thus, root growth may have caused a legacy effect that is visible in the SOC distribution in the subsoil.

This spatial legacy effect appeared to be primarily caused by small scale differences in clay, silt, $Fe_o$ and $Al_o$ leading to better nutrient and water availability at this local scale. Since the rooted soil samples contained more clay, silt, $Fe_o$ and $Al_o$, this preferential root growth could also result

from better nutrient and water availability than in the root-free soil. Still, the relationships found between SOC and soil mineralogical and textural parameters in the mixed model analyses (Table 5.2) showed that root densities only partly explain overall SOC variability and that therefore mineral-related stabilization mechanisms also control SOC variability.

To get information about the availability of SOC to microorganisms it might be interesting to look at the mean $C_{mic}$:SOC ratios. The rooted samples showed much lower ratios in comparison to the root-free samples ranging between 58 and 115 mg $g^{-1}$, which are excessively high values that are rarely found in topsoils (Blagodatskaya and Anderson 1998; Joergensen et al. 1995). It therefore is highly unlikely, that this is from active microbial biomass, but possibly reflects a high proportion of dormant or very slowly overturning microorganisms at these depths. Further studies show that the different microhabitats in the subsoil are preferentially colonized by oligotrophic microorganisms such as Acidobacteria that are characterized by their slow growth rates. In addition, the slow growth rate might be caused not only by specific slow growing microorganisms but also by oxygen as well as P and N limitation (Preusser et al. 2017). Further, the missing correlation of $C_{mic}$ with SOC in the subsoil can be explained by the spatial separation of SOC and microorganisms (Rumpel et al. 2012; Dungait et al. 2012). If the sampling would be conducted on a smaller scale (µm-mm scale) only reflecting the microbial habitat (Nunan 2017; Poll et al. 2006; Gaillard et al. 1999) the correlation to SOC might be stronger in the subsoil.

## 5.6 Conclusions

This study showed that the increasing spatial variability of SOC down to 185 cm depth can largely be explained by a complex interaction between soil texture and mineralogy with root growth. At our study site with its heterogeneous soil texture and mineral composition, roots preferentially grow into soil compartments with finer texture and higher metal oxyhydroxide contents and thus the observed SOC accumulation in these hot spots appears to be input-controlled. However, the mixed model analysis showed that texture and Fe oxides were also truly independent variables for explaining SOC variability in the subsoil, suggesting that the inhomogeneous distribution of these SOC stabilizing agents further control the degradation of fresh root derived inputs which is reflected in the lower $C_{mic}$:SOC ratios in the rooted samples. Therefore, the primary factor controlling the observed spatial SOC variability in the subsoil at our site is the textural and mineralogical variability as it influences both root distribution and SOC stabilization.

***Acknowledgements***

This project was supported by the German Research Foundation (DFG) within the Research Group FOR 1806 with participation of the subprojects: MA 1830/14-1, GU 406/28-1, HE 6877/1-1, KA 1590/11-1, LE 762, LU 583/15. Thank all the colleagues of the Research Group for measuring lots of samples and for the powerful helping hands in the field.

## Supplementary Material

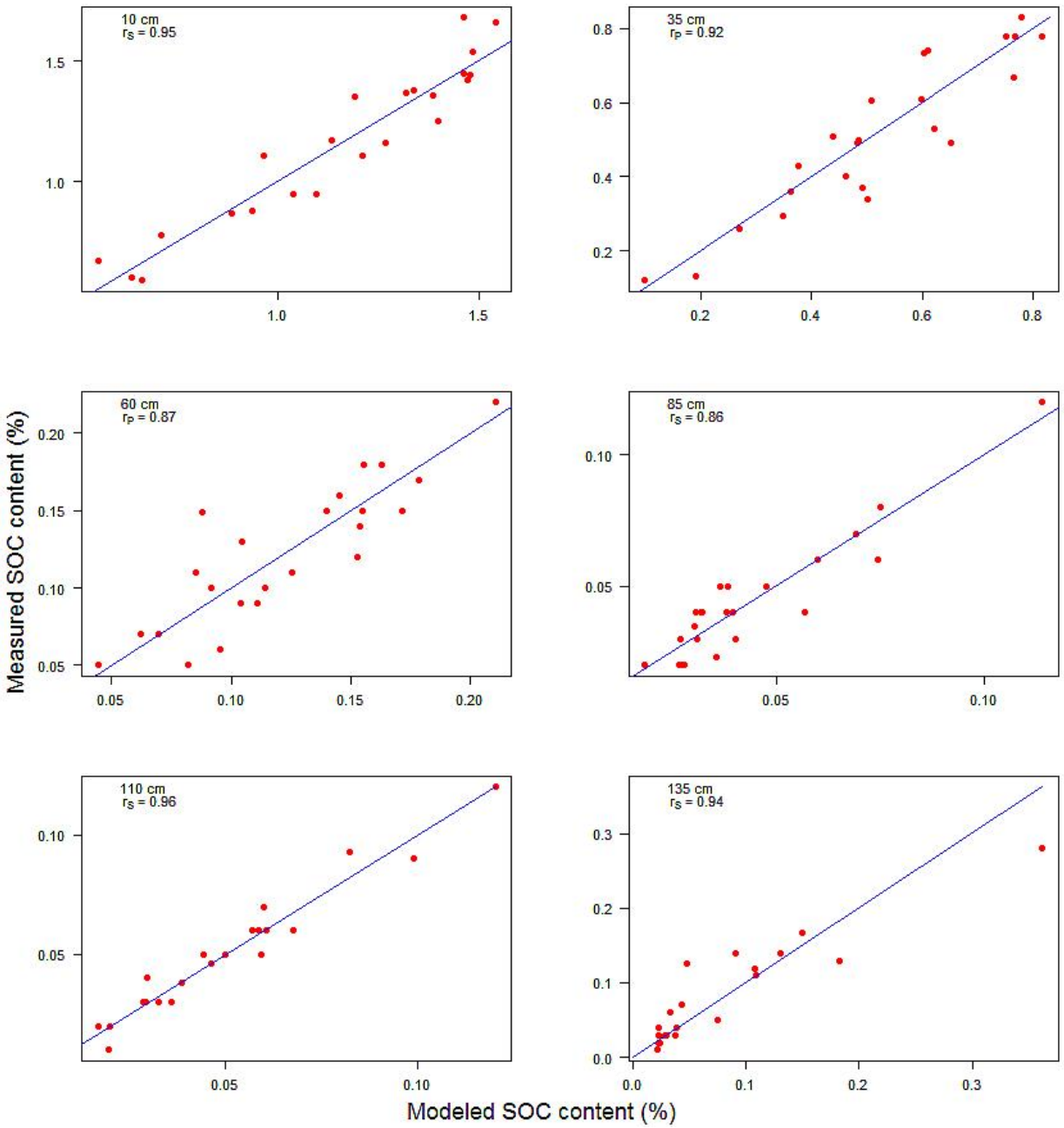


**FIGURE S5.1**: **Measured against modelled SOC contents for the different depths (n= 23 for each depth due to missing data for one of the factors considered in the regressions). Modelled data for 135 cm depth were back-transformed. Pearson correlation coefficients ($r_P$) or Spearman correlation coefficients ($r_S$) are also given.**

## 5.7 References

Angst, G., John, S., Mueller, C. W., Kögel-Knabner, I., and Rethemeyer, J. (2016a) Tracing the sources and spatial distribution of organic carbon in subsoils using a multi-biomarker approach. Scientific reports 6: 29478.

Angst, G., Kögel-Knabner, I., Kirfel, K., Hertel, D., and Mueller, C. W. (2016) Spatial distribution and chemical composition of soil organic matter fractions in rhizosphere and non-rhizosphere soil under European beech (*Fagus sylvatica* L.). Geoderma 264: 179-187.

Baisden, W. T., and Parfitt, R. L. (2007) Bomb 14 C enrichment indicates decadal C pool in deep soil?. Biogeochemistry 85(1): 59-68.

Barthès, B. G., Kouakoua, E., Larré-Larrouy, M. C., Razafimbelo, T. M., de Luca, E. F., Azontonde, A., ... and Feller, C. L. (2008) Texture and sesquioxide effects on water-stable aggregates and organic matter in some tropical soils. Geoderma 143(1-2): 14-25.

Batjes, N.H. (1996) Total carbon and nitrogen in the soils of the world. Eur. J. Soil Sci. 47: 151-163.

Bauhus, J., and Bartsch, N. (1996) Fine-root growth in beech (*Fagus sylvatica*) forest gaps. Canadian Journal of Forest Research 26(12): 2153-2159.

Blagodatskaya, E. V., and Anderson, T. H. (1998) Interactive effects of pH and substrate quality on the fungal-to-bacterial ratio and $qCO_2$ of microbial communities in forest soils. Soil Biology and Biochemistry 30(10-11): 1269-1274.

Blakemore, L.C., Searle, P.L., and Daly, B.K. (1987) Methods for Chemical Analysis of Soils. New Zealand Soil Bureau Scientific Report 80 Lower Hutt, New Zealand, Department of Scientific and Industrial Research.

Bundesanstalt für Bodenforschung (1973) Geologische Übersichtskarte 1:200000.

Bundt, M., Widmer, F., Pesaro, M., Zeyer, J., and Blaser, P. (2001) Preferential flow paths: biological 'hot spots' in soils. Soil Biology and Biochemistry 33(6): 729-738.

Chabbi, A., Kögel-Knabner, I., and Rumpel, C. (2009) Stabilised carbon in subsoil horizons is located in spatially distinct parts of the soil profile. Soil Biology and Biochemistry 41(2): 256-261.

Coleman, K., Jenkinson, D.S., Crocker, G.J., Grace, P.R., Klir, J., Körschens, P.R., and Richter, D.D. (1997) Stimulating trends in soil organic carbon in long-term experiments using Roth C-26.3 Geoderma 81: 29-44.

Curtin, D. (2002) Possible role of aluminum in stabilizing organic matter in particle size fractions of Chernozemic and Solonetizic soils. Canadian journal of soil science 82(2): 265-268.

Dahlgren, R. A., and Saigusa, M. (1994) Aluminum release rates from allophanic and nonallophanic Andosols. Soil science and plant nutrition 40(1): 125-136.

Don, A., Schumacher, J., Scherer-Lorenzen, M., Scholten, T., and Schulze, E. D. (2007) Spatial and vertical variation of soil carbon at two grassland sites—implications for measuring soil carbon stocks. Geoderma 141(3-4): 272-282.

Dungait, J. A., Hopkins, D. W., Gregory, A. S., and Whitmore, A. P. (2012) Soil organic matter turnover is governed by accessibility not recalcitrance. Global Change Biology 18(6): 1781-1796.

Eusterhues, K., Rumpel, C., and Kögel-Knabner, I. (2005) Organo-mineral associations in sandy acid forest soils: importance of specific surface area, iron oxides and micropores. European Journal of Soil Science 56(6): 753-763.

Eusterhues, K., Rumpel, C., and Kögel-Knabner, I. (2007) Composition and radiocarbon age of HF-resistant soil organic matter in a Podzol and a Cambisol. Organic Geochemistry 38(8): 1356-1372.

FAO-WRB (2014) World Reference Base for Soil Resources. World Soil Resources Reports 106. FAO, Rome, Italy.

Gaillard, V., Chenu, C., Recous, S., and Richard, G. (1999) Carbon, nitrogen and microbial gradients induced by plant residues decomposing in soil. European Journal of Soil Science 50(4): 567-578.

Gleixner, G. (2013) Soil organic matter dynamics: a biological perspective derived from the use of compound-specific isotopes studies. Ecological research 28(5): 683-695.

Hafner, S., Wiesenberg, G. L., Stolnikova, E., Merz, K., and Kuzyakov, Y. (2014) Spatial distribution and turnover of root-derived carbon in alfalfa rhizosphere depending on top-and subsoil properties and mycorrhization. Plant and soil 380(1-2): 101-115.

Helfrich, M., Flessa, H., Mikutta, R., Dreves, A., and Ludwig, B. (2007) Comparison of chemical fractionation methods for isolating stable soil organic carbon pools. European Journal of Soil Science 58(6): 1316-1329.

Hertel, D. (1999) Das Feinwurzelsystem von Rein- und Mischbeständen der Rotbuche: Struktur, Dynamik und interspezifische Konkurrenz. Dissertationes Botanicae 317. Gebrüder Borntraeger Verlagsbuchhandlung Berlin, Stuttgart.

Hertel, D., Strecker, T., Müller-Haubold, H., and Leuschner, C. (2013) Fine root biomass and dynamics in beech forests across a precipitation gradient–is optimal resource partitioning theory applicable to water-limited mature trees?. Journal of Ecology 101(5): 1183-1200.

Jenkinson, D. S., Poulton, P. R., and Bryant, C. (2008) The turnover of organic carbon in subsoils. Part 1. Natural and bomb radiocarbon in soil profiles from the Rothamsted long-term field experiments. European Journal of Soil Science 59(2): 391-399.

Jobbágy, E. G., and Jackson, R. B. (2000) The vertical distribution of soil organic carbon and its relation to climate and vegetation. Ecological applications 10(2): 423-436.

Joergensen, R. G., Anderson, T. H., and Wolters, V. (1995) Carbon and nitrogen relationships in the microbial biomass of soils in beech (*Fagus sylvatica* L.) forests. Biology and Fertility of Soils 19(2-3): 141-147.

Kaiser, K., and Guggenberger, G. (2003) Mineral surfaces and soil organic matter. European Journal of Soil Science 54(2): 219-236.

Kalbitz, K., and Kaiser, K. (2008) Contribution of dissolved organic matter to carbon storage in forest mineral soils. Journal of Plant Nutrition and Soil Science 171(1): 52-60.

Kleber, M., Eusterhues, K., Keiluweit, M., Mikutta, C., Mikutta, R., and Nico, P. S. (2015) Mineral–organic associations: formation, properties, and relevance in soil environments. Advances in agronomy 130:1-140.

Kögel-Knabner, I. (2002) The molecular organic composition of plant and microbial residues as inputs to soil organic matter Soil Biol. Biochem. 34: 139-162.

Kögel-Knabner, I., Guggenberger, G., Kleber, M., Kandeler, E., Kalbitz, K., Scheu, S., ... and Leinweber, P. (2008) Organo-mineral associations in temperate soils: Integrating biology,

mineralogy, and organic matter chemistry. Journal of Plant Nutrition and Soil Science 171(1): 61-82.

Krull, E. S., and Skjemstad, J. O. (2003) δ13C and δ15N profiles in $^{14}$C-dated Oxisol and Vertisols as a function of soil chemistry and mineralogy. Geoderma 112(1-2): 1-29.

Kubisch, P., Hertel, D., and Leuschner, C. (2016) Fine root productivity and turnover of ectomycorrhizal and arbuscular mycorrhizal tree species in a temperate broad-leaved mixed forest. Frontiers in plant science 7: 1233.

Leinemann, T., Mikutta, R., Kalbitz, K., Schaarschmidt, F., and Guggenberger, G. (2016) Small scale variability of vertical water and dissolved organic matter fluxes in sandy Cambisol subsoils as revealed by segmented suction plates. Biogeochemistry 131(1-2): 1-15.

Leuschner, C., Hertel, D., Coners, H., and Büttner, V. (2001) Root competition between beech and oak: a hypothesis. Oecologia 126(2): 276-284.

Leuschner, C., Wulf, M., Bäuchler, P., and Hertel, D. (2014) Forest continuity as a key determinant of soil carbon and nutrient storage in beech forests on sandy soils in Northern Germany. Ecosystems 17(3): 497-511.

Liang, C., and Balser, T. C. (2008) Preferential sequestration of microbial carbon in subsoils of a glacial-landscape toposequence, Dane County, WI, USA. Geoderma 148(1): 113-119.

Lomander, A., Kätterer, T., and Andrén, O. (1998) Carbon dioxide evolution from top-and subsoil as affected by moisture and constant and fluctuating temperature. Soil Biology and Biochemistry 30(14): 2017-2022.

Lorenz, K., Lal, R., and Shipitalo, M. J. (2011) Stabilized soil organic carbon pools in subsoils under forest are potential sinks for atmospheric $CO_2$. Forest Science 57(1): 19-25.

Lützow, M. V., Kögel-Knabner, I., Ekschmitt, K., Matzner, E., Guggenberger, G., Marschner, B., and Flessa, H. (2006) Stabilization of organic matter in temperate soils: mechanisms and their relevance under different soil conditions–a review. European Journal of Soil Science 57(4): 426-445.

Mikutta, R., Kleber, M., Torn, M. S., and Jahn, R. (2006) Stabilization of soil organic matter: association with minerals or chemical recalcitrance? Biogeochemistry 77(1): 25-56.

Mikutta, R., Schaumann, G. E., Gildemeister, D., Bonneville, S., Kramer, M. G., Chorover, J., ... and Guggenberger, G. (2009) Biogeochemistry of mineral–organic associations across a long-term mineralogical soil gradient (0.3–4100 kyr), Hawaiian Islands. Geochimica et Cosmochimica Acta 73(7): 2034-2060.

Mobley, M. L., Lajtha, K., Kramer, M. G., Bacon, A. R., Heine, P. R., and Richter, D. D. (2015) Surficial gains and subsoil losses of soil carbon and nitrogen during secondary forest development. Global change biology 21(2): 986-996.

Nunan, N. (2017) The microbial habitat in soil: Scale, heterogeneity and functional consequences. Journal of Plant Nutrition and Soil Science 180(4): 425-429.

Paul, E. A., Collins, H. P., and Leavitt, S. W. (2001) Dynamics of resistant soil carbon of Midwestern agricultural soils measured by naturally occurring $^{14}C$ abundance. Geoderma 104(3-4): 239-256.

Percival, H. J., Parfitt, R. L., and Scott, N. A. (2000) Factors controlling soil carbon levels in New Zealand grasslands is clay content important? Soil Science Society of America Journal 64(5): 1623-1630.

Poll, C., Ingwersen, J., Stemmer, M., Gerzabek, M. H., and Kandeler, E. (2006) Mechanisms of solute transport affect small-scale abundance and function of soil microorganisms in the detritusphere. European Journal of Soil Science 57(4): 583-595.

Porras, R. C., Pries, C. E. H., McFarlane, K. J., Hanson, P. J., and Torn, M. S. (2017) Association with pedogenic iron and aluminum: effects on soil organic carbon storage and stability in four temperate forest soils. Biogeochemistry 133(3): 333-345.

Preusser, S., Marhan, S., Poll, C., and Kandeler, E. (2017) Microbial community response to changes in substrate availability and habitat conditions in a reciprocal subsoil transfer experiment. Soil Biology and Biochemistry 105: 138-152.

Rasse, D. P., and Smucker, A. J. (1998) Root recolonization of previous root channels in corn and alfalfa rotations. Plant and Soil 204(2): 203-212.

Rethemeyer, J., Kramer, C., Gleixner, G., John, B., Yamashita, T., Flessa, H., ... and Grootes, P. M. (2005). Radiocarbon analysis of functional-defined and molecular organic matter fractions from agricultural soil profiles. Geoderma 128: 94-105.

Ross, G. J., and Wang, C. (1993) Extractable Al, Fe, Mn, and Si. Soil sampling and methods of analysis, 1993, 239-246.

Rumpel, C., and Kögel-Knabner, I. (2011) Deep soil organic matter—a key but poorly understood component of terrestrial C cycle. Plant and soil 338(1-2): 143-158.

Rumpel, C., Eusterhues, K., and Kögel-Knabner, I. (2004) Location and chemical composition of stabilized organic carbon in topsoil and subsoil horizons of two acid forest soils. Soil Biology and Biochemistry 36(1): 177-190.

Rumpel, C., Eusterhues, K., and Kögel-Knabner, I. (2010) Non-cellulosic neutral sugar contribution to mineral associated organic matter in top-and subsoil horizons of two acid forest soils. Soil Biology and Biochemistry 42(2): 379-382.

Rumpel, C., Rodríguez-Rodríguez, A., González-Pérez, J. A., Arbelo, C., Chabbi, A., Nunan, N., and González-Vila, F. J. (2012) Contrasting composition of free and mineral-bound organic matter in top-and subsoil horizons of Andosols. Biology and fertility of soils 48(4): 401-411.

Salome, C., Nunan, N., Pouteau, V., Lerch, T. Z., and Chenu, C. (2010) Carbon dynamics in topsoil and in subsoil may be controlled by different regulatory mechanisms. Global Change Biology 16(1): 416-426.

Scharlemann, J. P., Tanner, E. V., Hiederer, R., and Kapos, V. (2014) Global soil carbon: understanding and managing the largest terrestrial carbon pool. Carbon Management 5(1): 81-91.

Steinmann, T., Welp, G., Wolf, A., Holbeck, B., Große-Rüschkamp, T., and Amelung, W. (2016) Repeated monitoring of organic carbon stocks after eight years reveals carbon losses from intensively managed agricultural soils in Western Germany. Journal of Plant Nutrition and Soil Science 179(3): 355-366.

Stevenson, F.J. (1994) Biochemistry of the formation of humic substances. Humus Chem., 188-211.

Syswerda, S. P., Corbin, A. T., Mokma, D. L., Kravchenko, A. N., and Robertson, G. P. (2011) Agricultural management and soil carbon storage in surface vs. deep layers. Soil Science Society of America Journal 75(1): 92-101.

Tefs, C., and Gleixner, G. (2012) Importance of root derived carbon for soil organic matter storage in a temperate old-growth beech forest–Evidence from C, N and $^{14}C$ content. Forest Ecology and Management 263: 131-137.

Trumbore, S. (2009) Radiocarbon and soil carbon dynamics. Annu. Rev. Earth Planet. Sci. 37: 47-66.

Tückmantel, T., Leuschner, C., Preusser, S., Kandeler, E., Angst, G., Mueller, C. W., and Meier, I. C. (2017) Root exudation patterns in a beech forest: dependence on soil depth, root morphology, and environment. Soil Biology and Biochemistry 107: 188-197.

Van Praag, H. J., Sougnez-Remy, S., Weissen, F., and Carletti, G. (1988) Root turnover in a beech and a spruce stand of the Belgian Ardennes. Plant and soil 105(1): 87-103.

Vancampenhout, K., De Vos, B., Wouters, K., Swennen, R., Buurman, P., and Deckers, J. (2012) Organic matter of subsoil horizons under broadleaved forest: highly processed or labile and plant-derived?. Soil Biology and Biochemistry 50: 40-46.

Vance, E. D., Brookes, P. C., and Jenkinson, D. S. (1987) An extraction method for measuring soil microbial biomass C. Soil biology and Biochemistry 19(6): 703-707.

Wiseman, C.L.S., and Püttmann, W. (2006) Interactions between mineral phases in the preservation of soil organic matter. Geoderma 134(1-2): 109-118.

World Clim: Global Climate Data Model. http://www.worldclim.org/download, Accessed 3rd Feb 2016.

Wu, J. J. R. G., Joergensen, R. G., Pommerening, B., Chaussod, R., and Brookes, P. C. (1990) Measurement of soil microbial biomass C by fumigation-extraction-an automated procedure. Soil Biology & Biochemistry 22(8): 1167-1169.

# CHAPTER 6

# Spatial distribution and chemical composition of soil organic matter fractions in rhizosphere and non-rhizosphere soil under European beech (*Fagus sylvatica* L.)

Gerrit ANGST, Ingrid KÖGEL-KNABNER, Kristina KIRFEL, Dietrich HERTEL, Carsten W. MUELLER

GEODERMA, 2016, VOLUME 264, PAGES 179-187. DOI: 10.1016/j.geoderma.2015.10.016

## 6.1 Abstract

Little is known about how trees and their roots may influence the spatial distribution and chemical composition of soil organic matter (SOM) in subsoils with subsequent effects on soil organic carbon (SOC) storage and turnover. The aim of this study was to assess the impact of individual trees and their root system on the spatial distribution and chemical composition of SOM fractions and the storage of SOC in subsoils.

A Dystric Cambisol was sampled along three vertical replicate transects (3.15 m in length, 2.00 m in depth) in a regular grid (45 cm horizontal spaces, 25 cm vertical spaces) at increasing distance from three individual mature European beech trees (*Fagus sylvatica* L.). Soil OM fractions were obtained from rhizosphere soil and bulk soil samples taken at 10 and 85 cm depth increments by a combined density and particle size fractionation. Carbon and nitrogen measurements were performed, and the chemical composition of the SOM fractions was further characterized by solid state cross polarization magic angle spinning $^{13}C$ nuclear magnetic resonance spectroscopy.

The distance from the individual trees had no influence on the SOC contents and stocks or the chemical composition of the SOM fractions. This was ascribed to the dense and even rooting at 0–40 cm depth across all sampled distances. Instead, the SOC contents and stocks highly differed between 10 cm depth (11.4 g SOC $kg^{-1}$), where particulate organic matter (POM) dominated, and 85 cm depth (0.5 g SOC $kg^{-1}$), where clay associated SOC dominated. These differences seemed to be strongly influenced by the roots of the trees which were almost completely absent from depths ≥ 60 cm. Elevated SOC contents in the rhizosphere soil (40.1 g SOC $kg^{-1}$) were ascribed to root exudates in the root's vicinity and a very high amount (109.3 g $kg^{-1}$) of fresh POM (alkyl/O/N alkyl C ratio of 0.8). The data revealed that, besides root exudates, also root derived POM contributed significant amounts of SOC to the soil.

Although only low amounts of the clay fraction were found at 85 cm depth (22.8 g clay $kg^{-1}$), it accounted for high amounts of SOC and played a crucial role for the storage of SOM. The relatively high SOC stocks at 40–200 cm depth (1.4 kg C $m^{-2}$) compared to the SOC stocks at 0–40 cm depth (3.8 kg C $m^{-2}$) indicate that also sandy forest subsoils with low SOC contents have to be considered in terrestrial carbon inventories.

***Keywords:*** Grid sampling, Dystric Cambisol, Density and particle size fractionation, Solid state $^{13}C$ NMR spectroscopy, Soil organic carbon stocks, Subsoil

## 6.2 Introduction

Subsoils have received more attention in recent years (e.g., Eusterhues et al. 2005, Schöning and Kögel-Knabner 2006, Fontaine et al. 2007) because a substantial amount of soil organic carbon (SOC – C in soil derived from organic constituents) can be stored in subsoil horizons (Rumpel et al. 2002, Jobbágy and Jackson 2000). Forest soils are of particular interest because globally up to 70% of all SOC is stored in them (Jobbágy and Jackson 2000) and a considerable amount thereof in the subsoil (Lorenz and Lal 2005, Jobbágy and Jackson 2000). However, little quantitative information is available on the SOC contents and stocks, and the chemical composition of soil organic matter (SOM – the entirety of dead matter derived from plants and animals, and their organic transformation products) in subsoil (Rumpel and Kögel-Knabner 2011).

The distance from a tree can have a substantial influence on soil chemical (Lodhi 1977, Koch and Matzner 1993, Spielvogel et al. 2014) and physical properties (Chang and Matzner 2000b) as well as on the microbial community structure and activity (Saetre and Bååth 2000, Goemoeryova, 2004) and, therefore, on SOC storage and turnover. For example, Chang and Matzner (2000a), Chang and Matzner (2000b) found an increased channeling of dissolved organic carbon (DOC), increased water content, and a higher N-mineralization rate near the stem base of European beech trees. Spielvogel et al. (2014) found a pronounced gradient in lipid root biomarker concentrations with distance from beech trees. In another study SOC stocks have been found to be unaffected by the distance from individual trees (Schöning et al. 2006). However, all of these studies focused on bulk soil properties. Soil sampling designs in most studies have only involved samples being collected from different soil horizons at one horizontal distance from a tree (e.g., Rumpel et al. 2004, Eusterhues et al. 2005, Schrumpf et al. 2013). To the best of our knowledge, variations in the properties of functionally defined SOM fractions that are important for stabilization and turnover of SOC with distance from individual trees using a dense sampling grid have not been studied previously.

The storage of SOC in forest subsoils is thought to be mainly driven by rhizodeposition (Rasse et al. 2005, Tefs and Gleixner 2012). Rhizodeposits are root exudates and root litter (Kuzyakov and Domanski 2000). Most studies involving the rhizosphere have focused on enzyme activities (Brzostek et al. 2013), microbial biomass and community structure in rhizosphere soil (Koranda et al. 2011), or the influence of rhizodeposition on C turnover using carbon dioxide ($CO_2$) efflux measurements (Dijkstra and Cheng 2007, Schenck et al. 2012). To the best of our knowledge,

SOC contents in combination with the chemical composition of root-derived particulate organic matter (POM) and other functional SOM fractions in rhizosphere soil have not been studied.

The aim of this study was to assess the impact of individual mature European beech trees on the spatial distribution and chemical composition of SOM fractions, and evaluate the role of rhizosphere soil fractions for input and storage of SOC in subsoil. The hypothesis was that a measurable influence of individual trees on the measured chemical parameters existed, that decreased as the distance to the trees' stem bases increased. Soil samples were collected in a regular sampling grid from the profile walls of three transects, each of which started at a European beech tree. Rhizosphere soil and soil samples from 10 cm and 85 cm depth were subjected to a combined density and particle size fractionation. Beside C and N measurements of all samples, the chemical composition of the clay and POM fractions was further characterized by cross-polarization magic angle spinning $^{13}C$ nuclear magnetic resonance (CPMAS $^{13}C$ NMR) spectroscopy. Additionally, the specific surface area (SSA) of representative samples of the clay fraction was determined.

## 6.3 Materials and Methods

### *Study area and soil sampling*

The study was carried out at the Grinderwald which is located northwest of Hannover (52° 34′ 22″ N 9° 18′ 51″ E), Germany. Climate data were obtained from a German Meteorological Service monitoring station (Nienburg). The mean annual precipitation and temperature for the period 1981–2010 were 762 mm and 9.7 °C, respectively. Parent materials were Pleistocene glaciofluvial sandy deposits from the Saale glacial stage (Bundesanstalt für Bodenforschung 1973). The predominant soil type in the study area was an acid (pH 3.4–4.5), sandy (77.3% sand, 18.4% silt and 4.4% clay) Dystric Cambisol (IUSS Working Group WRB 2014) and the humus form was moder. The phyllosilicate mineralogy was characterized by XRD measurements. It revealed the presence of chlorite, mixed-layer minerals, kaolinite, and illite, whereas smectites were absent. The study area was covered with an even-aged European beech (*Fagus sylvatica* L.) forest established in 1916 (Forstamt Nienburg 2010). Mean stem density was 407 stems $ha^{-1}$, the mean diameter at breast height was 26.3 cm, and the mean basal area was 27.1 $m^2$ $ha^{-1}$. A mature beech forest was chosen, because aim was to study a climax forest association which commonly

occurs in Germany. In addition, European beech is the most abundant tree species in Central Europe (Geßler et al. 2007).

Three transects, each 2.00 m deep and 3.15 m long, were dug on flat terrain in June 2013 using a mechanical digger, each starting at the stem base of a mature beech tree. We oriented the transects North, South, and West facing, respectively, to avoid a systematic bias by cardinal direction. The depth was chosen to assure that the parent material below the B-horizons had been reached. To follow the spatial influence of a single tree on SOM properties, the direction of each transect was chosen to avoid the stem base of neighboring trees being reached. Furthermore, the locations of the transects were chosen so that they all had comparable soil and vegetation properties, i.e., soil texture and no vegetation cover other than European beech. Composite soil samples (each ~ 1 kg) and volumetric samples (taken using steel cylinders; diameter: 8.5 cm, height: 6.0 cm) were collected from the wall of each transect in a regular grid pattern with 45 cm horizontal spaces and 25 cm vertical spaces (Fig. 6.1). To ensure comparable volumetric sampling throughout the whole grid using the same steel rings unbiased by differing topsoil thicknesses, the uppermost sampled depth increment was set to 10 cm depth. The volumetric samples were used for the determination of the bulk density. A total of 192 soil samples were collected, 64 from each transect. Due to the sampling approach, the reported parameters are mean values for a specific soil increment (radius of 4.25 cm). Approximately 50 g of the organic layer were collected above the horizontal grid points. Leaf litter was randomly collected next to the profile walls of each transect. Fine roots (diameter $\leq$ 2 mm) were manually extracted from the volumetric soil samples taken from the profile walls. One composite rhizosphere soil sample was taken from each transect, predominantly from the uppermost, densely and evenly rooted 0–40 cm and at deeper soil depths where roots were present, close to the tree stems (Fig. 6.1, Fig. 6.2). Rhizosphere soil was defined as soil adhering to the roots after they had been shaken (Cieslinski et al. 1998, Gomes et al. 2003). The uppermost sampled depth increment at 10 cm depth was compared with the fourth sampled depth increment at 85 cm depth (Fig. 6.1). According to the WRB 2014 soil classification system, the AE horizon at the investigated soil ended at 2 cm depth and the first sampled depth increment at 10 cm depth was already located in the Bsw horizon. We consider subsoil as being the soil that is located below the A and E horizons (cf. IPCC 2000). Consequently, the sampled depth increment at 10 cm was referred to as "subsoil$_{10}$" and the depth

increment at 85 cm depth was referred to as "subsoil$_{85}$". The term "non-rhizosphere soil" refers to both the subsoil$_{10}$ and subsoil$_{85}$.

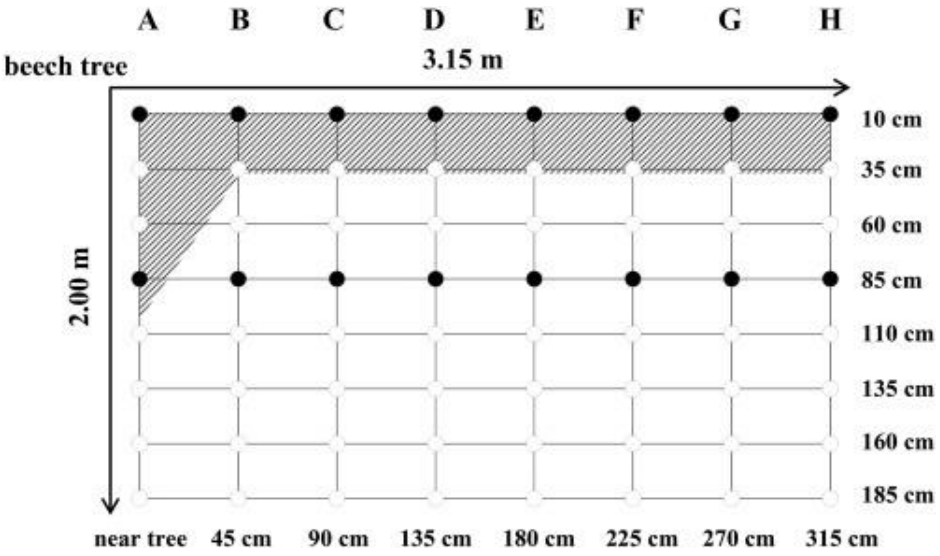


**FIGURE 6.1: Sampling grid applied to each transect wall (n = 64 samples per transect). Composite and volumetric soil samples (using steel cylinders; 8.5 cm diameter, 6 cm height) were taken. The black dots (n = 16 per transect) indicate the samples that were subjected to the combined density and particle size fractionation. The shaded area displays the regions from which the rhizosphere soil was collected. The letters above the graph represent the labels of the horizontal sampling spots, A being nearest to the tree. The distance between sampling spots were 45 cm in the horizontal and 25 cm and in the vertical, starting at a depth of 10 cm.**

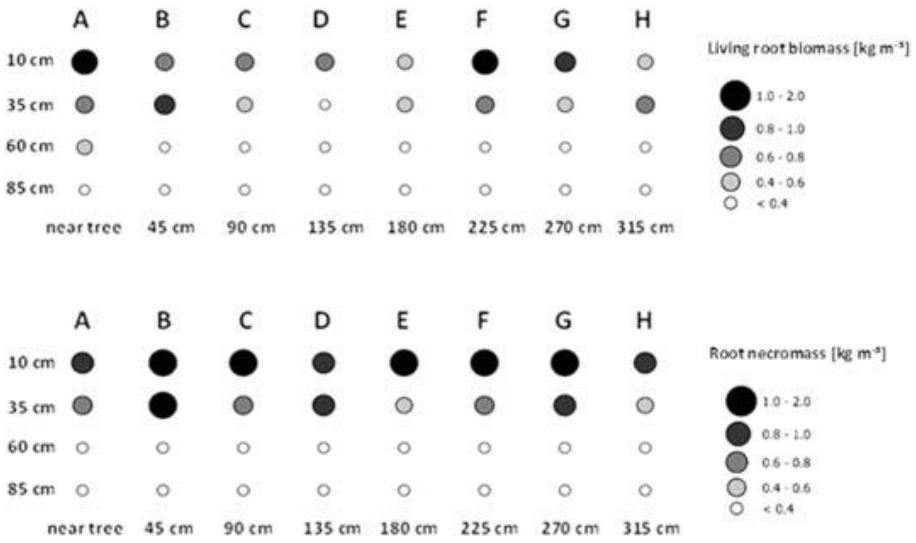


**FIGURE 6.2: Mean living and dead fine root concentration [kg $m^{-3}$] down to a depth of 85 cm. The letters above the plots are the labels of the horizontal sampling spots with A being nearest to the tree. n = 3 for each grid point.**

***Fine root biomass and necromass***

Roots were manually separated from the volume samples in the laboratory and cleaned in a sieve of 250 µm mesh size using deionized water (DI). Only fine roots (diameter ≤ 2 mm) could be detected in the samples, coarse roots (> 2 mm diameter) were absent. By inspection under a stereo microscope, the extracted rootlets were distinguished in living (biomass) and dead (necromass) fine roots following the criteria root color, elasticity, and cohesion of cortex, periderm and stele (e.g., Hertel et al. 2013, Hertel and Leuschner 2002, Persson 1978). The root biomass and necromass was dried for 48 h at 70 °C and weighed.

To keep the analysis viable, fine roots > 10 mm length were extracted from all samples but fine roots < 10 mm length were only extracted from representative samples. While the inclusion of only fine roots > 10 mm length and the negligence of fine roots < 10 mm length allows to quantify the majority of living fine root mass (> 95%), it fails to account for the mass of dead fine roots with sufficient accuracy, since a large proportion of fine root necromass consists of root fractions < 10 mm length (Bauhus and Bartsch 1996, Leuschner et al. 2001). In order to correct the fine root necromass for fine roots < 10 mm length, we extrapolated the mass of dead fine roots < 10 mm length of 30 representative samples per transect using soil depth-specific regression equations that relate the mass of fine dead roots < 10 mm length to fine dead roots >

10 mm length. These regression equations were established applying a method introduced by van Praag et al. (1988) and modified by Hertel (1999).

***Combined density and particle size fractionation***

Bulk soil samples were air dried and gently passed through a 2 mm sieve. Subsoil10 at sampling spots A to H (uppermost sampled depth increment at 10 cm), subsoil85 (fourth sampled depth increment at 85 cm) (Fig. 6.1), and rhizosphere soil from each transect were fractionated. Aim was to separate the combined fine silt and clay fractions because these are thought to contribute to the long-term stabilization of SOM (Mueller et al. 2009, Rumpel and Kögel-Knabner 2011).

A 30 g aliquot of air dried and sieved bulk soil was saturated with a sodium polytungstate (SPT) solution (TC Tungsten Compounds, Grub am Forst, Germany) adjusted to a density of 1.8 g $cm^{-3}$, and subsequently ultrasonicated at an energy of 600 J $ml^{-1}$ to break up soil aggregates and release the POM occluded within aggregates (oPOM). The samples were cooled during the ultrasonication treatment to reduce changes in SOM composition by heating the solution (Mueller et al. 2012b). Preliminary tests were performed using soil samples from the study site with densities of 1.6 and 1.8 g $cm^{-3}$, and ultrasonication energies of 400, 600 and 800 J $ml^{-1}$ to select experimental settings that separate the POM and mineral soil fractions most effectively. The results of the preliminary tests were evaluated against a particle size analysis of the respective samples, the C/N ratios, and reflectance light microscopy of the different fractions in order to ensure that the chosen parameters were appropriate. After ultrasonication, the POM fraction was removed using a water jet pump. The POM fraction was purged with DI until the electrical conductivity of the eluted water was below 5 µS, freeze-dried, and stored for further analysis. The remaining mineral residue was purged with DI until the conductivity of the eluted water was below 50 µS and wet sieved to obtain combined coarse and medium sand (200–2000 µm), fine sand (63–200 µm) and coarse silt (20–63 µm) fractions. The mineral soil that passed through all three sieves, i.e. medium silt, fine silt and clay, was subjected to sedimentation to separate the medium silt (6.3–20 µm) from the combined fine silt and clay fraction (< 6.3 µm). The mean recovery rate of the combined density and particle size fractionation on a mass basis was 98.4%. All of the fractions were freeze-dried and stored for further analysis. The coarse, medium, and fine sand fractions were referred to as the "sand fraction", the coarse and medium silt fractions

were referred to as the “silt fraction”, and the combined fine silt and clay fraction was referred to as the “clay fraction”.

### *Determination of carbon and nitrogen contents*

The C and N contents in the bulk soil were determined by weighing an aliquot of a soil sample into a ceramic cup and analyzing the sample by dry combustion with a VARIO MAX CNS analyzer (Elementar Analysensysteme, Hanau, Germany). The C and N contents in the mineral soil fractions and the POM were measured using an EA elemental analyzer (EuroVector, Milan, Italy). Both analyzers had a detection limit of 0.02% total C. The mineral soil fractions that were coarser than medium silt were finely ground prior to analysis. The pH value of the soil did not exceed 4.5 clearly indicating the absence of carbonates. Thus, the total C contents measured were equal to the SOC contents. All C and N measurements were run in duplicate.

### *Specific surface area measurements*

The specific surface area of representative samples of the clay fraction of the $subsoil_{10}$ and $subsoil_{85}$ from each transect was measured by the multi-point BET method (Brunauer et al. 1938) using an Autosorb-1 analyzer (Quantachrome, Syosset, NY, USA). Nitrogen adsorption data at 11 points were obtained in the partial pressure range 0.05–0.3 in liquid nitrogen. Prior to measurement, the samples were outgassed at 40 °C for at least 16 h to remove water. A total removal of SOM from the samples by further chemical pretreatments was omitted. Thus, the free surface areas of the clay fractions that were not obscured by SOM were measured.

### *$^{13}$C CPMAS NMR spectroscopy*

The leaf litter (n = 3), fine roots (n = 3), organic layer material (n = 24), POM (n = 24) and clay fractions (n = 24) of the $subsoil_{10}$, POM (n = 3) and clay fractions (n = 3) of the rhizosphere soil, and the clay fractions of the $subsoil_{85}$ (n = 4) (marked in Fig. 6.1) were subjected to solid state $^{13}$C CPMAS NMR spectroscopy. The POM and mineral associated SOM were analyzed as these fractions represented the largest SOC pool. Measurements were performed using a Bruker AvanceIII 200 Spectrometer. An aliquot was weighed into a zircon-oxide rotor that was spun at

5.0 kHz with a recycle delay time of 0.4 s for the clay fractions and 1 s for leave litter, roots, organic layer and the POM fractions. For the POM fractions, 4000 counts were acquired and more than 6 million counts were acquired for the clay fractions. Since SOC contents were very low in the clay fractions from the $subsoil_{85}$ and HF treatment of the samples (cf. Schmidt et al. 1997) was no option for us due to a loss of SOC and a possible alteration in SOC chemistry (Gonçalves et al. 2003, Rumpel et al. 2006), only four reasonable spectra could be obtained for the clay fractions of the $subsoil_{85}$. The spectra were processed with a line broadening of 50 Hz, phase adjusted and baseline corrected. Peaks were separated into four integration areas, 0–50 ppm (alkyl-C), 50–110 ppm (O/N-alkyl-C), 110–160 ppm (aromatic-C), and 160–220 ppm (carboxylic-C) (Kögel-Knabner et al. 1992).

The signals in the NMR spectra can be assigned to major chemical compound classes. O/N-alkyl C can be ascribed to amide C of proteins and the C2, C3, and C5 in polysaccharide molecules. The main signal at 30 ppm in the alkyl C region can be assigned to C in long chain aliphatic components from lipids, waxes, and other aliphatic biomacromolecules (Kögel-Knabner et al. 1992). Cellulose, hemicellulose, and proteins in plant residues are relatively easily decomposable, whereas aliphatic structures are thought to be more resistant to degradation. Thus, the ratio between alkyl C and O/N-alkyl C can be used as indicator for the degree of decomposition of OM (Baldock et al., 1997). Lignin, often detected in plant derived SOM, is indicated by signals at 56, 119, 130 and 150 ppm. High intensities at 130 ppm could also indicate the presence of pyrogenic C. The main peak around 175 ppm is assigned to carboxyl and amide groups in different compounds (Kögel-Knabner 1997).

### *Statistics*

Means and standard deviations (SD) of the field replicates were calculated using Microsoft Excel 2013 for Windows (Microsoft, Redmond, WA, USA). Correlation analysis (reported using the Pearson product–moment correlation coefficient, r) and all other statistics were carried out using the R 3.0.3 software for Windows (R Core Team 2013). The Shapiro–Wilk test was used to determine whether the data were normally distributed. Significant differences were tested using the one-way analysis of variance (ANOVA) or the Kruskal Wallis test. If not explicitly mentioned, all statistical analyzes were regarded as being significant when $p < 0.05$. Neither

ANOVA nor Kruskal Wallis test revealed any significant differences between the transects regarding SOC contents and stocks in the bulk soil and the fractions. Thus, the three transects were regarded as being replicates. Because there were also no significant differences between the horizontal sampling spots A to H, we refer to one mean value for each the subsoil10 and subsoil85 calculated from all three transects of sampling spots A to H.

The bulk soil densities were calculated from the weight of the dried soil volume samples relative to the volume of the steel cylinders used to collect the samples. Coarse particles (> 2 mm) were removed from the mineral soil during the sieving process (cf. chapter 2.3) and the bulk densities were adjusted accordingly. Soil OC stocks were calculated for 1 $m^2$ and a layer thickness of 1 cm from the SOC contents, soil densities and the amount (g [kg $soil^{-1}$]) of the respective soil fractions for the subsoil10 and the subsoil85. Soil OC stocks were also calculated for the depth layers 0–40 cm and 40–200 cm, representing the densely rooted upper soil layer and the lower soil layer with low root density. Soil OC stocks for the rhizosphere soil were not calculated due to missing soil densities. Carbon enrichment factors ($E_c$) were calculated using Eq. (1) (Guggenberger et al. 1994, Christensen 2001, Rumpel et al. 2004).

$$E_c = \text{g C kg}^{-1} \text{ fraction} / \text{g C kg}^{-1} \text{ whole soil} \quad (1)$$

The $E_c$ values were calculated for the soil samples obtained from 10 cm and 85 cm depth.

## 6.4 Results

### *Fine root biomass and necromass*

The fine root biomass and necromass did not show any significant differences between the sampling spots A to H and no significant correlations could be detected between the distance from the tree and the amount of the root biomass or necromass (Table S6.1). Instead, both showed significant negative correlations with an increasing depth ($r = -0.67$ and $r = -0.86$, respectively) and were less than 0.4 kg $m^{-3}$ at depths of 60 and 85 cm (Fig. 2). The only exception was at sampling point "A" at 60 cm depth, where the average living root biomass was greater than 0.4 kg $m^{-3}$.

### *Amount of recovered soil fractions, SOC contents and stocks*

Unexpectedly, no significant correlations were found between the distance from the tree and the amount of recovered soil fractions, the SOC contents, and stocks (Table S6.1). We thus focused our results on the comparison of vertical differences between average values for $subsoil_{10}$ and $subsoil_{85}$ (cf. Section 6.2), and on differences between rhizosphere and non-rhizosphere soil.

The amount of the sand fraction was significantly higher in the $subsoil_{85}$ compared to the $subsoil_{10}$ (Table 6.1). The amount of the clay and silt fractions of the $subsoil_{10}$ was more than twofold the amount of the respective fractions of the $subsoil_{85}$. Particulate OM was not detected in the $subsoil_{85}$ (Table 6.1).

The rhizosphere soil had the lowest amount of the sand fraction, an amount of the silt fraction comparable to the $subsoil_{10}$, and an intermediate amount of the clay fraction (Table 6.1). Interestingly, a six times higher amount of the POM fraction was obtained from the rhizosphere soil ($109.3 \pm 34.3$ g $kg^{-1}$) compared to the subsoil10 ($15.3 \pm 2.3$ g $kg^{-1}$).

**TABLE 6.1: Mean +/− SD recovered mass, soil organic carbon (SOC) content, carbon to nitrogen ratio (C/N), SOC stock, and carbon enrichment factor ($E_c$) of the unfractionated bulk soil and soil organic matter (SOM) fractions (here referred to as "sand", "silt", "clay" and "POM") from the $subsoil_{10}$, $subsoil_{85}$ and rhizosphere soil. Significant differences in SOM fraction or the bulk soil between the $subsoil_{10}$, $subsoil_{85}$ and rhizosphere soil are indicated by lowercase letters. The superscript † symbols mark observations that are not significantly different when comparing the individual SOM fractions to each other within the $subsoil_{10}$, $subsoil_{85}$ or rhizosphere soil.**

| | | $Subsoil_{10}$ | $Subsoil_{85}$ | Rhizosphere soil |
|---|---|---|---|---|
| **Recovered mass [g (kg soil)$^{-1}$]** | Sand | 639.5 ± 14.2b | 900.8 ± 26.6a | 584.7 ± 11.8c |
| | Silt | 285.2 ± 11.8a | 76.4 ± 23.1b | 264.9 ± 26.3a |
| | Clay | 59.9 ± 3.9a | 22.8 ± 4.2c | 41.0 ± 4.0b |
| | POM | 15.3 ± 2.3b | n.d. | 109.3 ± 34.3a |
| **SOC content [g C (kg fraction)$^{-1}$]** | Bulk soil | 11.4 ± 1.3b | 0.5 ± 0.2c | 40.1 ± 9.0a |
| | Sand | 0.3 ± 0.1a | 0.2 ± 0.1b | 0.4 ± 0.1a |
| | Silt | 2.7 ± 0.9a | 1.5 ± 0.6b | 4.0 ± 0.9a |
| | Clay | 53.2 ± 6.4b | 7.8 ± 1.7c | 84.0 ± 4.5a |
| | POM | 392.1 ± 18.1b | n.d. | 424.7 ± 3.9a |
| **C/N** | Bulk soil | 24.1 ± 3.1b | 7.5 ± 1.7c | 28.5 ± 1.4a |
| | Sand | n.d. | n.d. | n.d |
| | Silt | n.d. | n.d. | 17.3 ± 2.3† |
| | Clay | 15.9 ± 1.3a | 8.1 ± 1.6c | 14.3 ± 0.3b† |
| | POM | 48.5 ± 5.9a | n.d. | 26.9 ± 2.1b |
| **SOC stock [g m$^{-2}$]** | Bulk soil | 132.4 ± 23.4a | 8.1 ± 3.0b | n.d. |
| | Sand | 2.6 ± 0.7a | 3.2 ± 1.7a† | n.d. |
| | Silt | 9.9 ± 3.9a | 1.6 ± 0.8b | n.d. |
| | Clay | 41.3 ± 8.3a | 3.2 ± 1.3b† | n.d. |
| | POM | 78.5 ± 13.3 | n.d. | n.d. |
| **$E_c$** | Sand | 0.03 ± 0.01b | 0.4 ± 0.2a | 0.01 ± 0.00c |
| | Silt | 0.2 ± 0.1b | 3.4 ± 2.4a | 0.1 ± 0.0c |
| | Clay | 4.8 ± 0.6b | 17.3 ± 6.7a | 2.4 ± 0.4c |

N = 24 for $subsoil_{10}$, $subsoil_{85}$ & organic layer; n = 3 for leaves, roots & rhizosphere soil; n.d. = not determined.

The bulk $subsoil_{10}$ and fractions of the $subsoil_{10}$ had considerably higher SOC contents than the bulk $subsoil_{85}$ and the corresponding fractions (Table 6.1). The SOC contents of the clay fraction of the $subsoil_{10}$ were less variable (CV = 0.12) than those of the $subsoil_{85}$ (CV = 0.22). The differences in SOC contents between the rhizosphere soil and the non-rhizosphere soil were pronounced, especially regarding the bulk soil (Table 6.1). The rhizosphere soil had a more than three times higher SOC content compared to the bulk $subsoil_{10}$. Similarly, the SOC contents of the clay and POM fractions of the rhizosphere soil were also significantly higher than those of the non-rhizosphere soil. Apart from differences between the non-rhizosphere and rhizosphere soil, the clay and POM fractions always had the highest SOC contents, in contrast to the sand and silt fractions.

Similar to the SOC contents, the SOC stocks of the bulk $subsoil_{10}$ and its particle size fraction < 63 µm were significantly higher than the SOC stocks of the bulk $subsoil_{85}$ and the corresponding fractions (Table 6.1). Although very low in mass, the clay fraction of the $subsoil_{85}$ accounted for 3.2 ± 1.3 g C $m^{-2}$ (39.5%) of the bulk $subsoil_{85}$ SOC stocks (Table 6.1). This corresponds to a high $E_c$ value for the clay fraction of the $subsoil_{85}$ (Table 6.1), when compared to the clay fractions of the $subsoil_{10}$ and rhizosphere soil. Despite these higher $E_c$ values, there was a trend towards a higher specific surface area not covered by SOM of the clay fraction of the $subsoil_{85}$ (29.3 ± 5.3 $m^2$ $g^{-1}$) compared to the clay fraction of the $subsoil_{10}$ (18.6 ± 8.1 $m^2$ $g^{-1}$). Notably, the SOC stocks at deeper soil layers (40–200 cm) (1.4 ± 0.1 kg C $m^{-2}$), characterized by low amounts of root bio- and necromass, represented almost one third of the SOC stocks of the whole soil from 0 to 200 cm depth. The densely rooted soil at 0–40 cm depth accounted for 3.8 ± 0.9 kg C $m^{-2}$ (~ two thirds of the SOC stocks of 0–200 cm depth).The C/N ratios differed significantly between the subsoil10, subsoil85 and rhizosphere soil (Table 6.1). The C/N ratios of the subsoil85 were significantly lower compared to those of the $subsoil_{10}$. Interestingly, the C/N ratio of the POM fraction of the rhizosphere soil (26.9 ± 2.1) was about half the C/N ratio of the POM fraction of the $subsoil_{10}$ (48.5 ± 5.9). The C/N ratios and OC contents of the leaves and the roots were significantly higher than the C/N ratios and OC contents of the organic layer (Table 6.3).

### *$^{13}$C CPMAS NMR spectra*

A significant correlation between the distance from the tree and the chemical compound classes could not be detected (Table S6.1). Instead, differences between the $subsoil_{10}$ and $subsoil_{85}$, and between the non-rhizosphere and rhizosphere soil were observed.

In the clay fraction of the $subsoil_{85}$, the carboxyl and the aromatic C were higher compared to the corresponding compound classes of the clay fraction of the $subsoil_{10}$. This indicates a relative enrichment of aromatic compounds like lignin in $subsoil_{85}$. The relatively high O/N alkyl C peak of the clay fraction of the $subsoil_{85}$ points towards an accumulation of carbohydrates and proteins.

The NMR spectra of the clay and POM fractions of the $subsoil_{10}$ and the rhizosphere soil were dominated by alkyl C and O/N-alkyl C (Table 6.2, Fig. 6.3, Fig. 6.4). Carboxyl and aromatic C together accounted for less than 30% of the sum of integrated peak areas. In most cases, O/N-alkyl C was significantly higher than alkyl C. This indicates the presence of high amounts of presumably more labile carbohydrates. Strikingly, the O/N-alkyl C of the POM fraction of the $subsoil_{10}$ was significantly lower than the alkyl C of the same fraction. This resulted in higher alkyl/O/N-alkyl C ratios in the POM fraction of the $subsoil_{10}$ ($1.6 \pm 0.4$) compared to the POM fraction of the rhizosphere soil ($0.8 \pm 0.1$).

The spectra of the leaves, roots and organic layer material (Fig. 6.5) were dominated by O/N alkyl C, which accounted for approximately two thirds of the sum of integrated peak areas of leaves and roots (Table 6.3). This was indicative for a high amount of polysaccharides and resulted in very low alkyl/O/N-alkyl C ratios. Higher amounts of alkyl C in the organic layer resulted in alkyl/O/N-alkyl C ratios of $0.7 \pm 0.1$.

**TABLE 6.2: Relative peak intensities and alkyl/O/N alkyl C ratios of the clay and POM fractions of the subsoil$_{10}$, subsoil$_{85}$ and rhizosphere soil determined by solid state $^{13}$C NMR spectroscopy. Significant differences between the subsoil$_{10}$, subsoil$_{85}$, and rhizosphere soil are indicated by lowercase letters. The superscript † symbols mark observations that are not significantly different when comparing the chemical compound classes to each other within the clay or POM fraction from subsoil$_{10}$, subsoil$_{85}$ or rhizosphere soil. Standard deviation (SD) of field replicates after ±.**

| | Subsoil$_{10}$ | | Subsoil$_{85}$ | | Rhizosphere soil | |
|---|---|---|---|---|---|---|
| | **Clay** | **POM** | **Clay** | **POM** | **Clay** | **POM** |
| **Carboxyl C** | 12.6 ± 1.8b | 7.9 ± 0.8a | 22.7 ± 7.3a$^{\dagger}$ | n.d | 9.7 ± 0.9a | 6.5 ± 0.3b$^{\dagger}$ |
| **Aromatic C** | 14.9 ± 1.1b | 16.4 ± 2.4a | 28.5 ± 5.1a$^{\dagger}$ | n.d | 12.6 ± 2.1b | 15.3 ± 1.4a$^{\dagger}$ |
| **O/N alkyl C** | 36.9 ± 2.9b$^{\dagger}$ | 29.3 ± 3.9b | 30.1 ± 5.0c$^{\dagger}$ | n.d | 49.8 ± 1.3a | 43.1 ± 2.1a |
| **Alkyl C** | 35.2 ± 4.5a$^{\dagger}$ | 46.4 ± 6.1a | 17.5 ± 8.1b$^{\dagger}$ | n.d | 27.8 ± 2.3b | 34.7 ± 2.8b |
| **Alkyl/ O/N alkyl C** | 1.0 ± 0.2a | 1.6 ± 0.4a | 0.6 ± 0.2b | n.d | 0.6 ± 0.1b | 0.8 ± 0.1b |

N = 24 for subsoil$_{10}$ & organic layer; n = 4 for subsoil$_{85}$; n = 3 for leaves, roots & rhizosphere soil; n.d. = not determined.

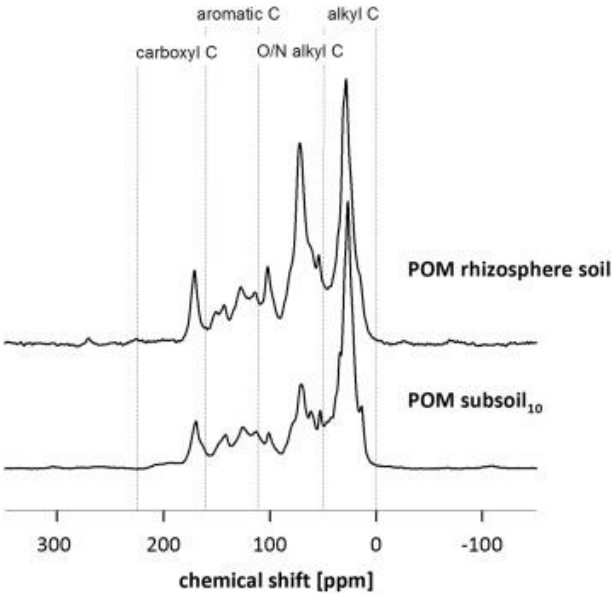


**FIGURE 6.3: $^{13}$C CPMAS NMR mean spectra of the POM fractions of the rhizosphere soil (calculated from three spectra) and the subsoil$_{10}$ (calculated from 24 spectra).**

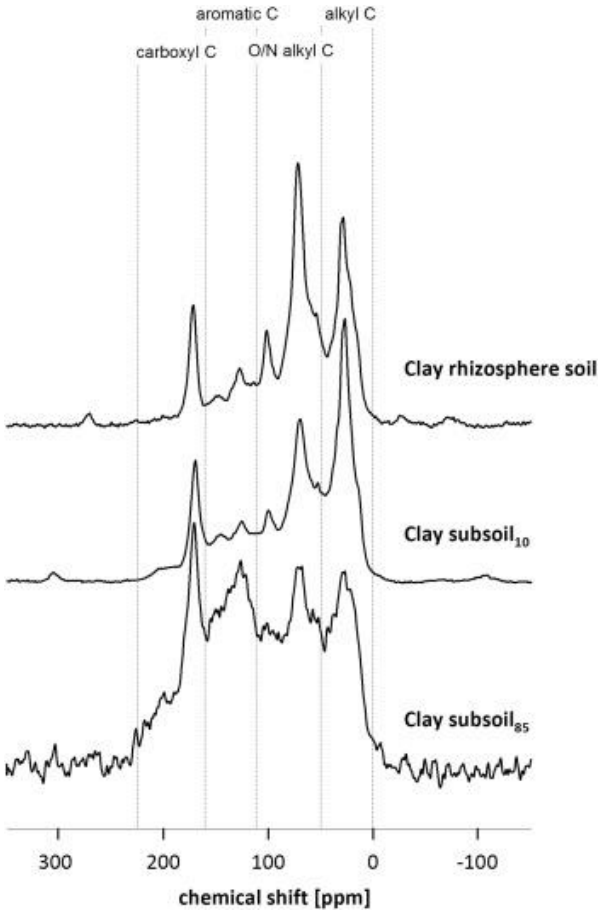


**FIGURE 6.4: $^{13}C$ CPMAS NMR mean spectra of the clay fractions of the rhizosphere soil (calculated from three spectra), subsoil$_{10}$ (calculated from 24 spectra) and subsoil$_{85}$ (calculated from four spectra).**

**TABLE 6.3: Mean +/− SD organic carbon (OC) content, carbon to nitrogen ratio (C/N), chemical compound classes (carboxyl C, aromatic C, O/N alkyl C, alkyl C) and alkyl/ O/N alkyl C ratio of the leaves, fine roots and organic layer. Significant differences of the OC contents, C/N ratios or peak intensities between the leaves, roots and the organic layer are indicated by lowercase letters.**

| | Leaves | Roots | Organic layer |
|---|---|---|---|
| **OC content [g (kg fraction)$^{-1}$]** | 453.1 ± 1.1a | 484.8 ± 10.9a | 112.9 ± 55.1b |
| **C/N** | 37.7 ± 2.0a | 93.8 ± 33.6a | 24.0 ± 1.0b |
| **Carboxyl C** | 5.9 ± 0.5b | 3.6 ± 0.4c | 10.6 ± 0.9a |
| **Aromatic C** | 18.6 ± 0.3b | 15.4 ± 1.9b | 18.7 ± 0.4a |
| **O/N alkyl C** | 62.2 ± 0.9a | 71.3 ± 5.9a | 40.5 ± 1.6b |
| **Alkyl C** | 13.3 ± 0.3b | 9.4 ± 4.3b | 30.2 ± 1.4a |
| **Alkyl/O/N alkyl C** | 0.2 ± 0.01b | 0.1 ± 0.1b | 0.7 ± 0.1a |

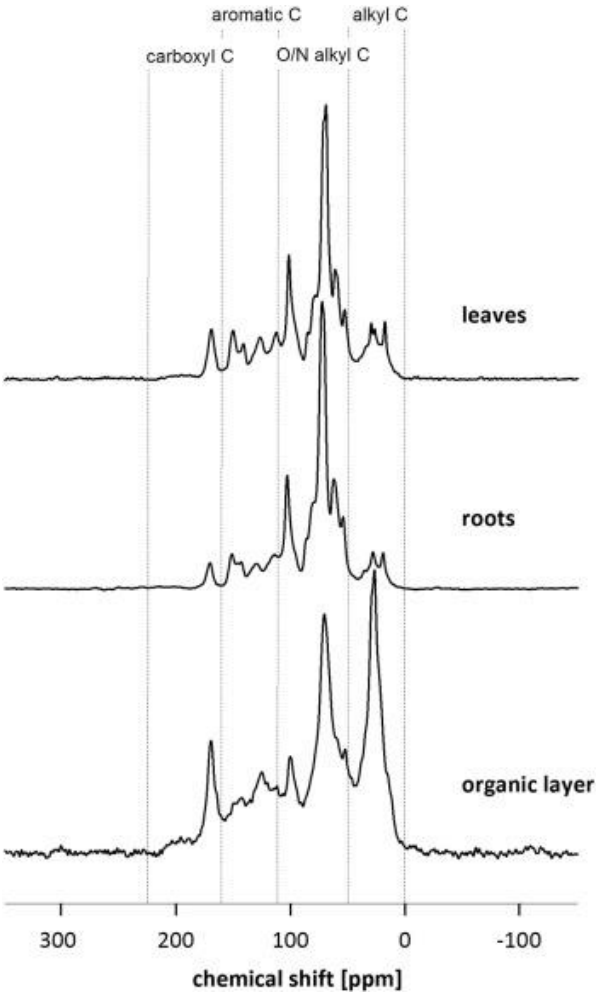


**FIGURE 6.5: $^{13}$C CPMAS NMR mean spectra of the leaves, fine roots (each calculated from three spectra) and the organic layer material (calculated from 24 spectra) from all transects.**

## 5.5 Discussion

***Impact of individual trees on SOM composition, SOC contents and stocks***

In contrast to our hypothesis, the SOC contents and stocks of the bulk soil and the soil fractions were independent of the distance to individual trees. The same was observed for the chemical composition of SOM evaluated by $^{13}$C NMR spectroscopy. For POM, this was probably because the beech roots and leaves, from which the POM is derived, have both been found to contain considerable amounts of similar alkanes, alcohols and carboxylic acids (Mueller et al. 2012a).

This might render it difficult to identify effects on major chemical compound classes caused by a tree, although differences in monomeric composition could exist (cf. Spielvogel et al. 2014).

Moreover, the fine roots of the trees were evenly distributed in the horizontal and used all of the soil to the depth increment of 35 cm but were low in abundance at deeper soil layers (Fig. 6.2). Because roots are highly important for the input of OC to the soil (Rasse et al. 2005), we ascribe the non-existence of horizontal trends in NMR spectra and SOC contents and stocks mostly to the distribution of the fine roots.

***Changes in chemical composition, SOC contents and stocks of the SOM fractions with depth***

Although individual trees did not have a horizontal influence on the investigated parameters, we measured a significant vertical difference between $subsoil_{10}$ and $subsoil_{85}$ regarding the amount of the recovered fractions, the SOC contents and stocks, and the chemical composition of SOM (Table 6.1, Table 6.2). We assume that the spatially varying inputs of OM derived from the fine roots and above-ground litter were a main driver of these differences. Our data suggest a high input of OM in the densely rooted upper soil layers (to the depth increment of 35 cm depth) (Fig. 6.2) whereas the concentration of root bio- and necromass was low in deeper soil layers.

The chemical composition of the SOM fractions was dominated by alkyl and O/N-alkyl C, whereas carboxylic and aromatic C accounted for a smaller amount, as was also observed by others (Rumpel et al. 2002, Mueller et al. 2009). Beech roots and leaves had wide C/N and narrow alkyl/O/N-alkyl C ratios, indicating a low degree of decomposition. A relative increase of alkyl C and a decrease of O/N-alkyl C from plant inputs to the organic layer and the POM fraction of the $subsoil_{10}$ (Table 6.2, Table 6.3; Fig. 6.3, Fig. 6.5) accompanied by decreasing C/N ratios can be ascribed to the decomposition of carbohydrates like cellulose and hemicellulose. Simultaneously, aliphatic components accumulate during decomposition relative to other compounds. These observations agree with the results of other studies (e.g., Quideau et al. 2001, Schöning and Kögel-Knabner 2006).

Notably, alkyl/O/N-alkyl C ratios of the POM fraction of the $subsoil_{10}$ were very high (Table 6.2). This has also been observed for oPOM by Mueller et al. (2009) and suggests that the POM fraction in this study had already reached an advanced stage of decomposition. This indicates

either that the aggregate turnover was rapid or very little macro-aggregation occurred, reducing physical protection (Six et al. 2000, Six et al. 2002, Swanston et al. 2005). The high sand contents, especially in the subsoil$_{85}$, suggest a minor degree of macro-aggregation. Particulate OM can therefore be assumed to be readily available to the decomposition by microorganisms. This can be seen as an important reason for the absence of POM in the subsoil$_{85}$, together with a limited bioturbation and a large root litter input confined to depths < 40 cm.

The SOC contents and stocks of the bulk soil were drastically lower in the subsoil$_{85}$ compared to the subsoil$_{10}$. Similar trends have also been observed by others (Rumpel et al. 2004, John et al. 2005, Schöning and Kögel-Knabner 2006). This was accompanied by a lower mass of the clay fraction of the subsoil$_{85}$ (Fig. 6.3). While the POM fraction was virtually absent in the subsoil$_{85}$, the clay fractions were enriched in SOC compared to the subsoil$_{10}$ (Table 6.3). A similar enrichment was also found by Rumpel et al. (2004) in the B horizons of a Dystric Cambisol under European beech. In contrast to our results, $E_c$ values for the clay fraction determined by Rumpel et al. (2004) were about four times lower than $E_c$ values detemined in our study. Clay was thus more important in stabilizing SOC by organo-mineral association in the sandy soils investigated in this study compared to soils with a lower sand content such as investigated by Rumpel et al. (2004). This conclusion was further corroborated by the SOC stocks (Table 6.1). The clay fraction of the subsoil$_{85}$ accounted for a considerable amount of the SOC stocks, although the mass of this fraction was only 22.8 ± 4.2 g kg− 1 (Table 6.1). The SOC stocks at 40–200 cm depth were almost one third of the SOC stocks of the whole soil from 0 to 200 cm depth (Table 6.1). This is remarkable because the POM fraction, which accounted for the highest SOC stock in the subsoil$_{10}$, (Table 6.1) was absent from the subsoil$_{85}$. Most of SOC in the subsoil$_{85}$ was thus associated with the clay fraction.

The clay fraction of the subsoil$_{85}$ provided more free surface area not covered by SOC than the clay fraction of the subsoil$_{10}$. In addition, SOC contents of the clay fraction of the subsoil$_{85}$ were more variable than those of the clay fractions of the subsoil$_{10}$. This indicates that the amount and spatial variability of the SOM inputs to the deeper soil layers, rather than the availability of free sorption surfaces, were decisive for the quantity and spatial distribution of SOC stored in the clay fractions of deeper subsoil layers. Our data set indicates a drastic change from POM dominated SOC pools in the upper soil layers to SOC almost exclusively associated with clay in deeper soil layers.

***Rhizosphere soil***

The rhizosphere soil had three times higher SOC contents compared to the bulk subsoil$_{10}$. The fractionation approach suggests that this may be due to two different SOM contributions from the roots. First, the higher SOC contents of the clay fraction of the rhizosphere soil compared to the clay fraction of the non-rhizosphere soil (Table 6.1) were probably due to root exudates. These induce high microbial activity and the formation of microbial extracellular polymeric substances (EPS) in the direct vicinity of the roots (Kuzyakov 2002, Koranda et al. 2011, Bengtson et al. 2012). Secondly, our data pointed towards a high and frequent supply of the rhizosphere soil with fresh POM. This was evidenced by a six times higher amount of the POM fraction derived from the rhizosphere soil compared to the amount of the POM fraction derived from the surrounding subsoil$_{10}$ (Table 6.1). Further, the POM fraction of the rhizosphere soil was significantly less processed than that of the subsoil$_{10}$ as indicated by lower alkyl/O/N-alkyl C ratios (Table 2).

Until now, root exudates have been considered to be the largest (Dennis et al. 2010) and most important contributor of SOC inputs to soils from roots (Kuzyakov et al. 2007). Our results suggest that root derived POM may also contribute considerable amounts of OC to the SOC pool.

## 5.6 Conclusions

In contrast to other studies, neither the SOC contents and SOC stocks nor the gross chemical composition of the SOM determined by $^{13}$C CPMAS NMR spectroscopy were affected by the distance from *F. sylvatica* L. We ascribed this to the uppermost soil layers being densely and evenly rooted across all distances.

The trees caused significant vertical differences with POM dominated SOC pools in the upper soil layers, and SOC pools that were dominated by organo-mineral associations with the clay fraction in the deeper soil layers. Our results imply that these differences were strongly influenced by the roots of the trees. The SOC contents of the rhizosphere soil were more than three times as high as the SOC contents of the subsoil$_{10}$. This was ascribed to root exudates as well as to a high and frequent supply of the rhizosphere soil with fresh POM. We conclude that, besides root exudates, also root derived POM may contribute considerable amounts of SOC to the rhizosphere soil. The clay fractions in the vicinity of roots showed higher SOC contents and

higher proportions of O/N alkyl C with respect to non-rhizosphere soil. This points to the rhizosphere as a hotspot for the formation of organo-mineral associations.

The clay fraction was specifically important for SOC storage at the deeper subsoil, where a low amount of organo-mineral associations comprised almost 40% of the bulk soil SOC stocks.

Soil OC stocks of deeper soil layers (40–200 cm) represented roughly one third of the total SOC stocks (0–200 cm depth). This indicates that sandy subsoils with low SOC contents have to be considered in C inventories and may be integral parts of the SOC pool.

***Acknowledgements***

Funding of the research unit "The Forgotten Part of Carbon Cycling: Organic Matter Storage and Turnover in Subsoils (SUBSOM)", which this project is part of, was granted by the Deutsche Forschungsgemeinschaft DFG (FOR1806). We would like to thank Dr. Stefanie Heinze and Prof. Dr. Bernd Marschner for the project coordination, Dr. Peter Schad for the help with soil classification and Dr. Werner Häusler for performing XRD analyses. We thank Maria Greiner and Robert Hagemann for their invaluable help in the laboratory, Gabriele Albert, Bärbel Angres and Sigrid Hiesch for assistance in the lab, and the many anonymous reviewers who helped us greatly improve the manuscript.

## Supplementary Material

**TABLE S6.1: P-values for the statistical correlation between the distance from the individual beech trees and the respective parameter.**

| | | $Subsoil_{10}$ | $Subsoil_{85}$ |
|---|---|---|---|
| **Recovered mass** | Sand | 0.40 | 0.47 |
| | Silt | 0.41 | 0.53 |
| | Clay | 0.74 | 0.33 |
| | POM | 0.53 | n.d. |
| **SOC content** | Bulk soil | 0.91 | 0.32 |
| | Sand | 0.68 | 0.36 |
| | Silt | 0.39 | 0.46 |
| | Clay | 0.89 | 0.08 |
| | POM | 0.10 | n.d. |
| **C/N** | Bulk soil | 0.70 | 0.05 |
| | Sand | n.d. | n.d. |
| | Silt | n.d. | n.d. |
| | Clay | 0.43 | 0.21 |
| | POM | 0.77 | n.d. |
| **SOC stock** | Bulk soil | 0.83 | 0.32 |
| | Sand | 0.14 | 0.21 |
| | Silt | 0.07 | 0.93 |
| | Clay | 0.40 | 0.71 |
| | POM | 0.85 | n.d. |
| **$E_c$** | Sand | 0.35 | 0.88 |
| | Silt | 0.21 | 0.83 |
| | Clay | 0.36 | 0.65 |
| **POM** | Carboxyl C | 0.45 | n.d. |
| | Aromatic C | 0.84 | n.d. |
| | O/N alkyl C | 0.57 | n.d. |
| | Alkyl C | 0.60 | n.d. |
| | Alkyl/O/N alkyl C | 0.53 | n.d. |
| **Clay** | Carboxyl C | 0.62 | 0.98 |
| | Aromatic C | 0.88 | 0.94 |
| | O/N alkyl C | 0.46 | 0.79 |
| | Alkyl C | 0.83 | 0.86 |
| | Alkyl/O/N alkyl C | 0.82 | 0.76 |
| **Root biomass** | | 0.73 | 0.98 |
| **Root necromass** | | 0.70 | 0.49 |

Df = 22 for all correlations except for the NMR data of the clay fraction from the subsoil85 (df = 2).

## 6.7 References

Baldock, J.A., Oades, J.M., Nelson, P.N., Skene, T.M., Golchin, A., and Clarke, P. (1997) Assessing the extent of decomposition of natural organic materials using solid-state bsup N 13b/sup N C NMR spectroscopy. Soil Res. 35 (5): 1061–1084.

Bauhus, J., and Bartsch, N. (1996) Fine-root growth in beech (*Fagus sylvatica*) forest gaps. Can. J. For. Res. 26 (12): 2153–2159.

Bengtson, P., Barker, J., and Grayston, S.J. (2012) Evidence of a strong coupling between root exudation, C and N availability, and stimulated SOM decomposition caused by rhizosphere priming effects. Ecol. Evol. 2 (8): 1843–1852.

Brunauer, S., Emmett, P.H., and Teller, E. (1938) Adsorption of gases in multimolecular layers. J. Am. Chem. Soc. 60 (2): 309–319.

Brzostek, E., Greco, A., Drake, J., and Finzi, A. (2013) Root carbon inputs to the rhizosphere stimulate extracellular enzyme activity and increase nitrogen availability in temperate forest soils. Biogeochemistry 115 (1–3): 65–76.

Bundesanstalt für Bodenforschung (1973) Geologische Übersichtskarte 1:200000.

Chang, S.-C., and Matzner, E. (2000a) The effect of beech stemflow on spatial patterns of soil solution chemistry and seepage fluxes in a mixed beech/oak stand. Hydrol. Process. 14 (1): 135–144.

Chang, S.-C., and Matzner, E. (2000b) Soil nitrogen turnover in proximal and distal stem areas of European beech trees. Plant Soil 218 (1–2): 117–125.

Christensen, B.T. (2001) Physical fractionation of soil and structural and functional complexity in organic matter turnover. Eur. J. Soil Sci. 52 (3): 345–353.

Cieslinski, G., Van Rees, K.C.J., Szmigielska, A.M., Krishnamurti, G.S.R., and Huang, P.M. (1998) Low-molecular-weight organic acids in rhizosphere soils of durum wheat and their effect on cadmium bioaccumulation. Plant Soil 203 (1): 109–117.

Dennis, P.G., Miller, A.J., and Hirsch, P.R. (2010) Are root exudates more important than other sources of rhizodeposits in structuring rhizosphere bacterial communities? FEMS Microbiol. Ecol. 72 (3): 313–327.

Dijkstra, F.A., and Cheng, W.X. (2007) Moisture modulates rhizosphere effects on C decomposition in two different soil types. Soil Biol. Biochem. 39 (9): 2264–2274.

Eusterhues, K., Rumpel, C., and Kögel-Knabner, I. (2005) Organo-mineral associations in sandy acid forest soils: importance of specific surface area, iron oxides and micropores. Eur. J. Soil Sci. 56 (6): 753–763.

Fontaine, S., Barot, S., Barre, P., Bdioui, N., Mary, B., and Rumpel, C. (2007) Stability of organic carbon in deep soil layers controlled by fresh carbon supply. Nature 450 (7167) (277-U210).

Forstamt Nienburg (2010) Bestandslagerbuch – status 01.01.2010.

Geßler, A., Keitel, C., Kreuzwieser, J., Matyssek, R., Seiler,W., and Rennenberg, H. (2007) Potential risks for European beech (*Fagus sylvatica* L.) in a changing climate. Trees 21 (1): 1–11.

Goemoeryova, E. (2004) Small-scale variation of microbial activities in a forest soil under a beech (*Fagus sylvatica* L.) stand. Pol. J. Ecol. 52 (3): 311–321.

Gomes, N.C.M., Fagbola, O., Costa, R., Rumjanek, N.G., Buchner, A., Mendona-Hagler, L., Smalla, K., 2003. Dynamics of fungal communities in bulk and maize rhizosphere soil in the tropics. Appl. Environ. Microbiol. 69 (7), 3758–3766.

Gonçalves, C.N., Dalmolin, R.S.D., Dick, D.P., Knicker, H., Klamt, E., and Kögel-Knabner, I. (2003) The effect of 10% HF treatment on the resolution of CPMAS $^{13}$C NMR spectra and on the quality of organic matter in ferralsols. Geoderma 116 (3–4): 373–392.

Guggenberger, G., Christensen, B.T., and Zech, W. (1994) Land-use effects on the composition of organic matter in particle-size separates of soil: I. Lignin and carbohydrate signature. Eur. J. Soil Sci. 45 (4): 449–458.

Hertel, D. (1999) Das Feinwurzelsystem von Rein- und Mischbeständen der Rotbuche: Struktur, Dynamik und Interspezifische Konkurrenz. Dissertationes Botanicae 317. Gebrüder Borntträger, Stuttgart.

Hertel, D., and Leuschner, C. (2002) A comparison of four different fine root production estimates with ecosystem carbon balance data in a *Fagus–Quercus* mixed forest. Plant Soil 239 (2): 237–251.

Hertel, D., Strecker, T., Müller-Haubold, H., and Leuschner, C. (2013) Fine root biomass and dynamics in beech forests across a precipitation gradient – is optimal resource partitioning theory applicable to water-limited mature trees? J. Ecol. 101 (5): 1183–1200.

IPCC (2000) Land Use, Land-Use Change, and Forestry – Special Report. Cambridge University Press, Cambridge CB2 2RU England (375 pp.).

IUSSWorking GroupWRB (2014)World Reference Base for Soil Resources 2014. International soil classification system for naming soils and creating legends for soil maps. World Soil Resources Reports No. 106. FAO, Rome.

Jobbágy, E.G., and Jackson, R.B. (2000) The vertical distribution of soil organic carbon and its relation to climate and vegetation. Ecol. Appl. 10 (2): 423–436.

John, B., Yamashita, T., Ludwig, B., and Flessa, H. (2005) Storage of organic carbon in aggregate and density fractions of silty soils under different types of land use. Geoderma 128 (1–2): 63–79.

Koch, A.S., and Matzner, E. (1993) Heterogeneity of soil and soil solution chemistry under Norway spruce (Picea abies Karst.) and European beech (*Fagus sylvatica* L.) as influenced by distance from the stem basis. Plant Soil 151 (2): 227–237.

Kögel-Knabner, I. (1997) $^{13}C$ and $^{15}$ N NMR spectroscopy as a tool in soil organic matter studies. Geoderma 80 (3–4): 243–270.

Kögel-Knabner, I., Hatcher, P.G., Tegelaar, E.W., and de Leeuw, J.W. (1992) Aliphatic components of forest soil organic matter as determined by solid-state $^{13}C$ NMR and analytical pyrolysis. Sci. Total Environ. 113 (1–2): 89–106.

Koranda, M., Schnecker, J., Kaiser, C., Fuchslueger, L., Kitzler, B., Stange, C.F., Sessitsch, A., Zechmeister-Boltenstern, S., and Richter, A. (2011) Microbial processes and community composition in the rhizosphere of European beech – the influence of plant C exudates. Soil Biol. Biochem. 43 (3): 551–558.

Kuzyakov, Y. (2002) Review: factors affecting rhizosphere priming effects. J. Plant Nutr. Soil Sci. 165 (4): 382–396.

Kuzyakov, Y., and Domanski, G. (2000) Carbon input by plants into the soil. Review. J. Plant Nutr. Soil Sci. 163 (4): 421–431.

Kuzyakov, Y., Hill, P., and Jones, D. (2007) Root exudate components change litter decomposition in a simulated rhizosphere depending on temperature. Plant Soil 290 (1–2): 293–305.

Leuschner, C., Hertel, D., Coners, H., and Büttner, V. (2001) Root competition between beech and oak: a hypothesis. Oecologia 126 (2): 276–284.

Lodhi, M.A.K. (1977) The influence and comparison of individual forest trees on soil properties and possible inhibition of nitrification due to intact vegetation. Am. J. Bot. 64 (3): 260–264.

Lorenz, K., and Lal, R. (2005) The Depth Distribution of Soil Organic Carbon in Relation to Land Use and Management and the Potential of Carbon Sequestration in Subsoil Horizons. In: Donald, L.S. (ed.), Advances in Agronomy. Academic Press, 35–66.

Mueller, K.E., Polissar, P.J., Oleksyn, J., and Freeman, K.H. (2012a) Differentiating temperate tree species and their organs using lipid biomarkers in leaves, roots and soil. Org. Geochem. 52: 130–141.

Mueller, C.W., Schlund, S., Prietzel, J., Kögel-Knabner, I., and Gutsch, M. (2012b) Soil aggregate destruction by ultrasonication increases soil organic matter mineralization and mobility. Soil Sci. Soc. Am. J. 76 (5): 1634–1643.

Mueller, C.W., Bruggemann, N., Pritsch, K., Stoelken, G., Gayler, S., Winkler, J.B., and Kögel-Knabner, I. (2009) Initial differentiation of vertical soil organic matter distribution and composition under juvenile beech (*Fagus sylvatica* L.) trees. Plant Soil 323 (1–2): 111–123.

Persson, H. (1978) Root dynamics in a young scots pine stand in central Sweden. Oikos 30 (3): 508–519.

Quideau, S.A., Chadwick, O.A., Benesi, A., Graham, R.C., and Anderson, M.A. (2001) A direct link between forest vegetation type and soil organic matter composition. Geoderma 104 (1–2): 41–60.

R Core Team (2013) R: A language and Environment for Statistical Computing. R Foundation for Statistical Computing, Vienna, Austria (URL http://www.R-project.org/).

Rasse, D., Rumpel, C., and Dignac, M.-F. (2005) Is soil carbon mostly root carbon? Mechanisms for a specific stabilisation. Plant Soil 269 (1–2): 341–356.

Rumpel, C., and Kögel-Knabner, I. (2011) Deep soil organic matter—a key but poorly understood component of terrestrial C cycle. Plant Soil 338 (1–2): 143–158.

Rumpel, C., Eusterhues, K., and Kögel-Knabner, I. (2004) Location and chemical composition of stabilized organic carbon in topsoil and subsoil horizons of two acid forest soils. Soil Biol. Biochem. 36 (1): 177–190.

Rumpel, C., Kögel-Knabner, I., and Bruhn, F. (2002) Vertical distribution, age, and chemical composition of organic, carbon in two forest soils of different pedogenesis. Org. Geochem. 33 (10): 1131–1142.

Rumpel, C., Rabia, N., Derenne, S., Quenea, K., Eusterhues, K., Kögel-Knabner, I., and Mariotti, A. (2006) Alteration of soil organic matter following treatment with hydrofluoric acid (HF). Org. Geochem. 37 (11): 1437–1451.

Saetre, P., and Bååth, E. (2000) Spatial variation and patterns of soil microbial community structure in a mixed spruce–birch stand. Soil Biol. Biochem. 32 (7): 909–917.

Schenck, z., Schweinsberg-Mickan, M., Jörgensen, R.G., and Müller, T. (2012) Rhizodeposition: its contribution to microbial growth and carbon and nitrogen turnover within the rhizosphere. J. Plant Nutr. Soil Sci. 175 (5): 750–760.

Schmidt, M.W.I., Knicker, H., Hatcher, P.G., and Kögel-Knabner, I. (1997) Improvement of $^{13}C$ and $^{15}N$ CPMAS NMR spectra of bulk soils, particle size fractions and organic material by treatment with 10% hydrofluoric acid. Eur. J. Soil Sci. 48 (2): 319–328.

Schöning, I., and Kögel-Knabner, I. (2006) Chemical composition of young and old carbon pools throughout Cambisol and Luvisol profiles under forests. Soil Biol. Biochem. 38 (8): 2411–2424.

Schöning, I., Totsche, K.U., and Kögel-Knabner, I. (2006) Small scale spatial variability of organic carbon stocks in litter and solumof a forested Luvisol. Geoderma 136 (3–4): 631–642.

Schrumpf, M., Kaiser, K., Guggenberger, G., Persson, T., Kögel-Knabner, I., and Schulze, E.D. (2013) Storage and stability of organic carbon in soils as related to depth, occlusion within aggregates, and attachment tominerals. Biogeosciences 10 (3): 1675–1691.

Six, J., Callewaert, P., Lenders, S., De Gryze, S., Morris, S.J., Gregorich, E.G., Paul, E.A., and Paustian, K. (2002) Measuring and understanding carbon storage in afforested soils by physical fractionation. Soil Sci. Soc. Am. J. 66 (6): 1981–1987.

Six, J., Elliott, E.T., and Paustian, K. (2000) Soil macroaggregate turnover and microaggregate formation: a mechanism for C sequestration under no-tillage agriculture. Soil Biol. Biochem. 32 (14): 2099–2103.

Spielvogel, S., Prietzel, J., Leide, J., Riedel, M., Zemke, J., and Kögel-Knabner, I. (2014) Distribution of cutin and suberin biomarkers under forest trees with different root systems. Plant Soil 381 (1–2): 95–110.

Swanston, C.W., Torn, M.S., Hanson, P.J., Southon, J.R., Garten, C.T., Hanlon, E.M., and Ganio, L. (2005) Initial characterization of processes of soil carbon stabilization using forest stand-level radiocarbon enrichment. Geoderma 128 (1–2): 52–62.

Tefs, C., and Gleixner, G. (2012) Importance of root derived carbon for soil organic matter storage in a temperate old-growth beech forest — evidence from C, N and C-14 content. For. Ecol. Manag. 263: 131–137.

Van Praag, H.J., Sougenez-Remy, S.,Weissen, F., and Carletti, G. (1988) Root turnover in a beech stand of the Belgian Ardennes. Plant Soil 105: 87–103.

# CHAPTER 7

# Soil organic carbon stocks in topsoil and subsoil controlled by parent material, carbon input in the rhizosphere, and microbial-derived compounds

Gerrit ANGST, Johanna MESSINGER, Maria GREINER, Werner HÄUSLER, Dietrich HERTEL, Kristina KIRFEL, Ingrid KÖGEL-KNABNER, Christoph LEUSCHNER, Janet RETHEMEYER, Carsten W. MUELLER

SOIL BIOLOGY AND BIOCHEMISTRY, 2018, VOLUME 122, PAGES 19-30. DOI: 10.1016/j.soilbio.2018.03.026

## 7.1 Abstract

Despite a large body of studies investigating soil organic carbon (SOC) stocks and potential influencing factors, the impact of contrasting parent material, particularly in the subsoil, has received little attention. To reveal potential effects varying parent materials exert on SOC stocks, we investigated chemical ($^{14}C$ content and overall chemical composition via $^{13}C$ NMR spectroscopy) and plant/microbial related parameters (root mass, amino sugars) of bulk soil and soil organic matter fractions from topsoil, subsoil, and rhizosphere soil at three European beech stands (*Fagus sylvatica* L.) only differing in parent material (Tertiary sand, Quaternary loess, and Tertiary basalt).

The results suggest that the clay fraction, its amount being largely dependent on the respective parent material, took a central role in shaping differences in SOC stocks among the investigated sites by affecting soil organic matter stabilization via organo-mineral association and aggregation. This fraction was particularly relevant in the subsoil, where it accounted for up to 80% of the bulk soil SOC stocks that decreased with decreasing amounts of the clay fraction (basalt > loess > sand site). Determining the soil's nutrient composition, parent material likely also indirectly affected SOC stocks by changing rhizosphere traits (such as fine root density or mortality) and by attracting root growth (and thus organic matter inputs) to subsoil with higher nutrient contents, where in situ root inputs in the form of rhizodeposits were likely the prime source of plant-derived SOC. However, root inputs also contributed in large part to topsoil SOC stocks and were associated with higher abundance of microbial compounds (amino sugars), whose relative importance increased with increasing soil depth.

Independent of soil depth and site, amino sugars and the amount of the clay fraction, combined with parameters related to the input of organic matter (root mass and amount of the particulate organic matter fraction) explained more than 90% of the variability in SOC stocks, indicating a key role of these measures in impacting SOC stocks. Because parent material directly or indirectly influenced these parameters, we demonstrate the necessity to consider differences in parent material when estimating and predicting SOC stocks.

***Graphical abstract***

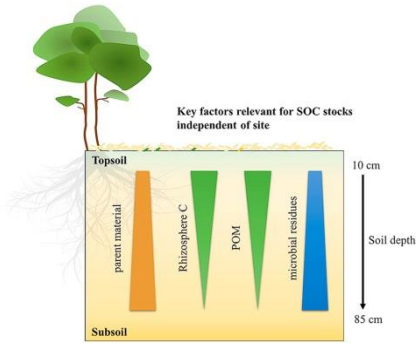


***Keywords***: *Fagus sylvatica* L., $^{14}C$, Physical fractionation, Amino sugars, $^{13}C$ NMR

## 7.2 Introduction

Soil constitutes a potential carbon (C) sink (Post et al. 1982) and many studies have been investigating soil organic C (SOC) stocks on different scales and possible controlling factors (e.g., Baritz et al. 2010; Janssens et al. 2005; Jobbágy and Jackson 2000; Jones et al. 2005; Saiz et al. 2012; Wiesmeier et al. 2014). On global or continental scale, differences in SOC stocks have been linked to vegetation type and climate (Gray et al. 2016; Jobbágy and Jackson 2000; Johnson et al. 2011; Saiz et al. 2012). On smaller scales, such as the stand scale, soil biota (particularly earthworms), soil acidity, or plant species (Mueller et al. 2015; Vesterdal et al. 2013) were identified as important driving factors. The influence of varying parent material, however, has received little attention (Barré et al. 2017; Heckman et al. 2009) and the way in which substrate properties affect the input of organic matter (OM) or translate into SOC stabilization mechanisms (e.g. Wagai et al, 2008), such as organo-mineral association or aggregation (von Lützow et al. 2006, 2008), is a widely unresolved matter (Prechtel et al. 2009).

Despite the wealth of studies dealing with SOC stocks, most of these studies were conducted in the topsoil (~upper 30 cm of the soil profile). The subsoil generally contains less SOC (Rumpel and Kögel-Knabner 2011), but given the fact that its volume often exceeds that of the topsoil, these low SOC contents can considerably contribute to SOC stocks of the whole soil (Angst et al. 2016b; Jandl et al. 2007; Richter and Billings 2015). An often very low $^{14}C$ content of SOC in the subsoil indicates its long residence time (also referred to as 'transit time'; Lorenz and Lal 2005; Manzoni et al. 2009; Rethemeyer et al. 2005; Rumpel and Kögel-Knabner 2011; Schöning and Kögel-Knabner 2006) and an increase of subsoil SOC stocks thus appears to be of central importance for sequestering C and mitigating climate change (Jobbágy and Jackson 2000; Lorenz et al. 2007). Organic matter inputs in the rhizosphere (by exudation and/or in particulate form) may already be relevant in the topsoil (Angst et al. 2016b; Tefs and Gleixner 2012), but seem to gain importance with increasing soil depth (Rasse et al. 2005) and have been proposed to increase subsoil SOC stocks (Lorenz et al. 2007). However, the consequences of additional C input for the SOC already stored in deeper soil layers is still uncertain and has been controversially discussed (e.g., Fontaine et al. 2007; Lorenz and Lal 2005). One reason for these uncertainties may be that studies including parent material variations are scarce. These variations may become particularly evident in the subsoil, where plant inputs are reduced and a direct effect of parent material mineralogy might be more directly perceptible as compared to the topsoil.

The aim of the present study, thus, was to disentangle the impact of different parent materials on the amount and distribution of SOC stocks in topsoil and subsoil by applying a combination of fractionation techniques and chemical methods. To control for the factors climate and vegetation, we chose pure mature European beech (*Fagus sylvatica* L.) stands with similar precipitation and temperature regimes, only differing in parent material: Tertiary sand, Quaternary loess, and Tertiary basalt. These substrates widely differ in their textural composition and nutrient supply. For example, sandy sedimentary materials can be expected to have substantially smaller nutrient contents than basaltic, more phyllosilicate rich rocks or soils developed from silt- and nutrient-rich Loess deposits (Anderson 1988; Catt 2001). These differences likely do not only influence the SOC preservation capacity of a soil (Hassink 1997) but also litter production (and thus input of OM or contribution of root as compared to shoot-derived OM (Crow et al. 2009; Kögel-Knabner 2002) via different levels of soil nutrients, such as phosphorus (Wright et al. 2011). The mentioned and other properties may not be uniformly distributed in developed soils with significant small-scale variability of SOC stocks (Chabbi et al. 2009; Schöning et al. 2006) and physical, chemical, and microbial soil properties that are often influenced by the distance to individual trees (Chang and Matzner 2000; Koch and Matzner 1993; Saetre and Bååth 2000). We thus relied on a spatially resolved sampling design taking into account possible horizontal heterogeneities at increasing distance to individual beech trees. We fractionated the investigated soils into compartments assignable to specific stabilization mechanisms (recalcitrance, organo-mineral association, and aggregation (von Lützow et al. 2007) and evaluated the $^{14}C$ content of stabilized soil OM (SOM) by performing radiocarbon measurements on mineral-associated SOM in the clay fraction. We additionally fractionated rhizosphere soil and measured the root mass (combined fine root biomass and necromass) to account for the relevance of the rhizosphere. Residues derived from soil microorganisms located in the rhizosphere and elsewhere may substantially contribute to SOM in organo-mineral associations and aggregate formation (e.g. Castellano et al. 2015; Cotrufo et al. 2013), but their role in affecting SOC stocks is unresolved. We thus determined the amount of amino sugars as indicators for microbial residues. The overall chemical composition of OM in the soil fractions, revealed by $^{13}C$ nuclear magnetic resonance spectroscopy (NMR; e.g. Baldock et al. 1997; Cepáková and Frouz 2015; Kögel-Knabner et al. 1992), completed our analyses.

## 7.3 Materials and Methods

### *Study sites and soil sampling*

Composite and volume soil samples were taken in May 2014 at three different study sites located near the city of Göttingen in central Germany. The study sites were covered by European beech forests, featured similar climatic conditions (average annual precipitation and temperature of ca. 650 mm and 9.2 °C in 1981–2010; Deutscher Wetterdienst, station 'Göttingen') but developed from different parent materials. The Haplic Cambisol at the site 'Hannoversch-Münden' (51° 26′ 25.64″ N 09° 41′ 24.25″ E, 270 m a.s.l.; termed 'sand site') developed from Tertiary sand and had a pH of 3.7–4.2 with Hemimor as forest floor type (65% sand, 27.3% silt, and 7.7% clay in mineral soil). The Haplic Luvisol at the site 'Rüdershausen' (51° 34′ 51.52″ N 10° 14′ 43.03″ E, 200 m a.s.l.; termed 'loess site') developed from Quaternary loess deposits, had a pH of 3.6–4.1, and a Leptomoder forest floor type (3.2% sand, 87.5% silt, and 9.3% clay in mineral soil). The Eutric Cambisol at the site 'Dransfeld' (51° 28′ 35.60″ N 09° 45′ 32.46″ E, 470 m a.s.l.; termed 'basalt site') developed from Tertiary basalt, had a pH of 3.7–4.8, and a Mullmoder forest floor type (1% sand, 87.5% silt, and 11.5% clay in mineral soil; forest floor data taken from Kirfel et al., unpublished data). All profiles were similar with respect to clay mineralogy (determined by X-ray diffraction) with dominance of illites, primary/secondary chlorites and smaller amounts of kaolinites present throughout the profiles. Some minor differences in the relative abundance of primary/secondary chlorites occurred across the study sites. However, these contribute only marginally to the cation exchange capacity of the soils because their interlayers are blocked with Al-octahedrons. Differences in the relative abundance of illites occurred at the sand site, where it was higher in the subsoil as compared to the respective topsoil. Smectites could not be confirmed at any of the study sites. At each study site, three different replicate soil ditches were dug reaching down to the parent material. One end of each ditch originated at the stem base of a mature European beech tree. Soil samples for all analyses were taken in 10 cm (from now on referred to as 'topsoil'; Al horizon at the loess and Ah-Bv horizon at the sand and basalt sites) and 85 cm depth (from now on referred to as 'subsoil'; Bt horizon at the loess and Cv horizon at the sand site; 60 cm at the basalt site due to solid parent material beneath this depth, Bv horizon) at two spots per depth increment to account for spatial variability: directly at the stem base of the tree and at 135 cm distance. The upper sampling spots were set to 10 cm depth to allow a representative volumetric sampling unbiased by varying topsoil thicknesses using the same steel

rings (diameter: 8.5 cm, height: 6.0 cm). Soil samples for calculation of SOC stocks only (see section 2.8), were collected in between the two vertical sampling spots at 35 and 60 cm depth. At the sand and basalt sites, these sampling depths were located in the B horizons, while they were part of the A horizon at the loess site. We sampled one composite rhizosphere soil sample at each transect from the whole extent of the densely rooted upper soil layers in between the two horizontal sampling spots (~top 40 cm of the soil profiles). Rhizosphere soil was defined as the soil sticking to a root after it had been thoroughly shaken (Cieslinski et al. 1998; Gomes et al. 2003). In the laboratory, the soil samples were air-dried and passed through a 2 mm-sieve. Soil densities were calculated from the volume samples considering soil moisture and coarse particles >2 mm. The sampling design enabled us to compare SOM properties in the topsoil vs. the subsoil vs. the rhizosphere soil, evaluate possible spatial variability and influence of the distance to individual trees, and investigate differences between sites differing in parent material.

***Determination of root mass***

Aliquots of the soil samples were sieved (0.25 mm mesh size) to separate roots from adhering soil particles. The sample remains were soaked in demineralized water and all roots larger than 10 mm in length were extracted with tweezers for further examination. Smaller root fractions were neglected during this first step to keep the workload viable. Under the stereo-microscope, the larger rootlets >10 mm length were separated into living (biomass) and dead (necromass) roots ≤ 2 mm (fine) and >2 mm (coarse) in diameter. The distinction of living and dead roots was made based on the parameters root and periderm color, tissue elasticity, and cohesion of cortex, periderm, and stele (e.g. Hertel et al. 2013). All roots were dried at 70 °C for 48 h and subsequently weighed. While omission of root fragments <10 mm in length captures the majority of the fine root biomass (>95%) well (Bauhus and Bartsch 1996; Leuschner et al. 2001), it leads to an underestimation of the fine root necromass, which thus has to be corrected for the root fragments < 10 mm length. This correction was made by extrapolating depth-specific regression equations with the mass of dead fine roots <10 mm regressed on the mass of dead fine roots ≥10 mm length. The data were collected from representative samples taken from the same plots for which the mass of small dead roots was quantified using a method introduced by van Praag et

al. (1988) and modified by Hertel (1999). Because the root necromass and biomass were highly correlated ($r = 0.84$), we consider the sum of both variables as a combined `root mass'.

***Extraction and quantification of microbial biomarkers***

The amino sugars glucosamine, mannosamine, galactosamine, and muramic acid were extracted from bulk soil samples following Zhang and Amelung (1996) and Liang et al. (2012). Aliquots of the samples were ground and hydrolyzed with 6 M HCl at 105 °C for 8 h. The extracts were purified by neutralization and precipitation of salts in MeOH and water, and derivatized to aldonitrile acetates. All extractions were performed in duplicate. Dried extracts were re-dissolved in ethyl acetate and hexane (1:1, v:v) and measured using a Trace GC Ultra coupled to an ISQ mass spectrometer (ThermoFisher Scientific, Waltham, USA) with myo-inositol as internal standard. The GC oven was run with the following temperature program: initial temperature of 120 °C held for 4 min, subsequent heating to 250 °C at 30 °C $min^{-1}$ held for 10 min, heating to 280 °C at 5 °C $min^{-1}$ held for 10 min, and heating to 320 °C at 30 °C $min^{-1}$ held for 10 min. Samples were injected in split mode (1:10) with an injector temperature of 260 °C and a constant He flow of 1 ml $min^{-1}$. The ISQ was operated in electron ionization mode and a scan mass range of 50–650 m $z^{-1}$. Quantification of amino sugars and muramic acid was achieved by applying calibration curves derived from an external standard consisting of different concentrations of the target analytes and normalized to the GC response factor that was always close to 1. Concentrations of the target analytes were normalized to the dry weight (DW) and organic C content of the respective sample.

***Combined density and particle size fractionation***

The air-dried and sieved soil samples were subjected to a modified combined density and particle size fractionation according to Angst et al. (2016b). Briefly, 30 g of soil were suspended in 150 ml of sodium polytungstate (SPT) solution with a density of 1.8 g $cm^{-3}$ and gently shaken to separate the lighter particulate OM fractions from the heavier mineral soil fractions. Because the soil from the sand site did not contain measurable amounts of occluded particulate OM, it was directly ultrasonicated with an energy of 600 J $ml^{-1}$ and free particulate OM (from now on referred to as 'POM') was removed by a water jet pump. Regarding the soils from the loess and basalt sites, floating POM was removed by a water jet pump prior to ultrasonication. Removed

SPT solution was replaced by fresh solution and floating POM was removed again. This step was repeated until no POM particles were floating in the solution. The soil from the loess site was subsequently ultrasonicated with an energy of 600 J $ml^{-1}$ and the soil from the basalt site was ultrasonicated with an energy of 800 J $ml^{-1}$ to release particulate OM occluded within aggregates. Based on pre-tests with different SPT densities and ultrasonication energies, the chosen parameters separated the particulate OM and mineral soil compartments most effectively. All samples were cooled during application of the ultrasound to avoid any heating and chemical changes of the SOM contained within the soils (Mueller et al. 2012). The occluded particulate OM was removed from the solutions analogous to the POM. The occluded particulate OM was further separated into fragments >20 μm (referred to as oPOM) and fragments < 20 μm (referred to as oPOMsmall) in a sieve of 20 μm mesh-size. Particulate OM fractions were washed with deionized water until the electrical conductivity of the eluted water was below 5 μS. The mineral soil residue was washed with distilled water until the electrical conductivity of the eluted water was below 50 μS. Subsequently, the mineral soil residue was successively wet-sieved through sieves of different mesh-size to obtain the sand fraction (63–2000 μm) and the coarse silt fraction (20–63 μm). The mineral soil that passed through all sieves was subjected to sedimentation to separate the medium silt (6.3–20 μm) from the combined fine silt and clay fraction (<6.3 μm; termed 'clay fraction'). The coarse and medium silt fractions were combined to the 'silt fraction'. The average mass recovery was 98.7% for the sand site, 97.3% for the loess site, and 97.1% for the basalt site. All fractions were freeze-dried. The reference to 'bulk' soil in the following chapters refers to non-fractionated soil and is not intended to distinguish rhizosphere from non-rhizosphere soil. Amounts of soil fractions and soil texture at the same site may differ due to methodological differences in their determination, such as a combination of fine-silt and clay in the fractionation, or the removal of OM prior to soil texture analysis.

### *Carbon and nitrogen measurements*

Aliquots of bulk soil and SOM fractions were analyzed for C and nitrogen (N) contents via dry combustion using an elemental analyzer (Eurovector, Milan, Italy). The SOM fractions larger than medium silt were finely ground prior to analysis. All measurements were run in duplicate. The pH of all investigated soils did not exceed a value of 4.8 clearly indicating the absence of inorganic C. Thus, total C contents were equal to organic C contents.

### *Radiocarbon analysis*

The radiocarbon analysis was performed on the clay fraction (<6.3 μm). All samples were treated using a modified protocol according to Rethemeyer et al. (2013) and Angst et al. (2016a). Briefly, all samples were extracted with 0.5% HCl, first for one hour at 60 °C and then over night at room temperature. The HCl was removed by washing with Milli-Q water. After drying, the samples were weighed into small tin cups, combusted, and graphitized using an elemental analyzer (Rethemeyer et al. 2013). The $^{14}C$ contents were measured on a 6 MV Tandetron AMS (HVE, The Netherlands) at the University of Cologne (Dewald et al. 2013). The results of the measurements are reported in $F^{14}C$ including blank correction and normalization for isotopic fractionation (Reimer et al. 2004).

### *Nuclear magnetic resonance spectroscopy*

The clay and particulate OM fractions (POM from the sand site; POM, oPOM, and oPOMsmall from the loess and basalt sites) commonly containing most SOC (Angst et al. 2016b) were measured using solid-state $^{13}C$ cross-polarization magic angle spinning (CPMAS) NMR spectroscopy. Samples were weighed into zircon oxide rotors that were spun at 5 kHz around a 'magic angle' of 54.74°. The recycle delay time was set to 0.4 s for the clay fraction and 1.0 s for all particulate OM fractions. The spectra were processed with a line broadening of 50–75 Hz, phase adjusted, corrected for spinning side bands, and baseline corrected. Peaks were separated into four integration areas: 0–45 ppm (alkyl-C), 45–110 ppm (O/N-alkyl-C), 110–160 ppm (aromatic-C), and 160–220 ppm (carboxylic-C). All spectra were well resolved (Supplementary

Fig. S7.1) indicating no interfering effects of paramagnetic compounds, such as iron, on the measurements.

***Statistics and calculations***

Soil OC stocks were calculated for each SOM fraction and the bulk soil at the respective sampling spot from SOC contents and soil densities for an area of 1 $m^2$ and normalized to a layer thickness of 1 cm (from now on referred to as 'SOC stocks'; cf. Angst et al. 2016b). For the calculation of rhizosphere SOC stocks, a mean density value was used, calculated from six volume soil samples taken at the topsoil sampling spots at each site. Because soil densities in the rhizosphere soil likely vary, e.g., due to soil compaction by roots, the rhizosphere SOC stocks calculated here can only be seen as an approximate estimate. Whole profile SOC stocks (down to 85 and 60 cm depth, respectively) separated into topsoil and subsoil were calculated by multiplying the SOC stocks by the thickness of the respective soil horizons. The additional sampling spots in between the 10 and 85 cm sampling depths (35 and 60 cm depth) were included for this calculation.

Aliphatic compounds (alkyl C) are usually more resistant against decomposition than e.g., polysaccharides (O/N-alkyl C). Thus, the alkyl/O/N-alkyl C ratio was calculated from the NMR spectra as an indicator of the degree of SOM degradation (Baldock et al. 1997).

The ratio between fungal and bacterial C was calculated according to Appuhn and Joergensen (2006) and Engelking et al. (2007) in order to distinguish the sources of the extracted microbial-derived compounds. Fungal C was determined by subtracting bacterial from total glucosamine, supposing that muramic acid and glucosamine occur at a molar ratio of 1–2 in bacterial cells (Engelking et al. 2007). Bacterial C was calculated by multiplying the content of muramic acid by 45 (Appuhn and Joergensen 2006; Engelking et al. 2007; Joergensen and Wichern 2008).

Arithmetic means and standard errors (SE) were calculated using Microsoft Excel 2013 for Windows (Microsoft, Redmond, WA, USA). All other statistics were performed using the statistical software R for Windows (R Core Team 2015). The data were tested for normality and homoscedasticity using the Shapiro-Wilk and Bartlett test, respectively. Depending on the tests' outcome, significant differences between the investigated parameters regarding horizontal

distance to each other, soil depth, and study sites were either assessed by the Kruskal-Wallis-test or one-way analysis of variance (ANOVA).

We performed best subset regression with the Akaike information criterion (AIC) for best model selection to identify possible site-independent parameters important to SOC stocks. We started with two predictor variables and only considered models with a higher set of predictors when their AIC was lower at least by a value of 2 than the AIC of the best model of the previous size. Using this approach, only predictors that added substantial information were included in the multiple regressions and overfitting was prevented. We tested the mass of fractions (clay, POM, oPOM, oPOMsmall), root mass, and amino sugars (per g DW) on SOC stocks of bulk soil across all sites and samples investigated in the present study. The data were screened for normality and log-transformed if needed. Multicollinearity was assessed by variance inflation factors (VIF), excluding variables from the multiple regression if VIF were larger than a value of 2.5. A low VIF cutoff (as used in the present study) prevents correlated predictors from frequently co-occurring in the same models. Residuals were tested for independence and normality. Statistical differences were regarded as significant at $p < 0.05$.

## 7.4 Results

None of the investigated parameters at each site significantly differed with respect to the horizontal distance to the individual beech trees. We thus decided to regard the two horizontal samples per depth increment (10 and 85 cm) and soil ditch at each site as replicates for that specific depth. This consolidation yielded six replicates for the topsoil and six replicates for the subsoil at each site. Consequently, only differences between topsoil, subsoil, and rhizosphere soil are considered in the following chapters.

### *Root mass*

In the topsoil, the root mass was highest at the sand site ($3.1 \pm 0.6$ g cm$^{-3}$) and lowest at the loess site ($1.1 \pm 0.4$ g cm$^{-3}$; Table 7.1). The basalt site took an intermediate position ($2.1 \pm 0.4$ g cm$^{-3}$) with a trend of a higher root mass in the topsoil as compared to the loess site (higher by 47.6%) and a trend of a lower root mass as compared to the sand site (lower by 32.3%; Table 7.1). The root mass generally decreased with depth (Table 7.1; significant at the sand and basalt sites, trend at the loess site (lower by 45.5%)).

**TABLE 7.1: Different biological and chemical parameters in topsoil, subsoil, and rhizosphere soil among the investigated sites ± S.E. Significant differences between the sites and topsoil, subsoil, and rhizosphere soil are indicated by lower case letters.**

| | | root mass [g cm$^{-3}$] | ∑ amino sugars [mg g$^{-1}$ DW] | ∑ amino sugars [mg g$^{-1}$ SOC] | fungal/bacterial C | $^{14}$C content of clay fraction [F$^{14}$C] |
|---|---|---|---|---|---|---|
| **sand** | topsoil | 3.1 ± 0.6a | 0.8 ± 0.2c | 46.1 ± 5.7bc | 2.2 ± 0.4cd | 0.98 ± 0.03a |
| | subsoil | 0.1 ± 0.04cd | 0.03 ± 0.01d | 45.5 ± 17.0bc | 3.2 ± 0.7bc | 0.57 ± 0.08c |
| | rhizosphere soil | n.d. | 1 ± 0.2bc | 50.9 ± 10.2abc | 2.5 ± 0.2bcd | 1.01 ± 0.01a |
| **loess** | topsoil | 1.1 ± 0.4bc | 0.7 ± 0.1c | 77.5 ± 14.0ab | 1.5 ± 0.4d | 0.99 ± 0.01a |
| | subsoil | 0.6 ± 0.03c | 0.2 ± 0.01d | 94.3 ± 15.0a | 1.3 ± 0.1d | 0.6 ± 0.05c |
| | rhizosphere soil | n.d. | 0.6 ± 0.1cd | 81.2 ± 7.9ab | 1.4 ± 0.3d | 0.96 ± 0.00a |
| **basalt** | topsoil | 2.1 ± 0.4ab | 1.4 ± 0.4ab | 40.5 ± 6.7c | 3.8 ± 0.6ab | 0.96 ± 0.01a |
| | subsoil | 0.6 ± 0.2c | 0.6 ± 0.3cd | 67.9 ± 6.5abc | 2.3 ± 0.3cd | 0.79 ± 0.03b |
| | rhizosphere soil | n.d. | 1.8 ± 0.3a | 56.7 ± 9.1abc | 4.7 ± 0.3a | 0.95 ± 0.02a |

n.d. = not determined, n = 6 for topsoil and subsoil; n = 3 for rhizosphere soil.

### *Microbial biomarkers*

The distribution of amino sugars normalized to DW was very similar within the sites with highest contents in the topsoil and rhizosphere soil and lower contents in the subsoil (Table 7.1; significant for the sand and basalt sites).

When comparing amino sugars per g DW between the sites, the values at the sand and loess sites did not significantly differ, neither in topsoil, subsoil nor rhizosphere soil. The amino sugars per g DW at the basalt site were significantly higher in the topsoil and rhizosphere soil and showed a trend of being higher in the subsoil as compared to the other two sites (higher by 95% as compared to the sand subsoil and 66.6% as compared to the loess subsoil).

The distribution of the amino sugars normalized to g C was substantially different from that of the amino sugars per g DW: within each site, significant differences did not exist but, as compared to the topsoil and rhizosphere soil, amino sugars tended to increase in the subsoil at the loess (by 16%) and basalt sites (by 29%; Table 7.1).

Within each site, the fungal/bacterial C ratio did not significantly differ, with the exception of the rhizosphere soil at the basalt site, where the ratio was significantly higher as compared to the topsoil. The loess site tended to have the lowest fungal/bacterial C ratios (Table 7.1).

### *Mass of soil fractions*

The sand site (the sand fraction accounted for up to 865 $g\,kg^{-1}$ bulk soil) had very small contents of the silt and clay fractions (at maximum 126 and 102 $g\,kg^{-1}$, respectively). In contrast, at the loess and basalt sites, considerably larger amounts of the same fractions could be recovered (loess site silt: 694 $g\,kg^{-1}$ and clay: 265 $g\,kg^{-1}$, and basalt site silt: 598 $g\,kg^{-1}$ and clay: 387 $g\,kg^{-1}$, respectively; Fig. 7.1), which significantly differed between the sites. Within each site, however, the amount of the mineral fractions did not change across topsoil, subsoil, or rhizosphere soil, with the exception of the sand site, where the amount of the sand fraction was significantly higher in the subsoil.

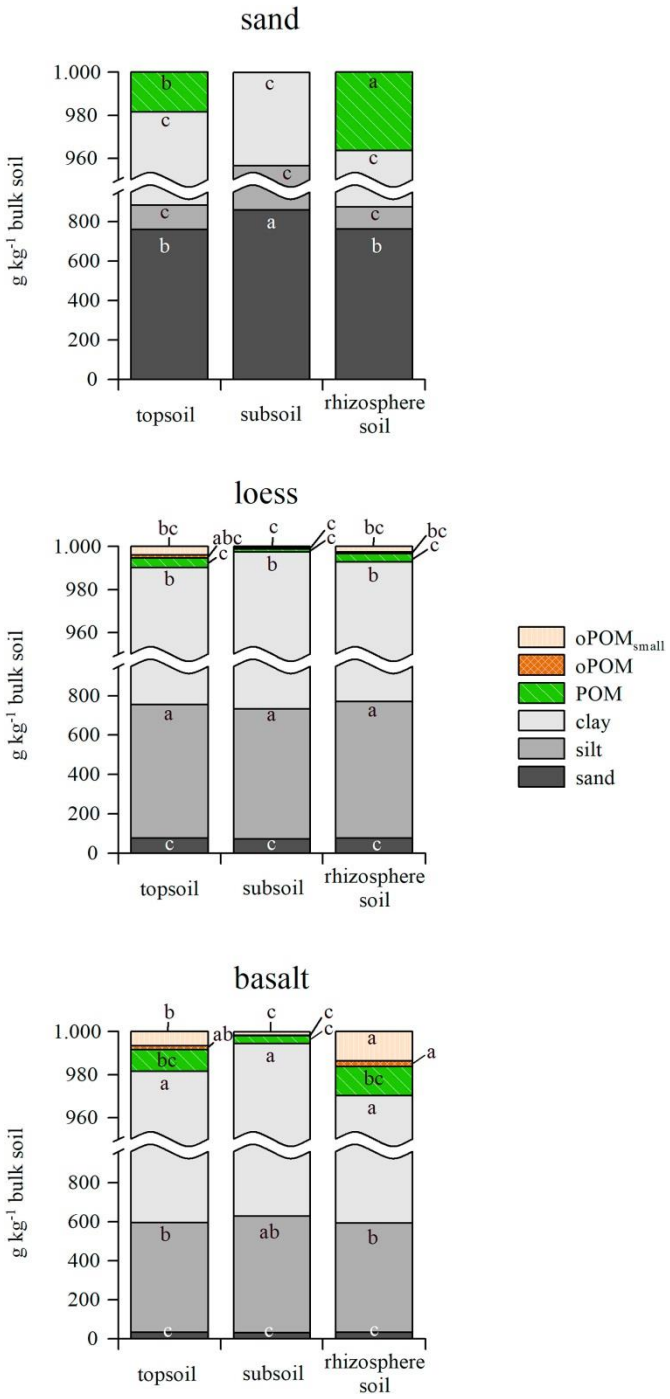


**FIGURE 7.1: Amount of fractions in g $kg^{-1}$ bulk soil at the sand, loess, and basalt sites. The various fractions (sand, silt, clay, POM, oPOM, oPOMsmall) are indicated by different colors. Significant differences of the respective fraction between the topsoil, subsoil, rhizosphere soil, and sites are indicated by different letters. (For interpretation of the references to color in this figure legend, the reader is referred to the Web version of this article.)**

The by far highest content of the POM fraction (36 g $kg^{-1}$; difference significant) was observed in the rhizosphere soil of the sand site, while it was lower in the rhizosphere soil of the loess and basalt sites (significant; Fig. 7.1). The POM fraction in the topsoil was highest at the sand and basalt sites (the latter showing a trend of lower values (by 45.6%) as compared to the sand site) and significantly lower at the loess site. At the loess and basalt sites, oPOM and oPOMsmall were recovered, while these fractions were below the detection limit at the sand site. Apart from the oPOMsmall fraction at the basalt site, the mass of these fractions did not significantly differ between topsoil and rhizosphere soil within each site, but was generally smaller in the subsoil (significant at the basalt site; trend for the loess site, 76% smaller for oPOM and 80% smaller for oPOMsmall). Though not statistically significant, the mass of the POM fraction was generally lower in the subsoil, while no POM could be detected in the subsoil of the sand site (Fig. 7.1).

***SOC stocks***

The bulk soil SOC stocks in the topsoil and rhizosphere soil were highest at the basalt site (up to 280 g C $m^{-2}$), followed by a tendency towards lower SOC stocks at the sand site (up to 218 g C $m^{-2}$, by on average 27% lower), and the lowest SOC stocks (significant) at the loess site (up to 101 g C $m^{-2}$; Fig. 7.2). The bulk soil SOC stocks in the subsoil did not significantly differ between the sites, but showed a clear decreasing tendency from the basalt (96 g C $m^{-2}$) to the loess (28 g C $m^{-2}$) and sand site (8 g C $m^{-2}$).

The bulk soil SOC stocks within each site were generally smallest in the subsoil (mostly significant) and similarly high in the topsoil and rhizosphere soil, with sometimes higher SOC stocks of bulk soil and particulate OM fractions in the rhizosphere soil of the sand and basalt sites (significant for oPOMsmall at the basalt site, trend for the bulk soil at the sand site; higher by 19%). Notably, the contribution of the POM fraction to bulk soil SOC stocks in the topsoil and rhizosphere soil at the sand site was similarly high (88 g C $m^{-2}$; topsoil) or even higher (133 g C m−2; rhizosphere soil) than that of the clay fraction (75 g C $m^{-2}$ in topsoil and 81 g C $m^{-2}$ in rhizosphere soil). In contrast, the clay fraction clearly featured the highest SOC stocks (up to 56 and 196 g C $m^{-2}$, respectively) at the loess and basalt sites (Fig. 7.2).

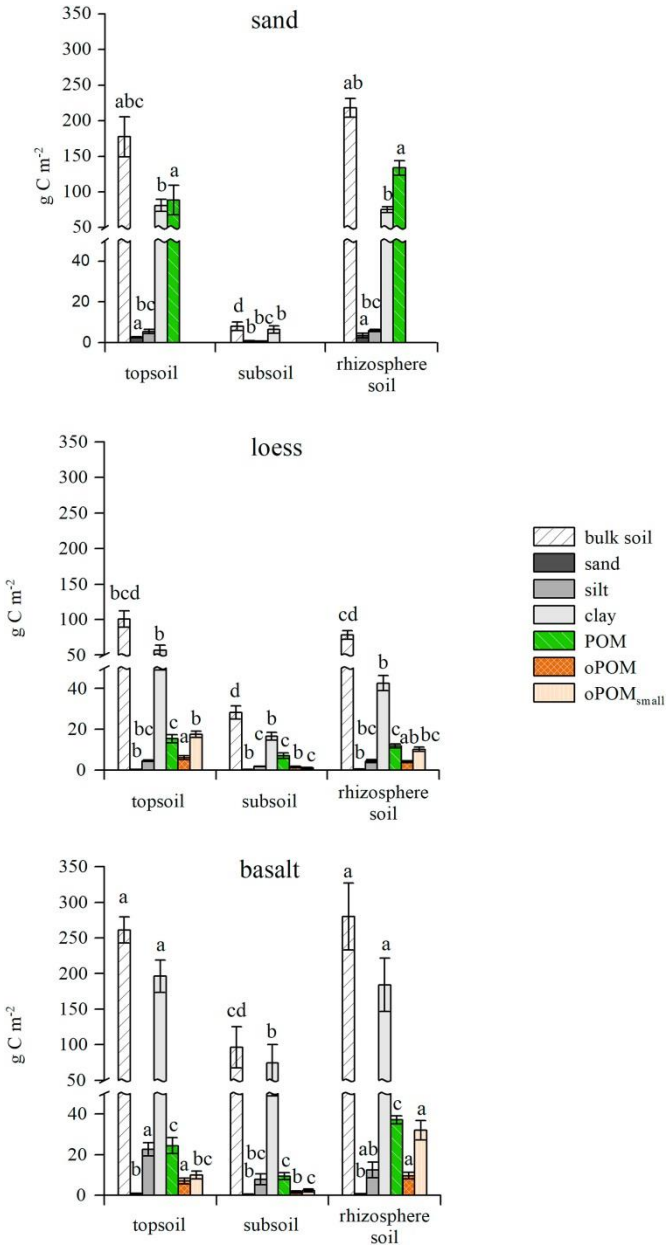


**FIGURE 7.2: Soil OC stocks (in g C $m^{-2}$ for a layer thickness of 1 cm) of bulk soil and fractions (sand, silt, clay, POM, oPOM, oPOMsmall) at the sand, loess, and basalt sites. The bulk soil and various fractions are indicated by different shadings and colors, respectively. Significant differences between the topsoil, subsoil, rhizosphere soil, and sites are indicated by different letters. (For interpretation of the references to color in this figure legend, the reader is referred to the Web version of this article.)**

The whole profile SOC stocks (calculated for the actual thickness of topsoil and subsoil horizons, respectively; cf. section 7.3) at the sand and basalt sites were significantly higher in the subsoil as compared to the respective topsoil, while this pattern was reversed at the loess site (Fig. 7.3). Among the sites, whole profile SOC stocks in the topsoil were lowest at the sand site (significant) but did not differ between the loess and basalt sites. Soil OC stocks in the subsoil were lowest at the loess site, intermediate at the sand site, and highest at the basalt site (differences significant; Fig. 7.3).

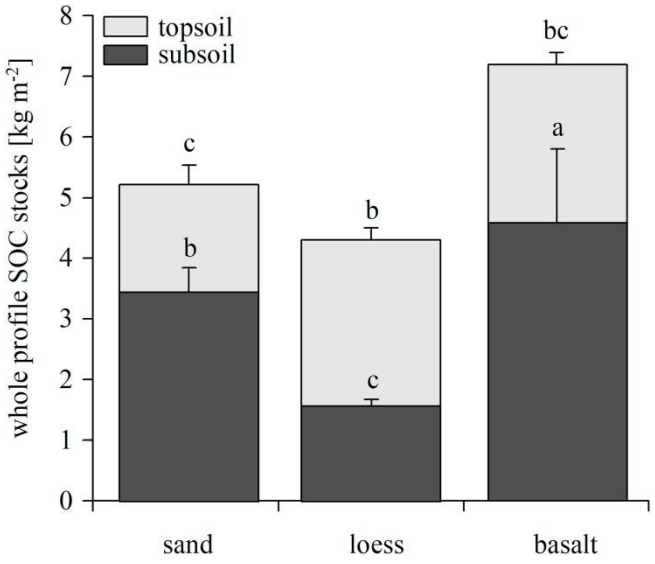


**FIGURE 7.3: Cumulative whole profile SOC stocks at the sand, loess, and basalt sites separated into topsoil and subsoil stocks. Significant differences between site, topsoil, and subsoil are indicated by different letters.**

### *$^{14}$C content of the clay fraction*

The $^{14}$C contents of the clay fractions were similar across the investigated sites: they ranged from 0.95 to 1.01 F$^{14}$C (modern) in the topsoil and rhizosphere soil and strongly decreased with depth (significantly; Table 7.1). This decrease was steepest at the sand and loess sites and lowest at the basalt site.

### *Chemical composition of fractions as inferred from NMR spectra*

The samples were dominated by alkyl C and/or O/N-alkyl C, while aryl and carboxyl C mostly contributed minor relative amounts to the spectra. The alkyl/O/N-alkyl C ratio of the topsoil clay

fractions were around 1.0 independent of investigated study site, while ratios were generally lower in the rhizosphere soil (0.6–0.8) and in the subsoil (0.7). The degree of decomposition of the particulate OM fractions mostly increased from the POM to the oPOM and oPOMsmall fractions (based on alkyl/O/N alkyl C ratios; Fig. 7.4).

Apart from these similarities, there were some notable differences between the study sites: the degree of decomposition for the POM fraction (in topsoil and rhizosphere soil) increased in the order loess < basalt < sand, while the advanced decomposition of the POM fraction from the latter site was only approximated by the oPOMsmall fractions from the loess site (Fig. 7.4). While the oPOM fractions from the loess and basalt site had similar alkyl C/O/N-alkyl C ratios (0.5–0.7 in subsoil and ~1 in topsoil and rhizosphere soil), the oPOMsmall was, apart from the subsoil, essentially less decomposed at the basalt as compared to the loess site.

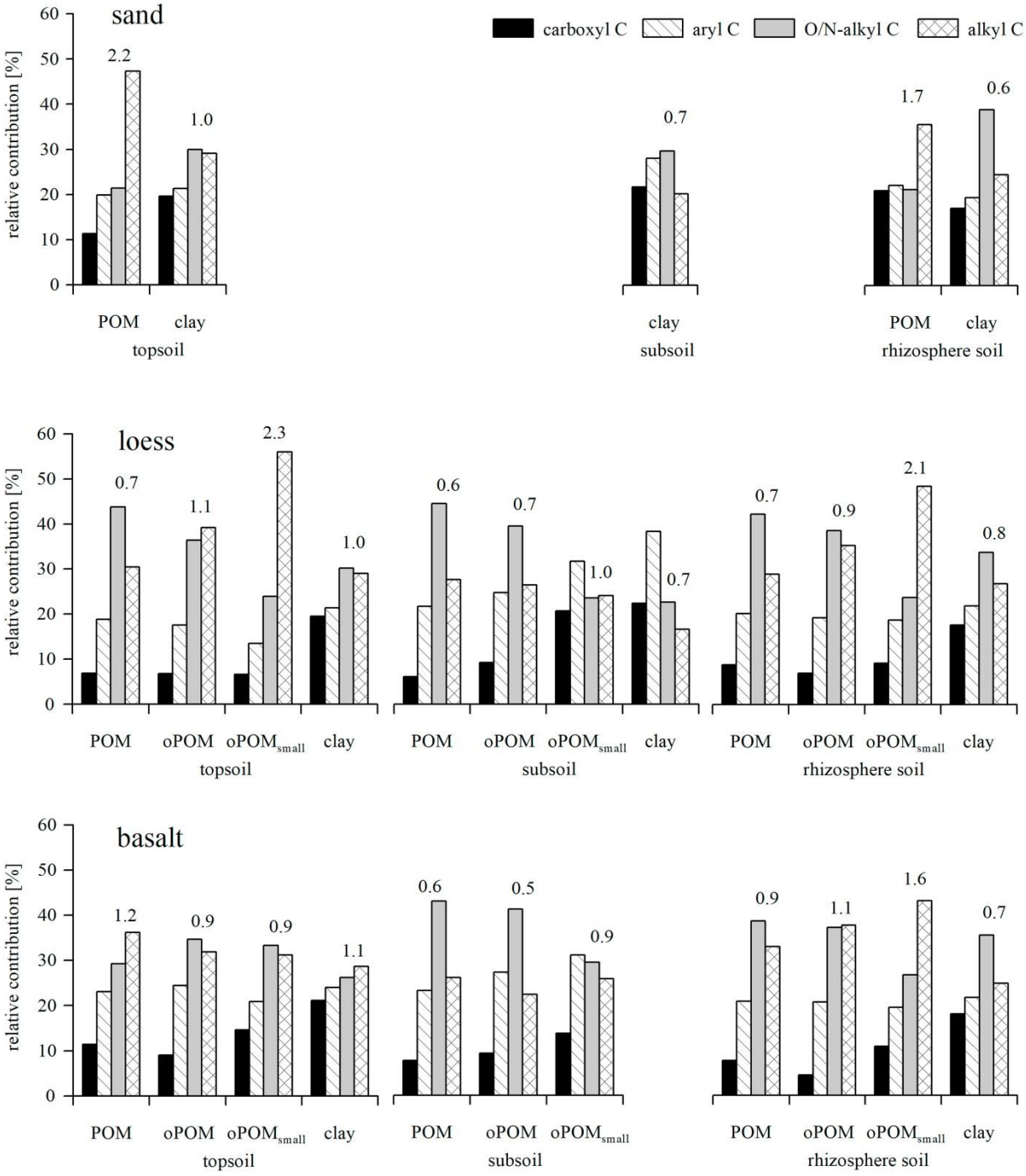


**FIGURE 7.4: Chemical composition as inferred from NMR spectra (relative intensity of carboxyl, aryl, O/N-alkyl, alkyl C; indicated by different shadings) of the clay, POM, oPOM, and oPOMsmall fractions in the topsoil, subsoil, and rhizosphere soil at the different study sites. The alkyl/O/N-alkyl C ratio is depicted by numbers above the bars. Note that the POM fraction could not be detected in the subsoil at the sand site. The signal intensity of the clay fraction in the subsoil at the basalt site was too low for obtaining a reasonable spectrum, probably due to the presence of paramagnetic materials.**

## *Multiple regression*

The root mass, amount of the clay and POM fractions, and amino sugars (per g DW) were included in the best model (Supplementary Table S7.1) and explained 90.1% of the variability in bulk soil SOC stocks independent of soil depth or investigated study site ($p < 0.001$; Fig. 7.5). Partial correlations of the variables, expressed as β coefficients, were 0.36 for the clay fraction, 0.18 for the root mass, 0.46 for the POM fraction, and 0.35 for the amino sugars. The oPOMsmall fraction had to be removed from the regression, due to strong collinearity with the clay fraction. Models including oPOMsmall instead of clay showed higher AIC values and explained less variability in SOC stocks. The amount of the oPOM fraction was not significantly related to the SOC stocks.

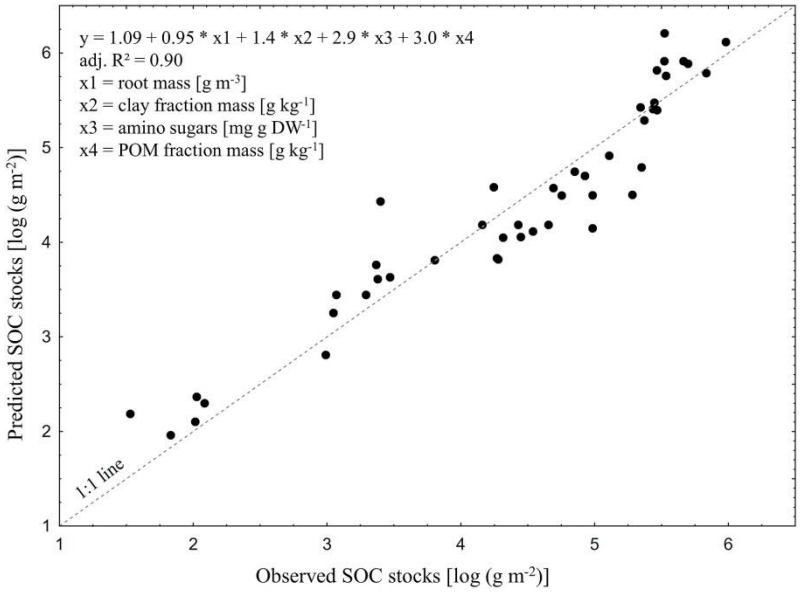


**FIGURE 7.5: Observed vs. predicted SOC stocks using the regression equation and predictors (root mass, mass of the clay and POM fraction, amino sugars) displayed in the upper left corner of the graph (note that predictors were log-transformed prior to analysis). The used predictors were significantly correlated with SOC stocks and appeared in the best model selected via AIC (see also Supplementary Table S7.1).**

## 7.5 Discussion

The distance to the individual beech trees did not have any detectable influence on the parameters investigated in the present study, which contradicts the findings of several previous studies that found chemical and microbial soil properties to vary with increasing or decreasing distance to individual trees (e.g., Chang and Matzner 2000; Saetre and Bååth 2000). However, the cited studies either sampled different parameters (e.g., phospholipid fatty acids) or chose a higher distance to the stem base (2 m). At the chosen scale, a horizontally relatively even distribution of fine roots (unpublished data) and probably also leaf litter across the whole horizontal extent of the soil profiles were likely responsible for the observed patterns. This leads to a vertical rather than a horizontal differentiation of soil properties, being in line with the results of others (Angst et al. 2016b; Schöning et al. 2006). We thus focused our discussion on these vertical differences (between topsoil and subsoil) and on the relevance of rhizosphere soil (cf. section 7.4) as influenced by the different parent materials.

### *Topsoil SOC stocks and the imprint of the rhizosphere*

The bulk topsoil SOC stocks substantially differed among the study sites (Fig. 7.2), where the basalt site had high ($261 \pm 18\ g\ m^{-2}$), the sand site intermediate ($177 \pm 28\ g\ m^{-2}$), and the loess site low SOC stocks ($100 \pm 11\ g\ m^{-2}$) at the 10 cm sampling depth (cf. section 7.4). These large variations may partly be ascribed to varying amounts of soil fractions at the individual study sites, determining the relevance of distinct SOM stabilization mechanisms, such as organo-mineral association and aggregation (Marschner et al. 2008; Schmidt et al. 2011; von Lützow et al. 2006). For example, high contents of the clay fraction at the basalt site (Fig. 7.1), in conjunction with the presence of expandable clay minerals (section 7.3), result in available surfaces for OM to be adsorbed. Thus, organo-mineral association was likely the dominant SOM stabilization mechanisms at the basalt site, considering the large contributions of the clay fraction to the bulk SOC stocks (Fig. 7.2). However, clay also positively affects aggregate formation and stability (Attou et al. 1998; Tisdall and Oades 1982), probably resulting in a higher degree of aggregation at the more ‘clay-rich’ basalt as compared to the loess site, where a lower degree of aggregation may have favored decomposition (higher alkyl/O/N-alkyl C ratios; Fig. 7.4) and led to smaller amounts of the oPOM and oPOMsmall fractions (Fig. 7.1; Mueller et al. 2009; Virto et

al. 2008). Aggregation can also enhance the stability of SOM contained within organo-mineral associations (Mueller et al. 2012; Angst et al. 2017) so that increased amounts of the clay fraction may have a twofold positive effect on bulk SOC stocks. In contrast, due to high sand and low clay contents, aggregation was likely of minor importance at the sand site (oPOM and oPOMsmall could not be detected) and due to the limited capacity for mineral SOM protection, inherent recalcitrance may have played a relatively greater role at this site (Angst et al. 2017).

Consequently, the specific proportions of soil fractions played a central role in shaping SOC stocks among the sites by having direct effects on the capacity of the soils to protect SOM via the formation of organo-mineral associations and aggregates. This capacity is at least to some extent dependent on the mineralogical characteristics of the parent material (Kölbl and Kögel-Knabner 2004; Torn et al. 2009; Wagai et al. 2008), which determines weathering and thus textural composition of the respective soil (Jenny 1994).

Also specific surface area or cation exchange capacity of (particularly) the clay fraction are determined by parent material mineralogy (Egli et al. 2004; Harrison et al. 1990) with potential consequences for SOM stabilization (Fernández-Ugalde et al. 2016; Wattel-Koekkoek et al. 2001). However, because the link between different clay mineralogy and SOM stabilization has not unequivocally been established (Barré et al. 2014) and, more importantly, clay mineralogy was similar among the investigated sites (dominated by illite, kaolinite, and chlorites), we regard qualitative effects on SOC stocks at the given pH values as minor in the present study (see also Rasmussen et al. 2018). This, however, may not exclude a potential clay type effect on SOM stabilization and SOC stocks at sites with more diverging clay mineralogy.

Apart from soil texture and clay mineralogy, parent material affects the soil's nutrient composition (Anderson 1988; Torn et al. 2009), which, in turn, may alter the extent of root exudation and the rooting system: At rather nutrient poor sites, such as the sand site (cf. Leuschner et al. 2006), trees may have increased root exudation, network density of their fine roots, and fine root mortality (Bertin et al. 2003; Leuschner et al. 2004; Vogt et al. 1987). These nutrient induced changes in rhizosphere traits may have been mirrored by wide ratios of root necromass to root biomass (~2.6 as compared to 1–2), indicating a higher fine root mortality, higher total root mass (3.1 g $cm^{-3}$ as compared to 1.1 g $cm^{-3}$ (loess) and 2.1 g $cm^{-3}$ (basalt); Table 7.1), amount of the POM fraction, and bulk soil SOC stocks at the sand site (Fig. 7.1, Fig. 7.2).

Particularly at the sand site, the rhizosphere soil thus seemed to be a hotspot for the input of OM (Angst et al. 2016b). Although the root mass was lower at the loess and basalt sites, likely due to a higher amount of nutrients present (Leuschner et al. 2004), our data suggest rhizosphere effects on SOC stocks and chemical composition of SOM also at the other sites investigated. The rhizosphere soil and topsoil were very similar with respect to the mass of fractions and SOC stocks, with a trend of or sometimes significantly higher values in the rhizosphere soil (Fig. 7.1, Fig. 7.2), pointing toward SOM in the topsoil being mainly derived from roots. This statement is supported by several indications: First, a moderate/low degree of bioturbation, and thus mixing of leaf litter with mineral soil, at all sites was evidenced by the mor/moder type forest floor present at the respective site (cf. section 7.3; Frouz 2017). Rhizodeposits/root litter inputs, which are already in direct contact with the mineral soil, as compared to leaf litter inputs may thus dominate (Mora et al. 2014). Second, an often substantially lower degree of degradation (as evidenced by alkyl C/O/N-alkyl C ratios; Fig. 7.4) and higher amounts of the rhizosphere soil POM (and oPOM) fractions as compared to the corresponding topsoil fractions (trend for the basalt site, significant for the Tertiary sand site; Fig. 7.1), indicate the input of fresh OM to the rhizosphere soil. Third, the higher contribution of generally easily decomposable polysaccharides (O/N-alkyl C) to the rhizosphere clay fractions as compared to the topsoil clay fractions (Fig. 7.4; cf. Angst et al. 2016b) probably derive from root exudates.

Combined, these results foster the importance of root-derived SOM for SOC contents and stocks and highlight their relevance not only in deeper soil layers (as found by e.g., Angst et al. 2016a; Nierop 1998; Rasse et al. 2005) but also in topsoil (similar to the results by Tefs and Gleixner 2012).

Beyond the input of fresh OM, our results indicate the importance of the rhizosphere for SOM stabilization and contribution of microbial compounds. Higher amounts of amino sugars in the rhizosphere soil of the sand and basalt sites (per g C, tendency; Table 7.1), which may partly contribute to the higher O/N-alkyl C values in the corresponding clay fractions (Cao et al. 2011), hint to a higher microbial (particularly fungal) abundance (increased fungal/bacterial ratios in the rhizosphere Table 7.1; Blagodatskaya and Kuzyakov 2013; Cheng and Coleman 1990), and/or to better preservation of amino sugars, perhaps due to an enhanced degree of aggregation. At the basalt site, an enhanced aggregation may be inferred from higher amounts of oPOM (by 28%; trend) and oPOMsmall (by 52%; significant) as compared to the corresponding topsoil (Fig. 7.1).

By an intensified stabilization of SOM in the rhizosphere soil, positive priming or exudation effects may be partly counteracted (Keiluweit et al. 2015; Kuzyakov et al. 2007; Mooshammer et al. 2014). Because parent material dependent nutrient composition likely affected the extent and characteristics of the rhizosphere, microbial abundance (and community composition) may in turn also depend on different parent materials.

It may be worth noting that the similar characteristics of topsoil and rhizosphere soil in the present study may at least partly be due to our sampling approach because we took our 'non-rhizosphere' samples with cylinders (cf. section 7.3) and could thus, particularly in the densely-rooted upper soil layers, not completely exclude a contribution of rhizosphere soil to these samples. The topsoil samples may thus be biased towards rhizosphere soil, so that these samples may even more differ with respect to SOC stocks, presence of fresh OM, and microbial-derived compounds than indicated by the present data.

In summary, SOC stocks and SOM chemical composition in the topsoil of the investigated beech stands seem to be a function of parent material effects on SOM stabilization mechanisms and on tree OM inputs mainly in the rhizosphere (root exudates and root-derived POM; see also Heinze et al. 2018).

***Subsoil SOC stocks mirror the substrate***

Most of the investigated parameters were significantly lower in the subsoil as compared to the corresponding topsoil: We observed a general decrease of the particulate OM fractions (POM, oPOM, and oPOMsmall), root mass, amino sugars per g DW, $F^{14}C$ (Fig. 7.1; Table 7.1), and decreasing SOC stocks (normalized to 1 cm layer thickness) with soil depth (mostly significant; Fig. 7.2) as previously observed by others (Angst et al. 2016a, 2016b; John et al. 2005; Rethemeyer et al. 2005; Rumpel et al. 2004; Schöning and Kögel-Knabner 2006). Although these patterns were consistent among the study sites, the decrease in SOC stocks from the topsoil to the subsoil was most pronounced at the sand site (Fig. 7.2): the bulk subsoil contained 4.5% of the bulk topsoil SOC stocks, while the bulk subsoil at the loess and basalt sites still contained 28.1 and 36.8% of the bulk topsoil SOC stocks. Considering the large volume of the subsoil, small changes in these SOC stocks (even at the sand site), calculated for a layer thickness of 1 cm, hold

the potential to substantially influence whole soil SOC stocks when extrapolated to the entire subsoil (cf. Angst et al. 2016b; Richter and Billings 2015).

Similar to the investigated topsoil but more pronounced, these site differences in SOC stocks seemed to be strongly affected by the amount of fractions, especially by that of the clay fraction (involved in physico-chemical protection of SOM; cf. chapter 7.5), accounting for 80% (sand), 59% (loess), and 78% (basalt) of the bulk subsoil SOC stocks, respectively (Fig. 7.2; see also Angst et al. 2016b; Rumpel et al. 2012). The mass of this fraction highly varied across the study sites (Fig. 7.1), reflecting the imprint of the respective parent material and explaining a large part of the variation in subsoil SOC stocks. Under similar vegetation and climate, subsoils with a higher amount of the clay fraction can thus be expected to feature higher SOC stocks than those with a higher contribution of larger SOM fractions (>6.3 μm).

However, differences in OM inputs likely also played a role for subsoil SOC stocks. Comparably low alkyl/O/N-alkyl C ratios of the POM fraction (not detected at the sand site; Fig. 7.1, Fig. 7.4) in the subsoil at the loess and basalt sites point to the presence of relatively fresh SOM. Further, despite the fact that $F^{14}C$ of the clay fraction in all investigated subsoils was very low, the site with the highest SOC stocks (basalt site) had the highest $F^{14}C$ and the site with the lowest SOC stocks in the subsoil (sand site) had the lowest $F^{14}C$ in the clay fraction. The basalt and loess sites probably receive more input of 'fresh' OM than the sand site, 'diluting' old (perhaps geogenic) SOM and additionally consolidating SOC stocks.

The major forms by which OM may reach deeper soil layers at the study sites are as dissolved (and partly particular) OM with percolating water (Cepáková et al. 2016; Kalbitz 2001; Ohta et al. 1986) or as in situ inputs by rhizodeposition (Rumpel and Kögel-Knabner 2011). Although we did not perform dissolved OM (DOM) measurements, the differences in $F^{14}C$ and subsoil SOC stocks among the sites may partly derive from the fact that DOM reaching the subsoil may be better retained in the fine textured subsoil at the basalt and loess sites than in the coarse textured subsoil at the sand site. A potential positive effect on SOC stocks via increased amounts of DOM reaching the subsoil at the sand site (due to a high permeability of the soil), may thus be offset by the lack of a sufficient amount of binding surfaces (with the clay fraction) (Kaiser et al. 1996; Kramer et al. 2012), perhaps resulting in leaching of DOM to even greater soil depths.

However, the contribution of DOM to SOC stocks in forest subsoils likely only accounts for a small portion (5–20% down to 1 m depth; Sanderman and Amundson 2008; Sheng et al. 2015) and several clues point to the relevance of in situ inputs by roots. First, the root mass at the basalt and loess sites, where bulk soil SOC stocks were higher by 92% and 72% than those at the sand site, tended to be higher by 83% (at both sites) as compared to the sand site (Table 7.1). Higher nutrient availability in deeper soil layers may attract fine root growth and extension of the fine root system to the subsoil, while the subsoil at nutrient-poor sites, such as the sand site, is exploited mainly by few pioneer roots and the bulk effort into root growth is invested in the upper part of the profile, where nutrients may be partly replenished by mineralization of SOM or where root exudation may enable microbes to mine for less bio-available SOM (Table 7.1; Tückmantel et al. 2017). Second, a higher root mass may stimulate aggregation, particularly in fine textured soils (e.g. Six et al. 2004), which might explain the presence of oPOM and oPOMsmall at the basalt and loess sites but its absence at the sand site (Fig. 7.1). A third indicator for the relevance of the rhizosphere is the high amount of O/N-alkyl C in the subsoil as compared to the topsoil fractions (Fig. 7.4). This may derive from root-exudates but also from microbial-derived compounds rich in N (Schöning et al. 2005). The contribution of the latter is fostered by a similar or even higher content of amino sugars (per g C) in the subsoil as compared to the topsoil (Table 7.1; see also Preusser et al. 2017). The contribution of microbial-derived compounds to SOM, and stabilized SOM in particular, has been highlighted recently (Castellano et al. 2015; Cotrufo et al. 2013; Rumpel et al. 2010) and our results indicate that their relative amount in SOM may even increase with soil depth. Because roots may foster microbial abundance (Blagodatskaya and Kuzyakov 2013), a combined contribution of root- and microbial-derived compounds to subsoil SOC stocks seems plausible.

Based on these considerations, subsoil SOC stocks were highly influenced by OM input and its retention by the soil mineral matrix, where we clearly emphasize the relevance of parent material traits, such as the amount of the clay fraction and nutrients, which at least partly control OM input and SOM stabilization, and thus to some extent also the contribution of microbial-derived compounds.

While differences among the investigated subsoils may partly be influenced by the fact that different soil horizons were sampled, the measured SOC stocks clearly point to the validity of the described patterns (as based on the sampled depth layers) independent from the designation of

soil horizons. However, a normalization of SOC stocks to a layer thickness of 1 cm (as discussed above) appears optimal for gaining a mechanistic understanding of how different factors influence SOC stocks, but we emphasize the need for the involvement of the whole soil volume when making statements on SOC storage with respect to the whole soil profile. This becomes particularly important when dealing with subsoils. For instance, OM input and amount of the fine fractions were low at the sand site. Nevertheless, the whole subsoil SOC stocks were twice as high as compared to those of the respective topsoil, due to the high subsoil volume (Fig. 7.3). In contrast, the subsoil volume at the loess site was comparably low (the topsoil was ~60 cm thick), resulting in higher whole topsoil as compared to subsoil SOC stocks. Thus, soil volume, maybe most importantly that of the subsoil, remains a decisive factor for the accuracy of C inventories.

***Factors site-independently driving SOC storage***

The results of the best subset regression we performed across all sites and samples taken in the present study indicate the existence of factors site-independently controlling SOC stocks at the stand scale. Changes in these factors (e.g., varying amounts of the clay fraction as a result of differing parent material) involve changes in SOC stocks: the predictors root mass, mass of the clay and POM fractions, and amino sugars per g DW explained more than 90% of the variability in SOC stocks (Fig. 7.5). Although we cannot exclude the existence of other reasonable predictors that were possibly not analyzed in the present study, the inclusion of root mass and microbial-derived compounds in addition to SOM fractions in C models may highly improve the prediction of SOC stocks (see also Dwivedi et al. 2017). While based on relatively few data points, the high amount of variability explained by only a few predictors at high significance ($p < 0.001$) points to a transferability of the relationships between SOC stocks and predictor variables to similar sites, such as to other broadleaf forest stands in temperate regions, and perhaps also to other parent materials and climatic zones (e.g., Paz et al. 2016). This statement may particularly be true for acidic forest soils, where bioturbation is limited and rhizodeposits/root-derived POM may be the most important sources of OM inputs to the soil and, in particular, to the subsoil (Angst et al. 2016b; Rasse et al. 2005). As elaborated in the previous sections, all the factors included in the best regression model were directly or indirectly

influenced by the respective parent material. We thus emphasize the necessity to consider parent material when estimating and predicting SOC stocks.

## 7.6 Conclusions

The parent material, predefining soil textural and nutrient composition, determined the capacity of the investigated soils to stabilize SOM via organo-mineral association and aggregation and governed OM inputs to the soil. These parent material effects were particularly perceivable in the subsoil, where sites with larger amounts of the clay fraction (decisive for SOM sequestration) and presumed higher nutrient contents (attracting root growth) had higher SOC stocks. While in situ root inputs in the form of rhizodeposits, including exudates and root-derived POM, were likely the prime source of plant-derived SOC in the subsoil at these sites, root-derived SOM also contributed in large part to topsoil SOC stocks. Associated with these root inputs were microbial-derived compounds, whose abundance (amino sugars per g C) increased in rhizosphere soil and with increasing soil depth.

When site-independently investigating combined effects of the above highlighted parameters, 90% of variability in SOC stocks were accounted for by the root mass, the amount of amino sugars and the clay and POM fractions, indicating a key role of these four measures in controlling SOC stocks. Because parent material directly or indirectly influenced these parameters, we demonstrate the necessity to consider differences in parent material when estimating and predicting SOC stocks.

***Acknowledgements***

This work was realized within the research unit "FOR1806: The Forgotten Part of Carbon Cycling: Organic Matter Storage and Turnover in Subsoils" funded by the Deutsche Forschungsgemeinschaft (DFG), grant No.: MU3021-4/1 and MU3021-4/2 and with the support of the SoWa Research Infrastructure funded by MEYS CZ grant No.: LM2015075 and EF16_013/0001782 – SoWa Ecosystems Research. We would like to thank Bärbel Angres and Pia Kuran for help in the laboratory, Dr. Peter Schad for help with soil classification, and two anonymous reviewers whose comments helped to improve the manuscript.

## Supplementary Material

**Table S7.1: Summary of the best subset regression with bulk soil SOC stocks as dependent variable. Predictors were amino sugars (per g DW), the mass of the clay, POM, and oPOM fractions, and the root mass. Measures shown are whole model $R^2$, AIC, number of predictors included in the respective model, and standardized beta coefficients for each predictor and model.**

| $R^2$ | AIC | # of included predictors | partial correlations of predictor variables (stand. β) | | | | |
|---|---|---|---|---|---|---|---|
| | | | amino sugars | clay | root mass | POM | oPOM |
| 0.9 | 72 | 4 | 0.35 | 0.36 | 0.18 | 0.46 | |
| 0.87 | 81.6 | 3 | 0.39 | 0.37 | | 0.5 | |
| 0.85 | 80.8 | 3 | | 0.53 | 0.21 | 0.67 | |
| 0.81 | 89.5 | 2 | | 0.56 | | 0.73 | |

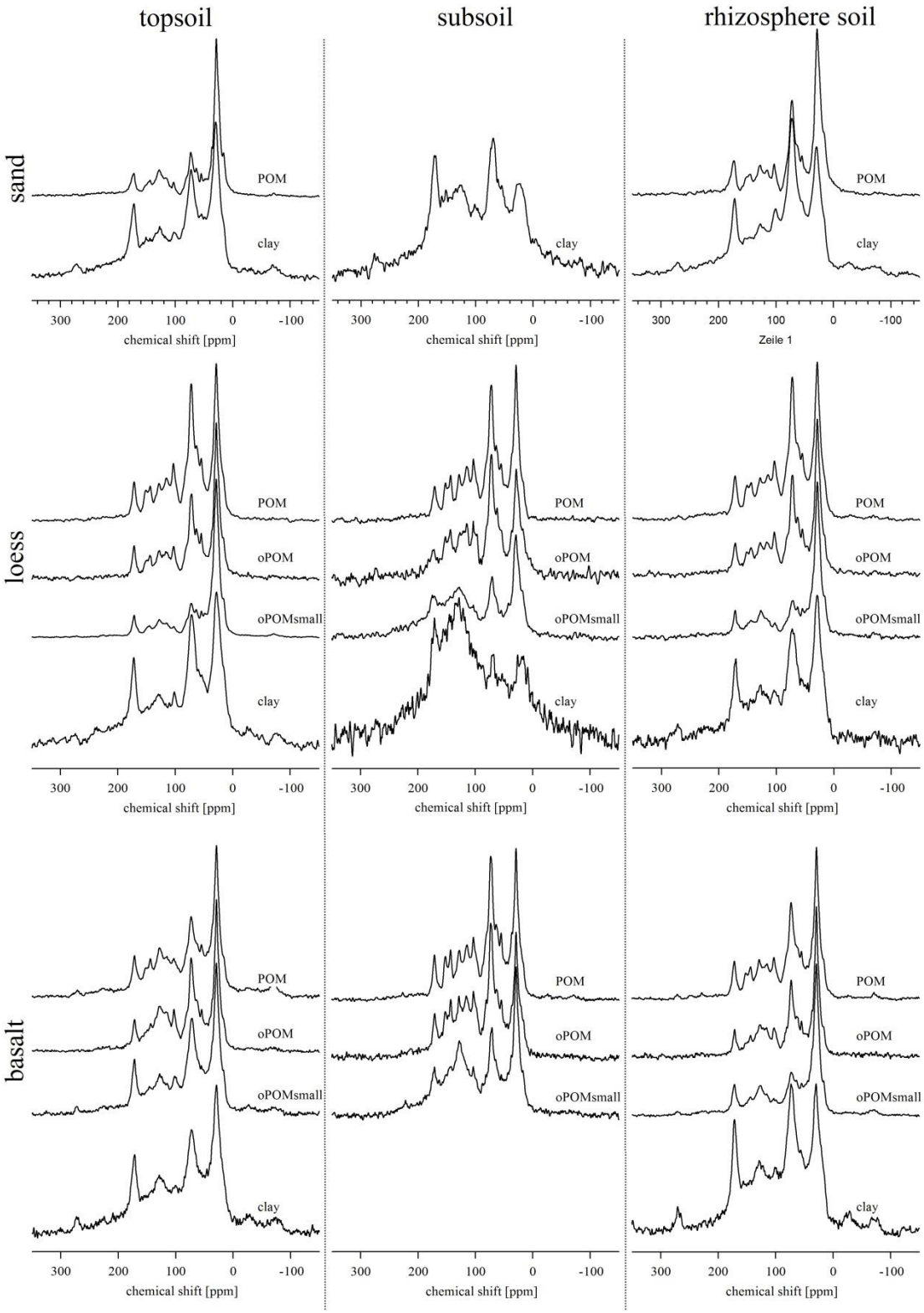


**FIGURE S7.1: Average $^{13}$C NMR spectra for the POM, oPOM, oPOMsmall, and clay fractions at the different study sites.**

## 7.7 References

Anderson, D.W. (1988) The effect of parent material and soil development on nutrient cycling in temperate ecosystems. Biogeochemistry 5: 71–97.

Angst, G., John, S., Mueller, C.W., Kögel-Knabner, I., and Rethemeyer, J. (2016a) Tracing the sources and spatial distribution of organic carbon in subsoils using a multi-biomarker approach. Scientific Reports 6. http://dx.doi.org/10.1038/srep29478.

Angst, G., Kögel-Knabner, I., Kirfel, K., Hertel, D., and Mueller, C.W. (2016b) Spatial distribution and chemical composition of soil organic matter fractions in rhizosphere and non-rhizosphere soil under European beech (*Fagus sylvatica* L.). Geoderma 264: 179–187. http://dx.doi.org/10.1016/j.geoderma.2015.10.016.

Angst, G., Mueller, K.E., Kögel-Knabner, I., Freeman, K.H., and Mueller, C.W. (2017) Aggregation controls the stability of lignin and lipids in clay-sized particulate and mineral associated organic matter. Biogeochemistry 132: 307–324. http://dx.doi.org/10.1007/s10533-017-0304-2.

Appuhn, A., and Joergensen, R.G. (2006) Microbial colonisation of roots as a function of plant species. Soil Biology and Biochemistry 38: 1040–1051. http://dx.doi.org/10.1016/j.soilbio.2005.09.002.

Attou, F., Bruand, A., and Le Bissonnais, Y. (1998) Effect of clay content and silt-clay fabric on stability of artificial aggregates. European Journal of Soil Science 49: 569–577. http://dx.doi.org/10.1046/j.1365-2389.1998.4940569.x.

Baldock, J.A., Oades, J.M., Nelson, P.N., Skene, T.M., Golchin, A., and Clarke, P. (1997) Assessing the extent of decomposition of natural organic materials using solid-state $^{13}C$ NMR spectroscopy. Soil Research 35: 1061–1084. http://dx.doi.org/10.1071/S97004.

Baritz, R., Seufert, G., Montanarella, L., and Van Ranst, E. (2010) Carbon concentrations and stocks in forest soils of Europe. Forest Ecology and Management 260: 262–277. http://dx.doi.org/10.1016/j.foreco.2010.03.025.

Barré, P., Durand, H., Chenu, C., Meunier, P., Montagne, D., Castel, G., Billiou, D., Soucémarianadin, L., and Cécillon, L. (2017) Geological control of soil organic carbon and

nitrogen stocks at the landscape scale. Geoderma 285: 50–56. http://dx.doi.org/10.1016/j.geoderma.2016.09.029.

Barré, P., Fernandez-Ugalde, O., Virto, I., Velde, B., and Chenu, C. (2014) Impact of phyllosilicate mineralogy on organic carbon stabilization in soils: incomplete knowledge and exciting prospects. Geoderma 235–236: 382–395. http://dx.doi.org/10.1016/j.geoderma.2014.07.029.

Bauhus, J., and Bartsch, N. (1996) Fine-root growth in beech (*Fagus sylvatica*) forest gaps. Canadian Journal of Forest Research 26: 2153–2159. http://dx.doi.org/10.1139/x26-244.

Bertin, C., Yang, X., and Weston, L.A. (2003) The role of root exudates and allelochemicals in the rhizosphere. Plant and Soil 256: 67–83.

Blagodatskaya, E., and Kuzyakov, Y. (2013) Active microorganisms in soil: critical review of estimation criteria and approaches. Soil Biology and Biochemistry 67: 192–211. http://dx.doi.org/10.1016/j.soilbio.2013.08.024.

Cao, Y., Wei, X., Cai, P., Huang, Q., Rong, X., and Liang, W. (2011) Preferential adsorption of extracellular polymeric substances from bacteria on clay minerals and iron oxide. Colloids and Surfaces B: Biointerfaces 83: 122–127. http://dx.doi.org/10.1016/j.colsurfb.2010.11.018.

Castellano, M.J., Mueller, K.E., Olk, D.C., Sawyer, J.E., and Six, J. (2015) Integrating plant litter quality, soil organic matter stabilization, and the carbon saturation concept. Global Change Biology 21: 3200–3209. http://dx.doi.org/10.1111/gcb.12982.

Catt, J.A. (2001) The agricultural importance of loess. Earth-Science Reviews 54: 213–229. http://dx.doi.org/10.1016/S0012-8252(01)00049-6.

Cepáková, Š., and Frouz, J. (2015) Changes in chemical composition of litter during decomposition: a review of published $^{13}C$ NMR spectra. Journal of Soil Science and Plant Nutrition 15: 805–815. http://dx.doi.org/10.4067/S0718-95162015005000055.

Cepáková, Š., Tošner, Z., and Frouz, J. (2016) The effect of tree species on seasonal fluctuations in water-soluble and hot water-extractable organic matter at post-mining sites. Geoderma 275: 19–27. http://dx.doi.org/10.1016/j.geoderma.2016.04.006.

Chabbi, A., Kögel-Knabner, I., and Rumpel, C. (2009) Stabilised carbon in subsoil horizons is located in spatially distinct parts of the soil profile. Soil Biology and Biochemistry 41: 256–261. http://dx.doi.org/10.1016/j.soilbio.2008.10.033.

Chang, S.-C., and Matzner, E. (2000) Soil nitrogen turnover in proximal and distal stem areas of European beech trees. Plant and Soil 218: 117–125. http://dx.doi.org/10.1023/A:1014931625707.

Cheng, W., and Coleman, D. (1990) Effect of living roots on soil organic matter decomposition. Soil Biology and Biochemistry 22: 781–787.

Cieslinski, G., Van Rees, K.C.J., Szmigielska, A.M., Krishnamurti, G.S.R., and Huang, P.M. (1998) Low-molecular-weight organic acids in rhizosphere soils of durum wheat and their effect on cadmium bioaccumulation. Plant and Soil 203: 109–117. http://dx.doi.org/10.1023/a:1004325817420.

Cotrufo, M.F., Wallenstein, M.D., Boot, C.M., Denef, K., and Paul, E. (2013) The Microbial Efficiency-Matrix Stabilization (MEMS) framework integrates plant litter decomposition with soil organic matter stabilization: do labile plant inputs form stable soil organic matter? Global Change Biology 19: 988–995. http://dx.doi.org/10.1111/gcb.12113.

Crow, S.E., Lajtha, K., Filley, T.R., Swanston, C.W., Bowden, R.D., and Caldwell, B.A. (2009) Sources of plant-derived carbon and stability of organic matter in soil: implications for global change. Global Change Biology 15: 2003–2019. http://dx.doi.org/10.1111/j.1365-2486.2009.01850.x.

Dewald, A., Heinze, S., Jolie, J., Zilges, A., Dunai, T., Rethemeyer, J., Melles, M., Staubwasser, M., Kuczewski, B., Richter, J., Radtke, U., von Blanckenburg, F., and Klein, M. (2013) CologneAMS, a dedicated center for accelerator mass spectrometry in Germany. Nuclear Instruments and Methods in Physics Research Section B: Beam Interactions with Materials and Atoms 294: 18–23. http://dx.doi.org/10.1016/j. nimb.2012.04.030.

Dwivedi, D., Riley, W.J., Torn, M.S., Spycher, N., Maggi, F., and Tang, J.Y. (2017) Mineral properties, microbes, transport, and plant-input profiles control vertical distribution and age of soil carbon stocks. Soil Biology and Biochemistry 107: 244–259. http://dx.doi.org/10.1016/j.soilbio.2016.12.019.

Egli, M., Mirabella, A., Mancabelli, A., and Sartori, G. (2004) Weathering of soils in Alpine areas as influenced by climate and parent material. Clays and Clay Minerals 52: 287–303. http://dx.doi.org/10.1346/CCMN.2004.0520304.

Engelking, B., Flessa, H., and Joergensen, R.G. (2007) Shifts in amino sugar and ergosterol contents after addition of sucrose and cellulose to soil. Soil Biology and Biochemistry 39: 2111–2118. http://dx.doi.org/10.1016/j.soilbio.2007.03.020.

Fernández-Ugalde, O., Barré, P., Virto, I., Hubert, F., Billiou, D., and Chenu, C. (2016) Does phyllosilicate mineralogy explain organic matter stabilization in different particlesize fractions in a 19-year C3/C4 chronosequence in a temperate Cambisol? Geoderma 264: 171–178. http://dx.doi.org/10.1016/j.geoderma.2015.10.017.

Fontaine, S., Barot, S., Barre, P., Bdioui, N., Mary, B., and Rumpel, C. (2007) Stability of organic carbon in deep soil layers controlled by fresh carbon supply. Nature 450. http://dx.doi.org/10.1038/nature06275. 277–U10.

Frouz, J. (2017) Effects of soil macro- and mesofauna on litter decomposition and soil organic matter stabilization. Geoderma. http://dx.doi.org/10.1016/j.geoderma.2017.08.039.

Gomes, N.C.M., Fagbola, O., Costa, R., Rumjanek, N.G., Buchner, A., Mendona-Hagler, L., and Smalla, K. (2003) Dynamics of fungal communities in bulk and maize rhizosphere soil in the tropics. Applied and Environmental Microbiology 69: 3758–3766. http://dx.doi.org/10.1128/aem.69.7.3758-3766.2003.

Gray, J.M., Bishop, T.F.A., and Wilson, B.R. (2016) Factors Controlling Soil Organic Carbon Stocks with Depth in Eastern Australia. http://dx.doi.org/10.2136/sssaj2015.06.0224.

Harrison, R., Swift, R.S., Campbell, A.S., and Tonkin, P.J. (1990) A study of two soil development sequences located in a montane area of Canterbury, New Zealand, I. Clay mineralogy and cation exchange properties. Geoderma 47: 261–282. http://dx.doi.org/10.1016/0016-7061(90)90033-6.

Hassink, J. (1997) The capacity of soils to preserve organic C and N by their association with clay and silt particles. Plant and Soil 191: 77–87. http://dx.doi.org/10.1023/A:1004213929699.

Heckman, K., Welty-Bernard, A., Rasmussen, C., and Schwartz, E. (2009) Geologic controls of soil carbon cycling and microbial dynamics in temperate conifer forests. Chemical Geology 267: 12–23. http://dx.doi.org/10.1016/j.chemgeo.2009.01.004.

Heinze, S., Ludwig, B., Piepho, H., Mikutta, R., Don, A., Wordell-dietrich, P., Helfrich, M., Hertel, D., Leuschner, C., Kirfel, K., Kandeler, E., Preusser, S., Guggenberger, G., Leinemann, T., and Marschner, B. (2018) Factors controlling the variability of organic matter in the top- and subsoil of a sandy Dystric Cambisol under beech forest.Geoderma 311: 37–44. http://dx.doi.org/10.1016/j.geoderma.2017.09.028.

Hertel, D. (1999) Das Feinwurzelsystem von Rein- und Mischbeständen der Rotbuche: Struktur, Dynamik und Interspezifische Konkurrenz. Gebrüder Bornträger, Stuttgart.

Hertel, D., Strecker, T., Müller-Haubold, H., and Leuschner, C. (2013) Fine root biomass and dynamics in beech forests across a precipitation gradient – is optimal resource partitioning theory applicable to water-limited mature trees? Journal of Ecology 101: 1183–1200. http://dx.doi.org/10.1111/1365-2745.12124.

Jandl, R., Lindner, M., Vesterdal, L., Bauwens, B., Baritz, R., Hagedorn, F., Johnson, D.W., Minkkinen, K., and Byrne, K.A. (2007) How strongly can forest management influence soil carbon sequestration? Geoderma 137: 253–268. http://dx.doi.org/10.1016/j.geoderma.2006.09.003.

Janssens, I.A., Freibauer, A., Schlamadinger, B., Ceulemans, R., Ciais, P., Dolman, a. J., Heimann, M., Nabuurs, G.-J., Smith, P., Valentini, R., and Schulze, E.-D. (2005) The carbon budget of terrestrial ecosystems at country-scale – a European case study.Biogeosciences 2: 15–26. http://dx.doi.org/10.5194/bg-2-15-2005.

Jenny, H. (1994) Factors of Soil Formation. A System of Quantitative Pedology. Dover Publications, New York. http://dx.doi.org/10.1016/0016-7061(95)90014-4.

Jobbágy, E.G., and Jackson, R.B. (2000) The vertical distribution of soil organic carbon and its relation to climate and vegetation. Ecological Applications 10: 423–436. http://dx.doi.org/10.1890/1051-0761(2000)010[0423:TVDOSO]2.0.CO;2.

Joergensen, R.G., and Wichern, F. (2008) Quantitative assessment of the fungal contribution to microbial tissue in soil. Soil Biology and Biochemistry 40: 2977–2991. http://dx.doi.org/10.1016/j.soilbio.2008.08.017.

John, B., Yamashita, T., Ludwig, B., and Flessa, H. (2005) Storage of organic carbon in aggregate and density fractions of silty soils under different types of land use. Geoderma 128: 63–79. http://dx.doi.org/10.1016/j.geoderma.2004.12.013.

Johnson, K.D., Harden, J., McGuire, A.D., Bliss, N.B., Bockheim, J.G., Clark, M., Nettleton-Hollingsworth, T., Jorgenson, M.T., Kane, E.S., Mack, M., O'Donnell, J., Ping, C.L., Schuur, E.A.G., Turetsky, M.R., and Valentine, D.W. (2011) Soil carbon distribution in Alaska in relation to soil-forming factors. Geoderma 167–168: 71–84. http://dx.doi.org/10.1016/j.geoderma.2011.10.006.

Jones, R.J.A., Hiederer, R., Rusco, E., and Montanarella, L. (2005) Estimating organic carbon in the soils of Europe for policy support. European Journal of Soil Science 56: 655–671. http://dx.doi.org/10.1111/j.1365-2389.2005.00728.x.

Kaiser, K., Guggenberger, G., and Zech, W. (1996) Sorption of DOM and DOM fractions to forest soils. Geoderma 74: 281–303. http://dx.doi.org/10.1016/s0016-7061(96)00071-7.

Kalbitz, K. (2001) Properties of organic matter in soil solution in a German fen area as dependent on land use and depth. Geoderma 104: 203–214. http://dx.doi.org/10.1016/S0016-7061(01)00081-7.

Keiluweit, M., Bougoure, J.J., Nico, P.S., Pett-Ridge, J., Weber, P.K., and Kleber, M. (2015) Mineral protection of soil carbon counteracted by root exudates. Nature Climate Change 5: 588–595.

Koch, A.S., and Matzner, E. (1993) Heterogeneity of soil and soil solution chemistry under Norway spruce (Picea abies Karst.) and European beech (*Fagus sylvatica* L.) as influenced by distance from the stem basis. Plant and Soil 151: 227–237. http://dx.doi.org/10.1007/BF00016288.

Kögel-Knabner, I. (2002) The macromolecular organic composition of plant and microbial residues as inputs to soil organic matter. Soil Biology and Biochemistry 34: 139–162. http://dx.doi.org/10.1016/S0038-0717(01)00158-4.

Kögel-Knabner, I., Hatcher, P.G., Tegelaar, E.W., and de Leeuw, J.W. (1992) Aliphatic components of forest soil organic matter as determined by solid-state $^{13}C$ NMR and analytical pyrolysis. The Science of the Total Environment 113: 89–106. http://dx.doi.org/10.1016/0048-9697(92)90018-N.

Kölbl, A., and Kögel-Knabner, I. (2004) Content and composition of free and occluded particulate organic matter in a differently textured arable Cambisol as revealed by solidstate $^{13}C$ NMR spectroscopy. Journal of Plant Nutrition and Soil Science 167: 45–53. http://dx.doi.org/10.1002/jpln.200321185.

Kramer, M.G., Sanderman, J., Chadwick, O.A., Chorover, J., and Vitousek, P.M. (2012) Longterm carbon storage through retention of dissolved aromatic acids by reactive particles in soil. Global Change Biology 18: 2594–2605. http://dx.doi.org/10.1111/j.1365-2486.2012.02681.x.

Kuzyakov, Y., Hill, P., and Jones, D. (2007) Root exudate components change litter decomposition in a simulated rhizosphere depending on temperature. Plant and Soil 290: 293–305. http://dx.doi.org/10.1007/s11104-006-9162-8.

Leuschner, C., Hertel, D., Coners, H., and Büttner, V. (2001) Root competition between beech and oak: a hypothesis. Oecologia 126: 276–284. http://dx.doi.org/10.1007/s004420000507.

Leuschner, C., Hertel, D., Schmid, I., Koch, O., Muhs, A., and Hölscher, D. (2004) Stand fine root biomass and fine root morphology in old-growth beech forests as a function of precipitation and soil fertility. Plant and Soil 258: 43–56. http://dx.doi.org/10.1023/B:PLSO.0000016508.20173.80.

Leuschner, C., Meier, I.C., and Hertel, D. (2006) On the niche breadth of *Fagus sylvatica*: soil nutrient status in 50 Central European beech stands on a broad range of bedrock types. Annals of Forest Science 63: 355–368. http://dx.doi.org/10.1051/forest:2006016.

Liang, C., Read, H.W., and Balser, T.C. (2012) GC-based detection of aldononitrile acetate derivatized glucosamine and muramic acid for microbial residue determination in soil. Journal of Visualized Experiments e3767. http://dx.doi.org/10.3791/3767.

Lorenz, K., and Lal, R. (2005) The depth distribution of soil organic carbon in relation to land use and management and the potential of carbon sequestration in subsoil horizons. In: Donald,

L.S. (ed.) Advances in Agronomy. Academic Press, 35–66. http://dx.doi.org/10.1016/S0065-2113(05)88002-2.

Lorenz, K., Lal, R., Preston, C.M., and Nierop, K.G.J. (2007) Strengthening the soil organic carbon pool by increasing contributions from recalcitrant aliphatic bio(macro)molecules. Geoderma 142: 1–10. http://dx.doi.org/10.1016/j.geoderma.2007.07.013.

Manzoni, S., Katul, G.G., and Porporato, A. (2009) Analysis of soil carbon transit times and age distributions using network theories. Journal of Geophysical Research 114: G04025.http://dx.doi.org/10.1029/2009JG001070.

Marschner, B., Brodowski, S., Dreves, A., Gleixner, G., Gude, A., Grootes, P.M., Hamer, U., Heim, A., Jandl, G., Ji, R., Kaiser, K., Kalbitz, K., Kramer, C., Leinweber, P., Rethemeyer, J., Schaeffer, A., Schmidt, M.W.I., Schwark, L., and Wiesenberg, G.L.B. (2008) How relevant is recalcitrance for the stabilization of organic matter in soils? Journal of Plant Nutrition and Soil Science 171: 91–110. http://dx.doi.org/10.1002/jpln.200700049.

Mooshammer, M., Wanek, W., Zechmeister-Boltenstern, S., and Richter, A. (2014) Stoichiometric imbalances between terrestrial decomposer communities and their resources: mechanisms and implications of microbial adaptations to their resources. Frontiers in Microbiology 5: 22. http://dx.doi.org/10.3389/fmicb.2014.00022.

Mora, J.L., Guerra, J.A., Armas-Herrera, C.M., Arbelo, C.D., and Rodríguez-Rodríguez, A. (2014) Storage and depth distribution of organic carbon in volcanic soils as affected by environmental and pedological factors. Catena 123: 163–175. http://dx.doi.org/10.1016/j.catena.2014.08.004.

Mueller, C.W., Bruggemann, N., Pritsch, K., Stoelken, G., Gayler, S., Winkler, J.B., and Kögel-Knabner, I. (2009) Initial differentiation of vertical soil organic matter distribution and composition under juvenile beech (*Fagus sylvatica* L.) trees. Plant and Soil 323:111–123. http://dx.doi.org/10.1007/s11104-009-9932-1.

Mueller, C.W., Schlund, S., Prietzel, J., Kogel-Knabner, I., and Gutsch, M. (2012) Soil aggregate destruction by ultrasonication increases soil organic matter mineralization and mobility. Soil Science Society of America Journal 76: 1634–1643. http://dx.doi.org/10.2136/sssaj2011.0186.

Mueller, K.E., Hobbie, S.E., Chorover, J., Reich, P.B., Eisenhauer, N., Castellano, M.J., Chadwick, O.A., Dobies, T., Hale, C.M., Jagodziński, A.M., Kałucka, I., Kieliszewska-Rokicka, B., Modrzyński, J., Rożen, A., Skorupski, M., Sobczyk, Ł., Stasińska, M., Trocha, L.K., Weiner, J., Wierzbicka, A., and Oleksyn, J. (2015) Effects of litter traits, soil biota, and soil chemistry on soil carbon stocks at a common garden with 14 tree species. Biogeochemistry 123: 313–327. http://dx.doi.org/10.1007/s10533-015-0083-6.

Nierop, K.G.J. (1998) Origin of aliphatic compounds in a forest soil. Organic Geochemistry 29: 1009–1016. http://dx.doi.org/10.1016/S0146-6380(98)00165-X.

Ohta, S., Suzuki, A., and Kumada, K. (1986) Experimental studies on the behavior of fine organic particles and water-soluble organic matter in mineral soil horizons. Soil Science & Plant Nutrition 32: 15–26. http://dx.doi.org/10.1080/00380768.1986.10557477.

Paz, C.P., Goosem, M., Bird, M., Preece, N., Goosem, S., Fensham, R., and Laurance, S. (2016) Soil types influence predictions of soil carbon stock recovery in tropical secondary forests. Forest Ecology and Management 376: 74–83. http://dx.doi.org/10.1016/j.foreco.2016.06.007.

Post, W.M., Emanuel, W.R., Zinke, P.J., and Stangenberger, A.G. (1982) Soil carbon pools and world life zones. Nature 298: 156–159.

Prechtel, A., Lützow, M. Von, Schneider, B.U., Bens, O., Bannick, C.G., Kögel-Knabner, I., and Hüttl, R.F. (2009) Organic Carbon in Soils of Germany : Status Quo and the Need for New Data to Evaluate Potentials and Trends of Soil Carbon Sequestration. pp. 601–614. http://dx.doi.org/10.1002/jpln.200900034.

Preusser, S., Marhan, S., Poll, C., and Kandeler, E. (2017) Microbial community response to changes in substrate availability and habitat conditions in a reciprocal subsoil transfer experiment. Soil Biology and Biochemistry 105: 138–152. http://dx.doi.org/10.1016/j.soilbio.2016.11.021.

R Core Team (2015) R: a Language and Environment for Statistic Computing. R Foundation for Statistical Computing, Vienna.

Rasmussen, C., Heckman, K., Wieder, W.R., Keiluweit, M., Lawrence, C.R., Berhe, A.A., Blankinship, J.C., Crow, S.E., Druhan, J.L., Hicks Pries, C.E., Marin-Spiotta, E., Plante, A.F., Schädel, C., Schimel, J.P., Sierra, C.A., Thompson, A., and Wagai, R. (2018) Beyond clay:

towards an improved set of variables for predicting soil organic matter content. Biogeochemistry 297–306. http://dx.doi.org/10.1007/s10533-018-0424-3.

Rasse, D.P., Rumpel, C., and Dignac, M.F. (2005) Is soil carbon mostly root carbon? Mechanisms for a specific stabilisation. Plant and Soil 269: 341–356. http://dx.doi.org/10.1007/s11104-004-0907-y.

Reimer, P., Brown, T., and Reimer, R. (2004) Discussion: reporting and calibration of postbomb $^{14}C$ data. Radiocarbon 46: 1111–1150.

Rethemeyer, J., Fülöp, R.H., Höfle, S., Wacker, L., Heinze, S., Hajdas, I., Patt, U., König, S., Stapper, B., and Dewald, A. (2013) Status report on sample preparation facilities for $^{14}C$ analysis at the new CologneAMS center. Nuclear Instruments and Methods in Physics Research Section B: Beam Interactions with Materials and Atoms 294: 168–172. http://dx.doi.org/10.1016/j.nimb.2012.02.012.

Rethemeyer, J., Kramer, C., Gleixner, G., John, B., Yamashita, T., Flessa, H., Andersen, N., Nadeau, M.-J., and Grootes, P.M. (2005) Transformation of organic matter in agricultural soils: radiocarbon concentration versus soil depth. Geoderma 128: 94–105. http://dx.doi.org/10.1016/j.geoderma.2004.12.017.

Richter, D.B., and Billings, S.A. (2015) "One physical system": tansley's ecosystem as earth's critical zone. New Phytologist 206: 900–912. http://dx.doi.org/10.1111/nph.13338.

Rumpel, C., Eusterhues, K., and Kögel-Knabner, I. (2010) Non-cellulosic neutral sugar contribution to mineral associated organic matter in top- and subsoil horizons of two acid forest soils. Soil Biology and Biochemistry 42: 379–382. http://dx.doi.org/10.1016/j.soilbio.2009.11.004.

Rumpel, C., Eusterhues, K., and Kögel-Knabner, I. (2004) Location and chemical composition of stabilized organic carbon in topsoil and subsoil horizons of two acid forest soils. Soil Biology and Biochemistry 36: 177–190. http://dx.doi.org/10.1016/j.soilbio.2003.09.005.

Rumpel, C., and Kögel-Knabner, I. (2011) Deep soil organic matter—a key but poorly understood component of terrestrial C cycle. Plant and Soil 338: 143–158. http://dx.doi.org/10.1007/s11104-010-0391-5.

Rumpel, C., Rodriguez-Rodriguez, A., Gonzalez-Perez, J.A., Arbelo, C., Chabbi, A., Nunan, N., and Gonzalez-Vila, F.J. (2012) Contrasting composition of free and mineral-bound organic matter in top- and subsoil horizons of Andosols. Biology and Fertility of Soils 48: 401–411. http://dx.doi.org/10.1007/s00374-011-0635-4.

Saetre, P., and Bååth, E. (2000) Spatial variation and patterns of soil microbial community structure in a mixed spruce–birch stand. Soil Biology and Biochemistry 32: 909–917. http://dx.doi.org/10.1016/S0038-0717(99)00215-1.

Saiz, G., Bird, M.I., Domingues, T., Schrodt, F., Schwarz, M., Feldpausch, T.E.D.R., Veenendaal, E., and Lloyd, J.O.N. (2012) Variation in Soil Carbon Stocks and Their Determinants across a Precipitation Gradient in West Africa. pp. 1670–1683. http://dx.doi.org/10.1111/j.1365-2486.2012.02657.x.

Sanderman, J., and Amundson, R. (2008). A comparative study of dissolved organic carbon transport and stabilization in California forest and grassland soils. Biogeochemistry 89: 309–327. http://dx.doi.org/10.1007/s10533-008-9221-8.

Schmidt, M.W.I., Torn, M.S., Abiven, S., Dittmar, T., Guggenberger, G., Janssens, I. a., Kleber, M., Kögel-Knabner, I., Lehmann, J., Manning, D. a. C., Nannipieri, P., Rasse, D.P., Weiner, S., and Trumbore, S.E. (2011) Persistence of soil organic matter as an ecosystem property. Nature 478: 49–56. http://dx.doi.org/10.1038/nature10386.

Schöning, I., and Kögel-Knabner, I. (2006) Chemical composition of young and old carbon pools throughout Cambisol and Luvisol profiles under forests. Soil Biology and Biochemistry 38: 2411–2424. http://dx.doi.org/10.1016/j.soilbio.2006.03.005.

Schöning, I., Morgenroth, G., and Kögel-Knabner, I. (2005) O/N-alkyl and alkyl C are stabilized in fine particle size fractions of forest soils. Biogeochemistry 73: 475–497. http://dx.doi.org/10.1007/s10533-004-0897-0.

Schöning, I., Totsche, K.U., and Kögel-Knabner, I. (2006) Small scale spatial variability of organic carbon stocks in litter and solum of a forested Luvisol. Geoderma 136: 631–642. http://dx.doi.org/10.1016/j.geoderma.2006.04.023.

Sheng, H., Zhou, P., Zhang, Y., Kuzyakov, Y., Zhou, Q., Ge, T., and Wang, C. (2015) Loss of labile organic carbon from subsoil due to land-use changes insubtropical China. Soil Biology and Biochemistry 88: 148–157. http://dx.doi.org/10.1016/j.soilbio.2015.05.015.

Six, J., Bossuyt, H., Degryze, S., and Denef, K. (2004) A history of research on the link between (micro)aggregates, soil biota, and soil organic matter dynamics. Soil and Tillage Research 79: 7–31. http://dx.doi.org/10.1016/j.still.2004.03.008.

Tefs, C., and Gleixner, G. (2012) Importance of root derived carbon for soil organic matter storage in a temperate old-growth beech forest – evidence from C, N and $^{14}C$ content. Forest Ecology and Management 263: 131–137. http://dx.doi.org/10.1016/j.foreco.2011.09.010.

Tisdall, J.M., and Oades, J.M. (1982) Organic matter and water-stable aggregates in soils. Journal of Soil Science 33: 141–163. http://dx.doi.org/10.1111/j.1365-2389.1982.tb01755.x.

Torn, M.S., Swanston, C.W., Castanha, C., and Trumbore, S.E. (2009) Storage and Turnover of Organic Matter in Soil. In: Senesi, N., Xing, B., Ming Huang, P. (eds.) Biophysico-Chemical Processes Involving Natural Nonliving Organic Matter in Environmental Systems, 219-261. Wiley, New Jersey, USA.

Tückmantel, T., Leuschner, C., Preusser, S., Kandeler, E., Angst, G., Mueller, C.W., and Christin, I. (2017) Soil Biology & Biochemistry Root exudation patterns in a beech forest : dependence on soil depth, root morphology, and environment. Soil Biology and Biochemistry 107: 188–197. http://dx.doi.org/10.1016/j.soilbio.2017.01.006.

Van Praag, H.J., Sougnez-Remy, S., Weissen, F., and Carletti, G. (1988) Root turnover in a beech and a spruce stand of the Belgian Ardennes. Plant and Soil 105: 87–103. http://dx.doi.org/10.1007/BF02371146.

Vesterdal, L., Clarke, N., Sigurdsson, B.D., and Gundersen, P. (2013) Do tree species influence soil carbon stocks in temperate and boreal forests? Forest Ecology and Management 309: 4–18. http://dx.doi.org/10.1016/j.foreco.2013.01.017.

Virto, I., Barré, P., and Chenu, C. (2008) Microaggregation and organic matter storage at the silt-size scale. Geoderma 146: 326–335. http://dx.doi.org/10.1016/j.geoderma.2008.05.021.

Vogt, K.A., Vogt, D.J., Moore, E.E., Fatuga, B.A., Mark, R., and Edmonds, R.L. (1987) Conifer and angiosperm fine-root biomass in relation to stand age and site productivity in douglas-fir forests. Journal of Ecology 75: 857–870.

Von Lützow, M., Kögel-Knabner, I., Ekschmitt, K., Matzner, E., Guggenberger, G., Marschner, B., and Flessa, H. (2006) Stabilization of organic matter in temperate soils: mechanisms and their relevance under different soil conditions - a review. European Journal of Soil Science 57: 426–445. http://dx.doi.org/10.1111/j.1365-2389.2006.00809.x.

Von Lützow, M., Kogel-Knabner, I., Ekschmittb, K., Flessa, H., Guggenberger, G., Matzner, E., and Marschner, B. (2007) SOM fractionation methods: relevance to functional pools and to stabilization mechanisms. Soil Biology and Biochemistry 39: 2183–2207. http://dx.doi.org/10.1016/j.soilbio.2007.03.007.

Von Lützow, M., Kögel-Knabner, I., Ludwig, B., Matzner, E., Flessa, H., Ekschmitt, K., Guggenberger, G., Marschner, B., and Kalbitz, K. (2008) Stabilization mechanisms of organic matter in four temperate soils: development and application of a conceptual model. Journal of Plant Nutrition and Soil Science 171: 111–124. http://dx.doi.org/10.1002/jpln.200700047.

Wagai, R., Mayer, L.M., Kitayama, K., and Knicker, H. (2008) Climate and parent material controls on organic matter storage in surface soils : a three- pool, density-separation approach. Geoderma 147: 23–33. http://dx.doi.org/10.1016/j.geoderma.2008.07.010.

Wattel-Koekkoek, E.J.W., van Genuchten, P.P.L., Buurman, P., and van Lagen, B. (2001) Amount and composition of clay-associated soil organic matter in a range of kaolinitic and smectitic soils. Geoderma 99: 27–49. http://dx.doi.org/10.1016/s0016-7061(00)00062-8.

Wiesmeier, M., Barthold, F., Spörlein, P., Geuß, U., Hangen, E., Reischl, A., Schilling, B., Angst, G., von Lützow, M., and Kögel-Knabner, I. (2014) Estimation of total organic carbon storage and its driving factors in soils of Bavaria (southeast Germany). Geoderma Regional 1: 67–78.

Wright, S., Yavitt, J., Wurzburger, N., Turner, B., Tanner, E., Sayer, E., Santiage, L., Kaspari, M., Hedin, L., Harms, K., Garcia, M., and Corre, M. (2011) Potassium, phosphorus, or nitrogen limit root allocation, tree growth, or litter production in a lowland tropical forest. Ecology 92: 1616–1625.

Zhang, X., and Amelung, W. (1996) Gas chromatographic determination of muramic acid, glucosamine, mannosamine, and galactosamine in soils. Soil Biology and Biochemistry 28: 1201–1206. http://dx.doi.org/10.1016/0038-0717(96)00117-4.

# CHAPTER 8

# Synthesis

## 8.1 Synthesis

The accurate assessment of distribution, abundance, morphology, and anatomy of trees' fine roots in forest ecosystems plays a vital role for understanding ecosystem functioning because

1) the roots of trees play a fundamental role in the acquisition of water and nutrients,

2) a large portion of trees' annually assimilated carbon is consumed by their root systems, and

3) tree roots contribute substantially to the belowground C fluxes in forest ecosystems.

Irrespective of these central functions, our knowledge on the belowground plasticity of trees under different environmental conditions is still incomplete, in particular with regards to the subsoil (Jackson et al. 1996; Gill and Burke 2002; Schenk and Jackson 2002, 2005). Despite a generally sharp decrease in fine root density with increasing soil depth and an increase in the heterogeneity of their distribution in deeper soil layers, fine roots in subsoils can be important in terms of water and nutrient supply (Stone and Kalisz 1991; Nepstad et al. 1994; Stone and Comerford 1994; Canadell et al. 1996; Jobbágy and Jackson 2001; Lehmann 2003). Furthermore, deep roots and rhizodeposits are assumed to be the primary source of SOC in deep soil layers (Rasse et al. 2005; Comas and Eissenstat 2009; Tefs and Gleixner 2012). Previous studies have shown that root distribution patterns govern the allocation of OC in soils (Jobbágy and Jackson 2000), which underlines the important role of fine root turnover in soil C cycling.

The largest terrestrial OC pool is located in soils, and with regards to ecosystem types, forest soils contain the largest share of SOC with up to 70% (Jobbággy and Jackson 2000; Janzen 2005). Thus, to accurately describe global C cycling, the quantification of forest belowground C-fluxes, including the subsoil, is one prerequisite (Pollierer et al. 2007).

The present thesis deals with the plasticity of the root system of European beech in the top- and subsoil in relation to different geological substrates. Belowground plastic responses to the temporally and spatially heterogeneous supply of nutrients and water in the soil are thought to be a major adaptation mechanism by which plants cope with the inherent heterogeneity of soils and variation in other external factors (e.g. water supply) (Hodge 2004). We investigated whether beech fine root system size, structure, morphology and anatomy vary in different soil depths and / or along an edaphic gradient. Furthermore, our goal was to highlight the role of beech fine roots

in the C cycle in the top- and subsoil – in particular their effect on SOC content, distribution, and quality.

For our comparative approach we selected six mature European beech forests in Northern Germany with comparable climatic conditions, age, and stand structure, but growing on different bedrock to be able to examine variation in root system traits and C cycling in the soil in relation to soil chemical properties and soil fertility. Since we particularly paid attention to subsoil processes, we investigated adaptations in the fine root system as well as the impact of roots on SOC storage and turnover in the top- and the subsoil of our stands, down to the bedrock or up to 200 cm soil depth.

The six study sites represent a broad spectrum of geological substrates from silicate-poor Pleistocene sandy deposits and Triassic sandstone to volcanic basalt and Triassic limestone. The base richness gradient in the topsoil (5-57 %) is less pronounced compared to the subsoil (6 to 100 %) due to topsoil acidification. Soil texture varied from loamy sand (site GR) to silt (GW and RU sites), which is reflected in the variation in the mass-specific cation exchange capacities from around 10 µmolc $g^{-1}$ in the sandy substrates (GR, HM) to >200 µmolc $g^{-1}$ at the limestone site (GW). A much higher soil carbon content at the basalt and limestone sites (2.5-3.6 % vs. 1.0-1.6 % at the other sites) contributed to the CEC at the GW and DR sites, while the highest C/N ratios were observed at the GR sites on Pleistocene sand (>25 in the topsoil); yet, no clear trend in C/N from base-poor to base-rich sites was observed. This was also true for topsoil pH ($CaCl_2$), which ranged between 3.5 and 4.3 at all six sites. Near-neutral pH values were found only at the limestone site in the subsoil (pH 6.6). All soil profiles were classified as Cambisols in different sub-types, ranging from dystric to chromic to eutric Cambisols. The profiles on sand, sandstone, and loess had Leptomoders or Hemimors as humus forms, while the biologically more active forms Mullmoder and Vermimull were found on basalt and limestone with higher base saturation in the mineral soil. Relatively thick organic layers (>35 mm) occurred on sand and basalt, thinner layers (<20 mm) on loess, sandstone, and limestone.

***Do total stand fine root biomass and necromass and fine root distribution patterns vary in dependence on soil acidity and depth?***

We did not observe any significant relationships between FRB profile totals and soil acidity or any other soil chemical or physical parameter (soil pH, base saturation, soil C/N ratio, clay content) (Chapter 3). On our sites, the depth of the profile appeared to be the most important determinant of the overall fine root system size (FRB). This result contrasts with a number of earlier studies, which concluded that on base-rich sites fine root biomass is smaller compared to more acidic, base-poor sites (Aber et al. 1985; Pregitzer et al. 1993; Poorter and Nagel 2000; Schmid 2002; Leuschner and Hertel 2003; Neatrour et al. 2005); higher FRB totals under nutrient deficient conditions are thought to be an adaptation directed at ensuring sufficient nutrient supply (Nadelhoffer 2000).

However, site nutrient availability and fine root biomass also do not appear to be unequivocally linked in other studies (Hertel 1999): e.g. Kern et al. (1961) reported a positive correlation between fine root biomass and site nutrient status in a comparison of conifer stands in the German Black Forest. Non-uniform adaptations in terms of root proliferation in response to differential nutrient availability are more the rule than an exception, across species, but also within one species. Moreover, increasing root biomass is only one strategy to increase the absorptive area of the root system – adaptations can also be made in the form of morphological alterations, most importantly by variations in root diameter, which is one determinant of specific root length (SRL), or root length per unit mass, which is indicative of the absorptive area of the root system (Eissenstat and Caldwell 1988). Additionally, plant roots are also physiologically plastic and may increase nutrient uptake by increasing their uptake capacity and / or their ion affinity without any changes in root biomass and morphology (Hodge 2004).

Another explanation could be that adaptations in the root system to soil acidity or low nutrient availability do not occur on a large, stand-related scale, but on a much smaller scale. Plants may react to small-scale soil heterogeneity with root proliferation into patches where nutrients are available; precision in foraging for certain nutrients on a small scale has been described earlier as an important mechanism of plants to cope with heterogeneous nutrient availability in soil (Hodge 2004). The higher silt and oxalate-extractable Fe ($Fe_o$) contents in the rooted soil samples from

the Tertiary sand site (GR) (Chapter 5) indicate that in soils with an overall relatively low nutrient availability, fine roots preferentially grow in spots where nutrients are available.

Other than FRB, we observed significantly higher amounts of fine root necromass (FRN) in the acidic profiles on sand (GR, HM), intermediate amounts on sandstone and basalt (EG, DR), and low amounts of FRN on the base-richer loess and limestone sites (RU, GW) (Chapter 3). Earlier studies on the fine root system of beech indicate that soil acidity and fertility strongly influence the mortality of fine roots; live:dead ratios of fine root mass were consistently found to be considerably higher in acidic soils compared to neutral to alkaline soils, which is hypothesized to be caused by a reduction in fine root longevity due to adverse soil chemical conditions (Leuschner et al. 1998; Godbold et a. 2003; Leuschner and Hertel 2003; Leuschner et al. 2004; Braun et al. 2005). Another explanation for a higher share of fine root necromass in acidic soils could be that necromass decomposition rates are lower at acidic sites due to reduced soil biological activity. Since root turnover and decomposition data is not available for our sites, we can only hypothesize about the causes for the differences in necromass amounts, but studies on fine root turnover in stands differing in terms of site fertility conclude that higher amounts of FRN at acidic sites are not due to altered decomposition rates, but for the main part caused by an increase in fine root mortality (Hertel 1999).

***Does beech fine root morphology differ in soils with different nutrient availability?***

Plastic responses in root morphology to environmental (soil) heterogeneity are another way in which trees may adapt to variation in soil conditions (Hodge 2006; Ostonen et al. 2007; Comas and Eissenstat 2009). Nutrient availability may have an effect on many root morphological traits, e.g. on root diameter (Forde and Lorenzo 2001; Pierret et al. 2007). Increased fineness of the rooting system might be directed at increasing the uptake efficiency per unit root mass under nutrient deficient conditions (Fitter 1985; Lõhmus et al. 1989; Eissenstat et al. 2000; Hertel and Wesche 2008; Ostonen et al. 2011). Specific root length (SRL) and specific root area (SRA) are measures which indicate the absorptive area of the root system. SRL and SRA vary with fine root biomass, but can also be increased by a decrease in fine root diameter, without any change in fine root biomass (Eissenstat and Caldwell 1988; Hodge 2004).

Across the investigated sites and across soil layers within one site, mean fine root diameter, SRL, and SRA varied considerably in this study. The largest differences appeared between the different layers within on profile: we observed the largest SRL and SRA in the organic layer (OL) at our sites. A consistent relation in root morphological traits to soil acidity or base saturation did not appear. We only found a significant correlation between base saturation and fine root diameter in the lower subsoil ($r^2 = 0.30$; $P < 0.05$) (Chapter 3). In an earlier study of the fine root morphology of *F. sylvatica*, a consistent change of SRA in relation to soil chemistry could neither be detected (Leuschner et al. 2004). In an overview of results with regards to responses in SRL to varying soil conditions, Ryser (1998) reported increases, decreases as well as no alteration in response to differential nutrient availability; thus, a clear relationship between soil chemical factors and SRL could not be established, yet.

Similar to increased root system fineness, an increased number of root tips might serve for enhancing the uptake efficiency per unit root mass under nutrient poor conditions (Leuschner et al. 2004). Separating fine roots into the two functional groups of absorptive fine roots and transport fine roots, root tips are classified as absorptive roots primarily functioning for nutrient acquisition and uptake from the surrounding soil solution (Guo et al. 2008; McCormack et al. 2015; Wang et al. 2015). Thus, the higher the number of root tips, the higher the absorptive area per soil volume.

At the investigated sites, a relationship between root tip frequency (RTF) and soil chemistry did not emerge (Chapter 3). In contrast to this result, other authors found RTF to be higher in acidic (Kottke and Agerer 1983; Leuschner et al. 2004) or nutrient-poor soils (Hertel 1999). Instead, RTF appeared to be depth-dependent on our sites: we observed high RTF values in the OL horizon followed by a decrease towards the upper subsoil. At half of the sites (GR, RU, GW) maximum RTF values were reached in the lower subsoil. Patterns of a vertical decrease in root tip density were reported in a number of studies (Olsthoorn 1991; Finér et al. 1997; Hertel 1999; Kalhoff 2000; Leuschner et al. 2004). We assume that the secondary peaks in RTF in the lower subsoil in GR, RU, and GW are due to increased nutrient availability in these horizons. These patterns suggest that rather than increasing the total number of root tips over the whole soil profile in response to low nutrient availability, adaptations happen on a smaller scale and the number of root tips is increased in soil horizons and / or soil patches, where nutrients are available to the plant.

***Do xylem anatomical and derived hydraulic traits of small- to medium-sized beech roots vary in dependence on soil depth?***

We measured mean vessel diameter (*D*), vessel density (VD), relative vessel lumen area (lumen area per xylem area) and derived potential hydraulic conductivity ($K_p$) in the xylem of 197 fine- to medium-diameter roots in the topsoil and subsoil (0-200 cm) in GR. A significant relation of the anatomical and functional traits to soil depth could not be established. Instead, all traits showed a strong dependence on root diameter and thus root age (Chapter 4).

Variation in xylem architecture and hydraulic performance of roots in relation to soil depth have only rarely been studied, yet (e.g. Gebauer and Volařík 2013; Maeght et al. 2013; Wang et al. 2015; Pierret et al. 2016). Some authors found increases in conduit diameter and hydraulic efficiency with increasing soil depth in the sinker roots of various Proteaceae species (Pate et al. 1995) and in the roots of various tree species (McElrone et al. 2004). The discrepancy to our results may be explained by the fact that the rooting system is highly responsive to external factors (Nardini et al. 2002; Christensen-Daalsgaard et al. 2008) like freeze-thaw events (Gebauer and Volařík 2013) or water availability (Rewald et al. 2011; Köcher et al. 2012), and mechanical demands (Dunham et al. 2007; Lintunen and Kalliokoski 2010); respective adaptations might overlay plant-internal architectural patterns. Secondly, the reported depth-dependent patterns in xylem anatomy and hydraulic conductivity in the cited studies may be due to differences in path length between the investigated root sections; variation in conduit diameters and hydraulic performance in relation to path length from the terminal branches to the stem and further to the roots is thought to be one general structural principle of the hydraulic architecture of trees (Aloni 1987; Tyree and Zimmermann 2002; Hacke et al. 2016). However, in this study we were not able to measure path length and therefore referred to soil depth, solely, which might explain the differences to the above-mentioned studies.

The number of studies investigating vessel diameter in relation to root diameter and thus with root age is yet very limited. In agreement with our findings, studies separating root branching orders concluded that conduit diameters tend to increase towards higher root orders (Valenzuela-Estrada et al. 2008; Huang et al. 2010; Long et al. 2013; Gu et al. 2014). Similarly, a vessel-diameter-stem diameter relation has been described in several other studies (e.g. Coomes et al. 2007; Olson and Rosell 2013; Olson et al. 2014; Pfautsch 2016; Rosell et al. 2017).

In the investigated roots, we found $D$ and $K_p$ to analogously increase linearly from the root tip to a maximum at root diameter of 6-7 mm; in thicker roots, $D$ remained constant, while $K_p$ even decreased slightly in roots of 8-10 mm in diameter. We assume that the maximum vessel diameter is restricted in roots in order to avoid drought- or frost-induced cavitation. A limitation in maximum vessel size may not only serve hydraulic safety, but may as well display a trade-off between hydraulic efficiency and mechanical requirements.

Another main result of this study is the high plasticity in xylem architectural and hydraulic traits of similar-sized beech roots independent of soil depth. In 8% of the roots, $K_p$ exceeded the average in their diameter class by 50-700%, which indicates the existence of different functional types of roots with respect to water uptake and conduction; we therefore termed these roots with at least 50% higher $K_p$ values 'high-conductivity roots'. The particularly high axial conductivity results from a large number of vessels >100 µm in diameter in these roots. As earlier studies indicate, functional specialization may develop in response to gradients in water availability, soil texture, and nutrient availability, with roots serving predominantly nutrient absorption, and others water uptake and conduction (Pierret et al. 2007; Rewald et al. 2011; Köcher et al. 2012; Hajek et al. 2014). Following this concept, 'high-conductivity roots' might develop in soil patches where water is, or was, more easily available. In general, anatomical and functional plasticity in secondary elements is thought to be an important mechanism for plants to adapt to differences in climatic conditions and other external factors (Carlquist 2001; Spicer and Groover 2010).

***What are the impacts of beech roots on the amount, the spatial distribution and chemical composition of soil organic matter (SOM)? And are there differences in the way they affect SOM storage and turnover on different parent materials?***

In the Dystric Cambisol developed from sandy glacio-fluviatile deposits from the Saale glaciation in the Grinderwald forest, the soil organic carbon (SOC) content in the topsoil appeared to be related to pH and dithionite-extractable Al, while the SOC content in the subsoil was shown to be related to root bio- and necromass as well as to the content of Fe oxides and/or silt (Chapter 5). On the horizontal axis, the distance from individual trees had neither influence on the SOC contents in the soil nor on the chemical composition of SOM fractions (Chapter 6). Vertically,

SOC contents and stocks, as well as the chemical composition of SOM differed significantly, assumably due to the spatial variability in organic matter (OM) inputs (Chapter 6).

Roots were present over the whole profile, from the topsoil down to 2 m depth, but the abundance of both fine root biomass and necromass sharply decreased and the heterogeneity of their distribution increased with increasing depth (Chapter 5,7); this asymptotic depth distribution of fine roots has been described in a number of other studies (e.g. Jackson et al. 1996; Hertel 1999; Jobbágy and Jackson 2001; Leuschner et al. 2004). Likewise, the SOC contents and stocks decreased strongly with increasing depth (Chapter 5,6), as reported by numerous other authors (e.g. Rumpel et al. 2004; Salomé et al. 2010; Rumpel and Kögel-Knabner 2011). The spatial variability in SOC contents increased as well with depth (Chapter 5), which suggests a locally higher amount of root-borne inputs or inputs in form of dissolved organic carbon (DOC) along preferential flow paths (Bundt et al. 2001; Chabbi et al. 2009; Salomé et al. 2010; Syswerda et al. 2011; Tefs and Gleixner 2012; Hafner et al. 2014; Leinemann et al. 2016). Below a depth of 35 cm inputs from above-ground litter were absent (Chapter 6), which supports the hypothesis that the main input of SOC in the subsoil originates from roots.

A comparison of root-free soil samples with rooted soil samples from the subsoil revealed an up to 10 times higher SOC content in the rooted samples, which further supports the assumption that root inputs are a major source of SOC in the subsoil. At the same time, the rooted soil samples contained significantly higher amounts of silt and oxalate-extractable Fe, indicating that roots preferentially grow in these spots with chemically and physically more favourable conditions. Furthermore, the higher, root-borne inputs in these spots were apparently better stabilized through sorption to Fe-oxides and silt in these zones, thereby leading to a longer-term storage of SOC in these hot-spots. Thus, the increasing spatial variability in SOC with depth can to a large part be explained by an interaction of soil texture and metal oxides with root abundance (Chapter 5).

According to the combined density and particle size fractionation, particulate organic matter (POM) dominated the SOC pools in the upper soil layers, while at greater soil depths, POM was virtually absent and most of the SOC was associated with the clay fraction. We hypothesize that the absence of POM in deeper soil layers is due to the high sand contents in the subsoil at the Grinderwald site, resulting in a minor degree of macroaggregation and a thereby increased

availability of POM for microbial decomposition. Compared to the upper soil layers, the clay fractions in the subsoil were enriched in SOC which suggests that by forming organo-mineral associations, clay is more important for stabilizing SOC in soils with high sand contents (Chapter 6).

Investigating the impact of differing parent materials (Tertiary sand (GR), Quaternary loess (RU), Tertiary basalt (DR)) on SOC stocks and SOM fractions further points to the importance of soil texture as a determinant of SOC contents and stocks (Chapter 7). The geological substrate predefines the texture and nutrient composition of the soil developing from it, including the clay content on different sites (Jenny 1994; Kölbl and Kögel-Knabner 2004; Wagai et al. 2008; Torn et al. 2009). Our results show that the clay fraction has a major role in shaping differences in SOC stocks between our sites, particularly in the subsoil: the clay fraction accounted for up to 80% of SOC in subsoils of our sites and SOC decreased with decreasing amount of the clay fraction. This relationship is attributed to SOM stabilization through organo-mineral association, which increases with increasing contents of the clay fraction. Furthermore, the quality of the parent material may have an indirect effect on SOC stocks via affecting root biomass, density, exudation, and longevity, and thereby shaping the amount root-borne SOC inputs to the soil. Independent of site and soil depth, more than 90 % of variation in SOC stocks could be explained by the amount of amino sugars (abundance of microbial compounds) and amount of the clay fraction in combination with OM-input-related parameters (root mass and amount of POM).

Comparing the bulk soil and rhizosphere soil at 10 cm depth, the rhizosphere soil had a more than three times higher SOC content than the bulk soil, which is ascribed to root exudates as well as to a considerable supply with fresh POM, which is evidenced by a six times higher amount of POM in the rhizosphere soil compared to the bulk soil. This result contrasts the common notion that root exudates are the largest and most important source of SOC inputs from roots to the soil (Kuzyakov et al. 2007; Dennis et al. 2010). Furthermore, the clay fractions in the rhizosphere soil had higher SOC contents compared to the non-rhizosphere soil, which suggests that rooting zones are hotspots for the formation of organo-mineral associations (Chapter 6).

***Overall conclusions***

The major aims of this study were to reveal species-specific adaptations in the size, structure, morphology and anatomy of the fine root system of beech to differences in soil conditions and to investigate the role of fine roots in SOC sequestration in the top- and subsoil of six mature beech forests growing on different parent materials in Northern Germany.

Comparing different sites and soil layers, great plasticity in the structure and morphology of the fine root system emerged, which is interpreted as an adaptation to the locally heterogenous supply of nutrients and water in the soil. Pronounced differences appeared primarily between the top- and subsoil, and less between the investigated sites. The higher silt and oxalate-extractable Fe contents in the rooted samples of the GR site suggest an increased foraging precision through root deployment in nutrient-rich patches in soils with low background fertility. Likewise, an increase in RTF in subsoil layers with increased nutrient availability points to a local response in fine root morphology to the availability of nutrients. In order to deepen our understanding of tree belowground adaptation to variable edaphic conditions, future studies on the variation in fine root system structure and morphology should investigate the variation of root traits in relation to soil chemistry and texture on a much smaller scale to be able to detect root responses to the inherent small-scale heterogeneity of soils. Furthermore, the investigation of root branching patterns (notably the 1st- and 2nd-order fraction) and root functioning (root longevity and uptake activity) could broaden our knowledge on adaptive belowground strategies of trees enabling the colonization of a wide range of soil types.

The high plasticity in xylem architectural and hydraulic traits of small- to medium-sized roots further supports the notion that the rooting system of European beech is highly responsive to external factors. The existence of ‘high conductivity roots’, which feature a 50-700% higher hydraulic conductivity compared to similar-sized roots, indicates the functional differentiation of roots with such serving predominantly water uptake and conduction, and others specialized for nutrient absorption. Functional specialization might develop in response to gradients in water and nutrient availability and soil texture - anatomical and functional plasticity in secondary elements is thought to be an important mechanism for plants to adapt to differences in climatic conditions and other external factors in general, but the exact relationships remain to be elucidated. Therefore, future studies should include the soil and moisture conditions surrounding the sampled

roots to learn about the mechanisms underlying functional differentiation of roots. Besides, accounting for path length, which is hypothesized to be a major determinant of anatomical and hydraulic properties in roots, could further serve to disentangle the key drivers of variation in xylem architecture and resulting hydraulic conductivity.

With regards to SOC stocks, this study showed that the main input of SOC in the subsoil originates from roots and that root-derived SOM also considerably contributes to SOC stocks in the topsoil. Moreover, the results emphasize the importance of soil texture and mineralogy as well as fine root mass as major determinants of the SOC contents and stocks in the subsoil. Most likely, soil texture and mineralogy have a twofold effect on SOC sequestration in the subsoil: firstly, through organo-mineral association by which SOM is stabilized and protected from microbial degradation. Organo-mineral association increases with increasing amounts of the clay fraction. Secondly, roots may grow preferentially in spots with chemically and physically more favourable conditions; thus, soil texture also indirectly asserts influence on SOC sequestration via shaping the amount of root-borne OM inputs to the soil. Another major result of this study is that SOC stocks in the subsoil may exceed those in the topsoil, even though SOC contents in deeper soil layers may be low. However, owing to the often great volume of subsoil horizons, SOC stocks in these soil layers may contribute substantially to the overall SOC pools and therefore have to be considered in C inventories.

## 8.2 References

Aber, J.D., Melillo, J.M., Nadelhoffer, K.J., McClaugherty, C.A., and Pastor, J. (1985) Fine root turnover in forest ecosystems in relation to quantity and form of nitrogen availability: a comparison of two methods. Oecologia 66:317–321.

Aloni, R. (1987) Differentiation of vascular tissues. Annu. Rev. Plant Physiol. 38: 179–204. doi: 10.1146/annurev.pp.38.060187.001143

Braun, S., Cantaluppi, L., Flückiger, W. (2005) Fine roots in stands of *Fagus sylvatica* and *Picea abies* along a gradient of soil acidification. Environmental Pollution 137:574-579.

Bundt, M., Widmer, F., Pesaro, M., Zeyer, J., and Blaser, P. (2001) Preferential flow paths: Biological "hot spots" in soils. Soil Biol. Biochem. 33: 729-738.

Canadell J, Jackson RB, Ehleringer JR, Mooney HA, Sala OE, Schulze E-D (1996) Maximum rooting depth of vegetation types at the global scale. Oecologia 108:583-595.

Carlquist, S. (2001) Comparative Wood Anatomy: Systematic, Ecological, and Evolutionary Aspects of Dicotyledon Wood. Springer-Verlag, Berlin. doi: 10.1007/978-3-662-04578-7

Chabbi, A., Kögel-Knabner, I., and Rumpel, C. (2009) Stabilised carbon in subsoil horizons is located in spatially distinct parts of the soil profile. Soil Biology and Biochemistry 41(2):256-261.

Christensen-Dalsgaard, K. K., Ennos, A. R., and Fournier, M. (2008). Are radial changes in vascular anatomy mechanically induced or an ageing process? Evidence from observations on buttressed tree root systems. Trees 22: 543–550. doi: 10.1007/s00468-008-0214-y

Comas, L.H., and Eissenstat, D.M. (2009) Patterns in root trait variation among 25 co-existing North American forest species. New Phytologist 182:919–928.

Coomes, D. A., Jenkins, K. L., and Cole, L. E. S. (2007) Scaling of tree vascular transport systems along gradients of nutrient supply and altitude. Biol. Lett. 3: 86–89. doi: 10.1098/rsbl.2006.0551

Dennis, P.G., Miller, A.J., and Hirsch, P.R. (2010) Are root exudates more important than other sources of rhizodeposits in structuring rhizosphere bacterial communities? FEMS Microbiol. Ecol. 72 (3): 313–327.

Dunham, S. M., Lachenbruch, B., and Ganio, L. M. (2007) Bayesian analysis of Douglas-fir hydraulic architecture at multiple scales. Trees 21: 65–78. doi: 10.1007/s00468-006-0097-8

Eissenstat, D. M., and Caldwell, M. M. (1988) Seasonal timing of root growth in favorable microsites. Ecology 69(3): 870-873.

Eissenstat, D.M., Wells, C.E., Yanai, R.D., and Whitbeck, J. L. (2000) Building roots in a changing environment: implications for root longevity. New Phytol. 147: 33-42.

Finér, L., Helmisaari, H.-S., Lõhmus, K., Majdi, H., Brunner, I., Børja, I., Eldhuset, T., Godbold, D., Grebenc, T., Konôpka, B., Kraigher, H., Möttönen, M.-R., Ohashi, M., Oleksyn, J., Ostonen, I., Uri, V., and Vanguelova, E. (2007) Variation in fine root biomass of three European tree species: Beech (*Fagus sylvatica* L.), Norway spruce (*Picea abies* L. Karst.), and Scots pine (*Pinus sylvestris* L.). Plant Biosystems 141:394–405.

Fitter, A.H. (1985) Functional significance of root morphology and root system architecture. In: Fitter, A.H., Atkinson, D., Read, D.J., and Usher, M.B. (eds.). Ecological Interactions in Soil (Special Publication of the British Ecological Society, No. 4), 87–106. Blackwell Scientific, Oxford.

Forde, B., and Lorenzo, H. (2001) The nutritional control of root development. Plant and soil 232(1-2):51-68.

Gebauer, R., and Volařík, D. (2013) Root hydraulic conductivity and vessel structure modification with increasing soil depth of two oak species: Quercus pubescens and Quercus robur. Trees 27: 523–531. doi: 10.1007/s00468-012- 0805-5

Gill, R.A., and Burke, I.C. (2002) Influence of soil depth on the decomposition of Bouteloua gracilis roots in the shortgrass step. Plant Soil 241: 233-242.

Godbold, D.L., Fritz, H.W., Jentschke, G., Meesenburg, H., and Rademacher, P. (2003) Root turnover and root necromass accumulation of Norway spruce (Picea abies) are affected by soil acidity. Tree Physiology 23:915-921.

Gu, J., Xu, Y., Dong, X., Wang, H., and Wang, Z. (2014) Root diameter variations explained by anatomy and phylogeny of 50 tropical and temperate tree species. Tree Physiol. 34: 415–425. doi: 10.1093/treephys/tpu019

Guo, D.L., Xia, M.X., Wie, X., Chang, W.J., Liu, Y., and Wang, Z.Q. (2008) Anatomical traits associated with absorption and mycorrhizal colonization are linked to root branch order in twenty-three Chinese temperate tree species. New Phytol 180:673–683. https://doi.org/10.1111/j.1469-8137.2008.02573.x

Hacke, U. G., Spicer, R., Schreiber, S. G., and Plavcová, L. (2016) An ecophysiological and developmental perspective on variation in vessel diameter. Plant Cell Environ. 40: 831–845. doi: 10.1111/pce.12777

Hafner, S., Wiesenberg, G.L.B., Stilnikova, E., Merz, K., and Kuzyakov, Y. (2014) Spatial distribution and turnover of root-derived carbon in alfalfa rhizosphere depending on top and subsoil properties and mycorrhization Plant Soil 380: 101-115.

Hajek, P., Leuschner, C., Herte, I. D., Delzon, S., and Schuldt, B. (2014) Trade-offs between xylem hydraulic properties, wood anatomy and yield in Populus. Tree Physiol. 34: 744–756. doi: 10.1093/treephys/tpu048

Hertel, D. (1999) Das Feinwurzelsystem von Rein-und Mischbeständen der-Rotbuche: Struktur, Dynamik und interspezifische Konkurrenz. Dissertationes Botanicae, 317. J. Cramer, Berlin, Stuttgart.

Hertel, D., and Wesche, K. (2008) Tropical moist Polylepis stands at the treeline in East Bolivia: the effect of elevation on stand microclimate, above-and below-ground structure, and regeneration. Trees 22(3): 303-315.

Hodge, A. (2004) The plastic plant: root responses to heterogeneous supplies of nutrients. New Phytologist 162: 9–24.

Hodge, A. (2006) Plastic plants and patchy soils. Journal of Experimental Botany 57(2): 401–411.

Huang, G., Zhao, X.-Y., Zhao, H.-L., Huang, Y.-X., and Zuo, X.-A. (2010) Linking root morphology, longevity and function to root branch order: a case study in three shrubs. Plant Soil 336: 197–208. doi: 10.1007/s11104-010-0466-3

Jackson, R.B., Canadell, J., Ehleringer, J.R, Mooney, H.A., Sala, O.E., and Schulze, E.D. (1996) A global analysis of root distributions for terrestrial biomes. Oecologia 108: 389-411.

Janzen, H. H. (2005) Soil carbon: A measure of ecosystem response in a changing world?. Canadian Journal of Soil Science 85(Special Issue): 467-480.

Jenny, H. (1994) Factors of Soil Formation. A System of Quantitative Pedology. Dover Publications, New York. http://dx.doi.org/10.1016/0016-7061(95)90014-4.

Jobbágy, E. G., and Jackson, R. B. (2000) The vertical distribution of soil organic carbon and its relation to climate and vegetation. Ecological applications 10(2): 423-436.

Jobbágy, E. G., and Jackson, R. B. (2001) The distribution of soil nutrients with depth: global patterns and the imprint of plants. Biogeochemistry 53(1): 51-77.

Kalhoff, M. (2000) Das Feinwurzelsystem in einem Kiefern-Eichen-Mischbestand. Dissertationes Botanicae, 332. J. Cramer, Berlin, Stuttgart.

Kern, K.G., Moll, W., and Braun, H.J. (1961) Wurzeluntersuchungen in Rein- und Mischbeständen des Hochschwarzwaldes (Vfl. Todtmoos 2,I-IV). Allg. Forst- u. Jagdztg. 132(10): 241-259.

Köcher, P., Horna, V., Beckmeyer, I., and Leuschner, C. (2012) Hydraulic properties and embolism in small-diameter roots of five temperate broad-leaved tree species with contrasting drought tolerance. Ann. For. Sci. 69: 693–703. doi: 10.1007/s13595-012-0189-0

Kölbl, A., and Kögel-Knabner, I. (2004) Content and composition of free and occluded particulate organic matter in a differently textured arable Cambisol as revealed by solidstate $^{13}C$ NMR spectroscopy. Journal of Plant Nutrition and Soil Science 167: 45–53. http://dx.doi.org/10.1002/jpln.200321185.

Kottke, I., and Agerer, R. (1983) Untersuchungen zur Bedeutung der Mykorrhiza in älteren Laub- und Nadelwaldbeständen des südwestlichen Keuperberglandes. Mitt Ver Forstl Standortsk Forstpflanzenzüchtung, Bundesrepublik Deutschl 30:30–39.

Kuzyakov, Y., Hill, P., and Jones, D. (2007) Root exudate components change litter decomposition in a simulated rhizosphere depending on temperature. Plant and Soil 290: 293–305. http://dx.doi.org/10.1007/s11104-006-9162-8.

Lehmann, J. (2003) Subsoil root activity in tree-based cropping systems. Plant and Soil 255: 319–331.

Leinemann, T., Mikutta, R., Kalbitz, K., Schaarschmidt, F., and Guggenberger, G. (2016) Small scale variability of vertical water and dissolved organic matter fluxes in sandy Cambisol subsoils as revealed by segmented suction plates Biogeochemistry 131: 1-15

Leuschner, C. and Hertel, D. (2003) Fine Root Biomass of Temperate Forests in Relation to Soil Acidity and Fertility, Climate, Age and Species. Progress in Botany 64: 405-438.

Leuschner, C., Hertel, D., Muhs, A., and Schmid, I. (1998) Feinwurzel-Bestandesmassen der Rotbuche an verschiedenen Standorten innerhalb ihrer oekologischen Amplitude in Nordwest- und Mittel-deutschland. VERHANDLUNGEN-GESELLSCHAFT FUR OKOLOGIE 28: 429-434.

Leuschner, C., Hertel, D., Schmid, I., Koch, O., Muhs, A., and Hölscher, D. (2004) Stand fine root biomass and fine root morphology in old-growth beech forests as a function of precipitation and soil fertility. Plant and Soil 258: 43–56.

Lintunen, A., and Kalliokoski, T. (2010) The effect of tree architecture on conduit diameter and frequency from small distal roots to branch tips in Betula pendula, Picea abies and Pinus sylvestris. Tree Physiol. 30: 1433–1447. doi: 10.1093/ treephys/tpq085

Lõhmus, K., Oja, T., and Lasn, R. (1989) Specific root area: a soil characteristic. Plant and Soil 119(2): 245-249.

Long, Y., Kong, D., Chen, Z., and Zeng, H. (2013) Variation of the linkage of root function with root branch order. PLoS ONE 8:e57153. doi: 10.1371/journal. pone.0057153

Maeght J.-L., Rewald, B., and Pierret, A. (2013) How to study deep roots — and why it matters. Frontiers in plant science 4: 1-14.

McCormack, M.L., Dickie, I.A., Eissenstat, D.M., Fahey, T.J., Fernandez, C.W., Guo, D., Helmisaari, H.-S., Hobbie, E.A., Iversen, C.M., Jackson, R.B., Leppälammi-Kujansuu, J., Norby, R.J., Phillips, R.P., Pregitzer, K.S., Pritchard, S.G., Rewald, B., and Zadworny, M. (2015) Redefining fine roots improves understanding of below-ground contributions to terrestrial biosphere processes. New Phytologist 207:505–518.

McElrone, A. J., Pockman, W. T., Martínez-Vilalta, J., and Jackson, R. B. (2004) Variation in xylem structure and function in stems and roots of trees to 20 m depth. New Phytol. 163: 507–517. doi: 10.1111/j.1469-8137.2004.01127.x

Nadelhoffer, K.J. (2000) The potential effects of nitrogen deposition on fine-root production in forest ecosystems. New Phytol. 147: 131-139.

Nardini, A., Salleo, S., and Tyree, M. T. (2002) Ecological aspects of water permeability of roots: In: Waisel, Y., Eshel, A., and Kafkafi, U. (eds.) Plant Roots: The Hidden Half, Marcel Dekker Inc., New York, 683–698.

Neatrour, M. A., Jones, R. H., and Golladay, S. W. (2005) Correlations between soil nutrient availability and fine-root biomass at two spatial scales in forested wetlands with contrasting hydrological regimes. Canadian Journal of Forest Research 35(12): 2934-2941.

Nepstad, D.C., de Carvalho, C.R., Davidson, E.A., Jipp, P.H., Lefebvre, P.A., Negreiros, G.H., da Silva, E.D., Stone, T.A., Trumbore, S.E., and Vieira, S. (1994) The role of deep roots in the hydrological and carbon cycles of Amazonian forests and pastures. Nature 372: 666–669.

Olson, M. E., Anfodillo, T., Rosell, J. A., Petit, G., Crivellaro, A., Isnard, S., et al. (2014) Universal hydraulics of the flowering plants: vessel diameter scales with stem length across angiosperm lineages, habits and climates. Ecol. Lett. 17: 988–997. doi: 10.1111/ele.12302

Olson, M. E., and Rosell, J. A. (2013) Vessel diameter–stem diameter scaling across woody angiosperms and the ecological causes of xylem vessel diameter variation. New Phytol. 197: 1204–1213. doi: 10.1111/nph.12097

Olsthoorn, A. F. M. (1991) Fine root density and root biomass of two Douglas-fir stands on sandy soils in The Netherlands. 1. Root biomass in early summer. Netherlands Journal of Agricultural Science 39:49-60.

Ostonen, I., Püttsepp, Ü., Biel, C., Alberton, O., Bakker, M. R., Lõhmus, K., Majdi, H., Metcalfe, D., Olsthoorn, A. F. M., Pronk, A., Vanguelova, E., Weih, M., and Brunner, I. (2007) Specific root length as an indicator of environmental change. Plant Biosystems - An International Journal Dealing with all Aspects of Plant Biology, 141(3): 426-442. DOI: 10.1080/11263500701626069.

Ostonen, I., Helmisaari, H. S., Borken, W., Tedersoo, L., Kukumägi, M., Bahram, M., ... and Asi, E. (2011) Fine root foraging strategies in N orway spruce forests across a E uropean climate gradient. Global Change Biology 17(12): 3620-3632.

Pate, J. S., Jeschke, W. D., and Aylward, M. J. (1995) Hydraulic architecture and xylem structure of the dimorphic root systems of South-West Australian species of Proteaceae. J. Exp. Bot. 46: 907–915. doi: 10.1093/jxb/46.8.907

Pfautsch, S. (2016) Hydraulic anatomy and function of trees—basics and critical developments. Curr. For. Rep. 2: 236–248. doi: 10.1007/s40725-016- 0046-8

Pierret, A., Doussan, C., Capowiez, Y., Bastardie, F., and Pagès, L. (2007) Root Functional Architecture: A Framework for Modeling the Interplay between Roots and Soil. Vadose Zone Journal 6(2): 269-281.

Pierret, A., Maeght, J. L., Clément, C., Montoroi, J. P., Hartmann, C., and Gonkhamdee, S. (2016) Understanding deep roots and their functions in ecosystems: an advocacy for more unconventional research. Annals of botany 118(4): 621-635.

Pollierer, M.M., Langel, R. Körner, C., Maraun, M., and Scheu, S. (2007) The underestimated importance of belowground carbon input for forest soil animal food webs. Ecology Letters 10: 729–736.

Poorter, H., and Nagel, O. (2000) The role of biomass allocation in the growth response of plants to different levels of light, $CO_2$, nutrients and water: a quantitative review. Australian Journal of Plant Physiology 27:595–607.

Pregitzer, K.S., Hendrick, R.L., and Fogel, R. (1993) The demography of fine roots in response to patches of water and nitrogen. New Phytol 125: 575–580.

Rasse, D.P., Rumpel, C., and Dignac, M.-F. (2005) Is soil carbon mostly root carbon? Mechanisms for a specific stabilization. Plant and Soil 269: 341-356.

Rewald, B., Leuschner, C., Wiesman, Z., and Ephrath, J. E. (2011) Influence of salinity on root hydraulic properties of three olive varieties. Plant Biosyst. 145: 12–22. doi: 10.1080/11263504.2010.514130

Rosell, J. A., Olson, M. E., and Anfodillo, T. (2017) Scaling of xylem vessel diameter with plant size: causes, predictions, and outstanding questions. Curr. For. Rep. 3: 46–59. doi: 10.1007/s40725-017-0049-0

Rumpel, C., and Kögel-Knabner, I. (2011) Deep soil organic matter—a key but poorly understood component of terrestrial C cycle. Plant and soil 338(1-2): 143-158.

Rumpel, C., Eusterhues, K., and Kögel-Knabner, I. (2004) Location and chemical composition of stabilized organic carbon in topsoil and subsoil horizons of two acid forest soils Soil Biol. Biochem. 36: 177-190.

Ryser, P. (1998) Intra- and interspecific variation in root length, root turnover and the underlying parameters. In: Lambers, H., Poorter, H., VanVuuren, M. (eds.) Inherent variation in plant growth: Physiological mechanisms and ecological consequences, Backhuys, Leiden, Netherlands, 441–465.

Salomé, C., Nunan, N., Pouteau, V., Lerch, T.Z., and Chenu, C. (2010) Carbon dynamics in topsoil and in subsoil may be controlled by different regulatory mechanisms Glob. Chang. Biol. 16: 416-426.

Schenk, H. J., and Jackson, R. B. (2002) The global biogeography of roots. Ecological Monographs 72: 311–328.

Schenk, H. J., and Jackson, R. B. (2005) Mapping the global distribution of deep roots in relation to climate and soil characteristics. Geoderma 126: 129-140.

Schmid, I. (2002) The influence of soil type and interspecific competition on the fine root system of Norway spruce and European beech. Basic Appl Ecol 3: 339–346.

Spicer, R., and Groover, A. (2010). Evolution of development of vascular cambia and secondary growth. New Phytol. 186: 577–592. doi: 10.1111/j.1469-8137.2010.03236.x

Stone, E. L., and Comerford, N. B. (1994) Plant and animal activity below the solum. Proceedings on a Symposium on Whole Regolith Pedology: 57-74.

Stone, E.L., and Kalisz, P.J. (1991) On the maximum extent of tree roots. Forest Ecology and Management 46: 59-102.

Syswerda, S.P., Corbin, A.T., Mokma, D.L., Kravchenko, A.N., and Robertson, G.P. (2011) Agricultural management and soil carbon storage in surface vs. deep layers Soil Sci. Soc. Am. J. 75: 92-101.

Tefs, C., and Gleixner, G. (2012) Importance of root derived carbon for soil organic matter storage in a temperate old-growth beech forest–Evidence from C, N and $^{14}C$ content. Forest Ecology and Management 263: 131-137.

Torn, M.S., Swanston, C.W., Castanha, C., and Trumbore, S.E. (2009) Storage and Turnover of Organic Matter in Soil. In: Senesi, N., Xing, B., Huang, P. M. (eds.) Biophysico-Chemical Processes Involving Natural Nonliving Organic Matter in Environmental Systems. Wiley, New Jersey, USA, 219-261.

Tyree, M. T., and Zimmermann, M. H. (2002) Xylem Structure and the Ascent of Sap. Springer Science & Business Media, Berlin. doi: 10.1007/978-3-662-04931-0

Valenzuela-Estrada, L. R., Vera-Caraballo, V., Ruth, L. E., and Eissenstat, D. M. (2008) Root anatomy, morphology, and longevity among root orders in Vaccinium corymbosum (Ericaceae). Am. J. Bot. 95: 1506–1514. doi: 10.3732/ajb.0800092

Wagai, R., Mayer, L.M., Kitayama, K., and Knicker, H. (2008) Climate and parent material controls on organic matter storage in surface soils : a three- pool, density-separation approach. Geoderma 147: 23–33. http://dx.doi.org/10.1016/j.geoderma.2008.07.010.

Wang, Y., Dong, X., Wang, H., Wang, Z., and Gu, J. (2015) Root tip morphology, anatomy, chemistry and potential hydraulic conductivity vary with soil depth in three temperate hardwood species. Tree Physiol. 36: 99–108. doi: 10.1093/treephys/tpv094

# CHAPTER 9

## Summary

## 9.1 Summary

Trees' rooting systems have a fundamental role in the acquisition of water and nutrients from the soil and they are thought to be inherently plastic with regards to their size, structure, morphology and anatomy in order to cope with the spatially and temporarily heterogeneous supply of nutrients and water in soil. Furthermore, fine roots have a prominent role in the C cycle of forest ecosystems. The largest terrestrial OC pool is located in soils, and forest soils are estimated to contain the largest share, with up to 70 % of SOC. A large portion of trees' annually assimilated carbon is consumed by fine roots and dead fine roots and rhizodeposits are a major source of OC in soils, particularly in subsoils. Therefore, to accurately assess the distribution, abundance, morphology and anatomy of trees' fine root system is of vital importance for understanding forest ecosystem functioning. Nonetheless, our knowledge on the belowground plasticity of trees and their role in the C cycle of forests is still incomplete, particularly with regards to the subsoil, although deep roots can be important for securing sufficient supply of nutrients and water and 30-60 % of the global SOC is stored in the horizons below the topsoil.

The present thesis deals with the variability in the size, structure, morphology, and anatomy of the fine root system of *Fagus sylvatica* as well as with the impact of beech fine roots on OC stocks in the topsoil and subsoil of six mature European beech forests Northern Germany. For this comparative approach, study sites with comparable climatic conditions, age and stand structure but growing on different bedrock were selected in order to be able to examine variation in root system traits and C cycling in the soil in relation to soil chemical properties and soil fertility. Major study aims were to i) quantify total stand fine root biomass and necromass and to analyze variation in fine root distribution patterns in dependence on soil acidity and depth, ii) investigate beech fine root morphological adaptations to different regimes of nutrient availability in soils, iii) analyze the intraspecific variability in xylem anatomical and derived hydraulic traits of small- and medium-sized beech roots with particular focus to soil depth-dependent variation, and iv) assess the impact of beech roots on the amount, spatial distribution and chemical composition of SOM with regards to the effect of different parent materials.

Quite unexpectedly, significant relationships between FRB profile totals and soil acidity did not appear. Instead, the depth of the profile was shown to be the most important determinant of overall fine root system size. Higher silt and oxalate-extractable Fe contents in the rooted samples of one site (GR) suggest an increased foraging precision through root deployment in nutrient-rich

patches in soils with low background fertility. Other than FRB, the amounts of necromass appeared to be related to site fertility, assumedly for the main part caused by an increase in fine root mortality. Across the investigated sites and across soil layers within one site, root morphological traits (mean fine root diameter, SRL, SRA, RTF) showed considerable variation. The largest differences emerged between the different layers within on profile, while a consistent relation in root morphological traits to soil acidity or base saturation did not appear. At half of the sites maximum RTF values were reached in the lower subsoil, presumably due to increased nutrient availability in these horizons.

A significant relation of the investigated xylem anatomical and functional traits ($D$, $K_p$, VD, relative vessel lumen area) to soil depth could not be established. Instead, all traits showed a strong dependence on root diameter and thus root age. The maximum vessel diameter appeared to be restricted in the investigated roots, which may display a trade-off between hydraulic efficiency and hydraulic safety as well as mechanical requirements. Another main result of this study is the high plasticity in xylem architectural and hydraulic traits of similar-sized beech roots independent of soil depth, which indicates the existence of different functional types of roots with respect to water uptake and conduction.

Furthermore, this study shows that the main input of SOC in the subsoil originates from roots and that root-derived SOM also considerably contributes to SOC stocks in the topsoil. The results emphasize the importance of soil texture and mineralogy as well as fine root mass as major determinants of the SOC contents and stocks in the subsoil. Most likely, soil texture and mineralogy have a twofold effect on SOC sequestration in the subsoil: firstly, through organo-mineral association by which SOM is stabilized and protected from microbial degradation. Secondly, soil texture may as well indirectly assert influence on SOC sequestration via shaping the amount of root-borne OM inputs to the soil.

Overall, this study supports the notion, that the rooting system of European beech is highly responsive to external (soil) factors, which is interpreted as an adaptive belowground strategy which enables the tree species to colonize a wide range of soil types. Furthermore, the results emphasize the prominent role of fine roots as a major determinant of SOC contents and stocks particularly in the subsoil and underline the importance of considering subsoil horizons in C inventories for accurately modeling terrestrial C cycling.

# CHAPTER 10

# Appendix

## 10.1 Index of Tables

**TABLE 1.1:** 13
Subprojects of the SUBSOM research unit.

**TABLE 2.1:** 25
Locational and soil characteristics of the six study sites grouped into deep and shallow profiles.

**TABLE 2.2:** 26
Overview of sampling designs, studies traits, and methods used.

**TABLE 3.1:** 37
Topographic, climatologic and stand structural characteristics of the six studied mature beech forests on different bedrock type in northern Germany. The sites are arranged from left to right in a sequence of increasing base richness of the soil, with the plots # 1-3 representing deep profiles (>2 m profile depth), while the profiles # 4-6 are shallow profiles (<0.8 m depth).

**TABLE 3.2:** 38
Soil characteristics of the six beech forests on different bedrock type. 'Upper subsoil' stands for 20-110 cm soil depth at the GR, RU and HM sites with deep profiles, and 20-50 cm depth in the shallow profiles of the EG, DR and GW sites. 'Lower subsoil' stands for 110-200 cm soil depth at the GR, RU and HM sites, and 50-80 cm depth at the EG, DR and GW sites.

**TABLE 3.3:** 47
Fine root biomass and necromass, and fine root live:dead ratio in the organic layer, mineral topsoil (0-20 cm), upper subsoil, and lower subsoil of the six investigated mature beech forests. 'Upper subsoil' stands for 20-110 cm soil depth at the GR, RU and HM sites with deep profiles, and 20-50 cm depth in the shallow profiles of the EG, DR and GW sites. 'Lower subsoil' stands for 110-200 cm soil depth at the GR, RU and HM sites, and 50-80 cm depth at the EG, DR and GW sites. Also given are ß-values, which characterize the depth distribution of root mass according to the expression: cumulative root mass $y = 1-\beta^d$. Shown are means + SE of three soil pits per site. Different small letters indicate significant differences ($P<0.05$) between the stands, capital letters significant differences between the soil horizons.

**TABLE 3.4:** 48
N content, specific root length (SRL), specific root area (SRA), root tip frequency (tips per root mass), tip abundance (tips per ground area), of living fine roots in the organic layer, topsoil, upper subsoil, and lower subsoil of the six investigated mature beech forest stands. Upper subsoil: 20-110 cm soil depth in GR, RU, HM, 20-50 cm soil depth in EG, DR, GW, lower subsoil: 110-200 cm soil depth in GR, RU, HM, 50-80 cm soil depth in EG, DR, GW. Shown are means + SE of three soil pits per field site. Different small letters indicate significant differences ($P<0.05$) between the stands, capital letters significant differences between the soil horizons.

**TABLE 3.5:** 53
Coefficients of linear Pearson correlations between fine root and soil and stand characteristics. * indicates significance at ≤ 0.05, ** significance at ≤ 0.01, and *** significance at ≤ 0.001 error probability. (FRB – Fine root biomass. FRN – Fine root necromass. FR – Fine root. RTD – Root tip density. SRA – Specific root area. OL- Organic layer.)

**TABLE 3.6:** 54
Results of multivariate regression analyses between fine root biomass and clay content (%), C/N ratio, and base saturation (BS, %), and between specific root area, average fine root diameter, and root tip frequency and clay content (%), C/N ratio, base saturation (BS, %), and fine root biomass (g $m^{-2}$). The regression analyses were conducted separately for the topsoil, upper subsoil and lower topsoil, and for all layers together. Shown are significant correlations with $P < 0.05$.
**TABLE 3.7:** 54
Results of the Principal Components Analysis with eigenvalues (EV) of the first for axes and loadings.

**TABLE S3.1:** 61
Fine root biomass (FRB) and necromass (FRN) in the organic layer and mineral top- and subsoil of the six investigated mature beech forests. Shown are means + SE of three soil pits per site.

**TABLE S3.2:** 62
Fine root biomass and necromass (fraction of profile average), coefficients of variation (CV) for fine root biomass and fine root necromass, fine root C/N ratio, and root tip density in the organic layer, mineral topsoil (0-20 cm), upper subsoil, and lower subsoil of the six investigated mature beech forests. 'Upper subsoil' stands for 20-110 cm soil depth at the GR, RU and HM sites with deep profiles, and 20-50 cm depth in the shallow profiles of the EG, DR and GW sites. 'Lower subsoil' stands for 110-200 cm soil depth at the GR, RU and HM sites, and 50-80 cm depth at the EG, DR and GW sites. Also given is the soil depth to which 50 or 90 %, of fine root biomass and necromass are found in the soil profile of the six investigated mature beech forests Shown are means + SE of three soil pits per site. Different small letters indicate significant differences ($P<0.05$) between the stands, capital letters significant differences between the soil horizons.

**TABLE S3.3:** 63
Specific root length, specific root area, and average fine root diameter for the organic layer and mineral top- and subsoil of the six investigated mature beech forests. Shown are means + SE of three soil pits per site.

**TABLE S3.4:** 64
Average fine root diameter and root tip frequency for the organic layer and mineral top- and subsoil of the six investigated mature beech forests. Shown are means + SE of three soil pits per site.

**TABLE S3.5:** 65
Root length index (RLI) and root area index (RAI) for the organic layer and mineral top- and subsoil of the six investigated mature beech forests. Shown are means + SE of three soil pits per site.

**TABLE 4.1:** 85
Results of linear mixed effects models on the influence of soil depth and root diameter as fixed continuous variables on eight wood anatomical variables in roots of European beech (*Fagus sylvatica*) (n = 197), and the interaction of both factors. Studied traits are root age (age, yr), cross-sectional xylem area ($A_{xylem}$, $mm^2$), relative vessel lumen area ($A_{lumen}$: $A_{xylem}$, %), vessel density (VD, n $mm^{-2}$), vessel diameter ($D$, µm), maximal vessel diameter ($D_{max}$, µm), hydraulically-weighted vessel diameter ($D_h$, µm) and potential hydraulic conductivity ($K_p$, kg $m^{-1}$ $MPa^{-1}$ $s^{-1}$). Also expressed is the variation of the traits (variance component, VC in %) within ($VC_{intra}$) and between ($VC_{inter}$) different root diameter classes (n = 9) and soil depth classes (n = 7). Given are the delta Akaike information criterion (Δi), the likelihood ratio (LR) and probability of error (*P*-value). Significant correlations ($P$<0.05) are shown in bold.

**TABLE 4.2:** 88
Results of regression analyses between the diameter of single root strands and the corresponding mean vessel diameter ($D$, µm), vessel density (VD, n mm-2) (shown in Figure 4.5) and potential hydraulic conductivity ($K_p$, kg $m^{-1}$ $MPa^{-1}$ $s^{-1}$) at the cross-section. Given are the number of observed segments along the individual root, the adjusted coefficient of determination ($r^2_{adj.}$), and the probability of error (*P*-value). Significant correlations ($P$<0.05) are shown in bold.

**TABLE S4.1:** 96
Root classification according to diameter after Sutton and Tinus (1983) and number of observations (n) per root class and soil depth (cm) across the three excavated soil pits.

**TABLE S4.2:** 96
Physical and chemical soil characteristics at different soil depths in the Grinderwald forest (June 2013). Classification of soil horizons according to FAO - WRB 2014.

**TABLE 5.1:** 115
Mean bulk density (BD), pH (0.01 M $CaCl_2$), texture, root biomass, root necromass, dithionite- and oxalate-extractable Fe ($Fe_d$; $Fe_o$) and aluminum ($Al_d$, $Al_o$), Fe in crystalline Fe oxides ($Fe_{(d-o)}$) of soil samples originating from three transects at the Grinderwald site at different depth (n = 24 for each depth). Numbers in brackets show coefficient of variation in % of the respective depth over three transects (n = 24).

**TABLE 5.2:** 124
Results (intercepts and regression coefficients) of the mixed effects models for the SOC content (%) or its natural logarithm (log) with different factors (n = 23 for each depth due to missing data for one of the factors). $Al_d$: dithionite-extractable Al, $Fe_o$: oxalate-extractable Fe, $Fe_{(d-o)}$: Fe in crystalline Fe oxides. Bold words represent significant parameters influencing SOC contents.

**TABLE 5.3:** 126
Mean soil properties in rooted and root-free soil in 85, 110, 135, and 185 cm depth and the mean variation shown as coefficient of variation (CV) in %. Numbers of samples are given in Fig. 5.2, respectively to each depth and soil sample.

**TABLE 6.1:** 153
Mean +/− SD recovered mass, soil organic carbon (SOC) content, carbon to nitrogen ratio (C/N), SOC stock, and carbon enrichment factor ($E_c$) of the unfractionated bulk soil and soil organic matter (SOM) fractions (here referred to as "sand", "silt", "clay" and "POM") from the $subsoil_{10}$, $subsoil_{85}$ and rhizosphere soil. Significant differences in SOM fraction or the bulk soil between the $subsoil_{10}$, $subsoil_{85}$ and rhizosphere soil are indicated by lowercase letters. The superscript † symbols mark observations that are not significantly different when comparing the individual SOM fractions to each other within the $subsoil_{10}$, $subsoil_{85}$ or rhizosphere soil.

**TABLE 6.2:** 156
Relative peak intensities and alkyl/O/N alkyl C ratios of the clay and POM fractions of the $subsoil_{10}$, $subsoil_{85}$ and rhizosphere soil determined by solid state $^{13}C$ NMR spectroscopy. Significant differences between the $subsoil_{10}$, $subsoil_{85}$, and rhizosphere soil are indicated by lowercase letters. The superscript † symbols mark observations that are not significantly different when comparing the chemical compound classes to each other within the clay or POM fraction from $subsoil_{10}$, $subsoil_{85}$ or rhizosphere soil. Standard deviation (SD) of field replicates after ±.

**TABLE 6.3:** 157
Mean +/− SD organic carbon (OC) content, carbon to nitrogen ratio (C/N), chemical compound classes (carboxyl C, aromatic C, O/N alkyl C, alkyl C) and alkyl/ O/N alkyl C ratio of the leaves, fine roots and organic layer. Significant differences of the OC contents, C/N ratios or peak intensities between the leaves, roots and the organic layer are indicated by lowercase letters.

**TABLE S6.1:** 163
P-values for the statistical correlation between the distance from the individual beech trees and the respective parameter.

**TABLE 7.1:** 184
Different biological and chemical parameters in topsoil, subsoil, and rhizosphere soil among the investigated sites ± S.E. Significant differences between the sites and topsoil, subsoil, and rhizosphere soil are indicated by lower case letters.

**TABLE S7.1:** 201
Summary of the best subset regression with bulk soil SOC stocks as dependent variable. Predictors were amino sugars (per g DW), the mass of the clay, POM, and oPOM fractions, and the root mass. Measures shown are whole model $R^2$, AIC, number of predictors included in the respective model, and standardized beta coefficients for each predictor and model.

## 10.2 Index of Figures

**FIGURE 1.1**: 8
Distribution map of *Fagus sylvatica*

**FIGURE 1.2**: 12
Project concept with four methodological approaches

**FIGURE 2.1**: 23
Map with the locations of the study sites in Lower Saxony

**FIGURE 3.1:** 45
Fine root biomass (left) and necromass (right) density (g L-1) in the soil profiles of the six investigated mature beech forest stands. Values are means of three soil pits per field site.

**FIGURE 3.2:** 49
Specific root length (cm g-1) (left) and specific root area (right) (cm² g-1) in the soil profiles of the six investigated mature beech forest stands. Values are means of three soil pits per field site.

**FIGURE 3.3:** 50
Stack diagram of fine root length index (RLI, m m-2) (left) and fine root area index (RLA, m² m-2) (right) in the soil profiles of the six investigated mature beech forest stands. Values are means of three soil pits per field site.

**FIGURE 4.1:** 82
Box-whisker plots (with median, 25 and 75% quantiles and extreme values) for the variation in root diameter (A), root age (B), mean vessel diameter (C, *D*), vessel density (D, VD), relative vessel lumen area (E, $A_{lumen}$: $A_{xylem}$), and potential hydraulic conductivity (F, $K_p$) in seven different soil depth classes.

**FIGURE 4.2:** 83
Root diameter in relation to root age in the sample of 197 roots.

**FIGURE 4.3:** 84
Root diameter in relation to mean vessel diameter (A, *D*), vessel density (B, VD), relative vessel lumen area (C, $A_{lumen}$: $A_{xylem}$), and potential hydraulic conductivity (D, $K_p$). Values are means ±1 SE.

**FIGURE 4.4:** 86
Cross-sections at 100× magnification for three pairs of roots of each similar diameter (A,B: 2.7 mm; C,D: 4.1 mm; E,F: 5.2 mm) displaying typical 'low conductivity' (left) and 'high conductivity' (right) characteristics, and relative contribution of eight vessel size classes to theoretical hydraulic conductivity ($K_h$). The depicted scale bars represent 1 mm.

**FIGURE 4.5:** 88
Root diameter of single root strands in relation to mean vessel diameter (A, *D*) and vessel density (B, VD). Regression functions, adjusted coefficients of determination ($r^2_{adj.}$) and probability of error (*P*-value) are given in Table 4.2.

**FIGURE S4.1:** 97
Influence of soil depth on mean vessel diameter (*D*) for nine different root diameter classes (RD). For each root diameter class, 9-44 samples were available, which subsequently were averaged for each soil depth class. For number of replicates per root diameter class see Table S1. Values are means ± SE; the slope (*b*), coefficient of determination ($r^2$) and probability of error (*P*-value) of the linear regressions are given.

**FIGURE S4.2:** 98
Box-whisker plots with median values for the variation in maximum vessel diameter ($D_{max}$) in seven soil depth classes (a); small letters indicate significant differences between depth classes. Additionally given is the relation between soil depth and mean values ± SE for $D_{max}$ (b). Please note the different scaling of the y-axis.

**FIGURE 5.1:** 122
Boxplots of a) SOC content (%), b) $\delta^{13}C/^{12}C$ (‰), c) root biomass (g $l^{-1}$) and d) microbial biomass C ($C_{mic}$, µg $g^{-1}$) within the soil profiles in different depth.

**FIGURE 5.2:** 123
Boxplot of OC-contents (g $kg^{-1}$) of roots, root-free and rooted soil in subsoil (85, 110, 135, 160, 185 cm). Italic numbers below the boxplot represent the number (n) of samples considered; number of root samples are conform to the number of rooted-soil samples.

**FIGURE S5.1**: 131
Measured against modelled SOC contents for the different depths (n= 23 for each depth due to missing data for one of the factors considered in the regressions). Modelled data for 135 cm depth were back-transformed. Pearson correlation coefficients ($r_P$) or Spearman correlation coefficients ($r_S$) are also given.

**FIGURE 6.1:** 146
Sampling grid applied to each transect wall (n = 64 samples per transect). Composite and volumetric soil samples (using steel cylinders; 8.5 cm diameter, 6 cm height) were taken. The black dots (n = 16 per transect) indicate the samples that were subjected to the combined density and particle size fractionation. The shaded area displays the regions from which the rhizosphere soil was collected. The letters above the graph represent the labels of the horizontal sampling spots, A being nearest to the tree. The distance between sampling spots were 45 cm in the horizontal and 25 cm and in the vertical, starting at a depth of 10 cm.

**FIGURE 6.2:** 147
Mean living and dead fine root concentration [kg $m^{-3}$] down to a depth of 85 cm. The letters above the plots are the labels of the horizontal sampling spots with A being nearest to the tree. n = 3 for each grid point.

**FIGURE 6.3:** 156
$^{13}C$ CPMAS NMR mean spectra of the POM fractions of the rhizosphere soil (calculated from three spectra) and the $subsoil_{10}$ (calculated from 24 spectra).

**FIGURE 6.4:** 157
$^{13}$C CPMAS NMR mean spectra of the clay fractions of the rhizosphere soil (calculated from three spectra), subsoil$_{10}$ (calculated from 24 spectra) and subsoil$_{85}$ (calculated from four spectra).

**FIGURE 6.5:** 158
$^{13}$C CPMAS NMR mean spectra of the leaves, fine roots (each calculated from three spectra) and the organic layer material (calculated from 24 spectra) from all transects.

**FIGURE 7.1:** 186
Amount of fractions in g kg$^{-1}$ bulk soil at the sand, loess, and basalt sites. The various fractions (sand, silt, clay, POM, oPOM, oPOMsmall) are indicated by different colors. Significant differences of the respective fraction between the topsoil, subsoil, rhizosphere soil, and sites are indicated by different letters. (For interpretation of the references to color in this figure legend, the reader is referred to the Web version of this article.)

**FIGURE 7.2:** 188
Soil OC stocks (in g C m$^{-2}$ for a layer thickness of 1 cm) of bulk soil and fractions (sand, silt, clay, POM, oPOM, oPOMsmall) at the sand, loess, and basalt sites. The bulk soil and various fractions are indicated by different shadings and colors, respectively. Significant differences between the topsoil, subsoil, rhizosphere soil, and sites are indicated by different letters. (For interpretation of the references to color in this figure legend, the reader is referred to the Web version of this article.)

**FIGURE 7.3:** 189
Cumulative whole profile SOC stocks at the sand, loess, and basalt sites separated into topsoil and subsoil stocks. Significant differences between site, topsoil, and subsoil are indicated by different letters.

**FIGURE 7.4:** 191
Chemical composition as inferred from NMR spectra (relative intensity of carboxyl, aryl, O/N-alkyl, alkyl C; indicated by different shadings) of the clay, POM, oPOM, and oPOMsmall fractions in the topsoil, subsoil, and rhizosphere soil at the different study sites. The alkyl/O/N-alkyl C ratio is depicted by numbers above the bars. Note that the POM fraction could not be detected in the subsoil at the sand site. The signal intensity of the clay fraction in the subsoil at the basalt site was too low for obtaining a reasonable spectrum, probably due to the presence of paramagnetic materials.

**FIGURE 7.5:** 192
Observed vs. predicted SOC stocks using the regression equation and predictors (root mass, mass of the clay and POM fraction, amino sugars) displayed in the upper left corner of the graph (note that predictors were log-transformed prior to analysis). The used predictors were significantly correlated with SOC stocks and appeared in the best model selected via AIC (see also Supplementary Table S7.1).

**FIGURE S7.1:** 202
Average $^{13}$C NMR spectra for the POM, oPOM, oPOMsmall, and clay fractions at the different study sites.

## 10.3 Acknowledgements

During my time as a doctoral student, many people supported me in so many different ways. Thank you very much!

First of all I want to thank my advisors Prof. Christoph Leuschner and Dr. Dietrich Hertel. You were at hand with help and advice in all time of research and writing of this thesis. Thank you for your guidance and support.

I would also like to thank my many technical and student assistants, who spent uncountable days with me in the field or helped me with processing my samples in the lab. I would like to mention in particular Mechthild Stange: without your commitment and skills it wouldn't have been possible to realize the practical part of my work. Besides, I really enjoyed our conversations and I sincerely appreciate your openness. I can think of no better field assistant. Furthermore, I would like to mention Frederic van Brock, who worked incredibly hard to help me finish my field work.

Thanks also to my colleague Prof. Bernhard Schuldt for the great and appreciative collaboration. I've learned a lot during the work on our joint study and it was fun, too. Thanks a lot!

I also want to thank the DFG for financing this project and my colleagues from the SUBSOM research unit for the good cooperation in the field and during the work on our joint papers.

My sincere thanks go also to my colleague and friend Robin Schwerbrock and to my friend Christine Brautzsch. Thank you for listening to all my complaints, for having too many drinks with me every now and then, for joking and laughing a lot together, for being there for me in times when I really needed good friends, and for all your practical support. You, together with your lovely daughter Josefine, are the ones who made me feel at home in Göttingen. I equally want to thank my colleague and friend Rebecca Liese: you were there for me in times of crisis, and you've always seen me as the person I am.

Last but not least: thank you very much for proof-reading, Steffen Klävers!

***Der Einsame***

Verhaßt ist mir das Folgen und das Führen.
Gehorchen? Nein! Und aber nein – Regieren!
Wer sich nicht schrecklich ist, macht niemand Schrecken:
Und nur wer Schrecken macht, kann andre führen.
Verhaßt ist mirs schon, selber mich zu führen!
Ich liebe es, gleich Wald- und Meerestieren,
Mich für ein gutes Weilchen zu verlieren,
In holder Irrnis grüblerisch zu hocken,
Von ferne her mich endlich heimzulocken,
Mich selber zu mir selber – zu verführen.

- FRIEDRICH NIETZSCHE -

## 10.4 Declaration of originality and certificate of ownership

I, Kristina Kirfel, hereby declare that I am the sole author of this dissertation entitled ‘BELOWGROUND PLASTICITY OF EUROPEAN BEECH – STUDIES ON THE VARIABILITY OF BEECH FINE ROOT SYSTEM SIZE, STRUCTURE, MORPHOLOGY, AND ANATOMY, AND ON THEIR IMPACT ON SOIL ORGANIC MATTER IN THE TOP- AND SUBSOIL OF SIX BEECH FORESTS WITH DIFFERENT BEDROCK TYPES IN NORTHERN GERMANY’. All references and data sources that were used in the dissertation have been appropriately acknowledged. I furthermore declare that this work has not been submitted elsewhere in any form as part of another dissertation procedure.